Stable isotopes as indicators of nitrate attenuation across landscapes

---

A thesis
submitted in partial fulfilment
of the requirements for the Degree of
Doctor of Philosophy

at
Lincoln University
by
Naomi S. Wells

Lincoln University
2013

Abstract of a thesis submitted in partial fulfilment of the
requirements for the Degree of Doctor of Philosophy.

Abstract

Stable isotope as indicators of nitrate attenuation across landscapes

by
Naomi S. Wells

Mitigating the cascade of environmental damage caused by the movement of excess reactive nitrogen (N) from land to sea is currently limited by difficulties in precisely and accurately measuring N fluxes due to variable rates of attenuation (denitrification) during transport. This thesis develops the use of the natural abundance isotopic composition of nitrate ($\delta^{15}N$ and $\delta^{18}O$ of NO_3^-) to integrate the spatial-temporal variability inherent to denitrification, creating an empirical framework for evaluating attenuation during land to water NO_3^- transfers. This technique is based on the knowledge that denitrifiers kinetically discriminate against 'heavy' forms of both N and oxygen (O), creating a parallel enrichment in isotopes of both species as the reaction progresses. This discrimination can be quantitatively related to NO_3^- attenuation by isotopic enrichment factors (ε_{denit}). However, while these principles are understood, use of NO_3^- isotopes to quantify denitrification fluxes in non-marine environments has been limited by, 1) poor understanding of ε_{denit} variability, and, 2) difficulty in distinguishing the extent of mixing of isotopically distinct sources from the imprint of denitrification. Through a combination of critical literature analysis, mathematical modelling, mesocosm to field scale experiments, and empirical studies on two river systems over distance and time, these short comings are parametrised and a template for future NO_3^- isotope based attenuation measurements outlined.

Published ε_{denit} values (n =169) are collated in the literature analysis presented in Chapter 2. By evaluating these values in the context of known controllers on the denitrification process, it is found that the magnitude of ε_{denit}, for both $\delta^{15}N$ and $\delta^{18}O$, is controlled by, 1) biology, 2) mode of transport through the denitrifying zone (diffusion v. advection), and, 3) nitrification (spatial-temporal distance between nitrification and denitrification). Based on the outcomes of this synthesis, the impact of the three factors identified as controlling ε_{denit} are quantified in the context of freshwater systems by combining simple mathematical modelling and lab incubation studies (comparison of natural variation in biological versus physical expression). Biologically-defined ε_{denit}, measured in sediments collected from four sites along a temperate stream and from three tropical submerged paddy fields, varied from -3‰ to -28‰ depending on

the site's antecedent carbon content. Following diffusive transport to aerobic surface water, ε_{denit} was found to become more homogeneous, but also lower, with the strength of the effect controlled primarily by diffusive distance and the rate of denitrification in the sediments. I conclude that, given the variability in fractionation dynamics at all levels, applying a range of ε_{denit} from -2‰ to -10‰ provides more accurate measurements of attenuation than attempting to establish a site-specific value. Applying this understanding of denitrification's fractionation dynamics, four field studies were conducted to measure denitrification/ NO_3^- attenuation across diverse terrestrial → freshwater systems.

The development of NO_3^- isotopic signatures (i.e., the impact of nitrification, biological N fixation, and ammonia volatilisation on the isotopic 'imprint' of denitrification) were evaluated within two key agricultural regions: New Zealand grazed pastures (Chapter 4) and Philippine lowland submerged rice production (Chapter 5). By measuring the isotopic composition of soil ammonium, NO_3^- and volatilised ammonia following the bovine urine deposition, it was determined that the isotopic composition of NO_3^- leached from grazed pastures is defined by the balance between nitrification and denitrification, not ammonia volatilisation. Consequently, NO_3^- created within pasture systems was predicted to range from +10‰ ($\delta^{15}N$) and -0.9‰ ($\delta^{18}O$) for non-fertilised fields (N limited) to -3‰ ($\delta^{15}N$) and +2‰ ($\delta^{18}O$) for grazed fertilised fields (N saturated). Denitrification was also the dominant determinant of NO_3^- signatures in the Philippine rice paddy. Using a site-specific ε_{denit} for the paddy, N inputs versus attenuation were able to be calculated, revealing that >50% of available N in the top 10 cm of soil was denitrified during land preparation, and >80% of available N by two weeks post-transplanting. Intriguingly, this denitrification was driven by rapid NO_3^- production via nitrification of newly mineralised N during land preparation activities.

Building on the relevant range of ε_{denit} established in Chapters 2 and 3, as well as the soil-zone confirmation that denitrification was the primary determinant of NO_3^- isotopic composition, two long-term longitudinal river studies were conducted to assess attenuation during transport. In Chapter 6, impact and recovery dynamics in an urban stream were assessed over six months along a longitudinal impact gradient using measurements of NO_3^- dual isotopes, biological populations, and stream chemistry. Within 10 days of the catastrophic Christchurch earthquake, dissolved oxygen in the lowest reaches was <1 mg l^{-1}, in-stream denitrification accelerated (attenuating 40-80% of sewage N), microbial biofilm communities changed, and several benthic invertebrate taxa disappeared. To test the strength of this method for tackling the diffuse, chronic N loading of streams in agricultural regions, two years of longitudinal measurements of NO_3^- isotopes were collected. Attenuation was negatively correlated with NO_3^- concentration, and was highly dependent on rainfall: 93% of calculated attenuation (20 kg NO_3^--N ha^{-1} y^{-1}) occurred within 48 h of rainfall.

The results of these studies demonstrate the power of intense measurements of NO_3^- stable isotope for distinguishing temporal and spatial trends in NO_3^- loss pathways, and potentially allow for improved catchment-scale management of agricultural intensification. Overall this work now provides a more cohesive understanding for expanding the use of NO_3^- isotopes measurements to generate accurate understandings of the controls on N losses. This information is becoming increasingly important to predict ecosystem response

to future changes, such the increasing agricultural intensity needed to meet global food demand, which is occurring synergistically with unpredictable global climate change.

Keywords: Nitrate, denitrification, nitrogen cascade, attenuation, grazed pastures, paddy soil, stable isotopes, biogeochemistry, nitrogen discharge, Rayleigh fractionation, diffusion

Acknowledgements

The most important first: thanks to my advisor Tim Clough. Armed with a reading speed which must surely be super-human, and possessing seemingly-endless scientific curiosity, he has guided through every step of this process. He let me pursue various non-linear ideas, and was always willing to lend his intellect to help mould them into something worthwhile: I always left our meetings ready to get out there and tackle 'big scientific questions'.

Thanks also to Troy Baisden, for always challenging me to take the research to the next level, and never let me get away with half-baked calculations. Troy both proposed the idea of using NO_3^- isotopes in 'simple and straightforward' ways and ensured a research budget that let me explore (and mess things up) well beyond this original scope. He enabled me to take advantage of workshops and conferences around the world that inestimably improved the quality and scope of this work.

This thesis could never have happened without the guidance of numerous mentors. Thanks to Dan Brabander for showing me that 'good questions' and 'good science' are one and the same, setting me on the path I'm on today. Liz Baggs at the University of Aberdeen took one look at me and told me that I needed to do a PhD. I've been fortunate to work with many scientist mentors who inspire me towards that elusive goal of 'good research': Sarah Johnson-Beebout, Roland Buresh, Bo Elberling, Eric Paterson, Gavin Lear. And, of course, at the start of it all: I'm indebted to my mother for teaching me the importance of a good question and the wonder of the natural world, and my father for tireless efforts to teach me the thrill of quantitative problem solving (it may have taken me ~20 years, but I think I'm getting there...).

The year I spent conducting research in the Philippines was made possible by the U.S. Student Fulbright program, so many thanks to all the PAEF staff for providing me with the opportunity to conduct this research, and Sarah Johnson-Beebout for supporting my work at IRRI. The quality of my scientific output from this project was greatly improved by the technical competence of Sonny, the analytical excellence of Mia, the physical assistance of Jerone and Angel, and the encyclopedic knowledge of all aspects of rice production shared with me by Jun, Wency, and RJB.

Thanks to all of the students and staff of the Lincoln soils department for their support and camaraderie, particularly Janet and Roger, who have provided assistance every step of the way, from teaching me how use the mass spec to finding me teaching work, and my fellow postgrads, Diana, Pal, Jack, Scott, Greg, Andre, Brendon, and Fiona. And special thanks to Nimlesh, who put up with sharing her office space with my smelly cycling gear for years, and provided quality conversation on diffusion, writing, marriage, and everything in between.

Building this thesis has been 'a journey'. And like any worthwhile epic journey, I would probably have been sucked into the morass by now if not for the support (and laughter) of many good friends and family. My peerless flatmates Volker and Vaughan made sure that I had cake (and also lasagna, goat curry,

macaroons...) to eat every day during these last few hectic months of writing; Sharon, Nick, Rose, and Jan have brought many adventures (without death!), and even managed to teach me a little about geology (and a lot about laughing under conditions that could objectively be described as mildly unpleasant). My parents and Emma, Todd, and Carl, who, against all odds, keep me in touch with reality, and are actually the best family.

Table of Contents

List of Figures

List of Tables

List of Images

Chapter 1
Introduction

Between 1900 and 1990 human activities have doubled the annual mass of nitrogen (N) entering the earth system, posing a threat to both the environment and sustainable food production (Gruber and Galloway 2008). This increase in N inputs is driven by the need to increase food production in order to meet the demands of the growing world population: although dinitrogen gas (N_2) makes up 78% of the atmosphere, it is unavailable to most organisms and thus biological production in most ecosystems is limited by N availability (Ju et al. 2009, Vitousek et al. 2009). Agricultural intensification has increased the release of available N into the biosphere through enhanced biological N_2 fixation (BNF) and the creation of synthetic N fertilisers via the Haber-Bosch process (as summarised in Table 1.1).

However, while N fertilizers have significantly increased global food production (Vitousek et al. 2009), the proportion of added N incorporated into crops has not improved and fertilisers are often applied well in excess of plant demand (Galloway et al. 2003, Dobermann and Cassman 2005, Vitousek et al. 2009). As a result, only 10% of N added to land for food production (including mineral fertilizers, animal waste, urea-based fertilizers, and biological N fixation (BNF)) ends up in the food itself. The remaining excess N is moved through the environment, creating a 'cascade' of environmental degradation as the multiple forms of N make it possible for each molecule to negatively impact a variety of systems along multiple pathways (Galloway et al. 2003).

Table 1.1 **Global sources and sinks of reactive N, with estimated sizes of fluxes in Tg N y^{-1} for present day (~1995- ~2005) (anthropogenic) and pre-industrial times (natural baseline). While in the pre-industrial era BNF was the primary pathway for available N creation (~89% of available N creation per annum), today BNF accounts for only ~46% of total N inputs to land. Nitrogen turnover in the terrestrial sphere has been further accelerated by increases in livestock production (Galloway et al. 2003), with livestock excreta accounting for as much as 24% of the excess N entering the environment in some catchments (e.g., Green et al. 2004). Synthetic N fertilisers account for the majority of new N entering the environment and ~20% of N total inputs on an annual basis (Erisman et al. 2008, Gruber and Galloway 2008). Tabulated inputs and outputs in the figure and table are based on data from Galloway et al. (2003), Gruber and Galloway (2008), Naqvi et al. (2008), and Schlesinger (2009). Error estimates are on the order of ±30%.**

		Anthropogenic *Tg N y^{-1}*	**Natural baseline** *Tg N y^{-1}*
Inputs			
Land	Industrial N_2 fixation	125	-
	BNF	35	110
	Atmospheric deposition	105	40
Oceans	BNF	-	140
	Atmospheric deposition	40	10
Total		*280*	*300*
Outputs (attenuation)			
Land	Denitrification	108	19
Rivers		50	30
Oceans		-	244
Total		*158*	*293*

Nitrogen transport through the environment occurs in gaseous and dissolved forms: N enters surface and ground water predominantly in the highly mobile form of nitrate (NO_3^-), where it can alter the ecosystem biogeochemical balance, before eventually flowing into marine environments, potentially creating anoxic zones and toxic algal blooms that degrade fish stocks (Galloway et al. 2003, Green et al. 2004, Bernal et al. 2012). At present ~40% of the estuaries in North America are now classified as eutrophic, and regions within the Gulf of Mexico and Baltic Sea are considered 'dead' due to seasonal anoxia (complete loss of oxygen (O_2)) driven by excess nutrient loading (Seitzinger 2008). Nitrate can also enter groundwater systems contaminating key freshwater resources (as discussed by Gruber and Galloway (2008) and references therein). Atmospheric N transfers come from the volatilisation of livestock excreta into gaseous ammonia (NH_3) as well as fossil fuel combustion (Table 1.1). These gases can be transported long distances, causing acidification and over-fertilization of 'downwind' areas (Bouwman et al. 1997, Law 2013). In order to mitigate the, "… severe damage to the environmental services at local, regional, and global scales..." (Galloway et al. 2008) caused by excess reactive N loading, improved fertilization techniques must be implemented and primary N loss pathways controlled (Ju et al. 2009).

Denitrification, the microbial process that completes the N cycling by reducing reactive N back to inert N_2, is the primary pathway through which reactive N is permanently removed from the

environment: it is hypothesized that the ~25% discrepancy between N inputs to freshwater and N exported to coastal environments is due almost entirely to denitrification – driven attenuation during transport. Yet the proportion of N inputs exported from land to the sea can vary dramatically between catchments from 0 to 80% (Howarth et al. 1996, Howarth et al. 2012) due to a complex array of proximal and distal controls on the rate and occurrence of denitrification (summarised in Fig. 1.1). The complexity of the N cycle and difficulties inherent in accurately quantifying denitrification have limited our ability to fully 'close the gap' on global sources and sinks of N. The ~50 Tg N y^{-1} unaccounted for globally (Schlesinger 2009), make creating and implementing effective management strategies difficult (Bernal et al. 2012).

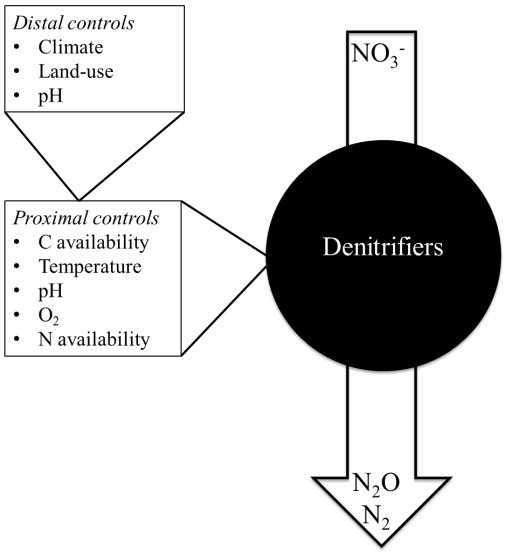

Figure 1.1 **The immediate (proximal) controls on denitrification (conversion of NO_3^- to N_2O and N_2) by microbes, fungi, and archaea, as well as the factors affecting denitrifier community composition (distal). (Modified from Wallenstein et al. (2006))**

Building on the growing use of the stable isotopes of N and oxygen (O) to identify N processes and sources, I hypothesise that NO_3^- dual isotopes can be used to construct an 'attenuation index'. While multiple stable isotopes of N and O occur naturally, their relative abundances are determined by local biological and chemical processes. The fractionation of NO_3^- isotopes during denitrification can be clearly related to changes in net concentration at the theoretical level using a Rayleigh model of kinetic fractionation (Eq. 1.1).

(1.1)
$$\frac{R}{R_0} = \left(\frac{C}{C_0}\right)^{1/(\alpha denit - 1)}$$

where the relationship between the change in the ratio of heavy to light isotopes (R/R_0) for a given change in substrate concentration (C/C_0) is defined by the reaction's fractionation factor (α). The degree of discrimination within the reaction for light isotopes can potentially be used to quantify net

NO_3^- removal rates from a given system based on measured changes in its isotopic composition over time and/or distance (Eq. 1.2) (Ostrom et al. 2002).

(1.2) $$Attenuation = 1 - e^{(R - R_0)/\alpha denit}$$

However, the implementation of such a stable-isotope based index for NO_3^- attenuation to natural systems has been severely limited by uncertainty in establishing precise fractionation factors for denitrification. By untangling N and O fractionation dynamics across scales and denitrifying zones, this research addresses these limitations and broadens the scope of use for NO_3^- isotopes to be viable indicators of catchment and field scale N attenuation.

1.1 Research objectives and thesis structure

In order to achieve the broad objective of quantitatively linked to the magnitude of attenuation/ denitrification NO_3^- isotopic composition across landscapes and scales, this thesis explores two fundamental questions,

1. What controls the magnitude (and variations in magnitude) of the relationship between NO_3^- concentration and isotopic composition (ε_{denit})?

2. When, where, and how should this relationship be used to quantify denitrification?

These questions are answered through a combination of literature analysis, mathematical modelling, mesocosm to whole-field scale manipulative experiments, and empirical measurements of rivers over length and time. The first chapter lays the foundation for the thesis through a meta-analysis of the literature, which re-integrates isotopic fractionation associated with NO_3^- production and reduction into the spatial-temporal gradient of denitrification across landscapes. The subsequent five chapters present findings from experimental work, each in the format of a prepared journal article. These five chapters move from diffusion-limited, microscale denitrification zones to N export measurements at the catchment scale (advection-transport dominated environments), the foundation of which will be laid out in Chapter 2. The relevant methodology and analytical methods (including equations) are presented independently in each of the five chapters, as are the chapter -specific acknowledgements, such that each section can be appreciated as a complete work. The final chapter synthesises the findings laid out in the previous sections and presents a template from which future work using NO_3^- stable isotopes in the natural environment can be based.

1.2 References

Bernal, S., L. O. Hedin, G. E. Likens, S. Gerber, and D. C. Buso. 2012. Complex response of the forest nitrogen cycle to climate change. Proceedings of the National Academy of Sciences of the United States of America **109**:3406-3411.

Bouwman, A. F., D. S. Lee, W. A. H. Asman, F. J. Dentener, K. W. VanderHoek, and J. G. J. Olivier. 1997. A global high-resolution emission inventory for ammonia. Global Biogeochemical Cycles **11**:561-587.

Dobermann, A. and K. G. Cassman. 2005. Cereal area and nitrogen use efficiency are drivers of future nitrogen fertilizer consumption. Science in China Series C-Life Sciences **48**:745-758.

Erisman, J. W., M. A. Sutton, J. Galloway, Z. Klimont, and W. Winiwarter. 2008. How a century of ammonia synthesis changed the world. Nature Geoscience **1**:636-639.

Galloway, J. N., A. R. Townsend, J. W. Erisman, M. Bekunda, Z. C. Cai, J. R. Freney, L. A. Martinelli, S. P. Seitzinger, and M. A. Sutton. 2008. Transformation of the nitrogen cycle: Recent trends, questions, and potential solutions. Science **320**:889-892.

Galloway, J. N., J. D. Aber, J. W. Erisman, S. P. Seitzinger, R. W. Howarth, E. B. Cowling, and B. J. Cosby. 2003. The nitrogen cascade. Bioscience **53**:341-356.

Green, P. A., C. J. Vorosmarty, M. Meybeck, J. N. Galloway, B. J. Peterson, and E. W. Boyer. 2004. Pre-industrial and contemporary fluxes of nitrogen through rivers: a global assessment based on typology. Biogeochemistry **68**:71-105.

Gruber, N. and J. N. Galloway. 2008. An Earth-system perspective of the global nitrogen cycle. Nature **451**:293-296.

Howarth, R., D. Swaney, G. Billen, J. Garnier, B. G. Hong, C. Humborg, P. Johnes, C. M. Morth, and R. Marino. 2012. Nitrogen fluxes from the landscape are controlled by net anthropogenic nitrogen inputs and by climate. Frontiers in Ecology and the Environment **10**:37-43.

Howarth, R. W., G. Billen, D. Swaney, A. Townsend, N. Jaworski, K. Lajtha, J. A. Downing, R. Elmgren, N. Caraco, T. Jordan, F. Berendse, J. Freney, V. Kudeyarov, P. Murdoch, and Z. L. Zhu. 1996. Regional nitrogen budgets and riverine N&P fluxes for the drainages to the North Atlantic Ocean: Natural and human influences. Biogeochemistry **35**:75-139.

Ju, X. T., G. X. Xing, X. P. Chen, S. L. Zhang, L. J. Zhang, X. J. Liu, Z. L. Cui, B. Yin, P. Christie, Z. L. Zhu, and F. S. Zhang. 2009. Reducing environmental risk by improving N management in intensive Chinese agricultural systems. Proceedings of the National Academy of Sciences of the United States of America **106**:3041-3046.

Law, B. 2013. BIOGEOCHEMISTRY Nitrogen deposition and forest carbon. Nature **496**:307-308.

Naqvi, S. W. A., M. Voss, and J. P. Montoya. 2008. Recent advances in the biogeochemistry of nitrogen in the ocean. Biogeosciences **5**:1033-1041.

Ostrom, N. E., L. O. Hedin, J. C. von Fischer, and G. P. Robertson. 2002. Nitrogen transformations and NO_3^- removal at a soil-stream interface: A stable isotope approach. Ecological Applications **12**:1027-1043.

Schlesinger, W. H. 2009. On the fate of anthropogenic nitrogen. Proceedings of the National Academy of Sciences of the United States of America **106**:203-208.

Seitzinger, S. 2008. Nitrogen cycle - Out of reach. Nature **452**:162-163.

Vitousek, P. M., R. Naylor, T. Crews, M. B. David, L. E. Drinkwater, E. Holland, P. J. Johnes, J. Katzenberger, L. A. Martinelli, P. A. Matson, G. Nziguheba, D. Ojima, C. A. Palm, G. P. Robertson, P. A. Sanchez, A. R. Townsend, and F. S. Zhang. 2009. Nutrient imbalances in agricultural development. Science **324**:1519-1520.

Wallenstein, M. D., D. D. Myrold, M. Firestone, and M. Voytek. 2006. Environmental controls on denitrifying communities and denitrification rates: Insights from molecular methods. Ecological Applications **16**:2143-2152.

Chapter 2

Expression of denitrification's intrinsic biochemical isotope fractionation measured in nitrate across terrestrial, freshwater, and marine environments: a synthesis

Sections of this chapter will be submitted for publication. Wells, N.S., T.J. Clough, S.E. Johnson-Beebout, W.T. Baisden. In prep. Environmental expression of denitrification's intrinsic biochemical isotope fractionation measured in nitrate: do 'site specific' enrichment factors exist? Biogeochemistry (Synthesis and Emerging Ideas)

2.1 Abstract

Variations in the natural isotopic abundance of nitrate ($\delta^{15}N$ and $\delta^{18}O$ of NO_3^-) have been proposed as a means of integrating the spatial-temporal variability of denitrification in order to accurately and precisely quantify NO_3^- attenuation across landscapes. This technique is based on the knowledge that denitrifiers kinetically discriminate against 'heavy' forms of both nitrogen and oxygen, creating a parallel enrichment in the isotopes of both species that can be quantitatively related to NO_3^- attenuation using isotopic enrichment factors (ε_{denit}). Yet application of this method is currently limited by the fact that, despite the >160 ε_{denit} values reported since the 1960s, the controls on its variations at both at the biochemical level and in the natural environment (e.g., at the catchment scale) are not understood. Systematic differences also exist in how NO_3^- isotope dynamics vary with denitrification activity between microbial culture, marine, and freshwater studies. By collating all published ε_{denit} values, I found that the distance and mode of NO_3^- transport to the denitrifying zone controlled the magnitude of ε_{denit} for both $\delta^{15}N$ and $\delta^{18}O$, enabling the construction of a global-scale framework of isotope effects. Contrary to expectations, there was no universal relationship between denitrification rates and fractionation strength. This synthesis provides key information for directing on-going efforts to use NO_3^- dual isotopes to identify sources and sinks, and highlights critical gaps in the understanding of nitrogen isotope cycling.

Keywords: denitrification, stable isotopes, nitrogen cascade, $\delta^{15}N$- $\delta^{18}O$- NO_3^-

Introduction

Although the productivity of agricultural systems often depend on nitrogen (N) additions, only 10% of the ~376 Tg N y^{-1} added to land for food production is consumed, posing a significant threat to environmental sustainability (Gruber and Galloway 2008, Schlesinger 2009). Excess N migrates through the environment (primarily as nitrate (NO_3^-)), creating a cascade of environmental degradation, including eutrophication of waterways and the production of the greenhouse gas nitrous oxide (N_2O), as its transported from land to the sea (Galloway et al. 2003). However, difficulty in determining NO_3^- sources and sinks across scales, especially for denitrification (heterotrophic reduction of NO_3^- to N_2O and dinitrogen (N_2)), the only permanent N removal pathway of global-scale significance (Groffman et al. 2009), means that ~50 Tg N y^{-1} are currently unaccounted globally (Schlesinger 2009).

Denitrification attenuates reactive N (converts it back to inert N_2) under anaerobic conditions, given available carbon (C) as an energy source. It is hypothesized that denitrification accounts for ~75% of N inputs to freshwater that don't reach the sea (Galloway et al. 2003). Yet the percentage of N inputs exported ranges from 0 to 80% between catchments, presumably reflecting divergent denitrification rates during transit (Howarth et al. 1996, Howarth et al. 2012). The rate and magnitude of denitrification are dependent on an array of physical and chemical conditions, both at the micro scale (defining the immediate environment of the microbes) and the biome scale (regulating development of denitrifying communities) (Wallenstein et al. 2006). However, the unreliable estimations of N attenuation caused by its variability can create a dramatic misrepresentation of N inputs (Boyer et al. 2002, Bernal et al. 2012). Without an understanding of when, where, and to what extent N attenuation occurs, assessments of the quantity of N entering and leaving a given system are inherently flawed, and N management schemes severely limited.

The isotopic composition of NO_3^- ($^{15}N/^{14}N$ and/or $^{18}O/^{16}O$, reported in δ values in ‰ with respect to international standards) has been identified as a potentially precise and accurate means of measuring denitrification rates in-situ. Nitrate isotopes are viable indicators of both the sources and sinks of reactive N as, while they exist in finite amounts (globally 99.6337‰ of N is ^{14}N and 0.3663‰ is ^{15}N (Junk and Svec 1958); and 99.759‰ of O is ^{16}O, 0.037‰ ^{17}O, and 0.024‰ ^{18}O (Cook and Lauer 1968)), biogeochemical processing distributes them unequally across landscapes (Fig. 2.1). This is caused by kinetic fractionation (α) as, in a given reaction, heavy isotopes will have a slower reaction rate (k_2) than light isotopes (k_1) (Eq. 2.1) (Kendall and Caldwell 1998).

(2.1) $$\alpha_k = k_1 / k_2$$

For example, atmospherically produced NO_3^- (from Haber-Bosch fertilisers or deposition) can be distinguished from microbially-cycled NO_3^- by its distinct $\delta^{18}O$ (~ +40‰) and $\delta^{15}N$ (~0‰) composition. However, once atmospherically derived N is microbially transformed its isotope

signature is modified and becomes indistinguishable from the typical 'soil-N' range (Fig. 2.1) (Curtis et al. 2011).

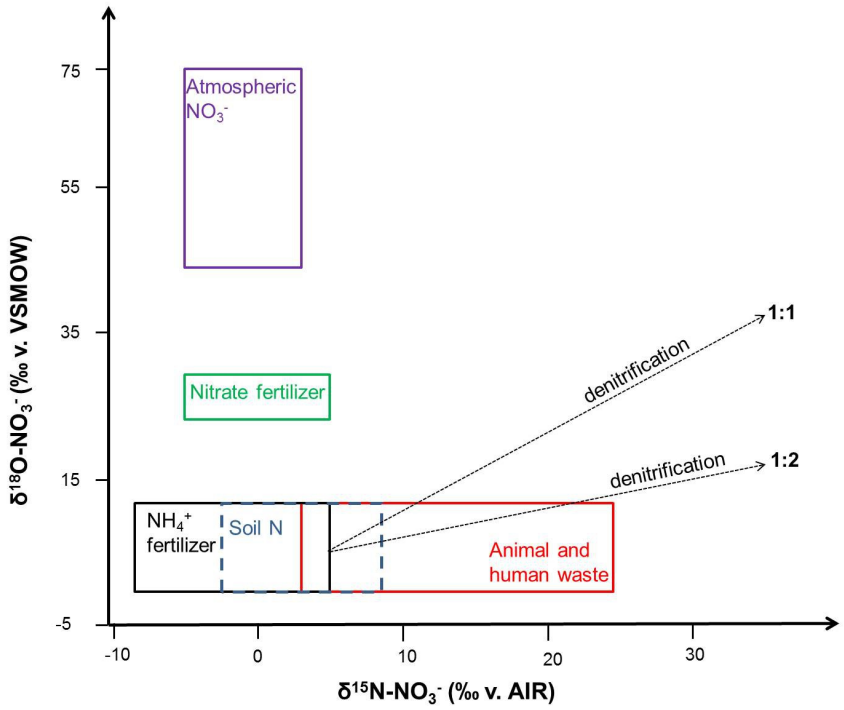

Figure 2.1 **Isotopic composition of global NO_3^- pools, plotted as $\delta^{18}O$- versus $\delta^{15}N$ (ranges from Xue et al. (2009), Nestler et al. (2011), and Kendall (1998)), where denitrification (dashed lines) causes parallel enrichment at a 1:2 (Kendall 1998) or 1:1 (Sigman et al. 2001, Granger et al. 2008) ratio.**

Recent methodological advances by Silva et al. (2000), Sigman et al. (2001), and McIlvin & Altabet (2005) increased the measurement precision of $\delta^{15}N$- $\delta^{18}O$- NO_3^- analyses and reduced sample volume requirements and preparation time, catalysing a dramatic increase in the use of NO_3^- dual isotopes (Fig. 2.2).

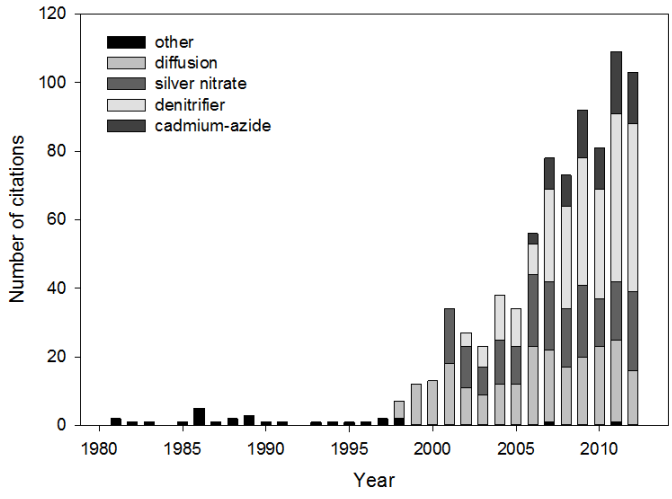

Figure 2.2 **Publications using the natural abundance isotopic composition of NO_3^- (either $\delta^{15}N\text{-}NO_3^-$, or both $\delta^{15}N$- and $\delta^{18}O$- NO_3^-) by year, as of Jan-2013. Numbers are approximations of total research papers published per year based on citations on ISI Web of Science of Sigman et al. (1997) (adaptation of diffusion method to natural abundance level precision), Silva et al. (2000) (silver nitrate method, which allowed dual isotope measurement), Sigman et al. (2001) (denitrifier method for simultaneous dual isotope measurements), and McIlvin and Altabet (2005) (cadmium-azide chemical method for simultaneous dual isotope measurements), plus anecdotal accounting of publications prior to these methods.**

The abundance of NO_3^- isotope data must now be considered within the theoretical framework of its sources and sinks across landscapes: three recent reviews focused on the growing use of NO_3^- isotope signatures to apportion N source contributions, a key issue for freshwater quality monitoring (Xue et al. 2009, Curtis et al. 2011, Nestler et al. 2011). These reviews described the clear 'added value' of incorporating NO_3^- isotopic measurements into groundwater and surface water monitoring schemes (Widory et al. 2013), but concluded that poor understanding of the factors controlling kinetic fractionation of NO_3^- isotopes, particularly during attenuation, create fundamental uncertainties in source apportionments. In contrast, marine scientists have focused on using NO_3^- isotopes to identify and quantify N transformations (Altabet et al. 1999, Sigman et al. 2009). However, lack of communication between the two research communities has created systematic differences in the handling of isotope kinetics.

Acknowledging that the use of NO_3^- isotopes as integrators of N cycling (and thus the ability to distinguish N sources in complex environments) is limited by poor understanding of the controls on isotopic fractionation during denitrification, the objective of this review is to create a cross-disciplinary framework for the isotope effects of denitrification. This framework is established by synthesising information from 129 publications that measured the impact of denitrification on $\delta^{15}N$-NO_3^- and/or $\delta^{18}O$-NO_3^- composition. The review is divided into two sections: part one evaluates denitrifier- driven fractionation (at the biochemical level and as expressed in the environment) based on factors that control the occurrence and rate of denitrification, and part two develops a global framework that relates variations in the degree of fractionation to environmental conditions and contexts.

2.2 Fractionation of NO_3^- isotopes

During denitrification the residual NO_3^- pool is fractionated as it is reduced to NO_2^-, causing progressive and parallel enrichment of the residual both N and O in the residual NO_3^- pool (Fig. 2.1). From the Rayleigh equation (Eq. 2.2):

$$\frac{R}{R_0} = \left(\frac{C}{C_0}\right)^{1/(\alpha denit - 1)} \tag{2.2}$$

the isotope abundance in the residual (or product) pool (R) relative to the original pool (R_0) can be quantitatively related to the corresponding change in substrate concentration (C/C_0), assuming that the degree of isotopic discrimination (α_{denit}) remains constant, and the product pool is continuously removed (as described in Kendall and Caldwell (1998)). As the reaction progresses, the residual substrate becomes increasingly enriched in heavy isotopes until its concentration reaches zero, at which point the isotopic composition of the product is equivalent to that of the initial substrate (Fig. 2.3a). The modified Rayleigh equations (written in delta notation) by Mariotti et al. (1981) provide the

most convenient method of relating the isotopic composition of $\delta^{15}N\text{-}NO_3^-$ and $\delta^{18}O\text{-}NO_3^-$ to the changing size of the NO_3^- pool during denitrification (Eq. 2.3).

$$\delta^{15}N_x = \delta^{15}N_0 + \varepsilon_{denit} \times \ln\left(\frac{f}{1-f}\right)$$

$$\delta^{18}O_x = \delta^{18}O_0 + \varepsilon_{denit} \times \ln\left(\frac{f}{1-f}\right) \quad (2.3)$$

The enrichment factor for denitrification ($\varepsilon_{denit} \approx (\alpha_{denit}\text{-}1)\times 1000$)) is used to calculate the fraction of the substrate pool remaining ($f = C_x/C_0$) based on the corresponding changes in its isotope composition ($\delta_x - \delta_0$). Accordingly, the more negative the value of ε_{denit}, the greater the magnitude of fractionation, and the closer ε_{denit} is to 0 the lower its effect (Fig. 2.3b). The relative strength of ε_{denit} for N ($^{15}\varepsilon_{denit}$) and O ($^{18}\varepsilon_{denit}$) ranges from 0.5 to 1.0, meaning $\delta^{18}O\text{-}NO_3^-$ and $\delta^{15}N\text{-}NO_3^-$ become enriched in parallel during denitrification (Fig. 2.1).

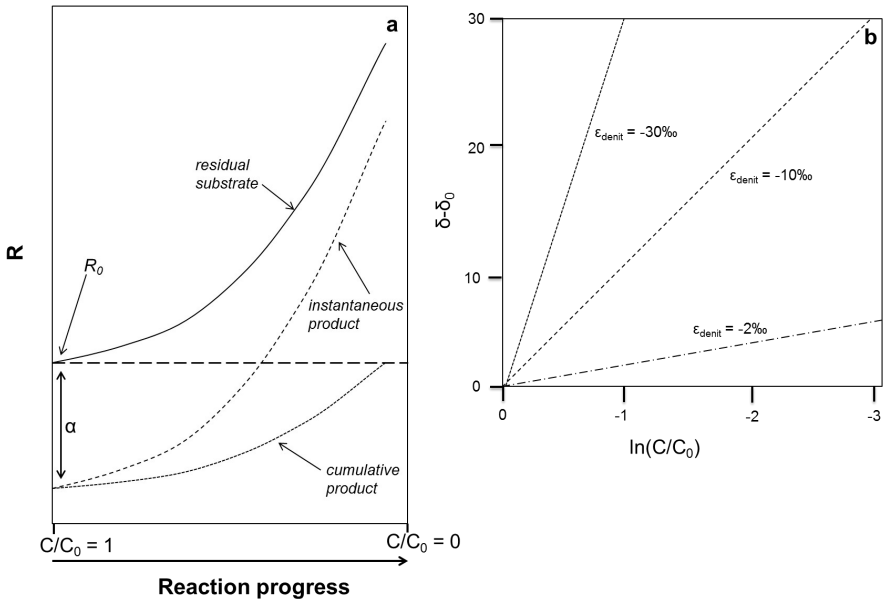

Figure 2.3 **Rayleigh fractionation of NO_3^- during denitrification, where the isotope ratio of the residual substrate (R, solid lines) becomes increasingly 'heavy' as the reaction progresses (i.e., concentration of substrate remaining (C) relative to the initial substrate concentration (C_0) approaches nil) and the isotopic composition of the cumulative product approaches the initial composition of the substrate (R_0) (reproduced with permission from Hogberg** (1997)) **(a); as per the modified Rayleigh equation of Mariotti et al.** (1981), the **changes in the isotopic composition (either $\delta^{18}O\text{-}NO_3^-$ or $\delta^{15}N\text{-}NO_3^-$) plotted versus the natural log of the proportion of substrate remaining ($\ln(C/C_0)$) define ε_{denit} (b).**

Given that δ_0 and C_0 are known (see Fig. 2.4 for summary of the processes affecting δ_0), increasingly 'heavy' NO_3^- as substrate concentration declines over time and/or distance indicates that these losses are caused by denitrification, as per Eq. 2.2. This relationship has been used to distinguish N lost to denitrification v. non-attenuating loss processes (e.g., dilution, plant uptake) in estuaries (Wankel et al. 2006), open oceans (Lehmann et al. 2007), aquifers (Aravena and Robertson 1998), riparian zones (Cey et al. 1999), lakes (Lehmann et al. 2003), and streams (Barnes et al. 2008, Pellerin

et al. 2009). Failure to find a relationship between NO_3^- concentration and $\delta^{15}N\text{-}NO_3^-$ has been used to rule out the presence of significant denitrification (Wassenaar 1995, Feast et al. 1998, Savard et al. 2007).

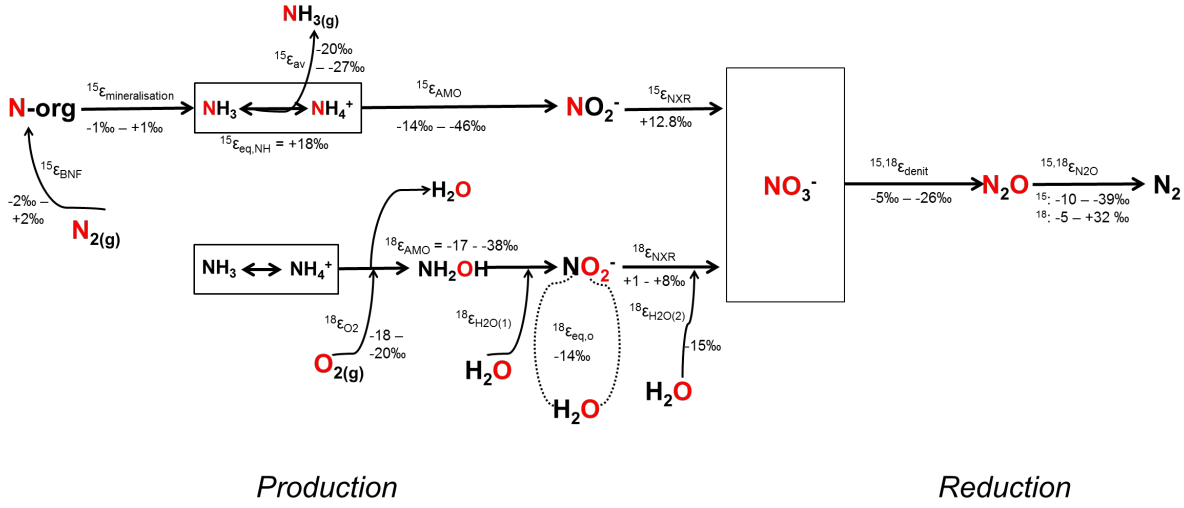

Figure 2.4 **Schematic representation of isotope effects during production (nitrification) and reduction (denitrification) of NO_3^-. During nitrification O from O_2 (atmospheric $\delta^{18}O\text{-}O_2$ = ~23.5‰ (Kroopnick and Craig 1972) (ε_{O2}) (Bender 1990) is incorporated during oxidation of NH_3 to hydroxylamine (NH_2OH) and then O from H_2O during subsequent oxidation of NH_2OH to NO_2^- (Andersson and Hooper 1983, Kumar et al. 1983). During ammonia oxidation O undergoes kinetic fractionation ($^{18}\varepsilon_{AMO}$) (Casciotti et al. 2010). Once formed, NO_2^- and the adjacent H_2O can exchange O atoms, with an associated equilibrium isotope effect ($\varepsilon_{aq,o}$) (Casciotti and McIlvin 2007). Incorporation of the second O from H_2O is also a fractionating process ($\varepsilon_{H2O(2)}$) (Buchwald and Casciotti 2010), and the oxidation step from NO_2^- to NO_3^- (ε_{NXR}) causes inverse kinetic fractionation (Buchwald and Casciotti 2010). The $\delta^{15}N$ of organic N is determined by mycorrhizal interactions and BNF ($\delta^{15}N\text{-}N_2$ = 0‰, fractionation (ε_{BNF}) = ~0 (Brandes and Devol 2002). This pool is then mineralised into NH_4^+ with negligible fractionation ($\varepsilon_{mineralisation}$) (Kendall 1998). Ammonia (NH_3) is in equilibrium with NH_4^+ in aqueous solution and the isotope balance between these two pools is dictated by an equilibrium isotope effect ($\varepsilon_{eq,NH}$)), but this pool can also be affected by kinetic fractionation from physical volatilisation of NH_3 to its gaseous form (ε_{av}). The isotope effect during oxidation to NO_2^- (ε_{AMO}) creates a 'lighter' product pool (Mariotti et al. 1981, Shearer and Kohl 1988, Casciotti et al. 2003). The final step, oxidation to NO_3^-, is thought to incur an inverse isotope effect on N (ε_{NXR}) (i.e., the $\delta^{15}N\text{-}NO_3^-$ produced from incomplete NO_2^- oxidation would be 'heavier' than that of the reactant) (Casciotti 2009). During denitrification, O and N of residual NO_3^- pool are enriched in parallel during reduction to N_2O ($^{15,18}\varepsilon_{denit}$) (Granger et al. 2008). During subsequent reduction of N_2O to N_2 the residual N will become more positive and the O more negative ($^{15,18}\varepsilon_{N2O}$) (Toyoda et al. 2005). Two intermediate steps of denitrification (NO_2^- to NO) are not shown here as they are environmentally unstable, not rate limiting steps of the process (Zumft 1997), and little is known about their impact on isotope composition (Bryan et al. 1983). (Negative ε values indicate preferential use of light isotopes, meaning the produced pool will be lighter than the residual)**

As $\delta^{18}O\text{-}NO_3^-$ measurements become routine, a linear relationship between variations in $\delta^{15}N\text{-}NO_3^-$ and $\delta^{18}O\text{-}NO_3^-$ can also be used to fingerprint denitrification (Fig. 2.1). This relationship was used to identify hot-spots of denitrification in, e.g., the hydrologically complex Changijiang River (China) (Li et al. 2010), the Platte River aquifer (USA) (Bohlke et al. 2007), and upwelling groundwater in Italy (Petitta et al. 2009). These examples highlight the potential to use NO_3^- isotopes to *identify* denitrification, but to convert these established relationships between NO_3^- concentrations and isotopic composition to quantitative attenuation rates requires a functional understanding of $^{15}\varepsilon_{denit}$ and $^{18}\varepsilon_{denit}$.

Since the first published $^{15}\varepsilon_{denit}$ value of -20‰ was measured for denitrification by a single-strain culture (Wellman et al. 1968), environmental inconsistencies in ε_{denit} have emerged. Variations are reported at both the cellular (e.g., Blackmer and Bremner 1977) and field level (e.g., Cline and Kaplan 1975), as well as in the relative strengths of $^{15}\varepsilon_{denit}$ v. $^{18}\varepsilon_{denit}$ (Casciotti et al. 2002, Lehmann et al. 2003, Burns et al. 2009). In the subsequent sections current knowledge of both the biochemical fractionation created by denitrifying microbes under controlled conditions ('intrinsic' fractionation) and the isotope effects associated with denitrification observed under field conditions ('effective' fractionation) are assessed in relationship to denitrification rates (k_{denit}). Data was collected from 124 studies, providing 65 original values for intrinsic ε_{denit} and 129 original values for effective ε_{denit} (see Appendix A for values and search details).

2.2.1 Biochemically-driven isotope fractionation (intrinsic)

Intrinsic ε_{denit} is imparted at the molecular level during the unidirectional enzymatic reduction of NO_3^- to NO_2^- (Granger et al. 2008), with strain-specific differences emerging from the relative rates of NO_3^- efflux v. uptake prior to bond breakage (Bryan et al. 1983, Shearer and Kohl 1988, Kritee et al. 2012). The 10 studies that measured ε_{denit} for pure microbial strains (total of 11 different strains) show that, even under ideal denitrifying conditions (non-limiting C, anaerobic, warm), intrinsic $^{15}\varepsilon_{denit}$ can vary from -5‰ to -31‰ (Fig. 2.5). Despite the range of analytical techniques and incubation set-ups used in the reviewed studies, intra-strain variation was lower than inter-strain ($p<0.05$) (e.g., Barford et al. (1999), Granger et al. (2008), and Kritee et al. (2012) all reported ε_{denit} values for *Paracoccus denitrificans* from -24‰ to -31‰ with a ~1:1 ratio between $\delta^{18}O$ and $\delta^{15}N$). However, new evidence from pure culture studies has revealed that the degree of preference for light isotopes by a given strain is also affected by the environmental factors, particularly oxygen concentration ($[O_2]$) and C. Specifically, Kritee et al. (2012) found that the magnitude of fractionation by three different denitrifier strains decreased in response to increasing environmental stress (e.g., variations in $[O_2]$ and C), concluding that the higher NO_3^- efflux across the cell wall led to 'complete' expression of the strain-specific fractionation by NO_3^- reductase enzymes outside of the cell under optimal conditions.

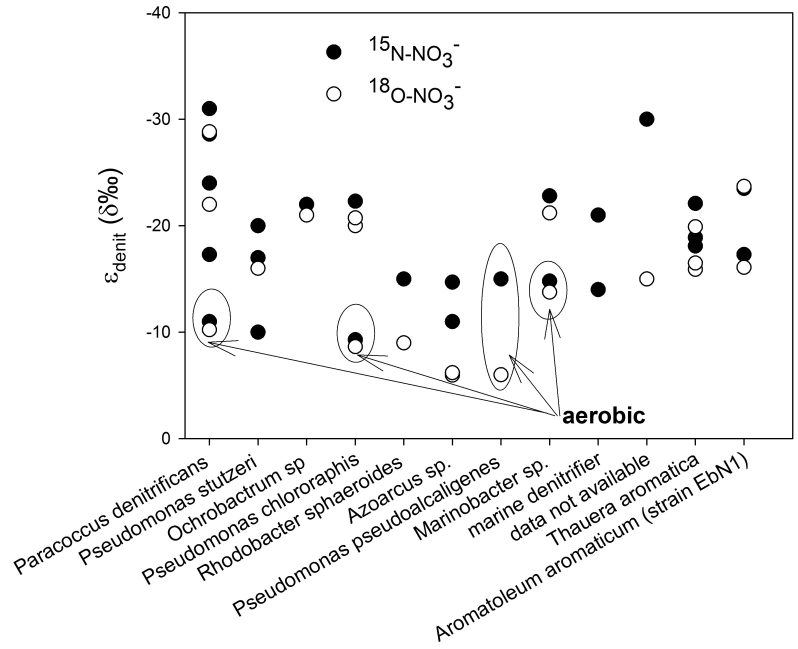

Figure 2.5 **Reported isotopic enrichment factors (ε_{denit}) for ^{15}N and ^{18}O of NO_3^- during denitrification by pure cultures of different bacteria ($^{15}\varepsilon_{denit}$: n = 69; $^{18}\varepsilon_{denit}$: n = 23) (see Appendix A for complete details and references). All culture were maintained under anaerobic ($[O_2]$<4 mg l^{-1}) conditions during the experiments unless otherwise indicated**

Aquatic denitrification typically occurs when dissolved $[O_2]$ is <4 mg l^{-1}, at which point NO_3^- becomes an energetically viable electron donor and denitrifying enzymes are activated (Rivett et al. 2008). However, this limitation on denitrification is not always obvious, as microscale variations in O_2 availability mean that denitrification can go forward in anaerobic microsites within systems classified as too oxic for the process to occur (e.g., Muller et al. 2004) and some denitrifier strains are also facultatively aerobic (Wallenstein et al. 2006). Surveying the published ε_{denit} values from pure culture studies revealed that aerobically produced ε_{denit} is routinely smaller than anaerobically produced ε_{denit} (Fig. 2.5), although the ratio of $^{18}\varepsilon_{denit}$ to $^{15}\varepsilon_{denit}$ is not affected. Kritee et al. (2012) hypothesised that the down regulation of NO_3^- availability caused by $[O_2]$ ≥4 mg l^{-1} decreases the magnitude of isotopic discrimination by denitrifiers. Denitrification in anaerobic versus aerobic conditions may cause a ~10‰ shift in ε_{denit}, representing roughly one third of the variation reported between strains (~30‰) (Fig. 2.5). More studies are needed to test the hypothesis that $[O_2]$ impacts the fundamental efflux of NO_3^- isotopes across cell walls (Appendix A)).

Denitrification rates (k_{denit}) are stoichiometrically limited by either NO_3^- or C availability, and tend to increase with rising temperatures. Contradicting the findings that environmental stress decreases ε_{denit} expression, kinetic isotope fractionation often decreases in magnitude as reaction rates increase (e.g., during reduction of N_2O to N_2 (Vieten et al. 2007), reduction of NO_2^- to N_2O (Bryan et al. 1983), and oxidation of NH_3 (Yun et al. 2011)). The first studies to test the relationship between k_{denit} and ε_{denit} concluded that increasing k_{denit} decreased the magnitude of ε_{denit} based on measurements

following manipulations in temperatures and C supply in anaerobically incubated soils (Mariotti et al. 1981, Mariotti et al. 1982). More recent studies of aquifer sediments amended with varying rates of C and N confirmed the inverse relationship between ε_{denit} and k_{denit} (Bates and Spalding 1998, Korom et al. 2012) This association could reveal a physical-chemical, rather than biological, control over isotope fractionation, as increasing temperatures (energy) decrease the strength of discrimination in, for instance, precipitation of H_2O (Bullen and Kendall 1998).

However, further in-vitro studies reveal that the relationship between k_{denit} and ε_{denit} cannot be fully explained by simple reaction kinetics. Some of this complexity comes from differences in C quality (i.e., energy required to access C), an increasingly recognised regulator of k_{denit} (Barnes et al. 2012). Two recent culture studies found that ε_{denit} strength decreased as the complexity of the available C increased. Wunderlich et al. (2012) measured a 4-6‰ decrease in the magnitude of ε_{denit} when complex (toluene), rather than simple (acetate), C was added to cultures; and Kritee et al. (2012) measured a ~3‰ decrease in ε_{denit} for three different denitrifier strains when the C source was shifted from acetate to casein. Yet the response to changing C quality and k_{denit} and ε_{denit} is not consistent across denitrifier strains and/or studies: Knoller et al. (2011) observed no change in ε_{denit} when changing C sources induced a six-fold increase in k_{denit}, while Granger et al. (2008) and Wunderlich et al. (2012) found that changing the C quality drove strong shifts in ε_{denit} but not k_{denit}. Over 50% of the ε_{denit} values reported for C-amended systems (n = 41) were generated using simple, readily biologically available C forms (acetate, ethanol, and glucose), but show no consistency in ε_{denit} with respect to either C availability or form. Carbon availability may be the key driver of k_{denit} (Taylor and Townsend 2010), but there is currently no conclusive evidence showing that it exerts similar control over the degree of isotopic discrimination during denitrification.

2.2.2 Relating intrinsic fractionation to field measurements

While intra-strain consistency of ε_{denit} supports the hypothesis that intrinsic ε_{denit} for a given location is defined by the local denitrifier population, field-scale implications of this finding cannot be fully understood until the distribution and function of microbial communities are better understood (e.g., Standing et al. 2007). Yet despite strong evidence for 'strain specific' ε_{denit} values, the mean $^{15}\varepsilon_{denit}$ reported for anaerobic incubations of C and N amended soils and sediments (presumably containing diverse denitrifier populations) were indistinguishable from those of pure-culture studies, with a mean ±SD $^{15}\varepsilon_{denit}$ of -17.5 ±8‰ (Table 2.1). Nor did a precise relationship between $^{18}\varepsilon_{denit}$ and $^{15}\varepsilon_{denit}$ emerge from this data set: while the majority of culture studies report consistent 1:1 ratios of $\delta^{18}O$:$\delta^{15}N$ (Granger et al. 2008, Kritee et al. 2012, Wunderlich et al. 2012), some denitrifiers seem to produce 1:2 fractionation ratios regardless of environmental conditions (Knoller et al. 2011) (Table 2.1). However, the finding that both freshwater and marine denitrifiers can become enriched according to a 1:1 ratio during denitrification, and that $[O_2]$ do not alter this relationship, provides compelling evidence that the differences in the ratio cited in freshwater (~1:2) v. marine (~1:1) studies is unlikely to be driven by population differences.

Culture studies have established that, 1) ε_{denit} can vary strongly between denitrifier strains, and, 2) the expression of ε_{denit} can be environmentally regulated. Overall, in-vitro studies have found $[O_2]$ to be the most consistent and powerful regulator intrinsic ε_{denit}. However, the interaction between these factors at the field level is unresolved, and variations in $^{18}\varepsilon_{denit}$ v. $^{15}\varepsilon_{denit}$ ratios unexplained.

Table 2.1 **Means (±SD) of comparable parameters reported in studies of isotopic fractionation during denitrification conducted under controlled/ laboratory conditions (intrinsic) (*n* = 59) versus empirical field measurements (effective) (*n* = 128). Temperature refers to laboratory temperature, reported water temperature for groundwater and marine systems, or mean annual air temperature for above-ground field studies; proportion anaerobic is the ratio of ε_{denit} measurements made under anaerobic conditions versus under aerobic conditions. Significant difference is based on 1-way ANOVA.**

	Controlled conditions *Intrinsic*	Field measurements *Effective*
Temperature (ºC)	20.4 ±8***	12.3 ±6
Proportion anaerobic	0.940***	0.705
$^{15}\varepsilon_{denit}$ (‰)	-17.8 ±10**	-12.2 ±10
$^{18}\varepsilon_{denit}$ (‰)	-14.0 ±6*	-8.16 ±7
$\delta^{18}O$:$\delta^{15}N$	0.802 ±0.2	0.711 ±0.2

***Significantly greater (at significance of $p<0.001$)
**Significantly greater (at significance of $p<0.001$)
*Significantly greater (at significance of $p<0.001$)

2.2.3 Isotope effects of denitrification at the field-scale (effective fractionation)

Corroborating the finding of Kritee et al. (2012) that sub-optimal denitrifying conditions decreases discrimination against heavy isotopes, the mean ε_{denit} obtained from field measurements were ~5‰ lower (for both $^{15}\varepsilon_{denit}$ and $^{18}\varepsilon_{denit}$) than those collected under relatively stress-free laboratory conditions (Table 2.1). The difference between 'laboratory' and 'field' datasets is particularly remarkable given the wide range of conditions (time scales, geographic locations, hydrology, spatial scales, analytical methods, etc.) under which these ε_{denit} values were determined (Fig. 2.6). However, the mean $^{18}\varepsilon_{denit}$:$^{15}\varepsilon_{denit}$ ratio of 0.71 ±0.2 did not differ from culture and mesocosms experiments, to empirical measurements in rivers, lakes, groundwater, and oceans (Table 2.1).

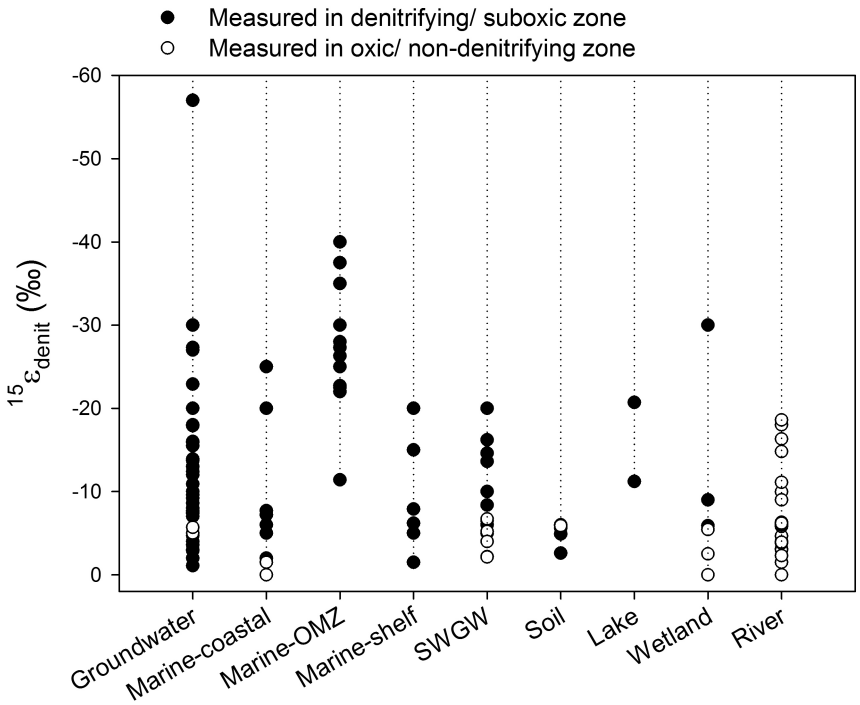

Figure 2.6 **Reported $^{15}\varepsilon_{denit}$ values from 129 empirical field measurements of NO_3^- isotopic fractionation during denitrification (representing 95 published journal articles). Unfilled circles indicate $^{15}\varepsilon_{denit}$ values based on measurements outside of the presumed denitrifying zone (e.g., oxic surface water in a river) and filled circles indicate $^{15}\varepsilon_{denit}$ values calculated based on measurements within the denitrifying zone (e.g., anoxic marine sediments). (See Appendix A for values and references.)**

Comparisons of field v. laboratory measurements must consider the possibility that the isotope effects observed in the field may not be entirely the result of denitrification. Evidence for relevant N transformations via anaerobic oxidation of ammonium (NH_4^+) (anammox), nitrifier-denitrification, co-denitrification, dissimilatory reduction of NO_3^- to NH_4^+ (DNRA), and abiotic NO_3^- removal has been found in a variety of environments (Burgin and Hamilton 2007, Thamdrup 2012) (Table 2.2). However, the paucity of information on when, where, and to what extent these processes occur, combined with a lack of direct isotope fractionation measurements (Table 2.2), makes assessing the impact of these processes on NO_3^- isotopic composition impossible. Furthermore, hypothesising isotope effects for anammox, nitrifier-denitrification, and co-denitrification is not straightforward as all three use NO_2^-, rather than NO_3^-, as an electron acceptor, meaning any effect on the NO_3^- pool would be integrated into the multiple fractionation factors associated with NO_2^- oxidation (as summarised in Fig. 2.4).

Table 2.2 **Summary of alternative NO_3^- loss processes in terms of the organisms responsible for their occurrence, their reactants and products (with the species whose fractionation is relevant to NO_3^- isotopic composition in bold), in what environments they've been found to occur, and their associated enrichment factors for N, and for O relative to N (question marks indicate data not available). Footnotes are used to list selected references.**

Organism	*Process*	*Reaction*		*Occurrence*	*N isotope effects*	*$\delta^{18}O$ v. $\delta^{15}N$*
Anammox bacteria[8]	***Anammox***	$NH_4^+ + \mathbf{NO_2^-} \rightarrow N_2 + 2H_2O$	*permanent DIN removal*	Anaerobic environments: marine,[1,2] freshwater sediments,[3] wetlands,[4] paddy soils,[5] groundwater[25]	? (may enrich residual $\delta^{15}N$-NH_4^+)[25]	?
Denitrifiers, or abiotic (?)[6]	***Co-denitrification***	$\mathbf{NO_2^-}$ → $NO_3^- \rightarrow N_2O \rightarrow N_2$; N_2 or N_2O; amino-N		Soil[6,7]	?	?
Nitrifiers[9]	***Nitrifier-denitrification***	$NH_3 \rightarrow NH_2OH \rightarrow \mathbf{NO_2^-} \rightarrow N_2O \rightarrow N_2$		Soil[10]	?	?
n/a	***Abiotic denitrification***	$\mathbf{NO_3^-} \rightarrow NO_2^- \rightarrow N_2O \rightarrow N_2$; Fe^{2+}		Anaerobic, with Fe(II) available: soil,[11] groundwater, and freshwater sediments[12]	-6.8 – -32‰[13, 14, 15]	0.36-0.86[15]
Denitrifiers with the nrf gene[16]	***DNRA***	$\mathbf{NO_3^-} \rightarrow NO_2^- \rightarrow NH_4^+$	*DIN recycling*	Anaerobic: coastal marine sediments,[17] soil,[18,19] freshwater sediments[20,21]	?	? (may suppress N fractionation relative to O)[22]
Eukaryotes and prokaryotes	***Assimilation***	$\mathbf{NO_3^-} \rightarrow NO_2^- \rightarrow$ N-org		Ubiquitous under aerobic conditions	0 to -4‰[23, 24, 22]	1.0[23,24]

[1](Lam et al. 2009), [2](Dalsgaard et al. 2012), [3](Zhu et al. 2013), [4](Erler et al. 2008), [5](Zhu et al. 2011), [6](Spott and Stange 2011), [7](Spott et al. 2011), [8](Thamdrup 2012), [9](Wrage et al. 2001), [10](Kool et al. 2010), [11](Matocha et al. 2012), [12](Sun et al. 2009), [13](Torrento et al. 2010), [14](Torrento et al. 2011), [15](Wankel, unpubl.), [16](An and Gardner 2002), [17](Gardner and McCarthy 2009), [18](Inselsbacher et al. 2010), [19](Rutting et al. 2011), [20](Nizzoli et al. 2010), [21](Revsbech et al. 2006), [22](Dhondt et al. 2003), [23](Granger et al. 2004), [24](Karsh et al. 2012) [25](Clark et al. 2008)

Biological assimilation of NO_3^- has also been suggested as a potentially interference when linking isotopic composition to denitrification fluxes in the field (e.g., Karsh et al. 2012). As assimilated N is eventually broken back down to NH_4^+ (ammonified), re-entering the inorganic N pool, distinguishing between assimilation and denitrification (which permanently removes reactive N from the biosphere) is necessary to accurately trace N flows (Galloway et al. 2003). Laboratory studies show that assimilation produces low levels of fractionation of the residual NO_3^- pool (ε of between 0 and -4‰) at a 1:1 ratio of $\delta^{18}O$:$\delta^{15}N$ enrichment (Table 2.2). On this basis, a shift in the $\delta^{18}O$:$\delta^{15}N$ ratio from 1:1 to 1:2 is frequently used as evidence for a shift from assimilation (1:1) to denitrification (1:2) of NO_3^- (Battaglin et al. 2001, Cohen et al. 2012). However, as the biochemical basis for denitrifiers to fractionate $\delta^{18}O$ and $\delta^{15}N$ at ratios from 1:1 to 1:2 is now clearly established, there is no scientific basis for using $\delta^{18}O$:$\delta^{15}N$ enrichment ratios as evidence for or against the occurrence of assimilation. Moreover, the fact that assimilation is not a permanent NO_3^- removal pathway (Galloway et al. 2003) must also be considered in terms of how the fractionation it creates would be expressed in the environment, if at all. Essentially, because assimilation and mineralisation, with variable fractionation

factors (Robinson et al. 1998) (Table 2.2), occur continuously and simultaneously, with rates dependent on season, species, etc., and could affect both NH_4^+ and NO_3^- pools (Kaye and Hart 1997, Waser et al. 1998), the 'net isotope effect' of assimilation on the NO_3^- pool of a given environment should be even lower than the intrinsic ε values found under ideal conditions (i.e., approaching 0‰).

Given both the consistency of the fingerprint $\delta^{18}O$:$\delta^{15}N$ fractionation ratio between laboratory and field studies and the lack of information on 'novel' NO_3^- removal pathways and their isotope effects, it is prudent to continue assessing NO_3^- dual isotopes in terms of a nitrification - denitrification continuum. Additionally, the hypothesis that $\delta^{15}N$ at the global scale reflects the degree of denitrification (Houlton and Bai 2009, Bai et al. 2012) illustrates the minor net effect of fractionation during assimilation versus during denitrification. Assuming that denitrification is the primary N removal pathway, the variation in ε_{denit} observed at the field scale could result from: 1) O_2 availability, 2) denitrifier community structure, and/or 3) the environmental variables regulating the availability of NO_3^- to denitrifiers.

Looking first at $[O_2]$, the most consistent controller of intrinsic NO_3^- isotope fractionation, the reviewed literature yielded relatively low ε_{denit} values for aerobic waters (particularly rivers) (mean of -7.2‰ for all reported field values, (p<0.01)). At the other end of the spectrum, ε_{denit} measured in marine oxygen minimum zones (OMZs) were consistently larger (-24‰ p<0.01) than the mean (Fig. 2.6). The consistency of low ε_{denit} values in aerobic conditions make it plausible that some of the systemic differences in the magnitude of ε_{denit} between freshwater and marine environments is created by O_2 down-regulating NO_3^- availability, and thus dampening the biochemical preference for light isotopes (Kritee et al. 2012). However, the fact that 1:2 ratios of $\delta^{18}O$:$\delta^{15}N$ fractionation were more frequently reported in aerobic freshwater environments (e.g., Burns et al. 2009) than in relatively low $[O_2]$ marine and groundwater systems cannot be explained by such a biochemical change, as in-vitro studies unanimously found $^{18}\varepsilon_{denit}$ and $^{15}\varepsilon_{denit}$ to be equally impacted by increasing $[O_2]$.

Despite strong evidence for ε_{denit} differing between denitrifier strains, the possibility that strain-specific ε_{denit} could combine to create unique 'community effects' for a given location has not been studied. Currently there is only indirect evidence: Chien et al. (1977) found that field cultivation history (now known to influence denitrifier community composition (Lo 2010, Tang et al. 2010)) caused a 10‰ difference in $^{15}\varepsilon_{denit}$ in saturated, non-C limited, soil cores; and Korom et al. (2005, 2012) measured a 13‰ difference in $^{15}\varepsilon_{denit}$ between two hydrologically similar aquifers in different parts of the United States. While similar responses in denitrification rates to N loading have been observed across biomes (Mulholland et al. 2008), the narrow climate range in which ε_{denit} values have been measured (~60% from temperate agricultural regions) means that the possible interactions resulting from varying microbial populations and k_{denit} on effective fractionation have not been fully explored. Measurements of ε_{denit} from 'extreme' climate locations, from a tropical Thai river (~27°C) (Miyajima et al. 2009) to a Mongolian wetland (~ -2.5°C) (Itoh et al. 2011) did not deviate from the

mean for field studies (Table 2.1). However, given the bias of the dataset, evidence against a biogeographic effect on denitrifier dynamics is not conclusive (Hall et al. 2011).

Local climate could also have a more direct (and measurable) impact on denitrification and ε_{denit}, as increasing temperature can increase k_{denit}, potentially decreasing ε_{denit}, as discussed previously. There is anecdotal evidence for this effect in the collated ε_{denit} dataset from field studies: larger fractionation of NO_3^--N in the Northern Pacific (Altabet et al. 1999, Lehmann et al. 2007) relative to in the Arabian Sea (Naqvi et al. 1998, Naqvi et al. 2006) was attributed to the warmer waters (and thus faster N turnover rates) at the latter location. However, such a temperature effect was not consistent between, or even within, studies. For instance, seasonal, temperature-driven, variations in k_{denit} coupled with constant ε_{denit} were found in a major river in China (Chen et al. 2009) and karst springs in Florida (Cohen et al. 2012). Moreover, the relatively cooler temperatures generally found in field studies versus lab studies does not translate into increased ε_{denit} magnitude (Table 2.1).

The role of C and N loading in driving k_{denit} (Seitzinger et al. 2006, Trimmer et al. 2012) could also contribute to observed differences in effective ε_{denit}. However, field-based evidence showing substrate (C and/or N) concentration effects on k_{denit} and ε_{denit} is contradictory. Relatively low $^{15}\varepsilon_{denit}$ values (-4‰ to -9‰) measured in aquifers by Mariotti et al. (1988), Smith et al. (1991), and Spalding et al. (1993) were attributed to fast k_{denit} induced by high N and C loading. Conversely, Singleton et al. (2007) hypothesised that extremely large fractionation ($^{15}\varepsilon_{denit}$ = -57‰) in an effluent contaminated aquifer was due to high N and C loading (and thus k_{denit}), while Vogel et al. (1981) ascribed large $^{15}\varepsilon_{denit}$ (-30‰) in a DOC-depleted aquifer below the Kalahari Desert to 'very slow' denitrification. Unfortunately, comparisons of isotope dynamics between nutrient-loaded and nutrient-limited regions are limited by the fact that the vast majority of stable isotope -based denitrification studies are undertaken in highly impacted systems (e.g., agricultural lands) (Appendix A).

The experimental finding that poor C quality can decrease ε_{denit} is also observed in field measurements. For instance, the magnitude of $^{15}\varepsilon_{denit}$, as well as k_{denit}, increased following labile C additions in multiple groundwater sites with and without C additions (Tsushima et al. 2002, Kellman and Hillaire-Marcel 2003, Kellman 2004, Tsushima et al. 2006). However, a biochemical response to changing C quality cannot fully explain the difference from ~ -4‰ to ~ -30‰ found for $^{15}\varepsilon_{denit}$ by Kellman and colleagues versus by Tsushima and colleagues.

Although differences in k_{denit} are often used to explain inter-site differences in effective ε_{denit}, there is little empirical evidence to support this argument, lending credence to recent laboratory studies demonstrating the complexity of this relationship (Kritee et al. 2012). These discrepancies over the role of C and k_{denit} in controlling the measured isotope effects for denitrification tie back to the many unknowns in how C regulates N cycling (Trimmer et al. 2012), highlighting the need for a more holistic approach to understanding the field-scale controls on ε_{denit} before NO_3^- isotopes can become an effective tool for disentangling N sources and sinks. Indeed, given the complexity of factors that can

impact ε_{denit}, it seems unlikely that a single environmental factor will be found to explain all of the variation in denitrification's isotopic fingerprint.

2.3 A global framework for assessing ε_{denit} dynamics

Given these poorly understood variations reported in ε_{denit} across scales, many studies opt to use literature-reported, rather than site-specific, ε_{denit} values as a basis for isotope-based attenuation calculations. For instance, Panno et al. (2006) used values of -15.9‰ and -8‰ for $^{15}\varepsilon_{denit}$ and $^{18}\varepsilon_{denit}$, respectively, to calculate that NO_3^- attenuation in the upper Mississippi River varied from 0-55% between sampling dates, and Bartoli et al. (2012) used a $^{15}\varepsilon_{denit}$ value of -20‰ to calculate that 20% of catchment's NO_3^- was attenuated within riparian and hyporheic zones. However, there is no environmental or biological rationale to select these ε_{denit} values. In the previous examples, Panno et al. (2006) used the ε_{denit} value found by Bottcher et al. (1990) for denitrification in an unconfined aquifer, and Bartoli et al. (2012) used the ε_{denit} range generated by Mariotti et al. (1981) for anaerobic soils and early culture experiments as reviewed by Kendall (1998). To increase the accuracy and precision of NO_3^- stable isotope -based assessments of denitrification, I propose a unifying framework for selecting an appropriate site-specific range of $^{18}\varepsilon_{denit}$ and $^{15}\varepsilon_{denit}$ based on the global denitrification model of Seitzinger et al. (2006) (Fig. 2.7).

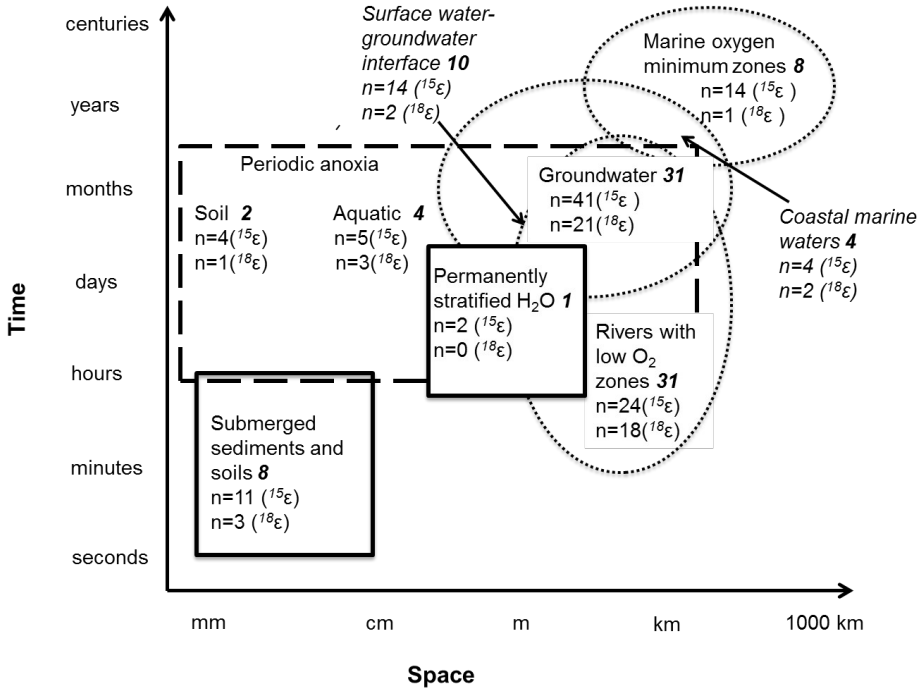

Figure 2.7 **The spatial-temporal distribution of enrichment factors (ε_{denit}) for $\delta^{15}N\text{-}NO_3^-$ and/or $\delta^{18}O\text{-}NO_3^-$ during denitrification based on 112 published empirical field measurements (from 79 publications). The number of unique ε_{denit} measurements per environment are indicated as *n* =x and the number of publications that generated these numbers is in bold. Environments are grouped as per Seitzinger et al. (2006), wherein 'space' and 'time' as indicators of the distance between NO_3^- production (nitrification) and consumption (denitrification) and the means of transport is defined as either diffusion-limited (rectangles with solid lines), temporally-limited (rectangles with dashed lines), or advective (ovals). (See Appendix A for details).**

The different zones of denitrification are delineated according to, 1) whether NO_3^- was transported to the denitrification zone by diffusion (passive) or advection (active), and, 2) the distance between the source and sinks of NO_3^- (i.e., distance between nitrification (or deposition) zone and denitrification zone). Accordingly, the values of ε_{denit} reported from field studies were categorised as being from environments where denitrification was limited by diffusion (A), periodic suboxia (B), or advection (C), and then binned based on the estimated distance and time between NO_3^- production and reduction (Fig. 2.7). Distances from the source to the denitrification zone were classified as either: (1) mm to cm, (2) cm to m, (3) m to km, or (4) km to 100 km, and estimated based on reported sources of NO_3^-, catchment size, and size of the denitrifying/ anaerobic area. Time of transport was defined as, (1) seconds to minutes, (2) minutes to hours, (3) hours to months, or, (4) months to centuries. Distance and time were estimated from reported flow rates, residence times, and/or catchment size. As this spatial-temporal framework hinges on the role of diffusion and the degree of coupling between nitrification-denitrification in controlling denitrification, integrating NO_3^- isotope data into this is validated by evaluating the reported effects of, 1) transport mode (diffusive v. advective), and, 2) mixing (fractionation during nitrification with that of denitrification, different sources) on $\delta^{15}N\text{-}NO_3^-$ and $\delta^{18}O\text{-}NO_3^-$.

2.3.1 Transportation

Diffusion is the primary mode of NO_3^- transport between aerobic flowing water, where measurements are typically taken, and the denitrifying zones in the anaerobic sediments (Lehmann et al. 2003, Sebilo et al. 2003). Solutes can be fractionated during diffusion as light isotopes are moved more easily than heavy isotopes (Abe and Hunkeler 2006, Aeppli et al. 2009). Direct evidence of diffusion impacting $\delta^{15}N\text{-}NO_3^-$, and decreasing the expression of ε_{denit}, was found by Tsushima et al. (2006), who established a direct relationship between the balance of advective v. diffusive transport and the magnitude of ε_{denit} in aquifer sediments. Accordingly, the effect of diffusion on NO_3^- moving from highly reducing marine sediments to the water column has been used to explain the discrepancy between the heavy (~ +30‰) $\delta^{15}N\text{-}NO_3^-$ measured within anaerobic sediments v. light $\delta^{15}N\text{-}NO_3^-$ (~ +5‰) found in the water column, leading to an estimation of ε_{denit} for marine sediments of ~0‰ (Brandes and Devol 1997, Lehmann et al. 2005, Sigman et al. 2009).

Across the reviewed literature, ε_{denit} values from aerobic environments (i.e., outside of the denitrifying zone) were lower (-5.64 ±5‰ (n = 38) for $^{15}\varepsilon_{denit}$ and -5.51 ±6‰ for $^{18}\varepsilon_{denit}$ (n = 23)) relative to anaerobic environments (i.e., within the denitrifying zone) (-14.9 ±10‰ for $^{15}\varepsilon_{denit}$ (n = 91) and -9.97 ±7‰ for $^{18}\varepsilon_{denit}$) (p<0.001 and p<0.05, respectively) (Fig. 2.6). The few studies of NO_3^- isotopes performed in aerobic soils also found consistently low ε_{denit} values (Fig. 2.6), confirming a diffusive limitation on the expression of intrinsic ε_{denit} (Kawanishi et al. 1993, 1996). However, it should be emphasised that diffusion limits the expression of intrinsic ε_{denit}, but should not negate any site-specificity of isotope dynamics (e.g., Ruehl et al. 2007).

2.3.2 Mixing

Distortion of fractionation factors and isotopic source signatures (R_0) by process mixing is well recognised in the literature (Xue et al. 2009, Nestler et al. 2011), with Green et al. (2010) noting that, ‘‘physical mixing tends to create the appearance of lower reaction rates and fractionation parameters when measured at larger scales and longer flow paths.’’ For instance, Schmidt et al. (2012) found that heterogeneous mixing of different sources within a shallow aquifer broke the relationship between NO_3^- attenuation and $\delta^{15}N\text{-}NO_3^-$. The ambiguity created by co-occurring N transformation pathways is exemplified by the finding of Farrell et al. (1996) that only 60% of the variation in $\delta^{15}N\text{-}NO_3^-$ leached from arid soils was explained by decreasing NO_3^- concentrations (i.e., denitrification was not the only process influencing NO_3^- concentration and/or $\delta^{15}N\text{-}NO_3^-$).

Coupling between nitrification and denitrification is recognised as the limiting factor for denitrification, as denitrification in anaerobic zones cannot progress until aerobically produced NO_3^- is transported to them (Seitzinger et al. 2006). The spatial and temporal separation between NO_3^- production and reduction, ranging from μm to 100 kms and from seconds to centuries (Fig. 2.7), can also modify the isotope effects associated with denitrification. Nitrification of NH_3 to NO_2^- and NO_3^- creates a $\delta^{15}N\text{-}NO_3^-$ pool significantly lighter than that of the original organic-N, unless the entire NH_3 pool is nitrified, although, again, the degree of fractionation incurred during the reaction is known to vary at the cellular and field scale (Casciotti et al. 2003, Yun et al. 2011).

When there is a strong spatial and/or temporal separation between nitrification and denitrification, as might be expected in the surface water of large rivers where the majority of denitrification occurs in hyporheic and riparian zones (e.g., Zarnetske et al. 2012), the NO_3^- isotopic composition is influenced by fractionation from both of the reactions. This effect is illustrated using a simple two-pool mixing dynamics (Kendall 1998) (Eq. 2.4):

$$R_{net} = \frac{R_{nit} \times C_{nit} + R_{denit} \times C_{denit}}{C_{net}} \tag{2.4}$$

where the isotopic composition of the measured NO_3^- pool (R_{net}) is calculated based on the composition of the nitrified NO_3^- (R_{nit}) and that of the residual denitrified pool (R_{denit}), weighted by their respective NO_3^- concentrations (C_{nit} v. C_{denit}) relative to the total (C_{net}).

At the other end of the spectrum, when nitrification and denitrification are co-occurring (as may happen within soil microsites or across steep redox gradients), the apparent isotope effect for denitrification (both N and O) is further convoluted since NO_3^- removal by denitrifiers (C_0 - C_{denit}) is obscured by production of NO_3^- by nitrifiers (C_{nit}), regardless of the fractionation associated with nitrification (Eq. 2.5):

(2.5)
$$\frac{R_{net}}{R_0} = \left(\frac{C_{net}}{C_0}\right)^{1/(\alpha denit - 1)}$$

where R_{net} and C_{net} are defined as Eq. 2.6:

(2.6)
$$R_{net} = \frac{R_{nit} \times C_{nit} + R_{denit} \times C_{denit}}{C_{net}}$$

$$C_{net} = C_{nit} + C_{denit}$$

This set of equations shows that coupling of these processes can cause $^{15}\varepsilon_{denit}$ to increase relative to $^{18}\varepsilon_{denit}$, as $\delta^{15}N\text{-}NO_3^-$ is dependent on the flux of both nitrification and denitrification, whereas $\delta^{18}O\text{-}NO_3^-$ from nitrification will have a roughly constant composition (Fig. 2.4). This relationship could explain previously discussed differences reported for fractionation during attenuation in OMZs (spatially and temporally distant from nitrified source) versus aerobic soils and surface waters (nitrification separated by mm or seconds from denitrification).

The mixing of N-fractionating processes led Barnes and Raymond (2010) to hypothesise that $\delta^{18}O\text{-}NO_3^-$ is a more accurate indicator of N cycling than $\delta^{15}N\text{-}NO_3^-$(Barnes and Raymond 2010). However, Eq. 2.4 – 2.6 emphasise that mixing of nitrification and denitrification can mask the relationship between isotopes and substrate concentration that would be clear if only one process was at play. Understanding N transformations, and their associated effects on $\delta^{15}N$ and $\delta^{18}O$, is thus a fundamental prerequisite for understanding the relationship between denitrification rates (k_{denit}) (as they control substrate availability (Seitzinger et al. 2006)) and NO_3^- isotopic signature prior to denitrification (R_0).

2.3.3 Framework outcomes

Distribution of the reviewed ε_{denit} values into a spatial-temporal framework for denitrification as proposed by Seitzinger et al. (2006) (Fig. 2.7) reveals distinct trends in ε_{denit} (Fig. 2.8). I therefore propose that the wide range of ε_{denit} values expressed within and across landscapes can be explained by the distance between sources and sinks, once the dominant transport mechanism is identified.

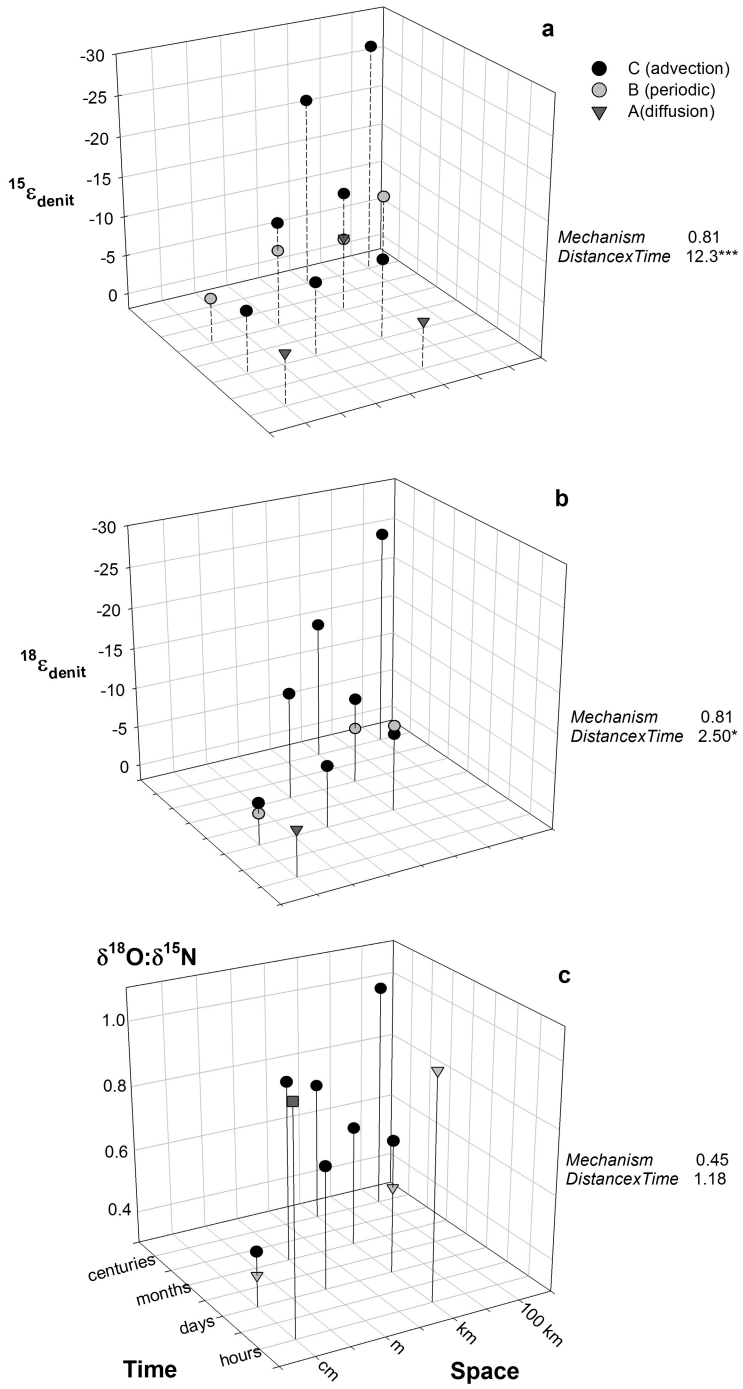

Figure 2.8 **The spatial-temporal distribution of published enrichment factors based on empirical field measurements for, (a) N ($^{15}\varepsilon_{denit}$), and, (b) O ($^{18}\varepsilon_{denit}$) isotopes of NO_3^- during denitrification ('effective fractionation'), as well as the relative ratio of $\delta^{18}O\text{-}NO_3^-$ to $\delta^{15}N\text{-}NO_3^-$ (c). Values are grouped by transportation mechanism: diffusion across an O_2 gradient (A), temporal separation based on periodic anoxia (B), or advective transport from distal sources through a consumption zone (C). The 'x' and 'y' axes plot space versus time for transportation of NO_3^- from production (nitrification) to consumption (denitrification), as per Seitzinger et al. (2006), and the means of transport is defined as either diffusion-limited (rectangles, solid lines), temporally-limited (rectangles, dashed lines), or advective (ovals). Statistical data on right are F values from 2-way ANOVA, where significance is indicated as *(p<0.05), **(p<0.01, and ***(p<0.001). (See Appendix A for values and references)**

(A) Diffusion – From the reviewed literature, denitrification within diffusion-limited denitrification zones was calculated to have a mean ±SD $^{15}\varepsilon_{denit}$ of -4.82 ±4‰, (lower (p<0.05) than measured in advection-limited zones) with no variation over transport distance. These results assist in explaining the findings of Ruehl et al. (2007) that $^{18}\varepsilon_{denit}$ and $^{15}\varepsilon_{denit}$ increased up to -20‰ in a California stream under high discharge rates (i.e., advective movement of water into the stream) and then decreased to between -1.6 and -9‰ under baseflow (diffusion-limited transport of NO_3^- from the sediments to the surface water), accompanied by a shift in $\delta^{18}O$:$\delta^{15}N$ ratios from 1:1 (high flow) to 1:2 (baseflow). However, a more detailed understanding of the spatial-temporal variation is limited by the fact that there are currently only nine published studies that have measured ε_{denit} in zones defined by diffusive transport of NO_3^-. Of these, only two involved transport distances at a scale greater than mm-sec (e.g., Alkhatib et al. (2012) measured denitrification of sinking particulate N in Gulf of Lawrence sediments). More rigorous examination of the fractionation effect of diffusion on NO_3^-, both in and out of denitrifying zones, is needed in order to better constrain effective ε_{denit} values for submerged sediments and soil microsites, especially as the only attempt to measure diffusive fractionation under abiotic conditions found no effect (Semaoune et al. 2012).

(B) Periodic suboxia – There is still very little information about isotope fractionation in environments with strong temporal separation between sources and sinks of NO_3^- (n =6) (Fig. 2.7). Available data for locations with periodic denitrification indicates that ε_{denit} is larger than at a similar space×time ranking in advection-dominated zones (C), although, due to the small sample size, these differences were not significant (Fig. 2.8). The distance and/or time between suboxic periods could regulate the magnitude of ε_{denit}. For instance, Sigman et al. (2003) measured an effective $^{15}\varepsilon_{denit}$ of -5‰ in the waters of the seasonally-hypoxic Santa Barbara Basin, significantly lower than their calculated intrinsic $^{15}\varepsilon_{denit}$ of -20‰. There is also evidence to indicate that using NO_3^- dual isotopes to calculate N fluxes during and following acute events (e.g., seasonal shifts in $[O_2]$ of coastal waters or flooding dried soils) is particularly effective due to, 1) the known δ_0 (i.e., nitrification completed prior to denitrification commenced), and, 2) the clear relationship between NO_3^- isotopes and composition while denitrification is dominating the N pool (e.g., Wells et al. 2013). I hypothesize that periodic NO_3^- sinks will have isotope effects similar to the intrinsic ε_{denit} for the local denitrifying populations, as diffusion should not influence $\delta^{15}N$- $\delta^{18}O$- NO_3^- and the distance/ time between nitrification and denitrification would minimise convolution of these two processes. This contrasts with diffusion-limited systems, where transport dampens and homogenises isotope effects.

(C) Advection – Denitrification zones dominated by advective solute transport can be treated as 'pipes': NO_3^- produced in a given zone is transported to a denitrifying zone and is gradually consumed as it passes through (i.e., Eq. 2.2). This scenario also describes laboratory incubation type studies, where NO_3^- is produced distally and then added in totality to an anaerobic system. The strong positive

correlation found between measured ε_{denit} and estimated travel distances (Fig. 2.8) indicates that the 'suppression' of intrinsic ε_{denit} values reported in shallow groundwater (Mariotti et al. 1988, Heffernan et al. 2012), hyporheic zones (Devito et al. 2000, Kellman and Hillaire-Marcel 2003), and rivers (Ruehl et al. 2007, Osaka et al. 2010, Wexler et al. 2011) could be a product of tightly coupled nitrification and denitrification, whereas increasing distance of advective transport between source and sink allow high magnitude intrinsic ε_{denit} values to be more fully expressed.

Moreover, different degrees of mixing between nitrification and denitrification within advection-dominated denitrification zones could explain the assigning of $\delta^{18}O$:$\delta^{15}N$ fractionation ratios of 1:1 for deepwater marine environments and 1:2 for shallow freshwater and soil environments. I found that reported $\delta^{18}O$:$\delta^{15}N$ ratios decreased with decreasing distance between source and sink, from a mean of 1 within OMZs to ~ 0.6 at metre scale transport distances (Fig. 2.8c). Similar shifts in $\delta^{18}O$:$\delta^{15}N$ ratios were used by Wankel et al. (2009) to constrain the importance of nitrification within California's Elkhorn Slough. However, potentially due to the paucity of $^{18}\varepsilon_{denit}$ data, this trend was not significant.

2.4 Key outcomes

The clear spatio-temporal distribution of ε_{denit} values across landscapes reveals the importance of 'macro-scale' variables in determining the effective magnitude of fractionation during denitrification at the field scale. These trends through doubt on the relevant of variations in intrinsic fractionation to field studies, particularly given our presently limited understanding of the role of microbial community structure and function. Thus I suggest that more research focus on constraining interactions between environmental factors (particularly hydrology) and ε_{denit}.

2.4.1 Future considerations

Oxygen strongly influences both intrinsic and effective fractionation (the latter a product of diffusive fractionation), and the consistent decreases in $^{18}\varepsilon_{denit}$ and $^{15}\varepsilon_{denit}$ caused by changing $[O_2]$ constrain a narrow range of relatively low enrichment factors relevant for aerobic environments. The lack of consistency in the relationship between the rate and fractionation strength of denitrification (k_{denit} and ε_{denit}) across the reviewed literature is an important consideration when interpreting new NO_3^- isotopic datasets. This finding emphasises the importance of the hydrologic environment, rather than biochemistry, in determining the expressed isotope effect. Yet within this variability ε_{denit} could be aligned to the spatial-temporal framework underpinning denitrification, confirming the validity of relationship between $\delta^{15}N$-NO_3^-, $\delta^{18}O$- NO_3^-, and NO_3^- attenuation across scale and disciplines. In this context, several key research gaps emerged:

- There is a need to resolve discrepancies in $\delta^{18}O$-NO_3^- dynamics, particularly with regards to $\delta^{18}O$:$\delta^{15}N$ fractionation ratios.

- Intrinsic variations in ε_{denit} must to be reconciled with 'effective' field-scale variations. Are effective fractionation factors driven by microbial community structure and/or function? Answering this question also necessitates filling in some of the gaps in the environmental distribution of field studies, particularly with respect to getting data from low-N environments.
- Measurements are needed of the impact of NO_3^- diffusion into and out of denitrifying zones on the expression of ε_{denit}, particularly in dynamic environments such as streams, where the distance and degree of diffusive transportation can vary widely over distance and time (Christensen et al. 1990).
- Field studies designed to disentangle nitrification and denitrification, enabling quantification of how their interactions impact measured $^{18}\varepsilon_{denit}$ and $^{15}\varepsilon_{denit}$, are required.

Building on the spatial-temporal framework developed through this review in order to address these identified knowledge gaps, the subsequent five chapters present original findings on NO_3^- isotope dynamics during denitrification from across the identified denitrification zones,

- Micro-scale experiments and modelling of diffusive versus intrinsic fractionation in soils and sediments (Chapter 3);
- Meso-scale measurements of the impact of mixing N-fractionating processes on NO_3^- isotopes under diffusion and spatial limitations on denitrification in pasture soils (Chapter 4);
- Field-scale empirical measurements of NO_3^- isotope dynamics in submerged (diffusion-limited) and wetting-drying (period-limited) paddy soils (Chapter 5);
- Nitrate removal and fractionation in a river as it transitioned from advection-limited to diffusion-limited denitrification (Chapter 6); and
- Catchment-scale NO_3^- removal with seasonal and climate driven variation in advection versus diffusion limitations on denitrification (Chapter 7).

2.5 Acknowledgements

Thanks to my co-authors, Tim Clough and Troy Baisden, both of whom provided invaluable assistance in polishing this manuscript and brainstorming titles, and provided some spirited debate on the 'most correct' way to describe isotopic enrichment factors.

2.6 References

Abe, Y. and D. Hunkeler. 2006. Does the Rayleigh equation apply to evaluate field isotope data in contaminant hydrogeology? Environmental Science & Technology **40**:1588-1596.

Aeppli, C., M. Berg, O. A. Cirpka, C. Holliger, R. P. Schwarzenbach, and T. B. Hofstetter. 2009. Influence of mass-transfer limitations on carbon isotope fractionation during microbial dechlorination of trichloroethene. Environmental Science & Technology **43**:8813-8820.

Alkhatib, M., M. F. Lehmann, and P. A. del Giorgio. 2012. The nitrogen isotope effect of benthic remineralization-nitrification-denitrification coupling in an estuarine environment. Biogeosciences **9**:1633-1646.

Altabet, M. A., C. Pilskaln, R. Thunell, C. Pride, D. Sigman, F. Chavez, and R. Francois. 1999. The nitrogen isotope biogeochemistry of sinking particles from the margin of the Eastern North Pacific. Deep-Sea Research Part I-Oceanographic Research Papers **46**:655-679.

An, S. M. and W. S. Gardner. 2002. Dissimilatory nitrate reduction to ammonium (DNRA) as a nitrogen link, versus denitrification as a sink in a shallow estuary (Laguna Madre/Baffin Bay, Texas). Marine Ecology-Progress Series **237**:41-50.

Andersson, K. K. and A. B. Hooper. 1983. O_2 and H_2O are each the source of one O in NO_2^- produced from NH_3 by nitrosomonas - N-15-NMR evidence. Febs Letters **164**:236-240.

Aravena, R. and W. D. Robertson. 1998. Use of multiple isotope tracers to evaluate denitrification in ground water: Study of nitrate from a large-flux septic system plume. Ground Water **36**:975-982.

Barford, C. C., J. P. Montoya, M. A. Altabet, and R. Mitchell. 1999. Steady-state nitrogen isotope effects of N_2 and N_2O production in Paracoccus denitrificans. Applied and Environmental Microbiology **65**:989-994.

Barnes, R. T. and P. A. Raymond. 2010. Land-use controls on sources and processing of nitrate in small watersheds: insights from dual isotopic analysis. Ecological Applications **20**:1961-1978.

Barnes, R. T., P. A. Raymond, and K. L. Casciotti. 2008. Dual isotope analyses indicate efficient processing of atmospheric nitrate by forested watersheds in the northeastern US. Biogeochemistry **90**:15-27.

Barnes, R. T., R. L. Smith, and G. R. Aiken. 2012. Linkages between denitrification and dissolved organic matter quality, Boulder Creek watershed, Colorado. Journal of Geophysical Research-Biogeosciences **117**.

Bartoli, M., E. Racchetti, C. A. Delconte, E. Sacchi, E. Soana, A. Laini, D. Longhi, and P. Viaroli. 2012. Nitrogen balance and fate in a heavily impacted watershed (Oglio River, Northern Italy): in quest of the missing sources and sinks. Biogeosciences **9**:361-373.

Bates, H. K. and R. F. Spalding. 1998. Aquifer denitrification as interpreted from in situ microcosm experiments. Journal of Environmental Quality **27**:174-182.

Battaglin, W. A., C. Kendall, C. C. Y. Chang, S. R. Silva, and D. H. Campbell. 2001. Chemical and isotopic evidence of nitrogen transformation in the Mississippi River, 1997-98. Hydrological Processes **15**:1285-1300.

Bai, E., B. Z. Houlton, and Y. P. Wang. 2012. Isotopic identification of nitrogen hotspots across natural terrestrial ecosystems. Biogeosciences **9**:3287-3304.

Bender, M. L. 1990. The $\delta^{18}O$ of dissolved O_2 in seawater - a unique tracer of circulation and respiration in the deep-sea. Journal of Geophysical Research-Oceans **95**:22243-22252.

Bernal, S., L. O. Hedin, G. E. Likens, S. Gerber, and D. C. Buso. 2012. Complex response of the forest nitrogen cycle to climate change. Proceedings of the National Academy of Sciences of the United States of America **109**:3406-3411.

Blackmer, A. M. and J. M. Bremner. 1977. Nitrogen isotope discrimination in denitrification of nitrate in soils. Soil Biology & Biochemistry **9**:73-77.

Bohlke, J. K., I. M. Verstraeten, and T. F. Kraemer. 2007. Effects of surface-water irrigation on sources, fluxes, and residence times of water, nitrate, and uranium in an alluvial aquifer. Applied Geochemistry **22**:152-174.

Bottcher, J., O. Strebel, S. Voerkelius, and H. L. Schmidt. 1990. Using isotope fractionation of nitrate nitrogen and nitrate oxygen for evaluation of microbial denitrification in a sandy aquifer. Journal of Hydrology **114**:413-424.

Boyer, E. W., C. L. Goodale, N. A. Jaworsk, and R. W. Howarth. 2002. Anthropogenic nitrogen sources and relationships to riverine nitrogen export in the northeastern USA. Biogeochemistry 57:137-169.

Brandes, J. A. and A. H. Devol. 1997. Isotopic fractionation of oxygen and nitrogen in coastal marine sediments. Geochimica Et Cosmochimica Acta **61**:1793-1801.

Brandes, J. A. and A. H. Devol. 2002. A global marine-fixed nitrogen isotopic budget: Implications for Holocene nitrogen cycling. Global Biogeochemical Cycles 16:14.

Bryan, B. A., G. Shearer, J. L. Skeeters, and D. H. Kohl. 1983. Variable expression of the nitrogen isotope effect associated with denitrification of nitrite. Journal of Biological Chemistry **258**:8613-8617.

Buchwald, C. and K. L. Casciotti. 2010. Oxygen isotopic fractionation and exchange during bacterial nitrite oxidation. Limnology and Oceanography **55**:1064-1074.

Bullen, T. D. and C. Kendall. 1998. Tracing of weathering reactions and water flowpaths:A multi-isotope approach. Pages 611-646 *in* C. Kendall and J. J. McDonnell, editors. Isotope Tracers in Catchment Hydrology Elsevier Science B.V., Amsterdam.

Burgin, A. J. and S. K. Hamilton. 2007. Have we overemphasized the role of denitrification in aquatic ecosystems? A review of nitrate removal pathways. Frontiers in Ecology and the Environment **5**:89-96.

Burns, D. A., E. W. Boyer, E. M. Elliott, and C. Kendall. 2009. Sources and transformations of nitrate from streams draining varying land uses: Evidence from dual isotope analysis. Journal of Environmental Quality **38**:1149-1159.

Casciotti, K. L. 2009. Inverse kinetic isotope fractionation during bacterial nitrite oxidation. Geochimica Et Cosmochimica Acta **73**:2061-2076.

Casciotti, K. L., M. McIlvin, and C. Buchwald. 2010. Oxygen isotopic exchange and fractionation during bacterial ammonia oxidation. Limnology and Oceanography **55**:753-762.

Casciotti, K. L. and M. R. McIlvin. 2007. Isotopic analyses of nitrate and nitrite from reference mixtures and application to Eastern Tropical North Pacific waters. Marine Chemistry **107**:184-201.

Casciotti, K. L., D. M. Sigman, M. G. Hastings, J. K. Bohlke, and A. Hilkert. 2002. Measurement of the oxygen isotopic composition of nitrate in seawater and freshwater using the denitrifier method. Analytical Chemistry **74**:4905-4912.

Casciotti, K. L., D. M. Sigman, and B. B. Ward. 2003. Linking diversity and stable isotope fractionation in ammonia-oxidizing bacteria. Geomicrobiology Journal **20**:335-353.

Cey, E. E., D. L. Rudolph, R. Aravena, and G. Parkin. 1999. Role of the riparian zone in controlling the distribution and fate of agricultural nitrogen near a small stream in southern Ontario. Journal of Contaminant Hydrology **37**:45-67.

Chen, F. J., G. D. Jia, and J. Y. Chen. 2009. Nitrate sources and watershed denitrification inferred from nitrate dual isotopes in the Beijiang River, south China. Biogeochemistry **94**:163-174.

Chien, S. H., G. Shearer, and D. H. Kohl. 1977. The nitrogen isotope effect associated with nitrate and nitrite loss from waterlogged soils. Soil Science Society of America Journal **41**:63-69.

Christensen, P. B., L. P. Nielsen, J. Sorensen, and N. P. Revsbech. 1990. Denitrification in nitrate-rich streams - diurnal and seasonal variation related to benthic oxygen-metabolism. Limnology and Oceanography **35**:640-651.

Clark, I., R. Timlin, A. Bourbonnais, K. Jones, D. Lafleur, and K. Wickens. 2008. Origin and fate of industrial ammonium in anoxic ground water - N-15 evidence for anaerobic oxidation (anammox). Ground Water Monitoring and Remediation **28**:73-82.

Cline, J. D. and I. R. Kaplan. 1975. Isotopic fractionation of dissolved nitrate during denitrification in the eastern tropical north pacific ocean. Marine Chemistry **3**:271-299.

Cohen, M. J., J. B. Heffernan, A. Albertin, and J. B. Martin. 2012. Inference of riverine nitrogen processing from longitudinal and diel variation in dual nitrate isotopes. Journal of Geophysical Research-Biogeosciences **117.**

Cook, G. A. and C. M. Lauer. 1968. Oxygen. Pages 499-512 *in* A. H. Clifford, editor. The Encyclopedia of the Chemical Elements Reinhold Book Corporation, New York.

Curtis, C. J., C. D. Evans, C. L. Goodale, and T. H. E. Heaton. 2011. What have stable isotope studies revealed about the nature and mechanisms of N saturation and nitrate leaching from semi-natural catchments? Ecosystems **14:**1021-1037.

Dalsgaard, T., B. Thamdrup, L. Farias, and N. P. Revsbech. 2012. Anammox and denitrification in the oxygen minimum zone of the eastern South Pacific. Limnology and Oceanography **57**:1331-1346.

Devito, K. J., D. Fitzgerald, A. R. Hill, and R. Aravena. 2000. Nitrate dynamics in relation to lithology and hydrologic flow path in a river riparian zone. Journal of Environmental Quality **29**:1075-1084.

Dhondt, K., P. Boeckx, O. Van Cleemput, and G. Hofman. 2003. Quantifying nitrate retention processes in a riparian buffer zone using the natural abundance of N-15 in NO3. Pages 2597-2604 *in* Meeting of the Stable-Isotope-Mass-Spectrometry-Users-Group. John Wiley & Sons Ltd, Bristol, England.

Erler, D. V., B. D. Eyre, and L. Davison. 2008. The contribution of anammox and denitrification to sedirnent N_2 production in a surface flow constructed Wetland. Environmental Science & Technology 42:9144-9150.

Farrell, R. E., P. J. Sandercock, D. J. Pennock, and C. VanKessel. 1996. Landscape-scale variations in leached nitrate: Relationship to denitrification and natural nitrogen-15 abundance. Soil Science Society of America Journal **60**:1410-1415.

Feast, N. A., K. M. Hiscock, P. F. Dennis, and J. N. Andrews. 1998. Nitrogen isotope hydrochemistry and denitrification within the Chalk aquifer system of north Norfolk, UK. Journal of Hydrology 211:233-252.

Galloway, J. N., J. D. Aber, J. W. Erisman, S. P. Seitzinger, R. W. Howarth, E. B. Cowling, and B. J. Cosby. 2003. The nitrogen cascade. Bioscience **53**:341-356.

Gardner, W. S. and M. J. McCarthy. 2009. Nitrogen dynamics at the sediment-water interface in shallow, sub-tropical Florida Bay: why denitrification efficiency may decrease with increased eutrophication. Biogeochemistry **95**:185-198.

Granger, J., D. M. Sigman, M. F. Lehmann, and P. D. Tortell. 2008. Nitrogen and oxygen isotope fractionation during dissimilatory nitrate reduction by denitrifying bacteria. Limnology and Oceanography **53**:2533-2545.

Granger, J., D. M. Sigman, J. A. Needoba, and P. J. Harrison. 2004. Coupled nitrogen and oxygen isotope fractionation of nitrate during assimilation by cultures of marine phytoplankton. Limnology and Oceanography **49**:1763-1773.

Green, C. T., J. K. Bohlke, B. A. Bekins, and S. P. Phillips. 2010. Mixing effects on apparent reaction rates and isotope fractionation during denitrification in a heterogeneous aquifer. Water Resources Research **46**:19.

Groffman, P. M., K. Butterbach-Bahl, R. W. Fulweiler, A. J. Gold, J. L. Morse, E. K. Stander, C. Tague, C. Tonitto, and P. Vidon. 2009. Challenges to incorporating spatially and temporally explicit phenomena (hotspots and hot moments) in denitrification models. Biogeochemistry **93**:49-77.

Gruber, N. and J. N. Galloway. 2008. An Earth-system perspective of the global nitrogen cycle. Nature **451**:293-296.

Hall, E. K., F. Maixner, O. Franklin, H. Daims, A. Richter, and T. Battin. 2011. Linking microbial and ecosystem ecology using ecological stoichiometry: A synthesis of conceptual and empirical approaches. Ecosystems **14**:261-273.

Heffernan, J. B., A. R. Albertin, M. L. Fork, B. G. Katz, and M. J. Cohen. 2012. Denitrification and inference of nitrogen sources in the karstic Floridan Aquifer. Biogeosciences 9:1671-1690.

Hogberg, P. 1997. Tansley review No 95 - N-15 natural abundance in soil-plant systems. New Phytologist **137**:179-203.

Houlton, B. Z. and E. Bai. 2009. Imprint of denitrifying bacteria on the global terrestrial biosphere. Proceedings of the National Academy of Sciences of the United States of America **106**:21713-21716.

Howarth, R., D. Swaney, G. Billen, J. Garnier, B. G. Hong, C. Humborg, P. Johnes, C. M. Morth, and R. Marino. 2012. Nitrogen fluxes from the landscape are controlled by net anthropogenic nitrogen inputs and by climate. Frontiers in Ecology and the Environment **10**:37-43.

Howarth, R. W., G. Billen, D. Swaney, A. Townsend, N. Jaworski, K. Lajtha, J. A. Downing, R. Elmgren, N. Caraco, T. Jordan, F. Berendse, J. Freney, V. Kudeyarov, P. Murdoch, and Z. L. Zhu. 1996. Regional nitrogen budgets and riverine N&P fluxes for the drainages to the North Atlantic Ocean: Natural and human influences. Biogeochemistry **35**:75-139.

Inselsbacher, E., N. Hinko-Najera Umana, F. C. Stange, M. Gorfer, E. Schuller, K. Ripka, S. Zechmeister-Boltenstern, R. Hood-Novotny, J. Strauss, and W. Wanek. 2010. Short-term competition between crop plants and soil microbes for inorganic N fertilizer. Soil Biology & Biochemistry **42**:360-372.

Itoh, M., Y. Takemon, A. Makabe, C. Yoshimizu, A. Kohzu, N. Ohte, D. Tumurskh, I. Tayasu, N. Yoshida, and T. Nagata. 2011. Evaluation of wastewater nitrogen transformation in a natural wetland (Ulaanbaatar, Mongolia) using dual-isotope analysis of nitrate. Science of the Total Environment **409**:1530-1538.

Junk, G. and H. J. Svec. 1958. The absolute abundance of the nitrogen isotopes in the atmosphere and compressed gas from various sources. Geochimica Et Cosmochimica Acta **14**:234-243.

Karsh, K. L., J. Granger, K. Kritee, and D. M. Sigman. 2012. Eukaryotic assimilatory nitrate reductase fractionates N and O Isotopes with a ratio near unity. Environmental Science & Technology **46**:5727-5735.

Kawanishi, T., Y. Hayashi, N. Kihou, T. Yoneyama, and Y. Ozaki. 1993. Dispersion effect on the apparent nitrogen isotope fractionation factor associated with denitrification in soil - evaluation by a mathematical-model. Soil Biology & Biochemistry **25**:349-354.

Kawanishi, T., Y. Hayashi, N. Kihou, T. Yoneyama, and Y. Ozaki. 1996. Difference in diffusion coefficients of (NO_3^-)-N^{14}-N and (NO_3^-)-N^{15}-N affects the apparent fractionation factor associated with denitrification in soil. Soil Science and Plant Nutrition **42**:407-411.

Kaye, J. P. and S. C. Hart. 1997. Competition for nitrogen between plants and soil microorganisms. Trends in Ecology & Evolution **12**:139-143.

Kellman, L. 2004. Nitrate removal in a first-order stream: reconciling laboratory and field measurements. Biogeochemistry **71**:89-105.

Kellman, L. M. and C. Hillaire-Marcel. 2003. Evaluation of nitrogen isotopes as indicators of nitrate contamination sources in an agricultural watershed. Agriculture Ecosystems & Environment **95**:87-102.

Kendall, C. 1998. Tracing Nitrogen Sources and Cycling in Catchments *in* C. Kendall and J. J. Mcdonell, editors. Isotope Tracers in Catchment Hydrology. Elsevier Science B.V., Amsterdam.

Kendall, C. and E. A. Caldwell. 1998. Fundamentals of Isotope Geochemistry *in* C. Kendall and J. J. McDonnell, editors. Isotope Tracers in Catchment Hydrology. Elsevier Science B.V., Amsterdam.

Knoller, K., C. Vogt, M. Haupt, S. Feisthauer, and H. H. Richnow. 2011. Experimental investigation of nitrogen and oxygen isotope fractionation in nitrate and nitrite during denitrification. Biogeochemistry **103**:371-384.

Kool, D. M., N. Wrage, S. Zechmeister-Boltenstern, M. Pfeffer, D. Brus, O. Oenema, and J. W. Van Groenigen. 2010. Nitrifier denitrification can be a source of N_2O from soil: a revised approach to the dual-isotope labelling method. European Journal of Soil Science **61**:759-772.

Korom, S. F., A. J. Schlag, W. M. Schuh, and A. K. Schlag. 2005. In situ mesocosms: Denitrification in the Elk Valley aquifer. Ground Water Monitoring and Remediation 25:79-89.

Korom, S. F., W. M. Schuh, T. Tesfay, and E. J. Spencer. 2012. Aquifer denitrification and in situ mesocosms: Modeling electron donor contributions and measuring rates. Journal of Hydrology **432:**112-126.

Kritee, K., D. M. Sigman, J. Granger, B. B. Ward, A. Jayakumar, and C. Deutsch. 2012. Reduced isotope fractionation by denitrification under conditions relevant to the ocean. Geochimica Et Cosmochimica Acta **92**:243-259.

Kroopnick, P. and H. Craig. 1972. Atmospheric oxygen: isotopic composition and solubility fractionation. Science **175**:54-55.

Kumar, S., D. J. D. Nicholas, and E. H. Williams. 1983. Definitive N-15 NMR evidence that water serves as a source of o during nitrite oxidation by nitrobacter-agilis. Febs Letters 152:71-74.

Lam, P., G. Lavik, M. M. Jensen, J. van de Vossenberg, M. Schmid, D. Woebken, G. Dimitri, R. Amann, M. S. M. Jetten, and M. M. M. Kuypers. 2009. Revising the nitrogen cycle in the Peruvian oxygen minimum zone. Proceedings of the National Academy of Sciences of the United States of America **106**:4752-4757.

Lehmann, M. F., P. Reichert, S. M. Bernasconi, A. Barbieri, and J. A. McKenzie. 2003. Modelling nitrogen and oxygen isotope fractionation during denitrification in a lacustrine redox-transition zone. Geochimica Et Cosmochimica Acta **67**:2529-2542.

Lehmann, M. F., D. M. Sigman, D. C. McCorkle, B. G. Brunelle, S. Hoffmann, M. Kienast, G. Cane, and J. Clement. 2005. Origin of the deep Bering Sea nitrate deficit: Constraints from the nitrogen and oxygen isotopic composition of water column nitrate and benthic nitrate fluxes. Global Biogeochemical Cycles **19**.

Lehmann, M. F., D. M. Sigman, D. C. McCorkle, J. Granger, S. Hoffmann, G. Cane, and B. G. Brunelle. 2007. The distribution of nitrate N^{15}/N^{14} in marine sediments and the impact of benthic nitrogen loss on the isotopic composition of oceanic nitrate. Geochimica Et Cosmochimica Acta **71**:5384-5404.

Li, S. L., C. Q. Liu, J. Li, X. L. Liu, B. Chetelat, B. L. Wang, and F. S. Wang. 2010. Assessment of the sources of nitrate in the Changjiang River, China using a nitrogen and oxygen isotopic approach. Environmental Science & Technology **44**:1573-1578.

Lo, C. C. 2010. Effect of pesticides on soil microbial community. Journal of Environmental Science and Health Part B-Pesticides Food Contaminants and Agricultural Wastes **45**:348-359.

Mariotti, A., J. C. Germon, P. Hubert, P. Kaiser, R. Letolle, A. Tardieux, and P. Tardieux. 1981. Experimental-determination of nitrogen kinetic isotope fractionation - some principles - illustration for the denitrification and nitrification processes. Plant and Soil **62**:413-430.

Mariotti, A., J. C. Germon, and A. Leclerc. 1982. Nitrogen isotope fractionation associated with the NO_2--N_2O step of denitrification in soils. Canadian Journal of Soil Science **62**:227-241.

Mariotti, A., A. Landreau, and B. Simon. 1988. N-15 isotope biogeochemistry and natural denitrification process in groundwater - application to the chalk aquifer of northern France. Geochimica Et Cosmochimica Acta **52**:1869-1878.

Matocha, C. J., P. Dhakal, and S. M. Pyzola. 2012. The role of abiotic and coupled biotic/abiotic mineral controlled redox processes in nitrate reduction. Pages 181-214 *in* D. L. Sparks, editor. Advances in Agronomy, Vol 115. Elsevier Academic Press Inc, San Diego.

McIlvin, M. R. and M. A. Altabet. 2005. Chemical conversion of nitrate and nitrite to nitrous oxide for nitrogen and oxygen isotopic analysis in freshwater and seawater. Analytical Chemistry **77**:5589-5595.

Miyajima, T., C. Yoshimizu, Y. Tsuboi, Y. Tanaka, I. Tayasu, T. Nagata, and I. Koike. 2009. Longitudinal distribution of nitrate delta N-15 and delta O-18 in two contrasting tropical rivers: implications for instream nitrogen cycling. Biogeochemistry **95**:243-260.

Mulholland, P. J., A. M. Helton, G. C. Poole, R. O. Hall, S. K. Hamilton, B. J. Peterson, J. L. Tank, L. R. Ashkenas, L. W. Cooper, C. N. Dahm, W. K. Dodds, S. E. G. Findlay, S. V. Gregory, N. B. Grimm, S. L. Johnson, W. H. McDowell, J. L. Meyer, H. M. Valett, J. R. Webster, C. P. Arango, J. J. Beaulieu, M. J. Bernot, A. J. Burgin, C. L. Crenshaw, L. T. Johnson, B. R. Niederlehner, J. M. O'Brien, J. D. Potter, R. W. Sheibley, D. J. Sobota, and S. M. Thomas. 2008. Stream denitrification across biomes and its response to anthropogenic nitrate loading. Nature **452**:202-U246.

Muller, C., R. J. Stevens, R. J. Laughlin, and H. J. Jager. 2004. Microbial processes and the site of N_2O production in a temperate grassland soil. Soil Biology & Biochemistry **36:**453-461.

Naqvi, S. W. A., H. Naik, A. Pratihary, W. D'Souza, P. V. Narvekar, D. A. Jayakumar, A. H. Devol, T. Yoshinari, and T. Saino. 2006. Coastal versus open-ocean denitrification in the Arabian Sea. Biogeosciences **3**:621-633.

Naqvi, S. W. A., T. Yoshinari, J. A. Brandes, A. H. Devol, D. A. Jayakumar, P. V. Narvekar, M. A. Altabet, and L. A. Codispoti. 1998. Nitrogen isotopic studies in the suboxic Arabian Sea. Proceedings of the Indian Academy of Sciences-Earth and Planetary Sciences **107**:367-378.

Nestler, A., M. Berglund, F. Accoe, S. Duta, D. M. Xue, P. Boeckx, and P. Taylor. 2011. Isotopes for improved management of nitrate pollution in aqueous resources: review of surface water field studies. Environmental Science and Pollution Research **18**:519-533.

Nizzoli, D., E. Carraro, V. Nigro, and P. Viaroli. 2010. Effect of organic enrichment and thermal regime on denitrification and dissimilatory nitrate reduction to ammonium (DNRA) in hypolimnetic sediments of two lowland lakes. Water Research **44**:2715-2724.

Osaka, K., N. Ohte, K. Koba, C. Yoshimizu, M. Katsuyama, M. Tani, I. Tayasu, and T. Nagata. 2010. Hydrological influences on spatiotemporal variations of delta N-15 and delta O-18 of nitrate in a forested headwater catchment in central Japan: Denitrification plays a critical role in groundwater. Journal of Geophysical Research-Biogeosciences **115**:14.

Panno, S. V., K. C. Hackley, W. R. Kelly, and H. H. Hwang. 2006. Isotopic evidence of nitrate sources and denitrification in the Mississippi River, Illinois. Journal of Environmental Quality **35**:495-504.

Pellerin, B. A., B. D. Downing, C. Kendall, R. A. Dahlgren, T. E. C. Kraus, J. Saraceno, R. G. M. Spencer, and B. A. Bergamaschi. 2009. Assessing the sources and magnitude of diurnal nitrate variability in the San Joaquin River (California) with an in situ optical nitrate sensor and dual nitrate isotopes. Freshwater Biology **54**:376-387.

Petitta, M., D. Fracchiolla, R. Aravena, and M. Barbieri. 2009. Application of isotopic and geochemical tools for the evaluation of nitrogen cycling in an agricultural basin, the Fucino Plain, Central Italy. Journal of Hydrology **372**:124-135.

Revsbech, N. P., N. Risgaard-Petersen, A. Schramm, and L. P. Nielsen. 2006. Nitrogen transformations in stratified aquatic microbial ecosystems. Antonie Van Leeuwenhoek International Journal of General and Molecular Microbiology 90:361-375.

Rivett, M. O., S. R. Buss, P. Morgan, J. W. N. Smith, and C. D. Bemment. 2008. Nitrate attenuation in groundwater: A review of biogeochemical controlling processes. Water Research **42**:4215-4232.

Robinson, D., L. L. Handley, and C. M. Scrimgeour. 1998. A theory for N-15/N-14 fractionation in nitrate-grown vascular plants. Planta **205**:397-406.

Ruehl, C. R., A. T. Fisher, M. Los Huertos, S. D. Wankel, C. G. Wheat, C. Kendall, C. E. Hatch, and C. Shennan. 2007. Nitrate dynamics within the Pajaro River, a nutrient-rich, losing stream. Journal of the North American Benthological Society **26**:191-206.

Rutting, T., P. Boeckx, C. Muller, and L. Klemedtsson. 2011. Assessment of the importance of dissimilatory nitrate reduction to ammonium for the terrestrial nitrogen cycle. Biogeosciences **8**:1779-1791.

Savard, M. M., D. Paradis, G. Somers, S. Liao, and E. v. Bochove. 2007. Winter nitrification contributes to excess NO_3 study. Water Resources Research **43**:W06422.

Schlesinger, W. H. 2009. On the fate of anthropogenic nitrogen. Proceedings of the National Academy of Sciences of the United States of America **106**:203-208.

Schmidt, C. M., A. T. Fisher, A. Racz, C. G. Wheat, M. Los Huertos, and B. Lockwood. 2012. Rapid nutrient load reduction during infiltration of managed aquifer recharge in an agricultural groundwater basin: Pajaro Valley, California. Hydrological Processes 26:2235-2247.

Sebilo, M., G. Billen, M. Grably, and A. Mariotti. 2003. Isotopic composition of nitrate-nitrogen as a marker of riparian and benthic denitrification at the scale of the whole Seine River system. Biogeochemistry **63**:35-51.

Seitzinger, S., J. A. Harrison, J. K. Bohlke, A. F. Bouwman, R. Lowrance, B. Peterson, C. Tobias, and G. Van Drecht. 2006. Denitrification across landscapes and waterscapes: A synthesis. Ecological Applications **16**:2064-2090.

Semaoune, P., M. Sebilo, J. Templier, and S. Derenne. 2012. Is there any isotopic fractionation of nitrate associated with diffusion and advection? Environmental Chemistry **9**:158-162.

Shearer, G. and D. H. Kohl. 1988. Nitrogen isotopic fractionation and o-18 exchange in relation to the mechanism of denitrification of nitrite by pseudomonas-stutzeri. Journal of Biological Chemistry **263**:13231-13245.

Sigman, D. M., M. A. Altabet, R. Michener, D. C. McCorkle, B. Fry, and R. M. Holmes. 1997. Natural abundance-level measurement of the nitrogen isotopic composition of oceanic nitrate: an adaptation of the ammonia diffusion method. Marine Chemistry **57**:227-242.

Sigman, D. M., K. L. Casciotti, M. Andreani, C. Barford, M. Galanter, and J. K. Bohlke. 2001. A bacterial method for the nitrogen isotopic analysis of nitrate in seawater and freshwater. Analytical Chemistry **73**:4145-4153.

Sigman, D. M., P. J. DiFiore, M. P. Hain, C. Deutsch, Y. Wang, D. M. Karl, A. N. Knapp, M. F. Lehmann, and S. Pantoja. 2009. The dual isotopes of deep nitrate as a constraint on the cycle and budget of oceanic fixed nitrogen. Deep-Sea Research Part I-Oceanographic Research Papers **56**:1419-1439.

Silva, S. R., C. Kendall, D. H. Wilkison, A. C. Ziegler, C. C. Y. Chang, and R. J. Avanzino. 2000. A new method for collection of nitrate from fresh water and the analysis of nitrogen and oxygen isotope ratios. Journal of Hydrology **228**:22-36.

Singleton, M. J., B. K. Esser, J. E. Moran, G. B. Hudson, W. W. McNab, and T. Harter. 2007. Saturated zone denitrification: Potential for natural attenuation of nitrate contamination in shallow groundwater under dairy operations. Environmental Science & Technology **41**:759-765.

Smith, R. L., B. L. Howes, and J. H. Duff. 1991. Denitrification in nitrate-contaminated groundwater - occurrence in steep vertical geochemical gradients. Geochimica Et Cosmochimica Acta **55**:1815-1825.

Spalding, R. F., M. E. Exner, G. E. Martin, and D. D. Snow. 1993. Effects of sludge disposal on groundwater nitrate concentrations. Journal of Hydrology **142**:213-228.

Spott, O., R. Russow, and C. F. Stange. 2011. Formation of hybrid N_2O and hybrid N_2 due to codenitrification: First review of a barely considered process of microbially mediated N-nitrosation. Soil Biology & Biochemistry **43**:1995-2011.

Spott, O. and C. F. Stange. 2011. Formation of hybrid N_2O in a suspended soil due to co-denitrification of NH_2OH. Journal of Plant Nutrition and Soil Science **174**:554-567.

Standing, D., E. M. Baggs, M. Wattenbach, P. Smith, and K. Killham. 2007. Meeting the challenge of scaling up processes in the plant-soil-microbe system. Biology and Fertility of Soils **44**:245-257.

Sun, W. J., R. Sierra-Alvarez, L. Milner, R. Oremland, and J. A. Field. 2009. Arsenite and ferrous iron oxidation linked to chemolithotrophic denitrification for the immobilization of arsenic in anoxic environments. Environmental Science & Technology 43:6585-6591.

Tang, H., K. Yan, L. P. Zhang, F. Q. Chi, Q. Li, S. J. Lian, and D. Wei. 2010. Diversity analysis of nitrite reductase genes (nirS) in black soil under different long-term fertilization conditions. Annals of Microbiology **60**:97-104.

Taylor, P. G. and A. R. Townsend. 2010. Stoichiometric control of organic carbon-nitrate relationships from soils to the sea. Nature **464**:1178-1181.

Thamdrup, B. 2012. New Pathways and Processes in the Global Nitrogen Cycle. Pages 407-428 *in* D. J. Futuyma, editor. Annual Review of Ecology, Evolution, and Systematics, Vol 43. Annual Reviews, Palo Alto.

Torrento, C., J. Cama, J. Urmeneta, N. Otero, and A. Soler. 2010. Denitrification of groundwater with pyrite and Thiobacillus denitrificans. Chemical Geology **278**:80-91.

Torrento, C., J. Urmeneta, N. Otero, A. Soler, M. Vinas, and J. Cama. 2011. Enhanced denitrification in groundwater and sediments from a nitrate-contaminated aquifer after addition of pyrite. Chemical Geology **287**:90-101.

Toyoda, S., H. Mutobe, H. Yamagishi, N. Yoshida, and Y. Tanji. 2005. Fractionation of N_2O isotopomers during production by denitrifier. Soil Biology & Biochemistry **37**:1535-1545.

Trimmer, M., J. Grey, C. M. Heppell, A. G. Hildrew, K. Lansdown, H. Stahl, and G. Yvon-Durocher. 2012. River bed carbon and nitrogen cycling: State of play and some new directions. Science of the Total Environment **434**:143-158.

Tsushima, K., S. Ueda, and N. Ogura. 2002. Nitrate loss for denitrification during high frequency research in floodplain groundwater of the Tama River. Water Air and Soil Pollution **137**:167-178.

Tsushima, K., S. Ueda, H. Ohno, N. Ogura, T. Katase, and K. Watanabe. 2006. Nitrate decrease with isotopic fractionation in riverside sediment column during infiltration experiment. Water Air and Soil Pollution **174**:47-61.

Vieten, B., T. Blunier, A. Neftel, C. Alewell, and F. Conen. 2007. Fractionation factors for stable isotopes of N and O during N_2O reduction in soil depend on reaction rate constant. Rapid Communications in Mass Spectrometry **21**:846-850.

Vogel, J. C., A. S. Talma, and T. H. E. Heaton. 1981. Gaseous nitrogen as evidence for denitrification in groundwater. Journal of Hydrology 50:191-200.

Wallenstein, M. D., D. D. Myrold, M. Firestone, and M. Voytek. 2006. Environmental controls on denitrifying communities and denitrification rates: Insights from molecular methods. Ecological Applications **16**:2143-2152.

Wankel, S. D., C. Kendall, C. A. Francis, and A. Paytan. 2006. Nitrogen sources and cycling in the San Francisco Bay Estuary: A nitrate dual isotopic composition approach. Limnology and Oceanography **51**:1654-1664.

Wankel, S. D., C. Kendall, and A. Paytan. 2009. Using nitrate dual isotopic composition (delta N-15 and delta O-18) as a tool for exploring sources and cycling of nitrate in an estuarine system: Elkhorn Slough, California. Journal of Geophysical Research-Biogeosciences **114**:15.

Waser, N. A. D., P. J. Harrison, B. Nielsen, S. E. Calvert, and D. H. Turpin. 1998. Nitrogen isotope fractionation during the uptake and assimilation of nitrate, nitrite, ammonium, and urea by a marine diatom. Limnology and Oceanography **43**:215-224.

Wassenaar, L. I. 1995. Evaluation of the origin and fate of nitrate in the Abbotsford aquifer using the isotopes of N-15 and O-18 in NO_3. Applied Geochemistry **10**:391-405.

Wellman, R. P., F. D. Cook, and H. R. Krouse. 1968. Nitrogen-15: microbiological alteration of abundance. Science (New York, N.Y.) **161**:269-270.

Wells, N.S., T.J. Clough, L.M. Condron, W.T. Baisden, J.S. Harding, Y. Dong, G.D. Lewis, G. Lear. 2013. Biogeochemistry and community ecology in a spring-fed urban river following a major earthquake. Environmental Pollution 182: 190-200.

Wexler, S. K., K. M. Hiscock, and P. F. Dennis. 2011. Catchment-scale quantification of hyporheic denitrification using an isotopic and solute flux approach. Environmental Science & Technology **45**:3967-3973.

Widory, D., E. Petelet-Giraud, A. Brenot, J. Bronders, K. Tirez, and P. Boeckx. 2013. Improving the management of nitrate pollution in water by the use of isotope monitoring: the delta(15)N, delta(18)O and delta(11)B triptych. Isotopes in Environmental and Health Studies **49**:29-47.

Wrage, N., G. L. Velthof, M. L. van Beusichem, and O. Oenema. 2001. Role of nitrifier denitrification in the production of nitrous oxide. Soil Biology & Biochemistry **33**:1723-1732.

Wunderlich, A., R. Meckenstock, and F. Einsiedl. 2012. Effect of different carbon substrates on nitrate stable isotope fractionation during microbial denitrification. Environmental Science & Technology **46**:4861-4868.

Xue, D. M., J. Botte, B. De Baets, F. Accoe, A. Nestler, P. Taylor, O. Van Cleemput, M. Berglund, and P. Boeckx. 2009. Present limitations and future prospects of stable isotope methods for nitrate source identification in surface- and groundwater. Water Research **43**:1159-1170.

Yun, S. I., H. M. Ro, W. J. Choi, and G. H. Han. 2011. Interpreting the temperature-induced response of ammonia oxidizing microorganisms in soil using nitrogen isotope fractionation. Journal of Soils and Sediments **11**:1253-1261.

Zarnetske, J. P., R. Haggerty, S. M. Wondzell, V. A. Bokil, and R. González-Pinzón. 2012. Coupled transport and reaction kinetics control the nitrate source-sink function of hyporheic zones. Water Resources Research **48**:n/a-n/a.

Zhu, G., S. Wang, W. Wang, Y. Wang, L. Zhou, B. Jiang, H. J. M. O. d. Camp, N. Risgaard-Petersen, L. Schwark, Y. Peng, M. M. Hefting, M. S. M. Jetten, and C. Yin. 2013. Hotspots of anaerobic ammonium oxidation at land-freshwater interfaces. Nature Geoscience **6**:103-107.

Zhu, G. B., S. Y. Wang, Y. Wang, C. X. Wang, N. Risgaard-Petersen, M. S. M. Jetten, and C. Q. Yin. 2011. Anaerobic ammonia oxidation in a fertilized paddy soil. Isme Journal **5**:1905-1912.

Zumft, W. G. 1997. Cell biology and molecular basis of denitrification. Microbiology and Molecular Biology Reviews **61**:533-+.

Plate 1 **Clockwise from top: the mesocosm incubation set-up for measuring denitrification and εdenit in paddy soils; Boggy Creek Ditch (site BC) in Doylston, Canterbury; ditch at the Lincoln University Dairy Farm (LUDF) where NO_3^- isotopes in sediments and surface water were measured in the winter of 2009, when these photos were taken.**

Chapter 3

Environmental controls on nitrate isotopes fractionation during denitrification in stream sediments and submerged soils, and its expression across the anaerobic-aerobic interface

Sections of this chapter will be submitted for publication. Wells, N.S., T.J. Clough, S.E. Johnson-Beebout, W.T. Baisden. In prep. Environmental expression of denitrification's intrinsic biochemical isotope fractionation measured in nitrate: do 'site specific' enrichment factors exist? Biogeochemistry (Synthesis and Emerging Ideas)

3.1 Abstract

Precise and accurate tracers of nitrate (NO_3^-) transformations in freshwater systems are needed to successfully mitigate the threat it poses to water quality. Measurements of NO_3^- isotopes ($\delta^{15}N$ and $\delta^{18}O$) could provide an integrative measure of N losses, as their composition reflects biogeochemical processing. However, quantitative use of $\delta^{15}N$ and $\delta^{18}O$ to measure NO_3^- attenuation (denitrification) is currently limited by a poor understanding of the factors controlling the strength of fractionation during denitrification (ε_{denit}), and the extent to which site-specific intrinsic ε_{denit} is expressed in in aerobic surface waters (ε_{eff}). Combining mathematical modelling with experimental results from field and lab studies, I lay out a practical framework for defining an appropriate ε_{denit} range for freshwater sites based on three layers of NO_3^- processing: 1) biological denitrification, 2) diffusive transport of NO_3^- through the denitrifying zone, and, 3) mixing with NO_3^- produced from nitrification. Biologically-defined ε_{denit}, measured in sediments from four sites along a temperate stream and from three tropical submerged paddy fields, varied with antecedent carbon content from -3‰ to -28‰. Following diffusive transport to aerobic surface water, ε_{denit} normalised around low ε_{eff} values: the measured ε_{denit} range (-17 ±15‰) is predicted to decrease to -2 ±4‰ following diffusion from the anaerobic sediment zone to the aerobic surface water. Mixing with nitrification likewise caused ε_{eff} to vary, depending on the relative rate of incoming NO_3^- from nitrification and removal of NO_3^- by denitrification. Inherent variability in fractionation at all three levels assessed leads to the suggestion that it is more accurate to apply a set range of ε_{denit} values for assessing attenuation in a given environment than to attempt to ascertain a unique value for a given catchment.

Keywords: stable isotopes, denitrification, nitrate, fractionation, diffusion, sediment-surface water interface

3.2 Introduction

Human activities have doubled the annual inputs of reactive nitrogen (N) to land, causing a cascade of environmental degradation as excess N is transported from land to the sea (e.g., eutrophication of water ways and emissions of the greenhouse gas nitrous oxide (N_2O)) (Galloway et al. 2008). Denitrification, the step-wise reduction of highly mobile nitrate (NO_3^-) to N_2O and dinitrogen (N_2), is the primary pathway for attenuating (permanently removing) reactive N and curtailing the N cascade (Galloway et al. 2003). At the global scale, 30% of N entering rivers is estimated to be denitrified during transport (Mulholland and Webster 2010), yet the extreme spatial and temporal variability of denitrification rates (k_{denit}) makes accurately quantifying attenuation fluxes, and thus N balances, within catchments inherently difficult (Seitzinger et al. 2006, Groffman et al. 2009).

The natural abundance isotopic composition of NO_3^- ($\delta^{15}N$ and $\delta^{18}O$) is recognised as a potential means of integrating N attenuation over time or distance as denitrifying microbes preferentially utilise 'light' isotopes (Groffman et al. 2006). The natural abundance composition of $\delta^{18}O\text{-}NO_3^-$ and $\delta^{15}N\text{-}NO_3^-$ in the residual NO_3^- pool can thus be used to calculate the proportion NO_3^- attenuated according to a Rayleigh fractionation process (Eq. 3.1):

$$\frac{R}{R_0} = \left(\frac{C}{C_0}\right)^{1/(\alpha denit - 1)} \quad (3.1)$$

where the ratio of heavy to light isotopes (R) at a given point divided by the original isotopic composition of the pool (R_0) is directly related to the difference between the measured substrate concentration (C) and the original substrate concentration (C_0) by the degree of preference for light isotopes during denitrification (fractionation factor: α_{denit}, referred to in the text in terms of ε_{denit}, where $\varepsilon_{denit} = (\alpha_{denit} - 1) \times 1000)$) (Kendall and Caldwell 1998). If ε_{denit} is known, the rate of NO_3^- attenuation ($1 - C/C_0$) could be calculated from measured $\delta^{15}N$ and $\delta^{18}O$ values (Ostrom et al. 2002). Currently, the large range of reported values, and poor understanding of what causes this range, limit the wide-scale use of isotopic methods to measure N attenuation (Fig. 3.1).

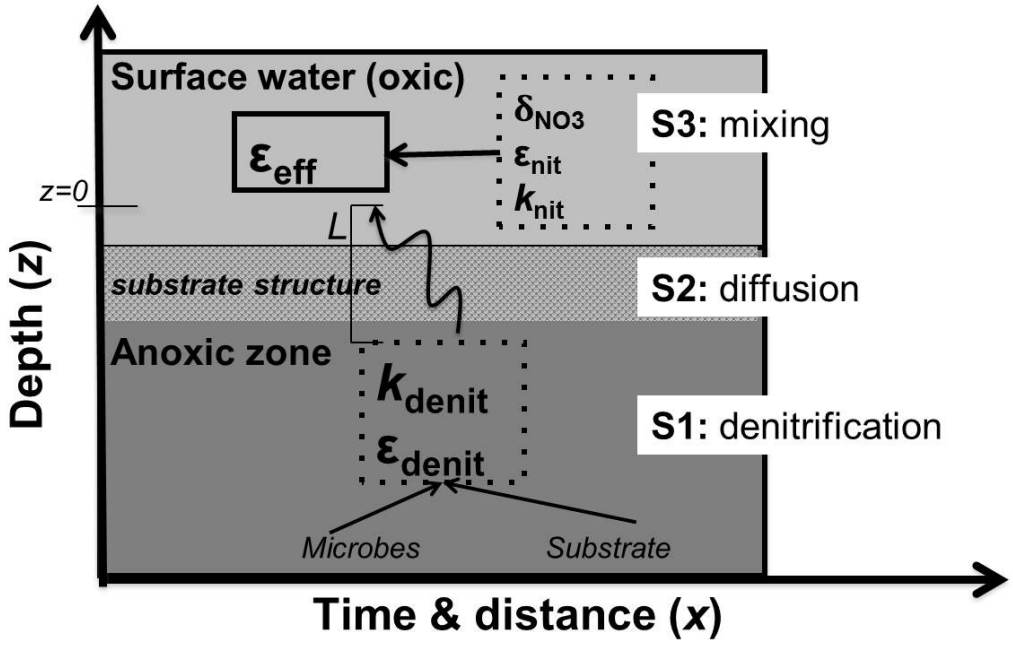

Figure 3.1 **The value of ε_{eff} (expression of ε_{denit} outside of the denitrifying zone in oxygenated stream water) depends on both site-specific intrinsic ε_{denit} conferred during denitrification (S1), the physical (diffusive v. advection) transport of NO_3^- from the denitrifying zone to the measurement zone (S2), and the mixing of the NO_3^- residual from denitrifcation (determined by k_{denit}, the denitrification rate) with the NO_3^- pool created by nitrification (determined by the nitrification rate, k_{nit}, and the isotopic composition defined by the $\delta^{15}N$ of the initial reduced N pool (δ_0) and the enrichment factor for nitrification (ε_{nit}) (S3).**

Isotopic fractionation occurs at the molecular level ('intrinsic') as NO_3^- is transported across the cell wall of the denitrifier (Kritee et al. 2012), where fractionation of N ($^{15}\varepsilon_{denit}$) and O ($^{18}\varepsilon_{denit}$) ranges from -5‰ (low) to -25‰ (high) between denitrifier strains (Granger et al. 2008), and typically occurs at a ~1:1 ratio for $\delta^{18}O$ v. $\delta^{15}N$. While this range of biologically-driven N fractionation is believed to result from variations in microbial metabolism (Kritee et al. 2012), the extent that these ranges are expressed in freshwater environments is unclear, particularly given how little is known about the environmental distribution and function of microbial populations (Standing et al. 2007). Indeed, while no differences in ε_{denit} have been observed between freshwater and marine denitrifiers (Granger et al. 2008, Wunderlich et al. 2012), empirical measurements of isotope effects (ε_{eff}, effective fractionation) in surface waters (e.g., rivers and lakes) consistently yield relatively low enrichment values with $\delta^{18}O$:$\delta^{15}N$ enrichment ratios closer to 1:2 than the expected 1:1 (Chapter 2).

In aerobic surface waters, ε_{denit} can be distorted by the diffusive transport that moves NO_3^- between the anaerobic denitrifying zones in the sediments and the aerobic waters where samples are typically collected (Christensen et al. 1990, Hondzo et al. 2005, Higashino et al. 2008) (Fig. 3.1). Diffusion is mass-dependent, meaning that light isotopes are moved faster than heavy isotopes, causing solute pools to become increasingly depleted in heavy isotopes over transport distance (Abe and Hunkeler 2006, Richter et al. 2006, LaBolle et al. 2008). Diffusive NO_3^- movement from anaerobic sediments to the water column was therefore hypothesised to drive observed discrepancies

in ε_{denit} measured within sediment porewater versus the water column by Brandes and Devol (1997, 2002) (ocean), Lehmann et al. (2003) (lake), and Sebilo et al. (2003) (river).

The aerobic-anaerobic gradient across the sediment-surface water interface also creates a zone for mixing residual NO_3^- from the denitrifying zone with NO_3^- created by nitrification (autotrophic oxidation of ammonia (NH_3) to NO_3^-) in the aerobic zone (Zarnetske et al. 2012) (Fig. 3.1). As O is consumed during nitrification, and denitrification is limited by both NO_3^- availability and the presence of O_2, nitrification (NO_3^- production) and denitrification (NO_3^- attenuation) are often tightly coupled in freshwater environments (Seitzinger et al. 2006). During nitrification, $\delta^{15}N\text{-}NO_3^-$ is isotopically light with respect to the residual $\delta^{15}N\text{-}NH_3$ (as per Eq. 3.1), while $\delta^{18}O\text{-}NO_3^-$ is defined by the incorporated O_2-O and H_2O-O (Casciotti et al. 2003, Buchwald et al. 2012). Therefore, mixing of 'nitrified' and 'denitrified' NO_3^- pools could mask the isotopic fractionation incurred during denitrification (e.g., Wankel et al. 2009).

By constraining ε_{eff} for NO_3^- attenuation in key freshwater systems, this study aims to understand the discrepancy between ε_{denit} and ε_{eff} based on three scenarios: 1) site-specificity of ε_{denit} (intrinsic variations, based on Rayleigh fractionation) (S1), 2) diffusive transport dampening the expression of biological fractionation in oxic zones (S2), and, 3) mixing between nitrification and denitrification in the measurement zone (S3). Site-specificity of ε_{denit} (S1) was determined via incubation of substrates collected from disparate locations, and the theoretical impact of S2 and S3 on these values was evaluated through models, and empirical measurements of $\delta^{15}N$- $\delta^{18}O$- NO_3^- in stream porewaters v. surface waters.

3.3 Materials and Methods

3.3.1 Model overview

Based on the assumptions of Rayleigh fractionation (continuous reaction with a continuous fractionation effect and finite substrate pool), reaction kinetics of denitrification are used to establish intrinsic fractionation for S1. The corresponding range of ε_{eff} was then calculated by overlaying this intrinsic framework with either mass-dependent isotopic fractionation from diffusive transport (S2) or the mixing effects of variable rates of nitrification (S3) using a range of reasonable input parameters (Table 2). In order to minimise assumptions, all of these calculations are based on changes in total isotopic abundance (R), rather than δ notation (‰).

Scenario 1 (intrinsic ε_{denit})

Under ideal conditions, intrinsic α_{denit} determines the relative abundance of 'heavy' isotopes (R^b) based on a 1st order k_{denit} and NO_3^- pool size (C) (Eq. 3.2):

(3.2) $$\frac{dC}{dx} = -k_{denit} C$$

and,

$$\frac{dR^b}{dx} = -\alpha_{denit} k_{denit} C$$

where the boundary conditions for both equations are defined by the initial isotopic composition (R_0) and concentration (C_0) of NO_3^- when x =0.

Scenario 2 (diffusion-limited fractionation)

Using Fick's Law, this model builds an isotopic dimension into the diffusion-based understanding of denitrification rates in sediments presented by Christensen et al. (1990), which defines k_{denit} and NO_3^- fluxes into and out of the denitrifying zone based on the depth of O_2 penetration (z) (Eq. 3.3).

(3.3)

$$0 = D_s \frac{\partial^2 C}{\partial z^2} - w \frac{\partial C}{\partial z} - F$$

where NO_3^- (as concentration, C) is transported vertically (over z) to and from the denitrifying zone (defined as an infinitely thin reactive layer, F, where denitrification occurs as per Eq 2) via diffusion (Christensen et al., 1990; House, 2003; O'Connor and Hondzo, 2008). Availability of C for diffusion or consumption is controlled by physical advection (w) (cm s^{-1}). The diffusion term (D_s) is dependent on molecular diffusivity (D_m) of NO_3^- (1.33 x10^{-5} cm^2 s^{-1}), temperature, and sediment porosity (Φ) (Boudreau, 1997). When the upper boundary layer at z = 0 is open, meaning substrate fluxes into the surface water in accordance with steady state demands, which is in turn controlled by downstream flow (w over x). Therefore, the NO_3^- concentration in the surface water reflects both the degree of denitrifcation and the effect of transport (w, D_s), and the flux across z = 0 can be solved as the first derivative of Fick's Law (Eq. 3.4).

(3.4)

$$\frac{D_s k_{denit} C_w}{D_s + k_{denit} L} = -w \frac{\partial C_w}{\partial x}$$

Accordingly, the isotopic composition at z =0 reflects fractionation resulting from denitrification (α_{denit}) and diffusive transport (α_D); α_D is defined by Eq. 3.5.

(3.5)

$$\alpha_D = \sqrt{\frac{m(m^b + M)}{m^b(m + M)}}$$

where the square root of the relative masses of the heavy (m^b) and light (m) forms of NO_3^- (i.e., $^{15}N^{16}O_3^-$, $^{14}N^{18}O_3^-$) diffused in water (M = mass of H_2O) define the diffusive fractionation factor (α_D)

(Richter et al. 2006, LaBolle et al. 2008). Using α_D and α_{denit}, the isotopic composition of NO_3^- (R) at depth *z* is calculated based on rates of consumption (k_{denit}) and transport (D_s) (Eq. 3.6).

$$R = \frac{C_0^b(D_s + k_{denit}L)(\alpha_D D_s + \alpha_{denit} k_{denit}(L-z))}{C_0(D_s + k_{denit}(L-z))(\alpha_D D_s + \alpha_{denit} k_{denit} L)} \quad (3.6)$$

The complete derivation of this equation is available in Appendix B.

Scenario 3 (mixing)

Nitrification (C_{nit} and R_{nit}) and denitrification (C_{denit} and R_{denit}) were treated as two isolated pools that react separately, and then continuously mix over time/distance to form R_{net} (Eq. 3.7):

$$R_{net} = \frac{R_{nit} \times C_{nit} + R_{denit} \times C_{denit}}{C_{net}} \quad (3.7)$$

where C_{denit} and R_{denit} are defined by Eq. 3.2; C_{nit} is determined by the rate of oxidation of NH_3 by nitrifiers (k_{nit}), and R_{nit} is the N isotopic composition of the nitrified NO_3^- (based on the Rayleigh equation for NH_3 oxidation from Casciotti et al. (2003)) (Fig. 3.1).

3.3.2 Incubation experiments

Substrates were collected from two locations: sediments from Harts Creek, a shallow spring-fed, gaining stream in the Canterbury plains region of New Zealand (43°46'S, 172°16'E), and submerged paddy soils from the International Rice Research Institute experimental farm (IRRI) in the Philippines (14º1'N, 121º15'E). Locations were selected to provide a snapshot of global (cross-biome) v. local (km) scale variation in freshwater ε_{denit}. Within Harts Creek, multiple sites were sampled to span variations in water depth, temperature, and organic matter content, factors known to influence k_{denit} (Garcia-Ruiz et al. 1998, Alexander et al. 2000) and denitrifier activity and abundance (Findlay 2010, Findlay et al. 2011). Sites within IRRI were selected based on changes in land-use / cultivation history, known to control k_{denit} and denitrifier community dynamics in submerged soils (Buresh et al. 2008, Bannert et al. 2011, Ahn et al. 2012).

Sample collection

In Harts Creek, streambed sediments were collected from four reaches at increasing distance from the source spring: 1.69 km (A), 3.69 km (B), 7.75 km (C), and, near the river mouth, 9.61 km (D). Prior to sediment collection, dissolved oxygen (DO) and water temperature were measured in-situ at each reach using a portable hand-held meter (550A YSI, Yellow Springs, OH). Stream depth was measured using a metre stick at upstream sites (A and B) and installed gauges at downstream sites (C and D). Harts Creek climate conditions were evaluated using data from the Leeston Harts Creek

climate station (43°46'1.99"S, 172°16'57.79"E) (<1 km from site A) (CliFlo: NIWA's Climate Database Online (http://cliflo.niwa.co.nz). Data retrieved 06-Jun-2011.)

Paddy soils were collected from three fields with different cultivation histories and clay contents (which reflects cultivation intensity (Kogel-Knabner et al. 2010)) at IRRI: E (two irrigated rice crops a year for >20 years, 61% clay), F (zero to two irrigated rice crops a year for ~10 years, 33% clay), and G (uncultivated soil within 500 m of E). Floodwater depth and soil temperature were recorded prior to sampling. Climate data was obtained from the on-farm climate station and soil characteristics from survey data (W. Lorenzo and R.J. Buresh, unpubl.).

At each location, 20 sediment samples (10 cm depth x 5 cm diameter) were collected (locations determined using a pre-prepared randomised grid) and bulked together to ensure that samples were representative of each site (Bissett et al. 2010). Samples were stored on ice until returned to the lab (<2 h), whereupon they were sieved through a 0.5 mm mesh to remove larger particles and soil fauna. Sub-samples (~50 g) from each location were stored at 4ºC until chemical analyses (water-holding capacity (WHC), total organic carbon (TOC), pH, and total C and N).

Intrinsic ε_{denit} incubations

Streambed sediments were incubated in 30 ml amber glass bottles (Alcom) sealed with Teflon-lined rubber septa. Three replicate incubations were made for each sampling time x treatment, plus an additional control. Each bottle was filled with 25 ml of sediment slurry (100% WHC), which were kept continuously mixed (i.e., no diffusive limitation to denitrification) using a rotary shaker table. For each paddy soil, the equivalent of 200 g dry weight was added to a 2 l mesocosm Pyrex jar and brought up to 1 kg with deionised H_2O (volume selected to ensure that the substrate surface area did not change significantly over time with sub-sampling), sealed, and then kept continuously mixed using a magnetic stirrer. Two replicate mesocosms were set-up for substrate from each site, each fitted with two platinum electrodes and one hydrogen probe for redox measurements (using an Ag/AgCl reference electrode), which were corrected based on hydrogen probe readings (simultaneously used to measure soil pH) (as per Johnson-Beebout et al. (2009)).

All incubations were continuously flushed with N_2 or He gas, and outflows from the incubations were bubbled through air-tight 12 ml Exetainer® filled with 10 ml of deionised water to ensure no air backflow. After 48 h of pre-incubation, C (as glucose; 1mM) and NO_3^- (25 mg N l^{-1} as KNO_3) were added to treatment incubations to ensure that the initial denitrification period was not substrate limited. Slurries were collected +1, 3, 6, 12, 24, and 36 h after substrate additions. For the Harts Creek sediments, sampling was destructive, consisting of opening mesocosms within an air-free bag (purged with He), where the slurries were transferred into a sterile 50 ml centrifuge tube for extraction. For paddy soils, three 50 ml sub-samples were collected from each mesocosm using a sterile syringe. These slurries were immediately injected into acid-washed centrifuge tubes. Once sediments and soils were in the centrifuge tubes, deionised water was added at a 5:1 w/w ratio and samples were centrifuged at 3500 rpm for 20 min, and supernatents pumped through GF/F (Whatman)

filter paper to remove particulates. Air temperature was measured continuously, and paddy slurry redox potential and pH were recorded at each sampling interval.

Layered incubations (ε_{eff})

Site C sediments were also used in incubations testing the impact of diffusion and nitrification on ε_{eff}. The sediments were placed in sterile 30 ml plastic vials (2.5 cm diameter x 6.0 cm height) and then brought to 100% WHC, and then overlain with either 0 cm (L_0), 2 cm (L_1) or 4 cm (L_2) of acid-washed quartz sand plus an additional 6 ml of deionised water. Treatments were replicated four times (including one control without added N or C) for each sampling interval. After 48 h, NO_3^- (25 mg N l^{-1} as KNO_3) and C (1 mM glucose) were slowly injected into the base of the sediment layer using a 1 ml syringe fitted with a 23 g (0.337 mm) needle. Incubations were destructively sampled 4, 8, 24, 48, and 96 h after substrate additions: surface water (SW) was removed using a 15 ml sterile syringe, sediment porewater (PW) extracted as in previous incubations, and both SW and PW samples passed through GF/F filter paper (Whatman).

Vertical profiles (500 μm depth intervals) of O_2 and N_2O concentrations in the sediments, sand, and water, were measured following the procedure of Elberling et al. (2010). Briefly, O_2 was determined using a miniaturised Clark-type O_2 micro-sensor (OX10, Unisense, Science Park, DK-8000 Aarhus, Denmark) equipped with an internal reference and a guard cathode (linearity was confirmed by recording the output current (pA) in water sparged with N_2, air and pure O_2). Standard micro-sensors were used to measure N_2O concentrations and substrate diffusivity (Elberling et al. (2010) and references therein).

3.3.3 Field sampling

Surface water and sediment samples were collected in winter 2009 from two ditches in Canterbury, New Zealand: adjacent to the Lincoln University Dairy Farm (LUDF) and Boggy Creek in the Lake Ellesmere catchment (BC). Four sites (~15 m apart over ditch length) were sampled in from the thalwag of each location. Sampling consisted of collecting 1 l of water in acetylene bottles from ~ 4 cm below the water surface (SW) and from 4 cm above the sediments (DW) using a reaching pole. Headspace air was immediately removed and samples were stored on ice until return to the lab. Porewater (PW) was collected from the underlying sediments: three cores (10 cm depth x 5 cm diameter) were collected, sealed in polythene bags, and kept on ice for <2 h. Cores were extruded and bulked upon return to the lab, and porewater samples obtained by centrifuging and filtration (as per method for incubation slurries).

3.3.4 Chemical and isotopic analyses

Following filtration, NO_3^- concentrations were measured in all samples using an ELIT 8021 ion selective electrode (detection limit: 0.01 μg l^{-1}) (www.nico2000.net). Approximately 10% of samples were re-analysed on a suppressed ion exchange chromatograph (Dionex DX-120 Ion

Chromatograph with an AS-50 Autosampler and an IonPac AG9-SC column) (Lincoln University, NZ) to ensure that there was no matrix interference to the ISE. Dissolved organic carbon (DOC) content was analysed on a Shimadzu TOC-5000A total organic C analyser fitted with an ASI-5000A auto sampler and total N and C via combustion on an Elementar EA-TCD (Lincoln University, NZ) (precision of ±0.04).

Nitrate isotopes ($\delta^{15}N$ and $\delta^{18}O$) were measured on two representative filtrates at each sampling interval (i.e., with NO_3^--N concentrations within ±1 SD). Samples were prepared using the Cd-azide method described by McIlvin and Altabet (2005) and analysed on a SerCon Europa 20/20 IRMS (Lincoln University, NZ). Results were calibrated using international standards USGS-32, USGS-34, IAEA-N3, giving an analytical range of -25‰ to +25‰ for $\delta^{18}O\text{-}NO_3^-$ and -4‰ to +178‰ for $\delta^{15}N\text{-}NO_3^-$ and internally-calibrated using KNO_3 and KNO_2 standards. Based on variations in international standards between runs, method accuracy was calculated as 0.8‰ for $\delta^{18}O\text{- }NO_3^-$ and 0.6‰ for $\delta^{15}N\text{- }NO_3^-$.

3.3.5 Quantitative analysis

Numerical solutions for theoretical R values for S1, S2 and S3 were generated iteratively for each unique combination of input parameters in Table 3.1 (see Appendix B for model details) (Mathematica ver. 7.0.2). The generated R values were then converted to δ notation and used to calculate ε_{eff} as per the simplified Rayleigh equations of Mariotti et al. (1981) (Eq. 3.8):

$$\delta^{15}N_x = \delta^{15}N_0 + {}^{15}\varepsilon \times \ln\left(\frac{f}{1-f}\right)$$

$$\delta^{18}O_x = \delta^{18}O_0 + {}^{18}\varepsilon \times \ln\left(\frac{f}{1-f}\right) \quad (3.8)$$

where ${}^{15}\varepsilon$ and ${}^{18}\varepsilon$ (either ε_{denit} (S1 solutions, intrinsic incubations) or ε_{eff} (S2 and S3 solutions, layered incubations, field samples) are equivalent to the linear slope between the natural log of the NO_3^- concentration relative to initial ($f = C/C_0$) and the equivalent change in isotopic enrichment ($\delta\text{-}\delta_0$). The slope, fit, and significance of regressions were determined using SPSS (ver.20).

Table 3.1 **Input parameters for numerical solutions to isotope fractionation models S1 (ideal), S2 (diffusion-limited) and S3 (mixing). Ranges are based on experimental findings from this study, as well as those of Garcia-Ruiz et al. (1998) and Buresh et al. (2008) for k_{denit}, Christensen et al. (1990) and House (2003) for L, Granger et al. (2008) for ε_{denit}, and Casciotti et al. (2003) for ε_{nit}. Values for $^{18}\varepsilon_D$ and $^{15}\varepsilon_D$ were calculated as per Eq. 3.5. (Isotope values are reported in δ‰ with respect to AIR for N and VSMOW for O).**

Variable	*Value*	
$\delta^{15}N\text{-}NO_3^-{}_0$	0‰	*(S1,S2,S3)*
$\delta^{18}O\text{-}NO_3^-{}_0$	0‰	*(S1,S2,S3)*
$C_0\ (NO_3^-)$	1 mg	*(S1,S2,S3)*
$C_0\ (NH_4^+)$	1 mg	*(S3)*
k_{denit}	$5.0\text{x}10^{-5} – 2.0\text{x}10^{-3}$ µg NO_3^- cm^{-2} s^{-1}	*(S2)*
	$1.0\text{x}10^{-3}$ µg NO_3^- cm^{-2} s^{-1}	*(S1,S3)*
k_{nit}	$2.5\text{x}10^{-4} – 2.0\text{x}10^{-3}$ µg NO_3^- cm^{-2} s^{-1}	*(S3)*
D_s	$3.0\text{x}10^{-4} – 1.4\text{x}10^{-3}$ cm^2 s^{-1}	*(S2)*
L	0.01 – 1.0 cm	*(S2)*
$^{15}\varepsilon_{denit}$	-2 – -31‰	*(S1,S2)*
	-17‰	*(S3)*
$^{18}\varepsilon_{denit}$	-2 – -31‰	*(S1,S2)*
	-17‰	*(S3)*
$^{15}\varepsilon_{nit}$	+20‰	*(S3)*
$^{18}\varepsilon_{nit}$	0‰	*(S3)*

Mixed models were used to assess differences between river sediments and paddy soils over time, with time and location as Type III factors (differences between effects were defined via the Least Significant Difference method) (SPSS ver.20). As dictated by experimental designs, time was treated as a repeated measure in only in paddy soil incubations. Differences between locations, sites, and treatments were tested using 1-way ANOVA (Tukey post-hoc). Pearson's correlation was used to establish relationships between chemistry, climate variables, and isotopes. Microsensor data for diffusion limitation incubations was converted into concentration profiles and fluxes using SensorTrace PRO® software and the PROFILE® model, which integrates concentration profiles to extrapolate fluxes and consumption rates, as described by Berg et al. (1998). Differences between LUDF and BC field samples were tested using a nested two-way ANOVA (with Sidak post-hoc), and paired t-tests to determine relationships within variables over depth. All results are reported as mean ±SD, unless otherwise noted, and significance is defined as $p<0.05$.

3.4 Results

3.4.1 Intrinsic fractionation (S1)

Despite the contrasting climates between IRRI and Harts Creek, there were no significant differences in denitrification dynamics or fractionation sediments between the locations (Table 3.2). Although there was no relationship between TOC and k_{denit}, substrate C/N was negatively correlated with k_{denit} (r = -0.972, p<0.001) (Table 3.2). In paddy soils, site G was less reducing (E_h = +65, compared to E (-221) and F (-158)) during the incubation period (Table 3.2).

Table 3.2 **Summary of physiochemical differences between sediments collected from different reaches along Harts Creek, a spring-fed stream (Canterbury, New Zealand) and from rice paddies with different cultivation history (International Rice Research Institute, Laguna, Philippines) (unique letters indicate significant differences (p<0.05)).**

	Air T *°C*	***Rain*** *mm*		***pH***	***TOC*** *mg C kg^{-1}*	***C/N***	***DO*** *mg O$_2$ l^{-1}*	***k_{denit}*** *mg N m^{-2} d^{-1}*
New Zealand streambed	10	600	*A*		41.1 ±11^{b}	11.8^{c}	7.42 ±0.2^{a}	34.7^{b}
			B		8.78 ±2^{a}	11.9^{c}	8.56 ±0.1^{b}	37.8^{b}
			C		707 ±40^{f}		9.11 ±0.1^{c}	11.4^{a}
			D		305 ±18^{e}	12.4^{d}	9.13 ±0.1^{c}	44.8^{b}
							Redox *mV*	
Philippine rice paddy	25	2500	*E*	7.32^{a}	130 ±3^{d}	10.4^{b}	-221 ±20^{a}	222^{c}
			F	7.30^{a}	79.2 ±3^{c}	9.00^{a}	-158 ±10^{b}	597^{d}
			G	8.19^{a}	46.5 ±10^{b,c}		64.5 ±21^{c}	274^{c}

The ratio of $\delta^{18}O\text{-}NO_3^-$ to $\delta^{15}N\text{-}NO_3^-$ in all seven sediments over the incubation period was 0.67 (p<0.001, r^2 = 0.92). Deviation from a 1:1 ratio was driven by C and G: the $\delta^{18}O$:$\delta^{15}N$ ratio was 0.80 (r^2 = 0.96, p<0.001) for only A, B, D, E, and F, versus 0.50 (r^2 = 0.95, p<0.001) for C and G (Fig. 3.2). The isotopic composition of NO_3^- in the control incubations for the substrates that produced 1:2 enrichment ratios was +3.94‰ ($\delta^{18}O$) and -3.58‰ ($\delta^{15}N$), lighter ($\delta^{18}O$: p<0.001; $\delta^{15}N$: p<0.01) than the values of +48.8‰ ($\delta^{18}O$) and +30.4‰ ($\delta^{15}N$) in controls for A, B, D, E, and F.

Enrichment factors ($^{15}\varepsilon_{denit}$ and $^{18}\varepsilon_{denit}$) varied by site (Fig. 3.2), as did k_{denit} (Table 3.2). However, both the highest (-28‰ at C) and lowest (-3‰ at B) $^{15}\varepsilon_{denit}$ values occurred in Harts Creek sediments (Fig. 3.2). Although the $^{15}\varepsilon_{denit}$ range was narrower in paddy soils (from -10‰ in E to -13‰ in F), variations in $^{15}\varepsilon_{denit}$, $^{18}\varepsilon_{denit}$, and k_{denit} between the three IRRI sites were significant (Table 3.2, Fig. 3.2). Overall, the range of $^{18}\varepsilon_{denit}$ was narrower than that of $^{15}\varepsilon_{denit}$, going from -17‰ (site D) to -3‰ (site B). Variations in $^{15}\varepsilon_{denit}$ between sites were controlled by sediment TOC content prior to glucose additions (Fig. 3.3) (r^2 = 0.82, p<0.001).

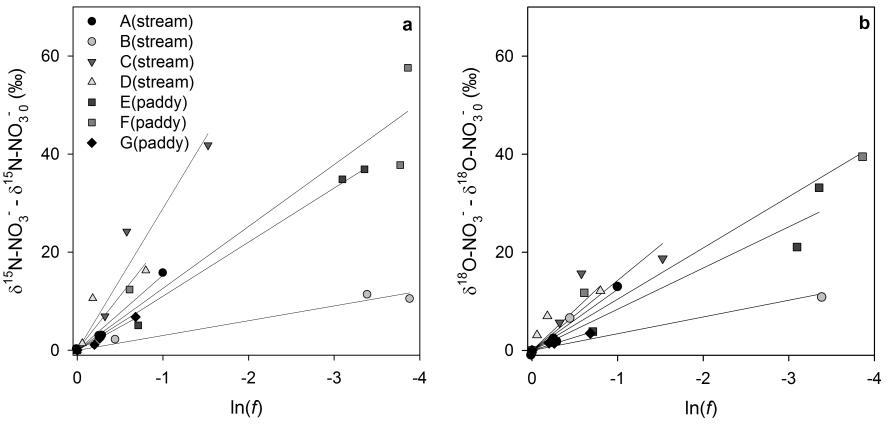

	$^{15}\varepsilon_{denit}$ (δ‰)	$^{18}\varepsilon_{denit}$ (δ‰)	$\delta^{18}O{:}\delta^{15}N$
A	-15.7 (0.99)^{d}	-13.5 (0.98)^{c}	0.89
B	-2.86 (0.98)^{a}	-2.58 (0.77)^{a}	1.03
C	-27.6 (0.94)^{e}	-11.7 (0.78)^{b}	0.50
D	-18.9 (0.86)^{e,d}	-16.5 (0.85)^{d,c}	0.96
E	-11.5 (0.99)^{c}	-8.83 (0.93)^{b}	0.77
F	-12.6 (0.91)^{c}	-10.4 (0.98)^{b}	0.77
G	-10.3 (0.98)^{b}	-4.97 (0.98)^{a}	0.55

Figure 3.2 **Isotope enrichment factors for (a) $\delta^{15}N\text{-}NO_3^-$ and (b) $\delta^{18}O\text{-}NO_3^-$ for denitrification in anaerobically incubated river sediments (A-D) (collected from four reaches along a spring-fed stream in Canterbury, New Zealand) and rice paddy soils (E-G) (collected from fields with different cultivation history at the International Rice Research Institute's experimental farm, Laguna, Philippines) following NO_3^- and C additions. Slopes of these lines define enrichment factors for $\delta^{15}N$ ($^{15}\varepsilon_{denit}$) and $\delta^{18}O$ ($^{18}\varepsilon_{denit}$), which are listed along with the ratio of $\delta^{18}O$ v. $\delta^{15}N$ enrichment, for each substrate (letters indicate significant difference at $p<0.05$).**

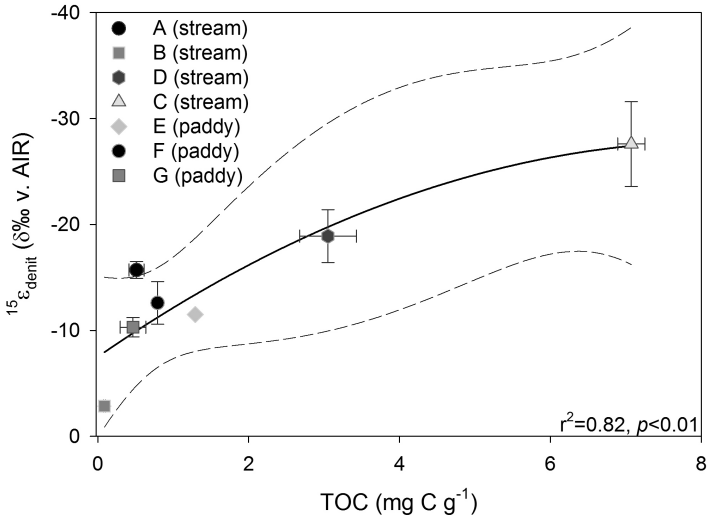

Figure 3.3 **Antecedent TOC content for four sediments and three paddy soils versus the strength of isotopic fractionation during denitrification ($^{15}\varepsilon_{denit}$) measured following glucose and KNO_3 additions under anaerobic conditions. Sediments were collected from four reaches along a spring-fed New Zealand stream and paddy soils from fields with varying cultivation histories in the Philippines. Symbols represent the mean (±SE) for each site, fitted to a 2nd order regression curve ($y = -7.5 - 0.05x + 3.0^{-5}x^2$) (solid line) with 95% confidence intervals (dashed lines).**

3.4.2 Effective fractionation (S2, S3)

Numerical solutions and model constraints

For all calculated diffusion-limited ε_{eff} (S2), change in $\delta^{15}N$ and $\delta^{18}O$ occurred linearly with respect to ln(*f*) (where *f* is equivalent to the concentration of NO_3^- at point *x* relative to initial NO_3^- concentration). As downstream flow velocity (*w*) controls the substrate supply to the sediments (Eq. 3.4), increasing *w* decreased ε_{eff} while simultaneously limiting the rate of NO_3^- consumption (data not shown). However, this effect was relatively small compared to that of other parameters (i.e., doubling *w* decreases ε_{eff} by only 0.02%).

Simultaneously increasing *L* and k_{denit} decreased the magnitude of $^{15}\varepsilon_{eff}$ and $^{18}\varepsilon_{eff}$ (Fig. 3.4). Due to the greater mass (larger α_D) of O relative to N, the magnitude of impact was greater for $^{18}\varepsilon_{eff}$ than $^{15}\varepsilon_{eff}$ (Fig. 3.4, Table 3.3). The ratio of $\delta^{18}O$:$\delta^{15}N$ decreased from the initial 1:1 under diffusion limited conditions (Table 3.3). The greater the diffusive limitation (i.e., the longer *L* and the steeper the diffusive gradient caused by faster rates of k_{denit}), the lower this ratio became, until eventually $\delta^{18}O$ became 'lighter' as NO_3^- concentration decreased, reflecting the $^{18}\alpha_D$ rather than $^{18}\varepsilon_{denit}$, creating an inverse relationship with $\delta^{15}N$, which reflected $^{15}\varepsilon_{denit}$ for longer (Table 3.3). The impact of diffusion (as measured via *L*, k_{denit}) on ε_{eff} was dependent on the initial ε_{denit} (-2 to -31‰), causing the range of ε_{eff} to decrease to as little as ±1‰ the more diffusion impacted the system (Table 3.3). Increasing D_s from $3.0x10^{-4}$ cm^2 s^{-1} (~ fine sediment) to $1.4x10^{-3}$ cm^2 s^{-1} (~sand) delayed the impact, but did not alter the magnitude, of these changes in ε_{eff} with respect to ε_{denit}, k_{denit}, and *L* (data not shown).

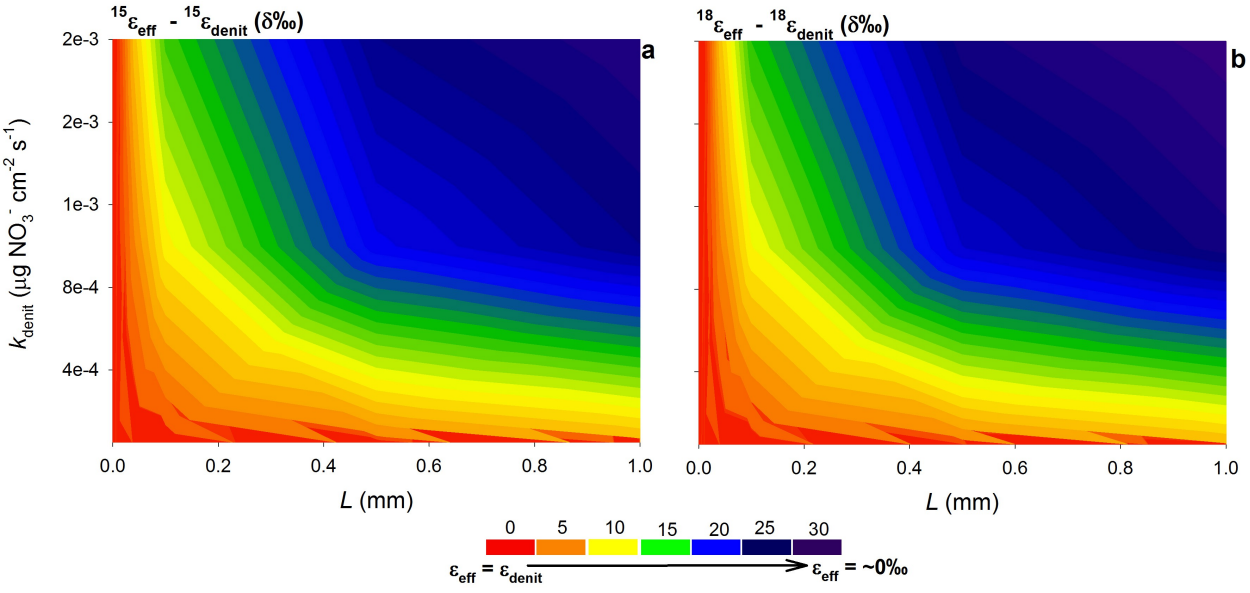

Figure 3.4 **Calculated effective (ε_{eff}) fractionation of $\delta^{15}N$-NO_3^- (a) and $\delta^{18}O$-NO_3^- (b) as influenced by diffusive transport of residual NO_3^- over distances (*L*) and varying rates of denitrification (k_{denit}) less the value of ε_{denit} prior to diffusion (either -2‰, -17‰, or -31‰) (input variables as per Table 3.1). Values of 0 (red) indicate no change from ε_{denit} to ε_{eff}, and large values (30) indicate that ε_{eff} is much less negative than ε_{denit}.**

Table 3.3 **Calculated effective enrichment factors for $\delta^{18}O\text{-}NO_3^-$ ($^{18}\varepsilon_{eff}$) and $\delta^{15}N\text{-}NO_3^-$ ($^{15}\varepsilon_{eff}$), as well as the ratio between the two, based on increasing distances of diffusive transport to/ from the denitrification zone (L), for denitrification rates (k_{denit}) from $5x10^{-5}$ (slow), to $1x10^{-3}$ (mid), to $2x10^{-3}$ (fast) µg NO_3^- cm^{-2} s^{-1}. All values are expressed as mean ±SD (n = 3 for each combination).**

Conditions		$^{18}\varepsilon_{eff}$ (‰ v. VSMOW)	$^{15}\varepsilon_{eff}$ (‰ v. AIR)	$\delta^{18}O$:$\delta^{15}N$
k_{denit}	L			
Slow	0 mm	-16.7 ±15	-16.7±15	1.0
	0.01 mm	-15.7 ±13	-15.6 ±13	1.0 ±0.01
	1.0 mm	-13.2 ±12	-12.9 ±12	0.92 ±0.1
Mid	0 mm	-16.7 ±15	-16.7±15	1.0
	0.01 mm	-11.5 ±10	-11.0 ±10	0.80 ±0.3
	1.0 mm	-2.11 ±4	-0.554 ±4	1.8 ±2
Fast	0 mm	-16.7 ±15	-16.7±15	1.0
	0.01 mm	-8.77 ±8	-7.97 ±8	0.36 ±1
	1.0 mm	-0.648 ±1	1.03 ±1	2.4 ±1

In S3, mixing NO_3^- from a nitrification pool (either on-going or a constant/ non-reacting) with a residual denitrification pool caused a non-linear relationship to develop between ln(f), $\delta^{18}O\text{-}NO_3^-$, and $\delta^{15}N\text{-}NO_3^-$ over x (time or distance) (Fig. 3.5a). Both the strength and slope of the intrinsic linear relationship between $\delta^{18}O\text{-}NO_3^-$, and $\delta^{15}N\text{-}NO_3^-$ from denitrification also decreased as a result of mixing. This relationship was controlled by the rate of k_{nit} relative to k_{denit}: the slope of the change in $\delta^{18}O$ v. the change in $\delta^{15}N$ increased from 0.42 (r^2 = 0.37, p<0.01,) when k_{nit} equalled $0.25k_{denit}$ to 0.56 (r^2 = 0.56, p<0.01) when k_{nit} equalled $2k_{denit}$ (Fig. 3.5b), but stayed at 1:1 (r^2 = 1, p<0.001) when the nitrification source was constant (i.e., k_{nit} = 0) (Fig. 3.5b).

Similarly, the faster k_{nit}, the larger the magnitude of $^{15}\varepsilon_{eff}$ (which actually became positive when $k_{nit} > k_{denit}$) (Fig. 3.5). The slope between $\delta^{15}N\text{-}NO_3^-$ and ln(f) stayed highly significant and strong (r^2 >0.98) for scenarios where k_{nit} and k_{denit} were co-occurring, while $\delta^{18}O\text{-}NO_3^-$ became relatively decoupled from NO_3^- concentrations (fit of $\delta^{18}O$ based Rayleigh diagrams ranged from 0.30 (k_{nit} = $0.25k_{denit}$) to 0.90 (k_{nit} = $1.5k_{denit}$) (Fig. 3.5). This breakdown in the $\delta^{18}O$:$\delta^{15}N$ relationship occurred at the point over x at which the concentration of NO_3^- began to increase as inputs from nitrification >> outputs from denitrification. There was no relationship between NO_3^- concentration and isotopic composition when mixing with a constant, rather than accumulating/fractionating, NO_3^- pool (Fig. 3.5).

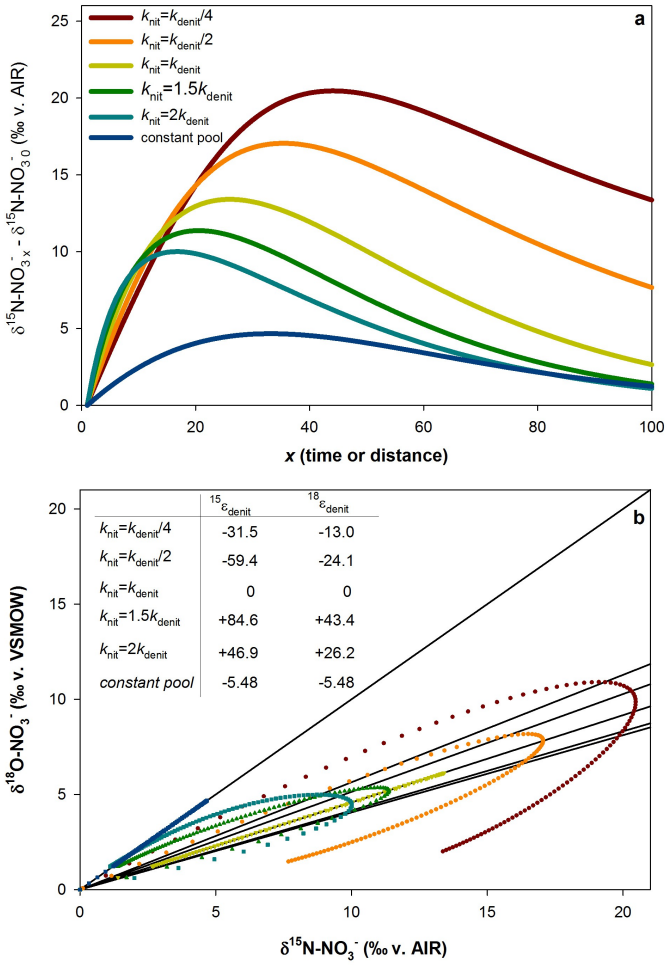

Figure 3.5 **Change in $\delta^{15}N\text{-}NO_3^-$ over x (time or distance) relative to its initial composition (a), and the composition of $\delta^{18}O\text{-}NO_3^-$ v. $\delta^{15}N\text{-}NO_3^-$ (b), as NO_3^- produced from nitrification mixes with residual NO_3^- from incomplete denitrification for varying rates of nitrification relative to denitrification (k_{nit} and k_{denit}, respectively), producing unique effective enrichment factors for both $\delta^{18}O$ ($^{18}\varepsilon_{eff}$) and $\delta^{15}N$ ($^{15}\varepsilon_{eff}$) for each.**

Layered incubations

The diffusivity of the sediments and sand used were $4.8x10^{-4}$ cm s^{-1} and $1.1x10^{-3}$ cm s^{-1}, respectively. The vertical distance between anaerobic (~0 µmol O_2 l^{-1}) and O_2 saturated (300 µmol O_2 l^{-1}) zones (L) was 4 mm in treatment L_0, 6 mm in L_1, and 10 mm in L_2 (Fig. 3.6a). There were no significant differences in net N_2O fluxes (production less reduction) between treatments, and steady-state N_2O concentration profiles showed the largest N_2O production between 30 mm and 45 mm depth (Fig. 3.6a). There was likewise no treatment effect on total (PW+SW) NO_3^- concentrations between treatments or over time. However, dynamics of NO_3^- in SW varied over time with diffusive layer thickness ($p<0.01$), with concentrations peaking 4 to 8 h after substrate additions in L_0 and L_1 and 96 h after additions in L_2.

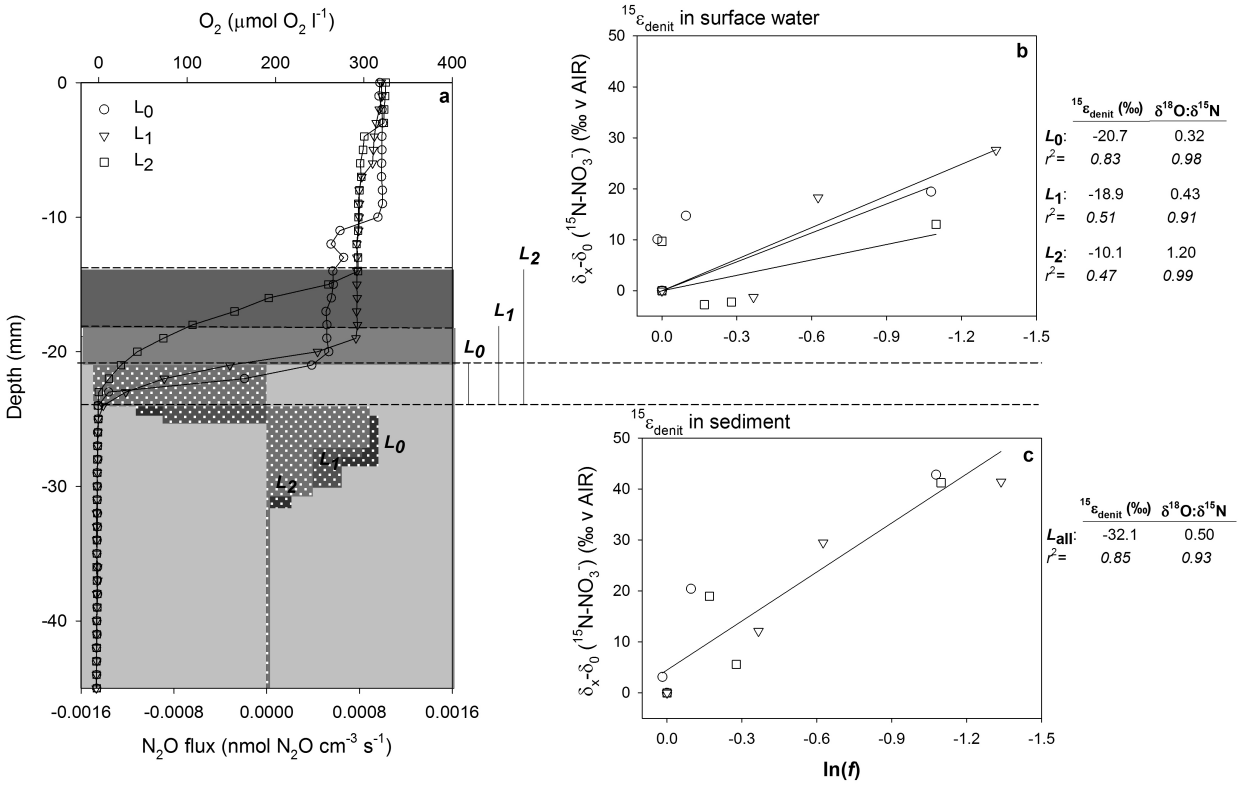

Figure 3.6 **Concentrations of O_2 (lines + symbols) and flux of N_2O (rectangles) over depth in layered sediment incubations, from surface water (0 mm) through sediments (a). Sediments (collected from Harts Creek, Canterbury, New Zealand) were overlain with either 0 mm (L_0), 4 mm (L_1), or 8 mm (L_2) of quartz sand, plus ~4 cm of water. The change in composition of $\delta^{15}N\text{-}NO_3^-$ in the surface water (b) and sediment porewater (c) was plotted versus the natural log of the change in NO_3^- concentration ($f = NO_3^-\text{-}N/NO_3^-\text{-}N_0$) to calculate $^{15}\varepsilon_{denit}$ (tabulated on left).**

There was a positive linear relationship between $\delta^{18}O\text{-}NO_3^-$ and $\delta^{15}N\text{-}NO_3^-$ ($\delta^{18}O_{pw}$ and $\delta^{15}N_{pw}$, respectively) in PW (x = 0.718, $r^2 = 0.718$, $p<0.001$). The relationship between the two isotopes in SW was linear (x = 0.262, $r^2 = 0.37$, $p<0.05$), but not as strong or as consistent as in PW. The $\delta^{18}O$ and $\delta^{15}N$ values in PW are positively correlated with, but not equal to, $\delta^{18}O$ and $\delta^{15}N$ in SW ($\delta^{18}O$: $r = 0.625$, $p<0.01$; $\delta^{15}N$: $r = 0.794$, $p<0.001$). All treatments had a $^{15}\varepsilon_{denit}$ value of -32‰ in PW, while $^{15}\varepsilon_{denit}$ in SW varied from -20‰ (L_0) to -10‰ (L_2) (Fig. 3.6). However, the difference between $^{15}\varepsilon_{denit}$ in SW v. PW was only significant in treatment L_2.

Interestingly, when the value of ln(*f*) for the whole incubation (PW + SW) was < -2 (90% NO_3^--N attenuated), $\delta^{18}O$ and $\delta^{15}N$ (concentration-weighted means for PW + SW) became *less* enriched relative to the previous measurement point (Fig. 3.7). These shifts in isotopic enrichment moved the $\delta^{18}O$ and $\delta^{15}N$ in treatments closer to that in controls (+9.19‰ for $\delta^{15}N$ and +5.20‰ for $\delta^{18}O$ over time) (Fig. 3.7a), and caused $^{15}\varepsilon_{eff}$ to shift from -28‰ ($r^2 = 0.95$) to -7.9‰ ($r^2 = 0.18$) and $^{18}\varepsilon_{eff}$ from -14‰ ($r^2 = 0.78$) to ~nil after 96 h (Fig. 3.7b).

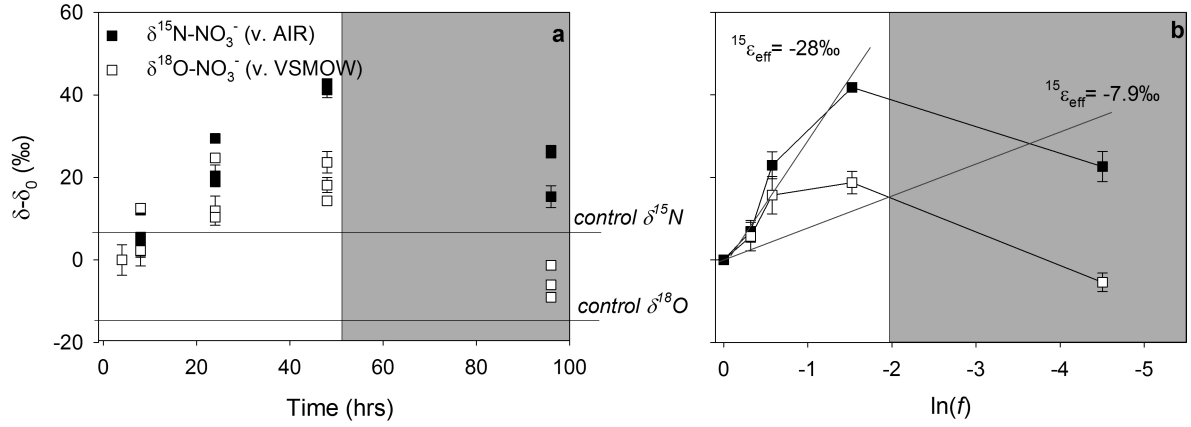

Figure 3.7 **Change in $\delta^{18}O\text{-}NO_3^-$ and $\delta^{15}N\text{-}NO_3^-$ in the sediment porewater of layered incubations over time following KNO_3 additions (symbols) or left as controls (horizontal lines) (a) and plotted v. the natural log of the change in substrate concentration ($f = NO_3\text{-}N/NO_3\text{-}N_0$) based on total NO_3^- concentrations per incubator (surface water + porewater), which yields a slope for $\delta^{15}N$ ($^{15}\varepsilon_{eff}$) of -28 ($r^2 = 0.95$) if the final sampling date is excluded, and a slope of -7.9 ($r^2 = 0.18$) if it is not (b). Symbols represent the mean (±SE) from sediments overlain by either 0, 4, or 8 mm of quartz sand, plus ~4 cm of water ($n = 3$ per treatment per time).**

Surface water v. porewater in streams

Sediments from BC had lower TOC and %C (loss on ignition) than those from LUDF (138 ±9 versus 267 ±8 µg TOC g^{-1} ($p<0.001$) and 10.5 ±3 versus 4.41 ±1 %C (w/w) ($p<0.05$), respectively). All locations and sites had a mean water column depth of 18 cm, water temperature of 3.92 ±1 ºC, DO (SW and DW) of 12.8 ±0.4 mg O_2 l^{-1}, and porewater DO of <1 mg O_2 l^{-1}. There were no significant differences in NO_3^- concentration or isotopic composition between SW and DW, but both had less enriched N and O relative to PW ($p<0.05$) (Fig. 3.8). The ratio of change in $\delta^{18}O$ to $\delta^{15}N$ over depth was 0.96 ($r^2 = 0.69$) in BC and 0.23 ($r^2 = 0.50$) in LUDF. Nitrate concentrations in SW decreased over distance by 0.02 mg NO_3^--N l^{-1} in LUDF and by 0.2 mg NO_3^--N l^{-1} in BC ($p<0.05$), while NO_3^- concentrations and isotopic compositions in PW did not vary over distance. Nitrate isotopes in SW and DW at both sites became enriched over stream length ($p<0.001$) at a $\delta^{18}O$ to $\delta^{15}N$ ratio of 1.2:1 ($r^2 = 0.8$, $p<0.01$). The relationship between changing concentration and isotopic composition in SW+DW over distance was used to calculate $^{15}\varepsilon_{eff}$ of -200‰ (LUDF) and -9‰ (BC), as per Eq. 3.8 (Fig. 3.8).

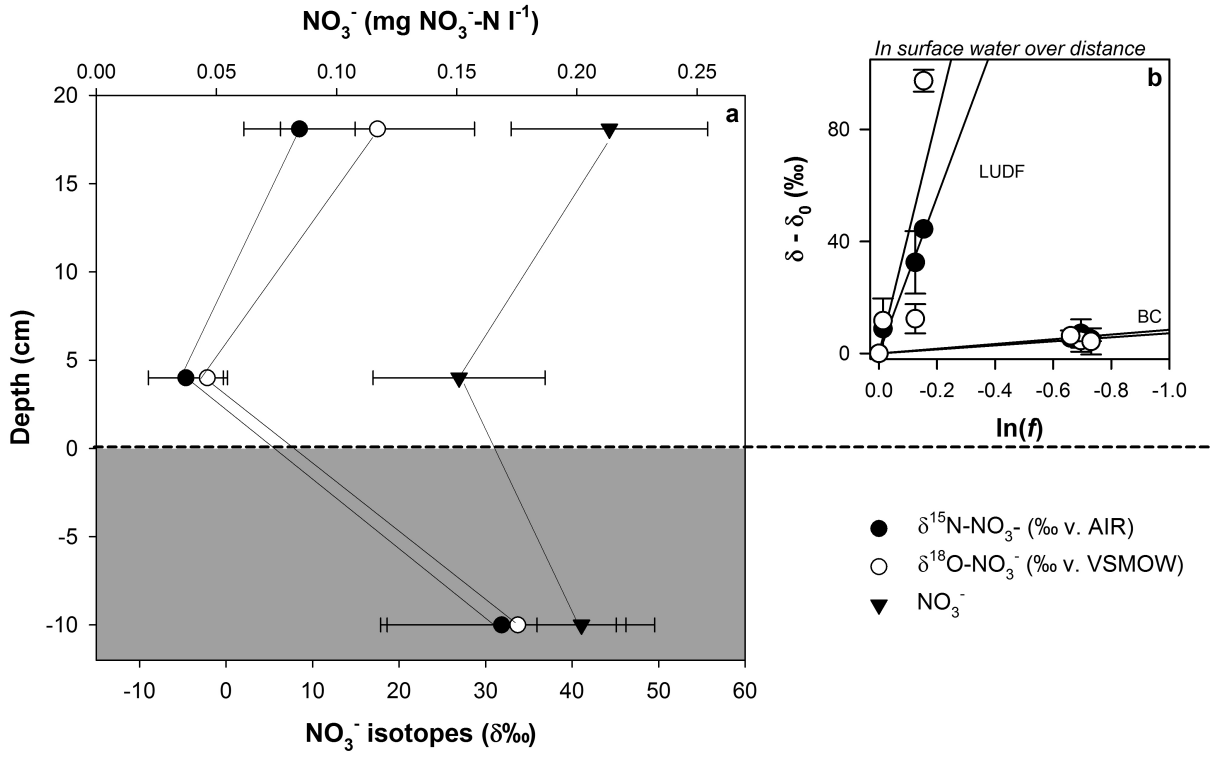

Figure 3.8 **The concentration and isotopic composition of NO_3^- over depth (with the sediment-surface water interface as 0), from samples taken at 4 cm below the water's surface, 4 cm above the sediments, and from porewater (0-10 cm depth) based on means (±SE) of samples collected from four sites along along two irrigation ditches in Canterbury, New Zealand (LUDF and BC) (a). Variations in $\delta^{15}N\text{-}NO_3^-$ and NO_3^- concentration in the surface water over distance yielded ε_{eff} values of -200‰ ($r^2 = 0.98$) -9‰ ($r^2 = 0.85$) for LUDF and BC, respectively (b).**

3.5 Discussion

3.5.1 Intrinsic variation

The ratio of $\delta^{18}O$:$\delta^{15}N$ during denitrification in anaerobic sediments / soils was not consistently 1:1. This ratio was lowest in the highly C enriched soils and sediments, where it was ~1:2. While 1:2 $\delta^{18}O$:$\delta^{15}N$ enrichment ratios have been found in pure culture studies by Knoller et al. (2011) and in a freshwater sediment incubation by Sebilo et al. (2003), the mechanism controlling the shift between 1:1 and 1:2 is not understood. However, the range from 1:1 to 1:2 for $\delta^{18}O$:$\delta^{15}N$ enrichment ratios found here for freshwater sediments and soils reveals that 1:2 is not a universal product of freshwater denitrification, as was previously hypothesised (e.g., Burns et al. 2009, Ostrom et al. 2002).

Despite the uniform C, N, and O_2 availability within the incubations, $^{15}\varepsilon_{denit}$ ranged from -3‰ to -28‰, spanning the published range for in-vitro studies (Chapter 2). This range did not separate between 'tropical' and 'temperate' locations, but was instead driven by differences at the km scale. While this is the first study to explicitly measure spatial variations in ε_{denit}, the site-specificity of $^{15}\varepsilon_{denit}$ is supported by the findings of Chien et al. (1977), who found that field cultivation history (now known to influence microbial community composition (Wang et al. 2009, Tang et al. 2010)) drove a 10‰ shift in soil ε_{denit} values.

The influence of antecedent C availability, rather than k_{denit}, on ε_{denit} supports the hypothesis that the site-specificity of intrinsic fractionation reflects fundamental differences in denitrifier populations, as C availability is known to control denitrifier community composition (Wallenstein et al. 2006). Pintar et al. (2008) also recorded significant differences between ε_{denit} in C rich surface soil v. C depleted subsoil following incubation with excess glucose-C and NO_3^-. However, unlike previous studies that linked faster k_{denit} induced by increased C availability to decreasing isotopic discrimination, and thus decreasing ε_{denit} (e.g., Mariotti et al. 1982, Pintar et al. 2008), here the relationship between C and ε_{denit} was independent of k_{denit}. The fact that antecedent C, rather than k_{denit} or glucose-C, dictated the strength of ε_{denit} supports the hypothesis that variation at the field scale is dictated by differences in denitrifier populations. This is further corroborated by the known ~20‰ variation in ε_{denit} between denitrifier strains (Granger et al. 2008) and evidence for site-to-site variation of denitrifier populations independent of environmental/ chemical variables (e.g., Singh et al. 2011, Liu et al. 2009).

In light of these findings, further research into the relationship between ε_{denit}, k_{denit}, and denitrifier composition may resolve questions of microbial structure v. function (i.e., 'who' is doing 'what'). The wide range of ε_{denit} values found to occur in natural sediments collected even within a few km to m of each-other, supports the diversity of expression produced by pure denitrifier cultures (Granger et al. 2008, Knoller et al. 2011, Kritee et al. 2012) and supports the supposition that environmental, rather than microbial, factors determine the relatively narrow range of $^{15}\varepsilon_{eff}$ measured in rivers and streams, as well as the commonly cited 1:2 enrichment ratio (Chapter 2). The potential expression of the measured ε_{denit} values in surface waters were evaluated by inputing a range of -2 to -30‰ ε_{denit} into S2 and S3 calculations.

3.5.2 Diffusive limitation

The developed model confirms that diffusive transport of NO_3^- through denitrifying zones and into the aerobic surface water, where measurements are typically collected, could account for the low ε_{eff} values typically found in rivers (Chapter 2). As O is relatively more impacted by diffusion than N (Eq. 3.5), meaning that, under diffusion-limited conditions, $^{18}\varepsilon_{eff}$ would be lower than $^{15}\varepsilon_{eff}$. Thus α_D could account for the consistent reporting of $\delta^{18}O{:}\delta^{15}N$ enrichment ratios of ~0.5 in aerobic freshwater environments (e.g., Burns et al. 2009, Barnes and Raymond 2010).

The differences in ε_{eff} measured in the surface water v. porewater of incubations with varying L distances confirmed the impact of diffusion across the sediment-water interface on ε_{denit} expression. Increasing L (i.e., deeper penetration of O_2 into the benthic (Christensen et al. 1990)), and finer sediments, also decreased $\delta^{18}O{:}\delta^{15}N$ ratio, a fact that adds nuance to the finding of Sebilo et al. (2003) that ε_{eff} strength decreased when sediments were incubated under stagnant, rather than continuously mixed, conditions. As indicated with the model, both ε_{eff} and $\delta^{18}O{:}\delta^{15}N$ in the 'layered' incubations were proportional to ε_{denit}.

The S2 equations reveal a synergistic relationship between increasing k_{denit} and L that can completely 'mask' denitrification's isotopic signature (i.e., under the most extreme diffusive limitation calculated, the relationship between $\delta^{18}O$:$\delta^{15}N$ reflects α_D rather than α_{denit}, and there is no relationship between $\delta^{18}O$, $\delta^{15}N$, and NO_3^- concentration). However, such complete masking would only occur in environments with rapid k_{denit} rates and long L, which are unlikely to co-occur in freshwater systems, where increasing L is caused by greater O_2 penetration, which in turn inhibits denitrification (Berg et al., 1998; House, 2003). Even though rapid sedimentary k_{denit} have been reported in response to organic matter additions in O_2-saturated water columns (Baxter et al. 2012), it is unlikely that such conditions could continue for an appreciable length of time in uncontrolled settings, as high organic inputs would drive rapid consumption of O_2 (House 2003, Glud et al. 2007), directly linking increasing k_{denit} to decreasing L.

This example highlights the difficulties inherit to up-scaling these interactions between ε_{denit} and diffusion to the catchment scale: both L and k_{denit} (identified here as the primary drivers of ε_{eff} in diffusion limited systems) vary dramatically over time and space with changes in hydrology and streambed biogeochemistry (Cook et al. 2006, Marzadri et al. 2012, Zarnetske et al. 2012). For instance, changes from wet to dry season flows can change the balance of advective v. diffusive water movement (O'Connor and Hondzo 2008), redox conditions of the streambed (Christensen et al. 1990, Berg et al. 1998), and k_{denit} (Mulholland et al. 2009). However, under the basis that ε_{denit} is unlikely to be completely masked by diffusion, these findings provide a functional framework for identifying the appropriate ε_{eff} range for a given location based on the k_{denit} capacity of the benthos (e.g., OM content, NO_3^- concentrations, water column DO (Rissanen et al. 2011, Johnson et al. 2012)) and diffusive v. advective transport (e.g., losing v. gaining streams (Ruehl et al. 2007), water residence time (Zarnetske et al. 2012), water column DO (House 2003), sediment porosity (Cook et al. 2006, Marzadri et al. 2012)). Considering the high degree of ε_{denit} variability found in sediments within the same stream, it seems that, rather than prohibiting the application of NO_3^- isotope based attenuation assessments, diffusion-limited environments may actually produce more uniform ε_{eff} than if they directly reflected highly variable ε_{denit}.

3.5.3 Nitrification

Mixing denitrification's residual NO_3^- pool with a growing NO_3^- pool (active nitrification) v. a constant NO_3^- pool (nitrification distal) reveal key differences in theoretical ε_{eff}: NO_3^- from a distal source (i.e., mixing of denitrified NO_3^- with a constant pool of NO_3^-) decreased/ masked $^{15}\varepsilon_{eff}$ and $^{18}\varepsilon_{eff}$, but maintained the intrinsic $\delta^{18}O$:$\delta^{15}N$ enrichment ratio, whereas the co-occurrence of nitrification and denitrification increased the magnitude of $^{15}\varepsilon_{eff}$ and dampened the $\delta^{18}O$:$\delta^{15}N$ ratio. Based on S3 calculations, the relative rate of nitrification to denitrification could determine $^{15}\varepsilon_{eff}$ and $^{18}\varepsilon_{eff}$ measured in surface water. Specifically, the 1:2 ratio of $\delta^{18}O$:$\delta^{15}N$ commonly found in freshwater systems could be a result of widespread NO_3^- production and reduction in hyporheic and riparian zones (a contrasted

to marine environments, where production of NO_3^- can centuries and 100 km distal to its reduction (denitrification)) (Seitzinger et al. 2006).

This role of nitrification in dictating ε_{eff} was evident in the 'layered' incubations, where an isotopic nitrification signature only became obvious once the NO_3^- concentration dropped below 10% of the original (Fig. 3.7), which was also the modelled 'inflection points' in $\delta^{15}N\text{-}NO_3^-$ enrichment (Fig. 3.5). According to the theoretical S3 solutions, co-occurring nitrification and denitrification could also explain the fact that NO_3^- isotopic composition in the layered incubations moved towards controls values. The output S3 also emphases that, while increasing isotope enrichment with decreasing ln(*f*) should always indicate the occurrence of denitrification, a lack of relationship between these two factors does not prove the absence of denitrification, but instead only that denitrification is not the dominant determinant of NO_3^- pool size.

3.5.4 Implications and field application

The advantage of basing attenuation calculations on this set range, as opposed to in-situ measurements, is highlighted by the $^{15}\varepsilon_{eff}$ value of -200‰ measured in LUDF. Based on S2 and S3 outcomes, this value is hypothesised to reflect a continuous mixing between the residual denitrified NO3- pool and an influxing NO_3^- pool from nitrification over stream length. This scenario is supported by the fact that $\delta^{15}N\text{-}NO_3^-$ enrichment during downstream transport did not correspond with changes in water column NO_3^- concentrations. Using an $^{15}\varepsilon_{eff}$ range of -2 to -10‰ to LUDF and BC yielded estimates of NO_3^- attenuation over distance of 0.99 ±0.01 and 0.58 ±0.01, respectively (where attenuation is defined as 1-*f* (Eq. 3.8) (Ostrom et al. 2002)). In contrast, if the empirically measured $^{15}\varepsilon_{eff}$ of -200‰ was used attenuation in LUDF was calculated to be only 0.39%. Using $^{15}\varepsilon_{eff}$ based on empirical surface water concentrations v. isotopic compositions would result in a dramatic underestimation of net attenuation. These case studies also emphasise the value that NO_3^- isotope measurements can bring to water quality monitoring: mixing nitrification and denitrification at LUDF meant that the concentration of NO_3^- varied minimally over the studied reach, which, without isotopic information, would lead to the erroneous conclusion that total N lost from the system was minimal.

The conducted field study highlights the necessity of accounting for intrinsic variation, diffusive transport, and source mixing in order to accurately use NO_3^- isotopes to describe biogeochemical cycling in a surface water ecosystem. However, neither of the two ε_{eff} scenarios (diffusion and mixing) discussed here satisfactorily explain why $^{18}\varepsilon_{denit}$ is often cited as the 'more reliable' variable for identifying and quantifying denitrification (e.g., Barnes and Raymond 2010). Indeed, tight coupling between nitrification and denitrification actually decreases the strength of the relationship between $\delta^{18}O$ composition and NO_3^- concentration, while a strong diffusive limitation inhibits expression of $^{18}\varepsilon_{denit}$ more than that of $^{15}\varepsilon_{denit}$. My measurements of ε_{denit} in sediments and soils found $^{18}\varepsilon_{denit}$ to be less variable than $^{15}\varepsilon_{denit}$, leading to the hypothesis that the perceived reliability of $\delta^{18}O$ over $\delta^{15}N$ as a process indicator could actually reflect an intrinsic, biologically driven factors. The

framework described in this paper provides a practical tool for evaluating an appropriate range of ε_{denit} to use for evaluating NO_3^- attenuation in a given freshwater environment.

3.6 Conclusions

The ~20‰ variation in $^{15}\varepsilon_{denit}$ found between sediments collected from different reaches along the same 20 km stream is of particular interest, given that a single, unique ε_{denit} values is often used to explain whole-system NO_3^- dynamics (e.g., Sebilo et al. 2003). Our findings suggest that assigning a precise value of ε_{denit} to environments such as streams, where the NO_3^- in the surface water represents an integrated $\varepsilon_{denit} \times f$ for each reach, could result in a misrepresentation of N cycling. Conversely, variation between relatively similar submerged paddy fields highlights the necessity of establishing a site-specific ε_{denit} even in such hydrologically homogeneous settings. Given the above illustration of the environmental variability of both ε_{denit} and ε_{eff}, the application of a precise ε_{eff} value to a highly heterogeneous system could mask variance, decreasing the precision of the resultant calculations.

Under the basis that ε_{denit} is unlikely to be completely masked by diffusion, these findings provide a functional framework for identifying the appropriate ε_{eff} range for a given location based on the k_{denit} capacity of the benthos (e.g., organic matter content, NO_3^- concentrations, water column DO (Rissanen et al. 2011, Johnson et al. 2012) and diffusive v. advective transport (e.g., losing v. gaining streams (Ruehl et al. 2007), water residence time (Zarnetske et al. 2012), water column DO (House 2003), sediment porosity (Cook et al. 2006, Marzadri et al. 2012)). Considering the high degree of ε_{denit} variability found in sediments within the same stream, it seems that, rather than prohibiting the application of NO_3^- isotope based attenuation assessments, diffusion-limited environments may actually produce more uniform ε_{eff} than if they directly reflected highly variable ε_{denit}. The measured broad range of intrinsic fractionation, combined with a variable yet, yet homogenising, effect from diffusive transport, it is proposed that an ε_{eff} range of -2‰ to -10‰ can be confidently applied to aerobic surface water isotopic measurements in order to assess attenuation fluxes (as per Eq. 3.1 and Eq. 3.8).

3.7 Acknowledgements

Samples from New Zealand streams were collected with assistance from Janet Bertram (Lincoln University) and those from the Philippines with assistance from Sonny Pantoja, Angel Bautista, and Jerone Onoya (International Rice Research Institute). Anoxic incubation chambers were set-up with assistance from Mia Bunquin and Sarah Johnson-Beebout (International Rice Research Institute). Thanks to Bo Elberling (University of Copenhagen) for assistance with the microsensors, Troy Baisden (GNS Science) for assistance with maths and Mathematica alike. Additionally, thanks to Roger Cresswell and Joy Jaio (Lincoln University) for assistance with chemical analyses. Research was funded by FRST (Foundation for Research, Science and Technology, New Zealand) grant C05X0803 to W.T. Baisden / GNS Science, with additional support from a U.S. Student Fulbright Scholarship to N.S. Wells. Troy Baisden and Tim Clough both provided feedback on early drafts of this manuscript.

3.8 References

Abe, Y. and D. Hunkeler. 2006. Does the Rayleigh equation apply to evaluate field isotope data in contaminant hydrogeology? Environmental Science & Technology **40**:1588-1596.

Ahn, J. H., J. Song, B. Y. Kim, M. S. Kim, J. H. Joa, and H. Y. Weon. 2012. Characterization of the bacterial and archaeal communities in rice field soils subjected to long-term fertilization practices. Journal of Microbiology **50**:754-765.

Alexander, R. B., R. A. Smith, and G. E. Schwarz. 2000. Effect of stream channel size on the delivery of nitrogen to the Gulf of Mexico. Nature **403**:758-761.

Bannert, A., K. Kleineidam, L. Wissing, C. Mueller-Niggemann, V. Vogelsang, G. Welzl, Z. H. Cao, and M. Schloter. 2011. Changes in diversity and functional gene abundances of microbial communities involved in nitrogen fixation, nitrification, and denitrification in a tidal wetland versus paddy soils cultivated for different time periods. Applied and Environmental Microbiology **77**:6109-6116.

Barnes, R. T. and P. A. Raymond. 2010. Land-use controls on sources and processing of nitrate in small watersheds: insights from dual isotopic analysis. Ecological Applications **20**:1961-1978.

Baxter, A. M., L. Johnson, J. Edgerton, T. Royer, and L. G. Leff. 2012. Structure and function of denitrifying bacterial assemblages in low-order Indiana streams. Freshwater Science **31**:304-317.

Berg, P., N. Risgaard-Petersen, and S. Rysgaard. 1998. Interpretation of measured concentration profiles in sediment pore water. Limnology and Oceanography **43**:1500-1510.

Bissett, A., A. E. Richardson, G. Baker, S. Wakelin, and P. H. Thrall. 2010. Life history determines biogeographical patterns of soil bacterial communities over multiple spatial scales. Molecular Ecology **19**:4315-4327.

Brandes, J. A. and A. H. Devol. 1997. Isotopic fractionation of oxygen and nitrogen in coastal marine sediments. Geochimica Et Cosmochimica Acta **61**:1793-1801.

Brandes, J. A. and A. H. Devol. 2002. A global marine-fixed nitrogen isotopic budget: Implications for Holocene nitrogen cycling. Global Biogeochemical Cycles **16**:14.

Buchwald, C., A. E. Santoro, M. R. McIlvin, and K. L. Casciotti. 2012. Oxygen isotopic composition of nitrate and nitrite produced by nitrifying cocultures and natural marine assemblages. Limnology and Oceanography **57**:1361-1375.

Buresh, R. J., K. R. Reddy, and C. van Kessel. 2008. Nitrogen Transformations in Submerged Soils. Pages 401-436 Nitrogen in Agricultural Systems.

Burns, D. A., E. W. Boyer, E. M. Elliott, and C. Kendall. 2009. Sources and transformations of nitrate from streams draining varying land uses: Evidence from dual isotope analysis. Journal of Environmental Quality **38**:1149-1159.

Casciotti, K. L., D. M. Sigman, and B. B. Ward. 2003. Linking diversity and stable isotope fractionation in ammonia-oxidizing bacteria. Geomicrobiology Journal **20**:335-353.

Chien, S. H., G. Shearer, and D. H. Kohl. 1977. The nitrogen isotope effect associated with nitrate and nitrite loss from waterlogged soils. Soil Science Society of America Journal **41**:63-69.

Christensen, P. B., L. P. Nielsen, J. Sorensen, and N. P. Revsbech. 1990. Denitrification in nitrate-rich streams - diurnal and seasonal variation related to benthic oxygen-metabolism. Limnology and Oceanography **35**:640-651.

Cook, P. L. M., F. Wenzhofer, S. Rysgaard, O. S. Galaktionov, F. J. R. Meysman, B. D. Eyre, J. Cornwell, M. Huettel, and R. N. Glud. 2006. Quantification of denitrification in permeable sediments: Insights from a two-dimensional simulation analysis and experimental data. Limnology and Oceanography-Methods **4**:294-307.

Elberling, B., H. H. Christiansen, and B. U. Hansen. 2010. High nitrous oxide production from thawing permafrost. Nature Geoscience **3**:332-335.

Findlay, S. 2010. Stream microbial ecology. Journal of the North American Benthological Society **29**:170-181.

Findlay, S. E. G., P. J. Mulholland, S. K. Hamilton, J. L. Tank, M. J. Bernot, A. J. Burgin, C. L. Crenshaw, W. K. Dodds, N. B. Grimm, W. H. McDowell, J. D. Potter, and D. J. Sobota. 2011. Cross-stream comparison of substrate-specific denitrification potential. Biogeochemistry **104**:381-392.

Galloway, J. N., J. D. Aber, J. W. Erisman, S. P. Seitzinger, R. W. Howarth, E. B. Cowling, and B. J. Cosby. 2003. The nitrogen cascade. Bioscience **53**:341-356.

Galloway, J. N., A. R. Townsend, J. W. Erisman, M. Bekunda, Z. C. Cai, J. R. Freney, L. A. Martinelli, S. P. Seitzinger, and M. A. Sutton. 2008. Transformation of the nitrogen cycle: Recent trends, questions, and potential solutions. Science **320**:889-892.

Garcia-Ruiz, R., S. N. Pattinson, and B. A. Whitton. 1998. Denitrification in river sediments: relationship between process rate and properties of water and sediment. Freshwater Biology **39**:467-476.

Glud, R. N., P. Berg, H. Fossing, and B. B. Jorgensen. 2007. Effect of the diffusive boundary layer on benthic mineralization and O_2 distribution: A theoretical model analysis. Limnology and Oceanography **52**:547-557.

Granger, J., D. M. Sigman, M. F. Lehmann, and P. D. Tortell. 2008. Nitrogen and oxygen isotope fractionation during dissimilatory nitrate reduction by denitrifying bacteria. Limnology and Oceanography **53**:2533-2545.

Groffman, P. M., M. A. Altabet, J. K. Bohlke, K. Butterbach-Bahl, M. B. David, M. K. Firestone, A. E. Giblin, T. M. Kana, L. P. Nielsen, and M. A. Voytek. 2006. Methods for measuring denitrification: Diverse approaches to a difficult problem. Ecological Applications **16**:2091-2122.

Groffman, P. M., K. Butterbach-Bahl, R. W. Fulweiler, A. J. Gold, J. L. Morse, E. K. Stander, C. Tague, C. Tonitto, and P. Vidon. 2009. Challenges to incorporating spatially and temporally

explicit phenomena (hotspots and hot moments) in denitrification models. Biogeochemistry **93**:49-77.

Higashino, M., B. L. O'Connor, M. Hondzo, and H. G. Stefan. 2008. Oxygen transfer from flowing water to microbes in an organic sediment bed. Hydrobiologia **614**:219-231.

Hondzo, M., T. Feyaerts, R. Donovan, and B. L. O'Connor. 2005. Universal scaling of dissolved oxygen distribution at the sediment-water interface: A power law. Limnology and Oceanography **50**:1667-1676.

House, W. A. 2003. Factors influencing the extent and development of the oxic zone in sediments. Biogeochemistry **63**:317-333.

Johnson-Beebout, S. E., O. R. Angeles, M. C. R. Alberto, and R. J. Buresh. 2009. Simultaneous minimization of nitrous oxide and methane emission from rice paddy soils is improbable due to redox potential changes with depth in a greenhouse experiment without plants. Geoderma **149**:45-53.

Johnson, L. T., T. V. Royer, J. M. Edgerton, and L. G. Leff. 2012. Manipulation of the dissolved organic carbon pool in an agricultural stream: Responses in microbial community structure, denitrification, and assimilatory nitrogen uptake. Ecosystems **15**:1027-1038.

Kendall, C. and E. A. Caldwell. 1998. Fundamentals of Isotope Geochemistry *in* C. Kendall and J. J. McDonnell, editors. Isotope Tracers in Catchment Hydrology. Elsevier Science B.V., Amsterdam.

Knoller, K., C. Vogt, M. Haupt, S. Feisthauer, and H. H. Richnow. 2011. Experimental investigation of nitrogen and oxygen isotope fractionation in nitrate and nitrite during denitrification. Biogeochemistry **103**:371-384.

Kogel-Knabner, I., W. Amelung, Z. H. Cao, S. Fiedler, P. Frenzel, R. Jahn, K. Kalbitz, A. Kolbl, and M. Schloter. 2010. Biogeochemistry of paddy soils. Geoderma **157**:1-14.

Kritee, K., D. M. Sigman, J. Granger, B. B. Ward, A. Jayakumar, and C. Deutsch. 2012. Reduced isotope fractionation by denitrification under conditions relevant to the ocean. Geochimica Et Cosmochimica Acta **92**:243-259.

LaBolle, E. M., G. E. Fogg, J. B. Eweis, J. Gravner, and D. G. Leaist. 2008. Isotopic fractionation by diffusion in groundwater. Water Resources Research **44**:15.

Lehmann, M. F., P. Reichert, S. M. Bernasconi, A. Barbieri, and J. A. McKenzie. 2003. Modelling nitrogen and oxygen isotope fractionation during denitrification in a lacustrine redox-transition zone. Geochimica Et Cosmochimica Acta **67**:2529-2542.

Liu, M. Q., F. Hu, X. Y. Chen, Q. R. Huang, J. G. Jiao, B. Zhang, and H. X. Li. 2009. Organic amendments with reduced chemical fertilizer promote soil microbial development and nutrient availability in a subtropical paddy field: The influence of quantity, type and application time of organic amendments. Applied Soil Ecology **42**:166-175.

Mariotti, A., J. C. Germon, P. Hubert, P. Kaiser, R. Letolle, A. Tardieux, and P. Tardieux. 1981. Experimental-determination of nitrogen kinetic isotope fractionation - some principles - illustration for the denitrification and nitrification processes. Plant and Soil **62**:413-430.

Mariotti, A., J. C. Germon, and A. Leclerc. 1982. Nitrogen isotope fractionation associated with the NO_2--N_2O step of denitrification in soils. Canadian Journal of Soil Science **62**:227-241.

Marzadri, A., D. Tonina, and A. Bellin. 2012. Morphodynamic controls on redox conditions and on nitrogen dynamics within the hyporheic zone: Application to gravel bed rivers with alternate-bar morphology. Journal of Geophysical Research-Biogeosciences **117**.

McIlvin, M. R. and M. A. Altabet. 2005. Chemical conversion of nitrate and nitrite to nitrous oxide for nitrogen and oxygen isotopic analysis in freshwater and seawater. Analytical Chemistry **77**:5589-5595.

Mulholland, P. J., R. O. Hall, D. J. Sobota, W. K. Dodds, S. E. G. Findlay, N. B. Grimm, S. K. Hamilton, W. H. McDowell, J. M. O'Brien, J. L. Tank, L. R. Ashkenas, L. W. Cooper, C. N. Dahm, S. V. Gregory, S. L. Johnson, J. L. Meyer, B. J. Peterson, G. C. Poole, H. M. Valett, J. R. Webster, C. P. Arango, J. J. Beaulieu, M. J. Bernot, A. J. Burgin, C. L. Crenshaw, A. M. Helton, L. T. Johnson, B. R. Niederlehner, J. D. Potter, R. W. Sheibley, and S. M. Thomas. 2009. Nitrate removal in stream ecosystems measured by ^{15}N addition experiments: Denitrification. Limnology and Oceanography **54**:666-680.

Mulholland, P. J. and J. R. Webster. 2010. Nutrient dynamics in streams and the role of J-NABS. Journal of the North American Benthological Society **29**:100-117.

O'Connor, B. L. and M. Hondzo. 2008. Enhancement and inhihition of denitrification by fluid-flow and dissolved oxygen flux to stream sediments. Environmental Science & Technology **42**:119-125.

Ostrom, N. E., L. O. Hedin, J. C. von Fischer, and G. P. Robertson. 2002. Nitrogen transformations and NO_3^- removal at a soil-stream interface: A stable isotope approach. Ecological Applications **12**:1027-1043.

Pintar, M., S. V. Bolta, and F. Lobnik. 2008. Nitrogen isotope enrichment factor as an indicator of denitrification potential in top and subsoil in the Apace Valley, Slovenia. Australian Journal of Soil Research **46**:719-726.

Richter, F. M., R. A. Mendybaev, J. N. Christensen, I. D. Hutcheon, R. W. Williams, N. C. Sturchio, and A. D. Beloso. 2006. Kinetic isotopic fractionation during diffusion of ionic species in water. Geochimica Et Cosmochimica Acta **70**:277-289.

Rissanen, A. J., M. Tiirola, and A. Ojala. 2011. Spatial and temporal variation in denitrification and in the denitrifier community in a boreal lake. Aquatic Microbial Ecology **64**:27-40.

Ruehl, C. R., A. T. Fisher, M. Los Huertos, S. D. Wankel, C. G. Wheat, C. Kendall, C. E. Hatch, and C. Shennan. 2007. Nitrate dynamics within the Pajaro River, a nutrient-rich, losing stream. Journal of the North American Benthological Society **26**:191-206.

Sebilo, M., G. Billen, M. Grably, and A. Mariotti. 2003. Isotopic composition of nitrate-nitrogen as a marker of riparian and benthic denitrification at the scale of the whole Seine River system. Biogeochemistry **63**:35-51.

Seitzinger, S., J. A. Harrison, J. K. Bohlke, A. F. Bouwman, R. Lowrance, B. Peterson, C. Tobias, and G. Van Drecht. 2006. Denitrification across landscapes and waterscapes: A synthesis. Ecological Applications **16**:2064-2090.

Singh, B. K., K. Tate, N. Thomas, D. Ross, and J. Singh. 2011. Differential effect of afforestation on nitrogen-fixing and denitrifying communities and potential implications for nitrogen cycling. Soil Biology & Biochemistry **43**:1426-1433.

Standing, D., E. M. Baggs, M. Wattenbach, P. Smith, and K. Killham. 2007. Meeting the challenge of scaling up processes in the plant-soil-microbe system. Biology and Fertility of Soils **44**:245-257.

Tang, H., K. Yan, L. P. Zhang, F. Q. Chi, Q. Li, S. J. Lian, and D. Wei. 2010. Diversity analysis of nitrite reductase genes (nirS) in black soil under different long-term fertilization conditions. Annals of Microbiology **60**:97-104.

Wallenstein, M. D., D. D. Myrold, M. Firestone, and M. Voytek. 2006. Environmental controls on denitrifying communities and denitrification rates: Insights from molecular methods. Ecological Applications **16**:2143-2152.

Wang, Y. A., X. B. Ke, L. Q. Wu, and Y. H. Lu. 2009. Community composition of ammonia-oxidizing bacteria and archaea in rice field soil as affected by nitrogen fertilization. Systematic and Applied Microbiology **32**:27-36.

Wankel, S. D., C. Kendall, and A. Paytan. 2009. Using nitrate dual isotopic composition (delta N-15 and delta O-18) as a tool for exploring sources and cycling of nitrate in an estuarine system: Elkhorn Slough, California. Journal of Geophysical Research-Biogeosciences **114**:15.

Wunderlich, A., R. Meckenstock, and F. Einsiedl. 2012. Effect of different carbon substrates on nitrate stable isotope fractionation during microbial denitrification. Environmental Science & Technology **46**:4861-4868.

Zarnetske, J. P., R. Haggerty, S. M. Wondzell, V. A. Bokil, and R. González-Pinzón. 2012. Coupled transport and reaction kinetics control the nitrate source-sink function of hyporheic zones. Water Resources Research **48**:n/a-n/a.

Plate 2 **Top to bottom: urine patches, evident by darker and thicker grass, covering a pasture in the Wairarapa region photographed in April (autumn) 2011; chamber set-up at Lincoln University for capturing ammonia gas following urine and urea applications (August 2012).**

Chapter 4

Isofluxes of reduced and oxidised nitrogen forms following application of urea fertiliser and bovine urine to pasture soil

A version of this chapter will be submitted for publication. Wells, N.S., W.T. Baisden, T.J. Clough. In prep. Isofluxes of reduced and oxidised nitrogen forms following application of urea fertiliser and bovine urine to pasture soil. Agriculture, Ecosystems & the Environment.

4.1 Abstract

Precise indicators of when and where reactive nitrogen is 'leaking' from grazed pasture ecosystems are needed in order to mitigate the threat that intensifying production poses to water quality. Acknowledging this need, the natural abundance isotopic composition of multiple inorganic N species (soil ammonium, nitrate, and nitrate, plus ammonia gas) were assessed for 17 days following deposition of bovine urine and urea fertilisers in order to quantify the importance of ammonia volatilisation on the $\delta^{15}N$ and $\delta^{18}O$ composition of NO_3^- leached from pastures. While net NH_3 volatilisation ranged from 5 to 40% of N inputs between treatments and had an associated isotopic enrichment factor of +35 ±5‰, the composition of residual $\delta^{15}N$-NH_4^+ did not differ significantly between treatments. This homogenisation is hypothesised to reflect mineralisation-immobilisation induced by urine deposition. As a results, the $\delta^{15}N$-NO_3^- composition across all treatments was primarily defined by nitrification of the reduced N sources, making it significantly lighter than the range typically ascribed to excreta N. However, the accumulation of nitrite up to 6 µg NO_2^--N g^{-1} soil in pasture receiving 600 kg N ha^{-1} was related to consistent $\delta^{18}O$-NO_3^- enrichment (+4‰). Based on the measured isofluxes for ammonia volatilisation, NO_3^- created within pasture systems was predicted to range from +10‰ ($\delta^{15}N$) and -0.9‰ ($\delta^{18}O$) for non-fertilised fields to -3‰ ($\delta^{15}N$) and +2‰ ($\delta^{18}O$) for grazed fertilised fields. Using an enrichment factor for denitrification calculated based on changes in NO_3^- concentration and isotopic composition following heavy rainfall at the end of the monitoring period, the impact of denitrification on the soil inorganic N pool was found to have a greater impact on whole-field $\delta^{15}N$ than ammonia volatilisation. These findings emphasise the importance of accounting for soil N immobilisation-mineralisation dynamics in soil zone N isofluxes, while laying a nitrification -denitrification baseline for identifying pasture NO_3^- sources in waterways.

Keywords: nitrate, grazed pastures, ammonia volatilisation, denitrification, nitrification

4.2 Introduction

A century of intensifying agricultural production has dramatically accelerated global nitrogen (N) turnover, with excess N inputs to farm lands cascading through the environment and jeopardising the ecosystem services of waterways and soils (Galloway et al. 2003). Pastoral livestock production has been identified as a particularly 'leaky' system, with nitrate (NO_3^-) leaching into the surrounding waterways (Di and Cameron 2002), release of ammonia (NH_3) gas, and production of the greenhouse gas nitrous oxide (N_2O) (Smith et al. 2008), combining to create a long-term decline in soil-N stocks (Stevenson et al. 2010). Moreover, as N inputs to pastures from fertilisers (typically urea) and animal excreta (of which urine contributes the majority of N) (Romera et al. 2012) increased with intensification of livestock production, N use efficiency (the proportion of inputs that ends up in food) has declined: from ~60% (low intensity) to as little as 8% (highly intensity) (Powell et al. 2010). In New Zealand, where grazed pastures account for 45% of land use (Stevenson et al. 2010) and declining water quality has been linked to intensifying dairy production (McDowell et al. 2011), the need for precise and accurate measurements of NO_3^- sources and sinks is particularly acute. However, the multiple biological and chemical pathways that transform N between seven redox states, combined with the diffuse nature of NO_3^- pollution, make assessing when are where N is 'leaked' from agroecosystems difficult (Groffman et al. 2009).

Once urea (from either fertiliser or urine) is deposited onto soil it hydrolyses to ammonium (NH_4^+) and HCO_3^-, increasing soil pH and pushing the equilibrium between NH_4^+ and ammonia (NH_3) towards NH_3 (Sherlock and Goh 1985, Clay et al. 1990). As a result, anywhere from 0 to 60% of N can be physically volatilised away from the soil as gaseous NH_3 over the two weeks following urea deposition (Cameron et al. 2013). Over the next ~20 days the residual soil NH_3 pool is oxidised to nitrite (NO_2^-) and then NO_3^- by nitrifying microbes (Clough et al. 2009). Nitrate in soil can then be taken up by plants, immobilised, leached, or biologically reduced to N_2O and dinitrogen (N_2) gasses (attenuated) (Fig. 4.1). The rates of these processes can vary widely between fields and over time, making it difficult to accurately quantify when and where N losses are occurring using traditional means, and thus to develop more effective N management strategies.

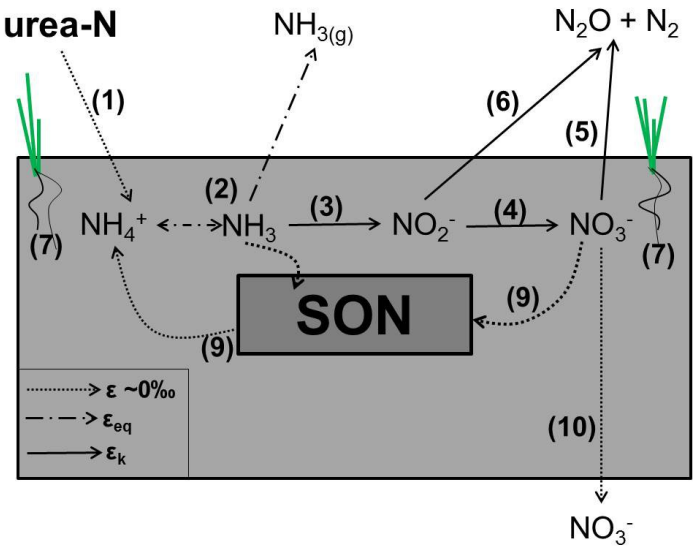

Figure 4.1 **Multiple, often co-occurring processes affect N turnover and isotopic composition in pasture systems: *(1)* Once urea (from fertiliser or urine) comes into contact with the soil, urea-N forms are immediately and completely hydrolysed to NH_4^+ with no apparent isotopic fractionation (ε~0‰); *(2)* NH_4^+ exists in equilibrium with NH_3, which will further equilibrate into aqueous and gaseous forms (the latter of which can be volatilised out of the soil zone), wherein the balance between the three pools is determined by soil pH, equilibrium fractionation (ε_{eq}) of N pool causes 'light' N to be preferentially volatilised (Sherlock and Goh 1985, Heaton 1986); *(3)* under aerobic conditions residual soil NH_3 is nitrified to NO_2^-, which causes kinetic fractionation (ε_k) of N (Casciotti et al. 2003), while O is incorporated from soil H_2O and O_2 (Casciotti et al. 2010); *(4)* NO_2^- is further oxidised to NO_3^- in the second step of nitrification, causing inverse kinetic fractionation of N (i.e., residual pool gets lighter as the reaction progresses) (Casciotti 2009) and O, in addition to incorporating another O from adjacent H_2O (Buchwald et al. 2012); *(5)* under anaerobic conditions, NO_3^- can be denitrified to N_2O and N_2, which causes parallel kinetic fractionation of both N and O (Granger et al. 2008); *(6)* new evidence suggests that NO_2^- can be directly reduced to N_2O and/or N_2 via co-denitrification (Spott et al. 2011) and nitrifier-denitrification (Kool et al. 2010), neither of which have known fractionation factors; (7) plants roots compete with these microbes to assimilate NO_3^- and NH_4^+ (Kaye and Hart 1997), both with minimal isotopes effects (Cernusak et al. 2009); *(8)* microbial immobilisation of inorganic N will reincorporate it into the large soil organic N (SON) pool; *(9)* SON can be mineralised back into the organic pool with minimal kinetic fractionation of N (and causing the O isotopes to be effectively 'reset') (Mengis et al. 2001, Mobius 2013); *(10)* any NO_3^- that is not taken up by plants, immobilised or attenuated to N gasses can be leached into the groundwater with no associated fractionation to N or O.**

The stable isotopes of NO_3^- ($\delta^{15}N$ and $\delta^{18}O$) potentially provide a means of quantifying the contribution of pasture sources across scales, based on the fact that both isotopes are modified by, and thus reflect, their environmental origin (Kendall 1998, Xue et al. 2009, Nestler et al. 2011). The theoretical 'pasture' N isotopic signature is believed to be the product of NH_3 volatilisation, during which lighter isotopes are preferentially removed and the residual $\delta^{15}N$-NH_3 pool becomes increasingly heavy (Heaton 1986, Hristov et al. 2011). This fractionation is the result of the different zero-point energies of the isotopically substituted molecules creating an unequal equilibrium distribution of heavy v. light isotopes.

The Rayleigh equation directly relates changes in substrate concentration (C/C_0) to changes in isotopic enrichment (R/R_0) based on the kinetic fractionation factor (α, $\varepsilon_k = (\alpha\text{-}1) \times 1000$)) for the reaction (Eq. 4.1).

(4.1) $$\frac{R}{R_0} = \left(\frac{C}{C_0}\right)^{\alpha-1}$$

Notably, while the residual pool becomes increasingly enriched as light isotopes are progressively removed, the composition of the product will be equivalent to that of the original substrate once the reaction is complete. Given that NH_3 volatilisation is known to both be strongly fractionating and cannot go to completion due to the constraints of soil pH, it is generally assumed that NO3- created from animal N sources will have $\delta^{15}N$ values >10‰ (Heaton 1986). However, $\delta^{15}N$ values for NO_3^- derived from animal excreta have since been reported to range from +5‰ to +35‰ (coupled with $\delta^{18}O$-NO_3^- values of -5‰ to + 5‰) (Xue et al. 2009). Some of this range may reflect post-deposition biological N cycling, rather than variations within the physical volatilisation process. Specifically, light isotopes are more readily processed during nitrification and denitrification due to the difference in reaction rates between heavy versus light isotopes for both processes. Incomplete turnover of NH_3 to NO_3^-, or of NO_3^- to N_2, could thus convolute the expression of the isotope effect of volatilisation within the leached NO_3^- pool.

Whereas previous studies of the impact of NH_3 volatilisation on residual $\delta^{15}N$ pools have either not directly measured volatilisation (i.e., urea was assumed to volatilise and cause fractionation) (e.g., Minet et al. 2012), or have assumed causality between volatilisation rates and increasingly heavy plant and/or soil total N pools without constraining other processes (e.g., Frank et al. 2004, Kriszan et al. 2009), this study measures the size and isotopic composition of the three main inorganic N pools (volatilised NH_3, soil NH_4^+, and soil NO_3^-). This enabled a mass-balance type approach to be used to assess the relative importance of multiple transformations on the isotopic composition of the soil N pool (Fig. 4.1) with the aim to, 1) assess the effect of N transformations (NH_3 volatilisation, nitrification, denitrification) on the isotopic composition of soil NH_4^+ and NO_3^-, and, 2) up-scale this information in order to constrain the isotopic signature of NO_3^- from pastoral agriculture.

4.3 Materials and Methods

4.3.1 Experimental set-up and design

The experiment was run at Lincoln University, Canterbury, New Zealand (E172°20.031', S43°39.375'), where mean annual precipitation and air temperature are 650 mm and 12ºC, respectively. The soil was a Templeton silt loam (Typic Immature Pallic Soil, New Zealand classification, C =3.4%, N =0.3%; 18% clay, 49% silt, 33% sand) (see Orwin et al. (2010) for more details). The study area was planted with rye grass (*Lolium perene*), which was trimmed to 4 cm height 48 h before the start of the experiment.

In August 2011 (winter) in-situ chambers (diameter: 0.23 m) were set up in a randomised design (five replicates per treatment), with soils receiving either: 600 kg N ha^{-1} of bovine urine (high),

80 kg N ha^{-1} of bovine urine (low), or 80 kg N ha^{-1} of urea fertiliser (Sigma Aldrich), or no N (controls). Eight litres of liquid were added to each chamber, with the difference made up in deionised water, when necessary (e.g., controls received 8 l deionised water). Urine addition rates were selected to span the range of reported N contents and deposition rates, which can vary significantly between herds due to diet (Oenema et al. 1997, Cheng et al. 2011). The urea fertiliser rate, chosen to enable direct comparison with the low urine treatment, falls within the typical range applied to New Zealand pastures (Cameron et al. 2013). Chambers were installed two-weeks prior to treatment application to minimise disturbance effects.

Fifty litres of urine were collected Jul-2012 from ~100 individual Fresian cows, grazed on kale (*Brassica oleracea*) and silver beet (*Beta vulgaris*), at the Lincoln University Ashley Dene experimental farm in Canterbury, New Zealand. Urine was immediately homogenised in two sealed 25 L drums and then stored for 12 h at 4ºC. The C and N content of the urine was 2.9 g N l^{-1} and 7.9 g C l^{-1} (measured on eight replicate subsamples via combustion (Elementar EA-TCD, Lincoln University, NZ) (precision of ±0.04)). The $\delta^{15}N$ composition of urea fertiliser was 0.67‰ and that of urine was1.6‰ (analysis described in Section 4.3.4). Urine was frozen at -20ºC until use.

4.3.2 Ammonia gas collection

The chamber set-up and gas collection follows the design of Black et al. (1987). Briefly, perspex lids were clamped onto chambers following treatment additions (creating a ~3 m^3 headspace) and air was continuously pumped through each chamber (headspace completely replaced every ~1 min) and flushed through individual acid traps containing 50 ml 0.5M H_2SO_4. Continuous flow ensured that any potential diurnal variations in $NH_{3(g)}$ fluxes(Sherlock and Goh 1985) were integrated into the measurement (Sherlock and Goh 1985). Sampling, during which acid from traps was removed for analysis and traps re-filled, was timed to to ensure capture of peak $NH_{3(g)}$ fluxes (Laubach et al. 2013): every 24 h over the first nine days, and then every 48 h over the last seven days.

In order to calculate $NH_{3(g)}$ fluxes over time, air flow rates into and out of each of the 20 traps were measured immediately prior to sample collection using manual flow metres to enable. The exact volume of acid collected from each trap was measured using a graduated cylinder to account for any evaporation, and then transferred to a 100 ml opaque Acetylene bottle for storage. Samples were stored in the dark at room temperature until analysis for NH_3-N concentration and isotopic composition (methods as described in the subsequent section).

4.3.3 Soil sampling and analyses

Soil samples were collected from each chamber 2, 5, 9, 15, and 17 days after treatment applications using individual corers (4 cm diameter x 10 cm height). Cores were extruded in the field and separated into two sections (0-2 cm and 2-10 cm), which were then sealed into polythene bags. Following extrusion, corers were reinserted into the soil and covered aluminium foil to minimise disturbance to the remaining sod. Upon return to the lab, plant biomass was separated from soil

samples, and the latter immediately extracted with 2M KCl (35 ml for 7 g dry soil) for inorganic N analyses. Extraction consisted of shaking the KCl-soil slurries in an end-over-end shaker for 30 min, centrifuging at 3500 rpm for 10 min, and then passing them through Whatman #1 filter paper (Blakemore et al. 1987). Filtrates were stored at 4ºC for <24 h, and then at -20ºC until isotopic analysis. Additional soil subsamples were weighed and dried at 105ºC for gravimetric moisture content (θ_g) quantification, or extracted with deionised water (1:10 ratio of soil (dry weight) to water) for total dissolved C (TOC) and pH analysis (Blakemore et al. 1987). To measure soil temperature a mercury thermometer was inserted into the soil to ~4 cm depth during sample collection.

Filtrates were analysed for NO_3^-, NO_2^-, and NH_4^+ concentrations within 24 h of extractions. Nitrate and NO_2^- concentrations were measured in 2M KCl soil extracts on an Alpkem FS3000 twin channel Flow Injection Analyser. Concentrations of NH_4^+ in the 2M KCl soil extracts and NH_3 trapped in 0.5M H_2SO_4 were measured using the salicylate method (Kempers and Zweers 1986), with absorbance read at 650 nm on a DU-730 UV-*vis* spectrophotometer. (Note: NH_4^+ measured in 2M KCl soil extracts includes both $NH_{3(aq)}$ and NH_4^+ (which are in equilibrium within the soil, Fig. 1) making it appropriate to treat this pool as the starting product for both nitrification and NH_3 volatilisation (Dobermann et al. 1994)) The TOC extracts were analysed on a Shimadzu TOC-5000A total organic C analyser fitted with an ASI-5000A auto sampler in water extracts from soils collected on days 1, 9 and 15. Soil pH was determined using a SevenEasy pH metre (Mettler Toledo).

4.3.4 Isotope measurements

The $\delta^{15}N$ composition of the treatment inputs (urine and urea) were determined by pipetting two replicate 5 µl aliquots into tin capsules filled with Chromosorb W (Supelco, Bellefonte, PA) (Cheng et al. 2011). These samples were analysed via combustion on a PDZ Europa 20-20 mass spectrometer (Lincoln University, New Zealand).

Ammonium isotopes ($\delta^{15}N$-NH_4^+) were measured in two representative 2M KCl soil extracts per treatment per sampling date using the diffusion method (Stark and Hart 1996): MgO was used to increase the pH to ~12, and NH_3 diffused onto GF/C (Whatman) filter paper acidified with 2.5M $KHSO_4$ over seven days in an enclosed headspace. In order to minimise ambient NH_3 contamination, glassware was acid washed and then combusted at 400ºC for 6 h and all work conducted in a fume hood. To measure $\delta^{15}N$-$NH_{3(g)}$ in the 0.5M H_2SO_4 acid traps, jars were shaken for ~2 h after MgO additions to prevent the hot reaction temperatures from causing it to solidify, and diffusions were continued for an additional seven days. All filter papers were analysed via combustion on a Europa Hydra mass spectrometer (coupled to a Carlo Erba NC 2500) (Otago University, New Zealand). Method precision and accuracy was established by running triplicates of two $\delta^{15}N$-$(NH_4)_2SO_4$ international standards (IAEA-N2 and USGS-25) plus solution blanks with each sample batch, and was calculated as ±0.9‰ for $\delta^{15}N$.

Nitrate isotopes ($\delta^{18}O$ and $\delta^{15}N$) in the 2M KCl extracts were measured using the cadmium-azide method (McIlvin and Altabet 2005): NO_3^- was reduced to NO_2^- using spongy cadmium buffered with MgO, and then reacted with azide to form N_2O. The same method, less the cadmium reduction step, was used to measure $\delta^{18}O$ and $\delta^{15}N$ of NO_2^- for six samples collected on days 15 and 17 from the high urine treatment. The $\delta^{15}N$ and $\delta^{18}O$ of the produced N_2O were analysed on a GVI Isoprime mass spectrometer (National Isotope Centre, GNS Science, New Zealand). Method precision was ±0.15‰ for N and ±0.22‰ for O. International standards for NO_3^- (IAEA, USGS-34) and NO_2^- (MAA1, MAA2), internal KNO_3 and KNO_2 standards, and blanks (made up with 2M KCl) were prepared with each sample batch in order to ensure method precision.

4.3.5 Statistical analyses and determination of fractionation factors

Changes in N species concentration and isotopic composition over time were analysed using a linear mixed model with individual chambers treated as repeated measures and treatments and sampling dates as fixed factors. Correlations between continuous variables were measured using Pearson's correlation (SPSS ver.20). Causal relationships between changing substrate concentrations and isotopic enrichment were quantified using linear regression, which were evaluated for goodness of fit (r^2) and significance (SigmaPlot ver.12, SPSS ver.20). These relationships were used to establish enrichment factors based on the simplified Rayleigh fractionation equations for denitrification, as described in discussion section (Mariotti et al. 1981). The isotopic enrichment factor for NH_3 volatilisation (ε_{AV}) was calculated based on the $\delta^{15}N$ composition of the captured NH_3 (R_A) versus the composition of the residual soil NH_4^+ pool (R_B) (Eq. 4.2)

(4.2) $$\varepsilon_{AV} = \{(R_A : R_B) - 1\} \times 1000$$

where ε_{AV} is the result of the equilibrium between the two species, and the larger the fractionation effect, the further ε is from 0 (Hogberg 1997). Within the text all values are reported as mean ±SD (unless otherwise noted), and significance defined as $p<0.05$.

4.4 Results

4.4.1 Overview of soil conditions

Soil moisture content was 25% (θ_g) over the first nine soil sampling days, but increased to 30% following rainfall on days 15 through 17. Over this period the mean soil temperature was 10 ±1°C. Soil TOC concentrations were greatest throughout the experiment in the high urine treatment (306 ±30 µg C g^{-1}, versus 149 ±40 µg C g^{-1} soil in the other treatments and controls) ($p<0.05$). Soil pH varied between treatments over time, and was consistently elevated in the high urine treatment (6.2 ±1) than in the low urine, urea, or control (5.7 ±0.5) ($p<0.05$). In high urine treatments both pH and

TOC concentration reached a maximum on day 9, with values of 7.35 ±1 and 540 ±400 µg C g^{-1} soil, respectively.

4.4.2 Ammonia volatilisation

Volatilisation rates varied with treatments over time (p<0.01), as did cumulative $NH_{3(g)}$ losses (p<0.001) (Fig. 4.2a). The highest proportion of applied N was volatilised from the low urine treatment, where a total of 48% of the urine-N was volatilised over the 17 days, in contrast to the 25% volatilised from the high urine treatment and 4% from the urea fertiliser treatment (treatment x time: p<0.05). The $\delta^{15}N$ was lightest on $NH_{3(g)}$ volatilised from the urea treatment (mean over time: -35.6 ±2‰), compared to mean compositions of -21.7 ±2‰ and -27.2 ±2‰ $\delta^{15}N$-$NH_{3(g)}$ volatilised from high and low urine treatments, respectively (p<0.001) (Fig. 4.2b). Across all treatments, $\delta^{15}N$-$NH_{3(g)}$ was positively correlated with the daily $NH_{3(g)}$ flux (r = 0.36, p<0.01), and the $NH_{3(g)}$ flux was positively correlated with the soil NH_4^+ concentration (r = 0.76, p<0.001) and negatively with soil NO_3^- (r = -0.21, p<0.05).

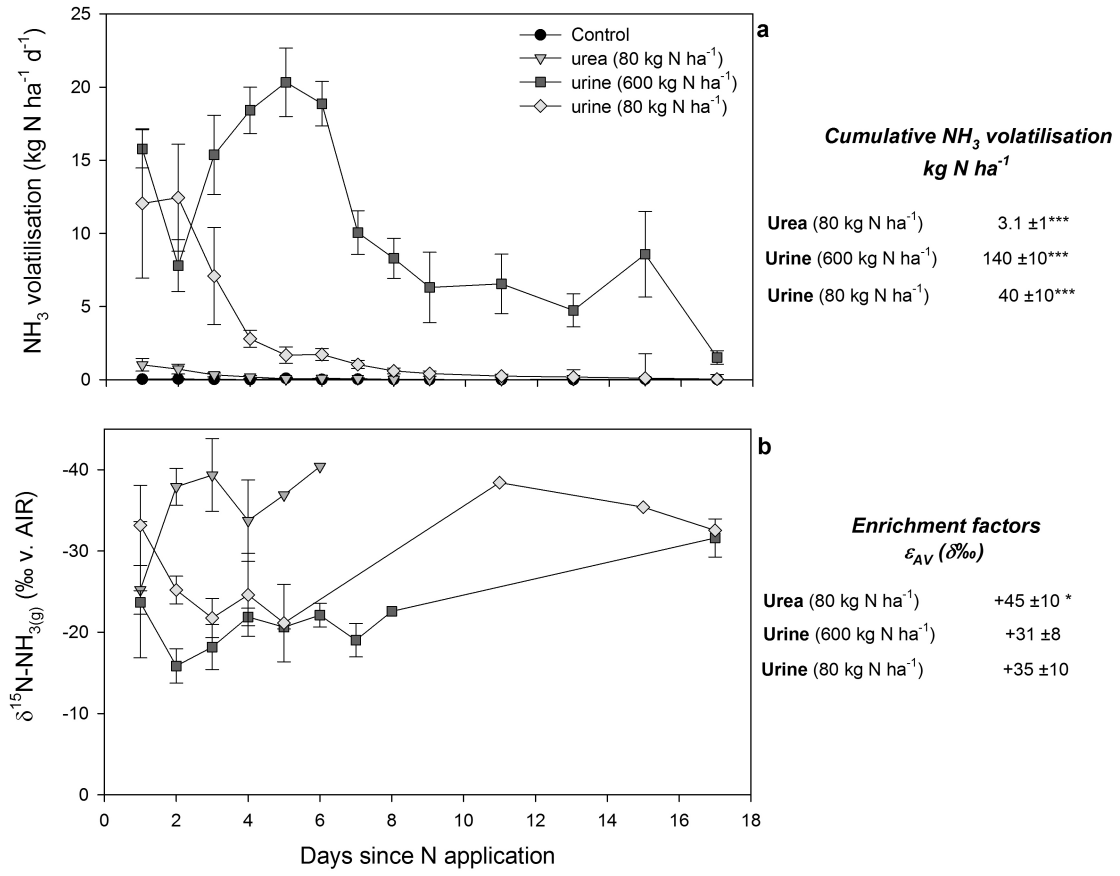

Figure 4.2 **Daily NH_3 volatilisation rates (a) and isotopic composition (b) following additions of either urea fertiliser (80 kg N ha^{-1}) or bovine urine (600 kg N ha^{-1} or 80 kg N ha^{-1}) to a pasture soil, and baseline NH_3 volatilisation rates from controls (which received no N inputs). The cumulative NH_3 volatilised (kg NH_3-N ha^{-1}) over the 17 day monitoring period and the ε_{AV} calculated from the $\delta^{15}N$ composition of volatilised NH_3 relative to residual $\delta^{15}N$-NH_4^+ in the top 2 cm of soil (Eq. 4.2) are also noted. (Symbols and error bars represent mean ±SD, n = 4 for concentrations, n = 2 for isotopes).**

4.4.3 Soil inorganic N

Soil NH_4^+ increased to a maximum on day 2 in all treatments, then decreased over the following days. The degree of change varied with treatment (treatment x time: $p<0.001$), but stayed relatively constant in the control (Fig. 4.3a,b). Within all treatments (including the control), NH_4^+ concentrations were lower at 0-2 cm than at 2-10 cm depth ($p<0.001$) (Fig. 4.3a,b). Decreases in NH_4^+ concentrations over time correlated with increasing NO_3^- concentrations ($r = -0.20$, $p<0.01$) (Fig. 4.3). Soil NO_2^- concentrations increased over time in all treatments up to 1.60 ±0.5 µg NO_2^--N g^{-1} soil by days 15 and 17 (Fig. 4.3c,d). Soils in the high urine treatment accumulated the most NO_2^- (mean of 2.02 ±0.2 µg NO_2^--N g^{-1} soil over the sampling period) and had a maximum concentration of ~8 µg NO_2^--N g^{-1} soil on day 15 ($p<0.001$) (Fig. 4.3c,d). There was no significant accumulation of NO_2^- in the control. Nitrate concentrations, which did not vary significantly with depth, were consistently higher ($p<0.001$) in the urea and low urine treatments than in the high urine treatment. Day 17, when there were no significant differences between treatments, was the exception to this trend (Fig. 4.3e,f). Nitrate accumulated over the first 15 days in all treatments, although this accumulation was somewhat delayed in the high urine treatment. Control soil NO_3^- concentrations did not change significantly over these 15 days (Fig. 4.3e,f). However, NO_3^- concentrations decreased in all soils (by 54.2 ±2% in all N amended soils and by 45% in controls) between the day 15 rainfall and the final sampling on day 17 (Fig. 4.3e,f).

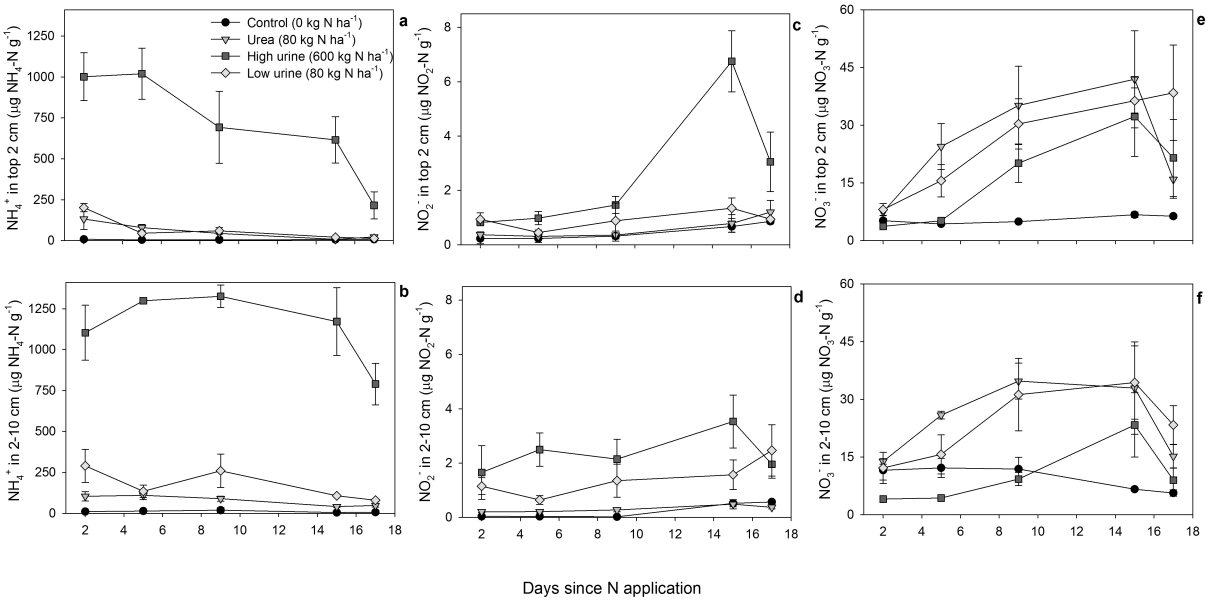

Figure 4.3 **Dissolved inorganic N concentrations (NH_4^+ (a, b), NO_2^- (c,d), and NO_3^- (e,f)) over time in pasture soils at 0-2 cm and 2-10 cm depths following additions of either urea (80 kg N ha^{-1}) or bovine urine (80 kg N ha^{-1} or 600 kg N ha^{-1}), or left as controls. Symbols and error bars represent mean ±SD ($n = 4$).**

4.4.4 Soil inorganic N isotopes

In contrast to the ~1‰ value for $\delta^{15}N$ of the applied urine and urea, soil $\delta^{15}N\text{-}NH_4^+$ across all treatments and depths was 10.2 ±1‰ within two days of N additions. By the final sampling on day 17, $\delta^{15}N\text{-}NH_4^+$ within all treatments was 16.3 ±2‰ (p<0.05) (Fig. 4.4b), while the $\delta^{15}N$ of the control NH_4^+ pool did not deviate from a mean of 10 ±4‰ over depth or time.

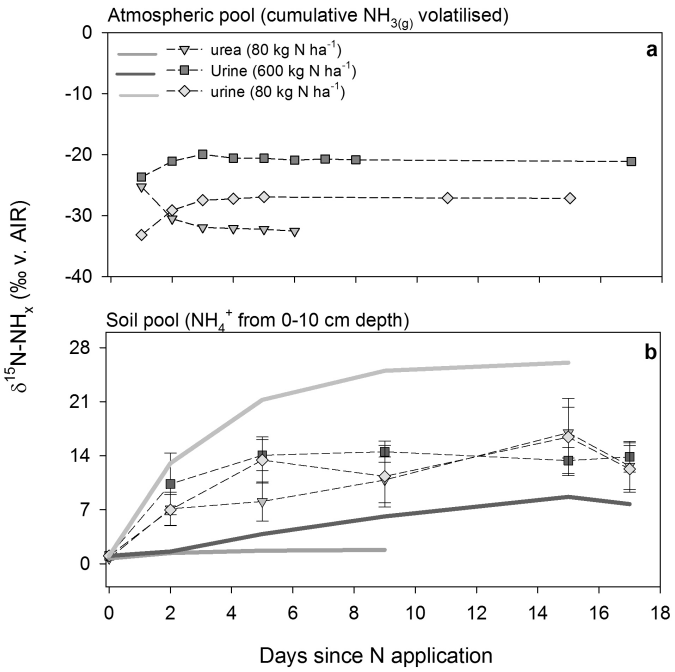

Figure 4.4 **Partitioning of $\delta^{15}N\text{-}NH_x$ between the atmosphere (as $NH_{3(g)}$) (a) and soil (as NH_4^+) (b) following application of either 80 kg N ha^{-1} urea fertiliser, 600 kg N ha^{-1} bovine urine, or 80 kg N ha^{-1} bovine urine. In (a), the $\delta^{15}N$ composition of the total volatilised NH_3 pool was calculated based on flux-weighted daily measurements to reflect. In (b) symbols represent concentration-weighted mean of the $\delta^{15}N\text{-}NH_4^+$ measured in 2M KCl extracts of soils from 0-2 and 2-10 cm depth concentration-weighted mean (±SD), as compared to lines representing the expected soil $\delta^{15}N\text{-}NH_4^+$ composition based on the $\delta^{15}N$ isoflux for NH_3 volatilisation from each treatment shown in (a).**

The $\delta^{15}N$ of NO_3^- in the control was 10.2 ±3‰ over time and depth, higher than in any of the treatments, while $\delta^{15}N\text{-}NO_3^-$ was lowest in the urea fertiliser treatment, with a mean of -0.884 ±3‰ (Fig. 4.5b). The $\delta^{15}N\text{-}NO_3^-$ composition at both 0-2 cm and 2-10 cm depths varied with treatments over time (p<0.01). Across all three treatments and depths, $\delta^{15}N\text{-}NO_3^-$ was lowest on day 9 (-5.50 ±7‰) and highest on day 17 (10.7 ±3‰). In contrast, $\delta^{18}O\text{-}NO_3^-$ increased over time in all treatments from 0.059 ±0.3‰ on day 5 to 4.76 ±2‰ on day 17 (p<0.05). As with $\delta^{15}N\text{-}NO_3^-$, $\delta^{18}O\text{-}NO_3^-$ was most enriched (p<0.001) on the last day of sampling in both depths (Fig. 4.5). Nitrate $\delta^{18}O$ in the high urine treatment had a concentration-weighted mean composition of 4.60 ±1‰ over depth and time, higher (p<0.001) than in the controls, low urine, or urea fertiliser treatments (Fig. 4.5b). Nitrite $\delta^{15}N$ (measured in the high urine treatment on days 15 and 17) was negatively correlated with NO_2^- concentration (r = -1, p<0.05), but not with $\delta^{15}N\text{-}NO_3^-$ or NO_3^- concentration (Fig. 6). While $\delta^{15}N\text{-}NO_2^-$ was consistently isotopically depleted relative to $\delta^{15}N\text{-}NO_3^-$ (p<0.001), the difference between the two decreased between days 15 and 17.

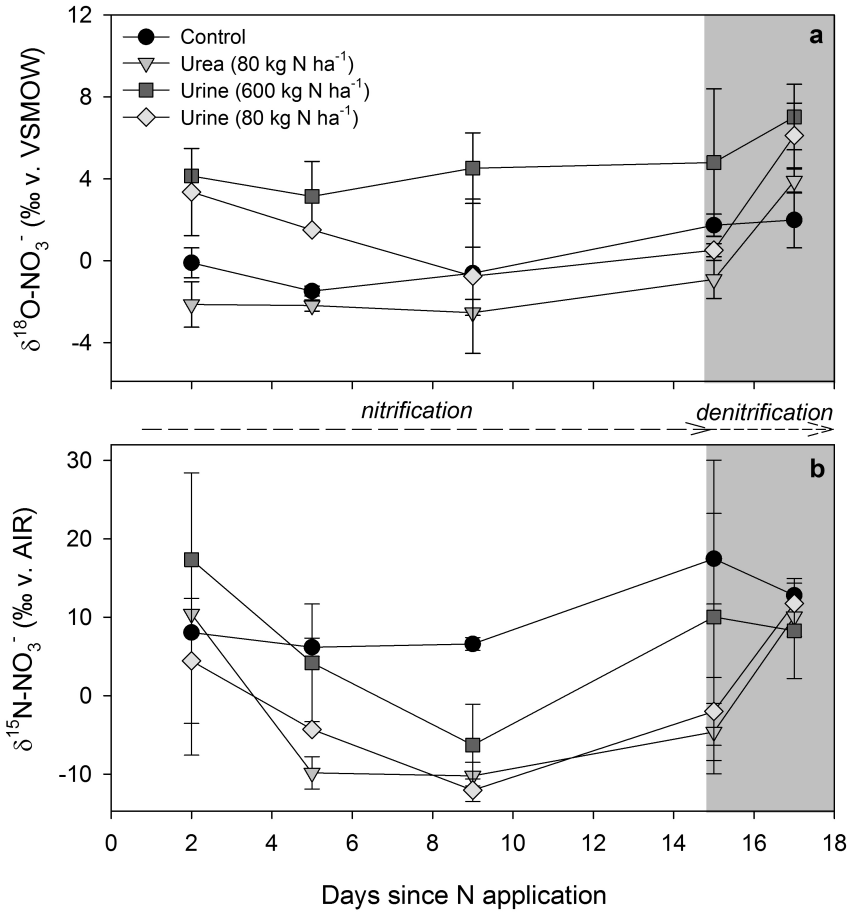

Figure 4.5 **Changes in $\delta^{18}O$ (a) and $\delta^{15}N$ (b) composition of soil NO_3^- over the 17 days following additions of either 80 kg N ha^{-1} urea fertiliser, 600 kg N ha^{-1}, bovine urine, 80 kg N ha^{-1} bovine urine, or a commensurate volume of DI H_2O (control). Following heavy rain on days 15-17, conditions shifted to favour denitrification (shaded area). Values represent the concentration-weighted mean of samples from 0-2 and 2-10 cm depth, ±SE (*n* =2 per depth).**

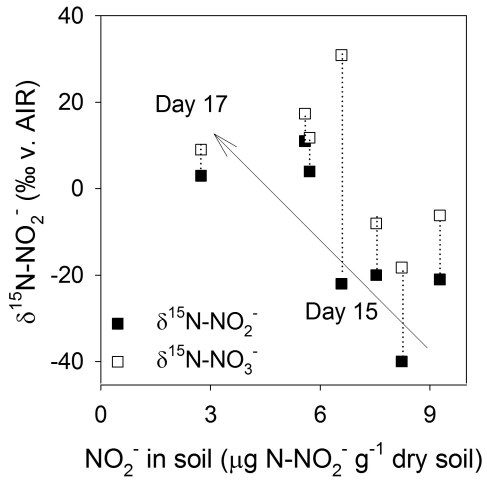

Figure 4.6 **Soil $\delta^{15}N\text{-}NO_2^-$ and $\delta^{15}N\text{-}NO_3^-$ composition with respect to NO_2^- concentration measured 15 and 17 days after 600 kg N ha^{-1} of bovine urine was applied to the pasture. The arrow represents the slope of the linear regression between $[NO_2^-\text{-}N]$ and $\delta^{15}N\text{-}NO_2^-$: $y = 29 - 6.3x$ ($r^2 = 0.54$, $p<0.05$), and the dotted lines sketch the difference in ^{15}N enrichment between $\delta^{15}N\text{-}NO_3^-$ and $\delta^{15}N\text{-}NO_2^-$ within a given sample.**

4.5 Discussion

Soil inorganic N dynamics are consistent with the finding that nitrification is complete within ~2 weeks of urine application (Laubach et al. 2013), and NH_3 volatilisation rates from the different treatments bracket the reported range for pasture systems (Cameron et al. 2013). From this basis, changes in the isotopic composition of the measured reduced (NH_3, NH_4^+) and oxidised (NO_3^-, NO_2^-) inorganic N pools can be confidently used to represent typical patterns within pasture soils.

4.5.1 Reduced N

The calculated mean ε_{AV} for all treatments and sampling dates was +35 ±0.4‰, with the strength of fractionation increasing from +30‰ to +52‰ over time as volatilisation rates decreased (p<0.01) (Fig. 4.2a). These ε_{AV} values fall within the range established based on patterns of $\delta^{15}N\text{-}NH_3$ in rainfall (Hogberg 1997, Jia and Chen 2010), and is roughly equivalent to the value of +35‰ reported in the only previous study to measure $\delta^{15}N\text{-}NH_{3(g)}$ fluxes at the soil-atmosphere interface (Frank et al. 2004). Accordingly, the initial enrichment of the soil $\delta^{15}N\text{-}NH_4^+$ pool can be attributed to volatilisation -induced fractionation (Fig. 4.4).

The N isoflux for volatilisation was calculated from the cumulative NH_3 loss times its measured $\delta^{15}N$ value on discrete sampling dates (Fig. 4.4a). These flux values were then used to calculate the theoretical impact of NH_3 volatilisation on the residual isotopic composition of the residual NH_4^+ pool for each treatment over time (Fig. 4.4b). Based on these calculations, the predicted $\delta^{15}N$ composition of the NH_4^+ soil pool in the low urine treatment after 17 days would be ~30‰ if NH_3 volatilisation was the only process affecting NH_4^+ pool size and isotopic composition, significantly higher than what the measured value of 14‰. On the opposite end, $\delta^{15}N\text{-}NH_4^+$ pools in the high urine and fertiliser treatments were more enriched than was expected based on their respective volatilisation rates (Fig. 4.4).

These findings indicate that, in urine-treated soils, was N recycled through the SON pool, muting the effect of volatilisation, and that NH_3 volatilisation was not the primary N fractionating process in the urea fertilised soils. The rapidly mineralisation (ammonification) and immobilisation that is known to occur within urine patches (Decau et al. 2004, McFarland et al. 2010, Schrama et al. 2013) may explain the under-expression of volatilisation's isotope effects found in the low urine treatment (i.e., urine deposition stimulated mineralisation of organic N that diluted the heavy residual NH_3 pool). Based on the measured accumulation of NO_3^- over time in all soils, it seems probable that $\delta^{15}N\text{-}NH_4^+$ enrichment over time was also influenced by incomplete nitrification. Specifically, the fact that ~80% of non-volatilised NH_3 was converted to NO_3^- in the low urine and urea treatments, and ~60% in the high urine treatment by day 15 would also add to the 'heavy' $\delta^{15}N\text{-}NH_4^+$ pool as light isotopes are preferentially oxidised (Casciotti et al. 2003).

The co-occurrence of equilibrium fractionation from NH_3 volatilisation and kinetic fractionation from nitrification made their individual roles in driving the enrichment of the $\delta^{15}N\text{-}NH_4^+$

composition difficult to distinguish. However, the importance of nitrification in controlling inorganic N isotopic composition is emphasised by the fact that there was no quantifiable relationship between either the flux or cumulative proportion of NH_3 volatilisation and $\delta^{15}N\text{-}NO_3^-$ either within or between treatments (i.e., nitrification limited NO_3^- production, and thus controlled its $\delta^{15}N$). Overall, this data set reveals that dynamic N cycling within urine patches (or following concentrated urea fertiliser applications) can homogenise the residual $\delta^{15}N\text{-}NH_4^+$ pool, and that this pool therefore does not always reflect the magnitude of NH_3 volatilisation.

4.5.2 Oxidised N

Nitrification

Nitrate isotopic composition over the first ~9 days following urine and urea applications clearly reflects the imprint of nitrification: $\delta^{15}N\text{-}NO_3^-$ values decreased over time as NO_3^- accumulated. Over this period the $\delta^{18}O\text{-}NO_3^-$ remained relatively constant, as expected for nitrification-induced mixing of atmospheric $\delta^{18}O\text{-}O_2$ and $\delta^{18}O$ from local H_2O (as discussed in Buchwald et al. (2012)) (Fig. 4.1). While the relatively slow nitrification rates caused by winter conditions (wet and cold soil) could minimising the evidence for NH_3 volatilisation carried over to the NO_3^- pool by increasing the expression of nitrification-induced fractionation, the similarity in the $\delta^{15}N\text{-}NH_4^+$ composition across the treatments (from which from 5 and 48% of N inputs were volatilised, and for which nitrification rates were comparable) makes this seem unlikely. Specifically, on day 15, when ~80% of the non-volatilised NH_4^+ in both the low urine and the urea fertiliser treatments had been nitrified, meaning the ~40% difference in volatilisation rates between the should be expected in the NO_3^- isotopes, the $\delta^{15}N\text{-}NO_3^-$ composition actually became more similar across the treatments (Fig. 4.5).

While previous studies relied on NH_3 volatilisation altering $\delta^{15}N$ to identify effluent-derived NO_3^- (e.g., Choi et al. 2011), in the current study the most consistent treatment difference was unexpectedly found in $\delta^{18}O\text{-}NO_3^-$ composition. As denitrification would cause parallel enrichment of both NO_3^- isotopes, rather than just $\delta^{18}O$ (Xue et al. 2009), this process could not be used to explain the relatively heavy $\delta^{18}O\text{-}NO_3^-$ values in the high urine treatments. Based on the accumulation of NO_2^- in these soils, it is hypothesised that $d18O\text{-}NO_3^-$ is instead the product of the decoupling of NH_3 oxidation and NO_2^- oxidation (Fig. 4.1) in high urine treatments. Nitrite accumulation is a well-documented occurrence in N-rich urine patches (e.g., Clough et al. 2009) believed to result from NH_3 toxicity to NO_2^- oxidising bacteria (Chung et al. 2005, Uemura et al. 2011) and/or the delayed recovery from the shock caused by pH changes and salt additions of NO_2^- oxidisers relative to NH_3 oxidisers (Orwin et al. 2010, Bertram et al. 2012, Venterea et al. 2012). Longer residence times for NO_2^- could influence $\delta^{18}O\text{-}NO_3^-$ by increasing the opportunity for O exchange between NO_2^- and H_2O (wherein equilibrium fractionation preferentially leaves heavy O with NO_2^-). The observed delay in NO_2^- oxidation could also increase the expression of the inverse fractionation of both N and O isotopes from NO_2^- oxidation (Buchwald and Casciotti 2013), an effect which is further supported by the decreasing difference between $\delta^{15}N\text{-}NO_3^-$ and $\delta^{15}N\text{-}NO_2^-$ as the concentration of NO_2^- relative to NO_3^- declined (Fig. 4.5). The

possibility that NO_2^- attenuation processes such as nitrifier-denitrification (Wrage et al. 2001) or co-denitrification (Spott et al. 2011), hypothesised to play a role in soil N cycling following urea N additions due to positive correlations between NO_2^- concentrations and N_2O emissions (Oenema et al. 1997), could create the unique $\delta^{18}O\text{-}NO_3^-$ composition in the high urine treatment must also be acknowledge. However, the severely information on these processes and their isotope effects (Chapter 2) make it difficult to arrive at a concrete explanation for these $\delta^{18}O\text{-}NO_3^-$ values difficult.(Venterea et al. 2012)Future efforts need to focus on identifying and quantifying the fractionation dynamics of the NO_2^- transformation pathways in order to fully understand the measured differences between N application rates and sources within complex pasture systems. Specifically, the processes driving the unique relationship found between NO_2^- accumulation and elevated $\delta^{18}O\text{-}NO_3^-$ should be further explored in order to determine the prevalence of this relationship in NO_3^- produced under soil affected by high NH_3 loadings.

The data here emphasises that the NO_3^- leached from pasture systems will only reflect the isotopic fingerprint of NH_3 volatilisation if, 1) mineralisation – immobilisation do not homogenise $\delta^{15}N$ of the reaction substrate, 2) nitrification occurs only after NH_3 volatilisation stops, and, 2) nitrification of the NH_3 pool is complete prior to leaching. These findings add functional depth to previous observations that soil zone nitrification – denitrification and active immobilisation-mineralisation can rapidly homogeneous isotopically- distinct N pools (Mengis et al. 2001, Billy et al. 2010, Minet et al. 2012).

Denitrification

The decrease in NO_3^- concentrations combined with the parallel enrichment of $\delta^{15}N\text{-}NO_3^-$ and $\delta^{18}O\text{-}NO_3^-$ between days 15 and 17, when heavy rainfall saturated the soil, provided unambiguous evidence of denitrification in all treatments and the control. A switch to denitrification as the dominant N process is further supported by the rapid loss of NO_2^- and increase in $\delta^{15}N\text{-}NO_2^-$ in the high urine treatment soil. Based on these relationships, it is useful to use data from these two sampling dates to estimate the effective enrichment factor for denitrification (ε_{denit}) in this setting. Thus ε_{denit} was calculated using the modified Rayleigh equation of Mariotti et al. (1981) (Eq. 4.3):

$$\delta^{15}N_x = \delta^{15}N_0 + \varepsilon_{denit} \times \ln\left(\frac{f}{1-f}\right)$$
$$\delta^{18}O_x = \delta^{18}O_0 + \varepsilon_{denit} \times \ln\left(\frac{f}{1-f}\right) \quad (4.3)$$

which directly relates the composition of $\delta^{15}N$ and $\delta^{18}O$ at point *x* (day 17) to that prior to significant modification by denitrification (δ_0) (day 15) using ε_{denit} and the natural log of the relative NO_3^- concentration between the two dates (*f*). By plotting ln(*f*) versus the changes in NO_3^- isotopes, ε_{denit} was measured to be -12.4‰ for $\delta^{15}N\text{-}NO_3^-$ ($r^2 = 0.84$, $p<0.01$) and -4.54‰ for $\delta^{18}O\text{-}NO_3^-$ ($r^2 = 0.72$, $p<0.01$).

The 0.25 enrichment ratio of $\delta^{18}O$ to $\delta^{15}N$ during this period is lower than the 0.5 to 1.0 range typically associated with denitrification (Xue et al. 2009), most likely indicating that some level of nitrification continued to occur even post rainfall-induced saturation, which would distort the denitrification signal, causing enrichment of $\delta^{15}N$ to increase relative to that of $\delta^{18}O$ per unit of substrate attenuation (Chapter 3). The mean ε_{denit} reported for aerobic soils under 'natural' conditions (i.e., no C or N additions) is ~ -4‰, placing the value of -12.4‰ measured here for N enrichment closer to the range reported for anaerobic soil incubations with simple C additions (Chapter 2). Regardless of how close these calculated ε_{denit} values may be to the biochemically fractionation of the site's denitrifiers, this quantification of how attenuation affects NO_3^- isotopic composition provides fundamental information needed in order to fully parametrise the relative impact of the two main N loss pathways (NH_3 volatilisation and denitrification) on pasture ecosystems.

4.5.3 Calculating whole-pasture isotopic signatures

The concurrent effects of nitrification and NH_3 volatilisation on the isotopic signature of the produced NO_3^- was evaluated over depth and time using an isotope mass balance compiled from measured NO_3^- concentrations and isotopic composition over time. A whole-field NO_3^- isotopic signature was calculated by applying an isotope mixing model (Kendall 1998) (Eq. 4.4) to the pasture N leaching model for determining total N losses from Cameron et al. (2013) (Eq.4. 5).

(4.4) $$\delta_{net} = \frac{\{(\delta_{urine} N_{urine} P_{urine}) + (\delta_{field} N_{field} P_{field})\}}{N_{net}}$$

(4.5) $$N_{net} = (N_{urine} P_{urine}) + (N_{field} P_{field})$$

where the total N exported from a pasture (N_{net}) is the sum of N from urine deposition (N_{urine}) and N from the non-urine affected soil (N_{field}), which contains N from soil organic N and/or fertilisers. Combining this framework with the spatial distribution of urine patches per grazing and per-annum described by Moir et al. (2011) and the isotope data generated in this study, the NO_3^- produced in urea fertilised and non-fertilised pastures with and without grazing animals were calculated (Fig. 4.7).

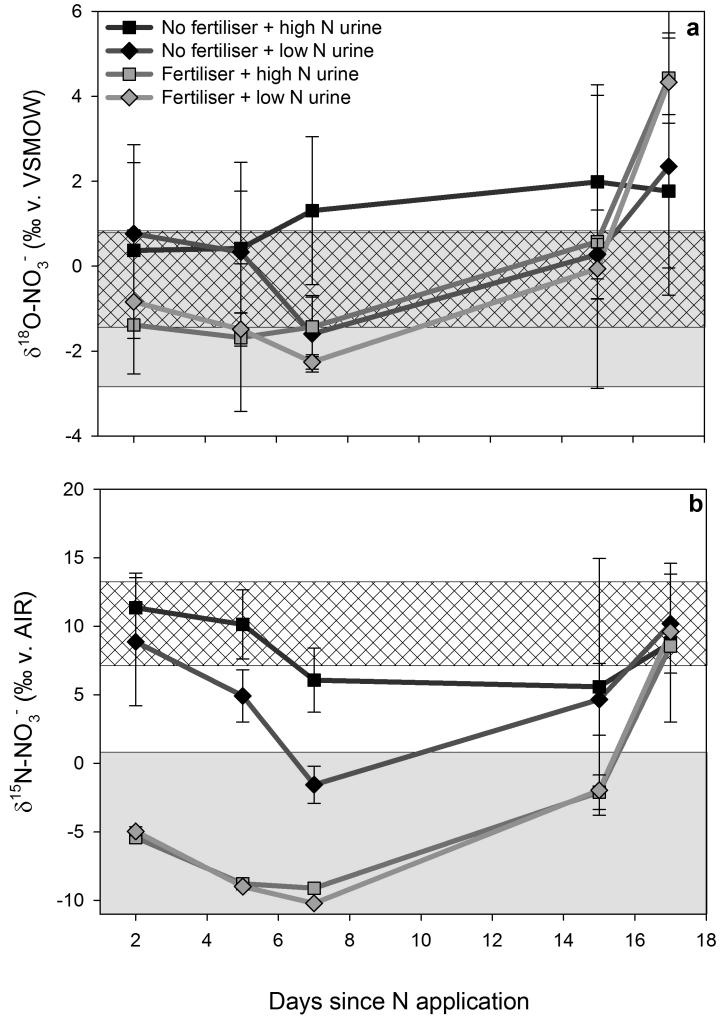

Figure 4.7 **The calculated $\delta^{18}O$ (a) and $\delta^{15}N$ (b) composition of the whole-pasture NO_3^- pool over time following high (600 kg N ha-1) and low (80 kg N ha-1) of urine deposition, as compared with NO_3^- isotopic composition in fertilised (grey rectangle spans mean ±1 SD) v. non-fertilised fields (cross hatched rectangle spans mean ±1 SD) without grazing (urine deposition). All values were calculated based on the isotope mass balance (concentration × δ) and reported spatial distribution of urine patches (Moir et al. 2011).**

Within this framework, the theoretical versus measured influence of the primary fractionating N loss pathways (NH_3 volatilisation and denitrification) on soil $\delta^{15}N$- $\delta^{18}O$- NO_3^- were calculated (Table 4.1). Nitrate $\delta^{15}N$ were based either on measured values at the 'end' of nitrification (maximum NO_3^- accumulation) or the $\delta^{15}N$-NO_3^- value calculated based on 100% nitrification of the treatment's NH_4^+ pool. Nitrification produced $\delta^{18}O$-NO_3^- in this experiment would theoretically have fairly negative values (from -4.1‰ (if $\delta^{18}O$-H_2O were -1‰, as calculated based on 1:1 mixing of $\delta^{18}O$-O_2 (+23.5‰) and $\delta^{18}O$-NO_2^-) to -13‰), based on reported local $\delta^{18}O$-H_2O of -8‰ (Blackstock 2011). The uncertainty in these calculations stems from potential variations in the degree of O exchange (and associated equilibrium fractionation) between O-NO_2^- and adjacent O-H_2O, plus the degree of kinetic fractionation of O-NO_2^- during the oxidisation step to NO_3^- (Buchwald and Casciotti 2010, Fang et al. 2012).

Table 4.1 **The calculated isotopic composition of NO_3^- ($\delta^{15}N$ and $\delta^{18}O$) of NO_3^- exported from grazed pastures on a whole-field basis, using NO_3^- concentrations to weight means of $\delta^{15}N$-NO_3^- and $\delta^{18}O$-NO_3^- in the top 10 cm. Fields were considered as either non-fertilised (control plots, receiving no N inputs) or fertilised (urea fertiliser at a rate of 80 kg N ha^{-1}) with or without grazing/ urine additions (either low, 80 kg N ha^{-1} per urination; or high, 600 kg N ha^{-1} per urination); or on calculated $\delta^{15}N$- $\delta^{18}O$- NO_3^- from complete nitrification of non-volatilised NH_3 occurring without denitrification ('ideal'). Isotope values are reported in δ‰, with respect to AIR for N and VSMOW for O.**

N sources[a]		Calculated (100% nitrification)				Measured			
		R_0 (no denitrification)[b]		*50% denitrification*[c]		*R_0 (no denitrification)*[d]		*50% denitrification*[e]	
urea	*urine*	*$\delta^{15}N$-NO_3^-*	*$\delta^{18}O$-NO_3^-*	*$\delta^{15}N$-NO_3^-*	*$\delta^{18}O$-NO_3^-*	*$\delta^{15}N$-NO_3^-*	*$\delta^{18}O$-NO_3^-*	*$\delta^{15}N$-NO_3^-*	*$\delta^{18}O$-NO_3^-*
Un-fertilised	*nil*	+10.6 (3)	-0.090 (2)	+16.2 (6)	+5.78 (5)	+10.6 (3)	-0.090 (2)	+19.2 (3)	+13.5 (2)
	high	+8.25 (9)	-5.11 (5)	+14.1 (3)	+0.761 (5)	+5.59 (9)	+1.98 (2)	+14.2 (9)	+5.13 (2)
	low	+13.8 (3)	-6.29 (5)	+19.7 (9)	-0.419 (2)	+4.34 (3)	+0.290 (1)	+12.9 (3)	+3.44 (1)
Fertilised	*nil*	+0.413	-10.3 (5)	+6.30 (3)	-4.43 (8)	-4.98 (7)	-0.759 (3)	+3.62 (4)	+2.89 (0.8)
	high	+1.86		+7.73 (2)		-3.84 (1)	+0.454 (2)	+4.75 (6)	+3.60 (2)
	low	+5.51		+11.4 (2)		-3.38 (3)	-0.317 (1)	+5.22 (3)	+2.83 (0.3

a Whole pasture mean for one grazing, based on measured distribution, volume, and occurrence of urine patches in Moir et al. (2011), as per Eq. 4.4 and Eq. 4.5

b Calculated using % ammonia volatilisation and ε_{AV} for each treatment, assuming 100% of the non-volatilised N retained the $\delta^{15}N$ of urea (~1‰) and equilibrium fractionation of NH_3-N (Eq. 4.2, Fig. 4.1) for $\delta^{15}N$-NO_3^-; and using equation of Fang et al. (2012) for $\delta^{18}O$-NO_3^- from nitrification: $\delta^{18}O_{NO3}=1/3\delta^{18}O_{O2} + 2/3\delta^{18}O_{H2O} + 1/3(^{18}\varepsilon_{k,O2} + {}^{18}\varepsilon_{k,H2O,1} + {}^{18}\varepsilon_{kH2O,2}$ (see text for complete explanation)

c From mean ±SD of ε_{denit} measured experimentally (-8.5 ±6‰), which covers range of reported values for terrestrial denitrification (Chapter 2)

d Based on samples collected 15 days post N application, at maximum NO_3^--N concentration and prior to intensive leaching

e Based on samples collected 17 days post N application, following leaching in which ~50% of NO_3^--N was lost from the top 10 cm of soil

Outcomes

As urine patches only accounts for 3-5% of pasture area (Moir et al. 2011), the clearest difference in terms of $\delta^{15}N$-NO_3^- composition is found between the fertilised and non-fertilised fields (Fig. 4.7). If nitrification is assumed to go to completion urine inputs at any concentration to either 'fertilised' or 'non-fertilised' fields causes either a relative increases (in fertilised fields) or decreases (in non-fertilised fields) of $\delta^{15}N$-NO_3^- (Table 4.1). This slight effect of urine patches on whole-field $\delta^{15}N$-NO_3^- driven by their higher rates of NH_3 volatilisation, demonstrates that NH_3 volatilisation can play a role in creating the frequently cited 'heavy' $\delta^{15}N$ signatures in grazed pastures. The high $\delta^{18}O$-NO_3^- values measured within the high urine treatments also had an impact on the calculated whole-field NO_3^- (with or without fertiliser additions) that could not be satisfactorily explained by nitrification (Table 4.1), emphasising the need for continuing research into NO_2^- dynamics within urine patches.

The stark differences between $\delta^{15}N$-NO_3^- in fertilised versus non-fertilised pastures emphasises that systems receiving high N inputs, which lead to a de-coupling of nitrification and denitrification, can drive the 'pasture-N' signature created within the soil zone towards 'light' values. This reveals a rarely considered mechanism for distinguishing agricultural N inputs from background soil N: excess N inputs to pastures create an isotopically 'light' NO_3^- pool due to the ongoing nitrification of NH_3, regardless of the proportion which volatilised at the soil surface (corroborating the assumptions in

Chapter 7). In addition, the homogenisation of the residual $\delta^{15}N\text{-}NH_4^+$ pool noted here following urine deposition further limits the possibility of ε_{AV} being expressed within a pasture NO_3^- pool (Table 4.1).

These results indicate that the incorporation of 'heavy' $\delta^{15}N$ into plant and soil biomass following, e.g., slurry applications (Kriszan et al. 2009) could be driven equally by increasing denitrification within urine patches (e.g., Clough et al. 2009) and NH_3 volatilisation, as both caused changed $\delta^{15}N$ of the residual pool by ~ +10‰. Therefore the source of whole-system ^{15}N enrichment would depend on the relative uptake of NH_4^+ versus NO_3^- (Schimel and Bennett 2004), and the magnitude of this enrichment would depend on, 1) NH_3 volatilisation enriching the $\delta^{15}N\text{-}NH_4^+$ pool, 2) the relative rate of nitrification partitioning light isotopes into the NO_3^- pool, and, 3) the timing NO_3^- removal via leaching (non-fractionating) versus via denitrification (causing enrichment of both NO_3^- isotopes). The balance of these processes under winter conditions, when biological nitrification and denitrification are most retarded and NO_3^- leaching is maximised (Decau et al. 2004), would then create a seasonal 'light' $\delta^{15}N\text{-}NO_3^-$ pool reflecting the nitrification limitation. Drier and warmer soils in the summer would increase nitrification rate, resulting in the slightly heavier $\delta^{15}N\text{-}NO_3^-$ composition predicted for ideal conditions in Table 4.1.

4.6 Conclusion

By measuring changes in the isotopic composition of inorganic N species following urine and urea deposition I was able to precisely identify the causes of enrichment and depletion of the N different pools. Although $\delta^{15}N\text{-}NH_4^+$ of surface soils increased during the most intense volatilisation period, this effect was ultimately indistinguishable from fractionation incurred during incomplete nitrification, and the $\delta^{15}N$ of neither NH_4^+ nor NO_3^- correlated to the proportion of N volatilised. My results necessitate a re-evaluation of the $\delta^{15}N$- $\delta^{18}O$- NO_3^- values typically ascribed to 'animal excreta' (Xue et al. 2009) within the context of soil cycling: at the whole-field scale, I found $\delta^{15}N\text{-}NO_3^-$ reflected the balance between nitrification and denitrification, with increasingly 'light' values the greater the disconnect between creation and attenuation, while $\delta^{18}O\text{-}NO_3^-$ composition was consistently heavier in soils with the highest urine-N inputs. In light of the homogenised response of $\delta^{15}N\text{-}NH_4^+$ and $\delta^{15}N\text{-}NO_3^-$ to extremely different rates of NH_3 volatilisation, future research should focus on quantifying the effect of SON turnover of the natural abundance composition of specific N compounds.

4.7 Acknowledgements

Thanks to Neil Smith for assistance with the ammonia gas trapping set-up, Qian Liang and Roger Cresswell for analytical assistance, and Keith Cameron for lending his high quality equipment. Brenda Lynch (Animal Sciences, Lincoln University) arranged urine collection and access to the Ashley Dene herd. Research was funded by FRST (Foundation for Research, Science and Technology, New Zealand) grant C05X0803 to W.T. Baisden / GNS Science.

Tim Clough helped with editing, and provided a wealth of knowledge on pasture systems and ammonia volatilisation that was invaluable to both developing and writing this manuscript. Troy Baisden provided valuable perspective on the isoflux calculations and data presentation.

4.8 References

Bertram, J. E., K. H. Orwin, T. J. Clough, L. M. Condron, R. R. Sherlock, and M. O'Callaghan. 2012. Effect of soil moisture and bovine urine on microbial stress. Pedobiologia **55**:211-218.

Billy, C., G. Billen, M. Sebilo, F. Birgand, and J. Tournebize. 2010. Nitrogen isotopic composition of leached nitrate and soil organic matter as an indicator of denitrification in a sloping drained agricultural plot and adjacent uncultivated riparian buffer strips. Soil Biology & Biochemistry **42**:108-117.

Black, A. S., R. R. Sherlock, and N. P. Smith. 1987. Effect of timing of simulated rainfall on ammonia volatilization from urea, applied to soil of varying moisture-content. Journal of Soil Science **38**:679-687.

Blackstock, J. M. 2011. Isotope study of moisture sources, recharge areas, and groundwater flow paths within the Christchurch Groundwater System. University of Canterbury, Christchurch.

Blakemore, L. C., P. L. Searle, and B. K. Daly. 1987. Methods for chemical analysis of soils. NZ Soil Bureau Scientific report 80:7.

Buchwald, C. and K. L. Casciotti. 2010. Oxygen isotopic fractionation and exchange during bacterial nitrite oxidation. Limnology and Oceanography **55**:1064-1074.

Buchwald, C., A. E. Santoro, M. R. McIlvin, and K. L. Casciotti. 2012. Oxygen isotopic composition of nitrate and nitrite produced by nitrifying cocultures and natural marine assemblages. Limnology and Oceanography **57**:1361-1375.

Cameron, K. C., H. J. Di, and J. L. Moir. 2013. Nitrogen losses from the soil/plant system: a review. Annals of Applied Biology **162**:145-173.

Casciotti, K. L., M. McIlvin, and C. Buchwald. 2010. Oxygen isotopic exchange and fractionation during bacterial ammonia oxidation. Limnology and Oceanography **55**:753-762.

Cernusak, L. A., K. Winter, and B. L. Turner. 2009. Plant $\delta^{15}N$ correlates with the transpiration efficiency of nitrogen acquisition in tropical trees. Plant Physiology **151**:1667-1676.

Cheng, L., E. J. Kim, R. J. Merry, and R. J. Dewhurst. 2011. Nitrogen partitioning and isotopic fractionation in dairy cows consuming diets based on a range of contrasting forages. Journal of Dairy Science **94**:2031-2041.

Choi, B. Y., S. T. Yun, B. Mayer, and K. H. Kim. 2011. Sources and biogeochemical behavior of nitrate and sulfate in an alluvial aquifer: Hydrochemical and stable isotope approaches. Applied Geochemistry **26**:1249-1260.

Chung, J., H. Shim, Y. W. Lee, and W. Bae. 2005. Comparison of influence of free ammonia and dissolved oxygen on nitrite accumulation between suspended and attached cells. Environmental Technology **26**:21-33.

Clay, D. E., G. L. Malzer, and J. L. Anderson. 1990. Ammonia volatilization from urea as influenced by soil-temperature, soil-water content, and nitrification and hydrolysis inhibitors Soil Science Society of America Journal **54**:263-266.

Clough, T. J., J. L. Ray, L. E. Buckthought, J. Calder, D. Baird, M. O'Callaghan, R. R. Sherlock, and L. M. Condron. 2009. The mitigation potential of hippuric acid on N2O emissions from urine patches: An in situ determination of its effect. Soil Biology & Biochemistry **41**:2222-2229.

Decau, M. L., J. C. Simon, and A. Jacquet. 2004. Nitrate leaching under grassland as affected by mineral nitrogen fertilization and cattle urine. Journal of Environmental Quality **33**:637-644.

Di, H. J. and K. C. Cameron. 2002. Nitrate leaching in temperate agroecosystems: sources, factors and mitigating strategies. Nutrient Cycling in Agroecosystems **64**:237-256.

Dobermann, A., J. L. Gaunt, H. U. Neue, I. F. Grant, M. A. Adviento, and M. F. Pampolino. 1994. Spatial and temporal variability of ammonium in flooded rice fields. Soil Science Society of America Journal **58**:1708-1717.

Fang, Y. T., K. Koba, A. Makabe, F. F. Zhu, S. Y. Fan, X. Y. Liu, and M. Yoh. 2012. Low delta O-18 values of nitrate produced from nitrification in temperate forest soils. Environmental Science & Technology **46**:8723-8730.

Frank, D. A., R. D. Evans, and B. F. Tracy. 2004. The role of ammonia volatilization in controlling the natural N-15 abundance of a grazed grassland. Biogeochemistry **68**:169-178.

Galloway, J. N., J. D. Aber, J. W. Erisman, S. P. Seitzinger, R. W. Howarth, E. B. Cowling, and B. J. Cosby. 2003. The nitrogen cascade. Bioscience **53**:341-356.

Groffman, P. M., K. Butterbach-Bahl, R. W. Fulweiler, A. J. Gold, J. L. Morse, E. K. Stander, C. Tague, C. Tonitto, and P. Vidon. 2009. Challenges to incorporating spatially and temporally explicit phenomena (hotspots and hot moments) in denitrification models. Biogeochemistry **93**:49-77.

Heaton, T. H. E. 1986. Isotopic studies of nitrogen pollution in the hydrosphere and atmosphere - a review. Chemical Geology **59**:87-102.

Hogberg, P. 1997. Tansley review No 95 - N-15 natural abundance in soil-plant systems. New Phytologist **137**:179-203.

Jia, G. D. and F. J. Chen. 2010. Monthly variations in nitrogen isotopes of ammonium and nitrate in wet deposition at Guangzhou, south China. Atmospheric Environment **44**:2309-2315.

Kaye, J. P. and S. C. Hart. 1997. Competition for nitrogen between plants and soil microorganisms. Trends in Ecology & Evolution **12**:139-143.

Kempers, A. J. and A. Zweers. 1986. Ammonium determination in soil extracts by the salicylate method. Communications in Soil Science and Plant Analysis **17**:715-723.

Kendall, C. 1998. Tracing Nitrogen Sources and Cycling in Catchments *in* C. Kendall and J. J. Mcdonell, editors. Isotope Tracers in Catchment Hydrology. Elsevier Science B.V., Amsterdam.

Kool, D. M., N. Wrage, S. Zechmeister-Boltenstern, M. Pfeffer, D. Brus, O. Oenema, and J. W. Van Groenigen. 2010. Nitrifier denitrification can be a source of N_2O from soil: a revised approach to the dual-isotope labelling method. European Journal of Soil Science **61**:759-772.

Kriszan, M., W. Amelung, J. Schellberg, T. Gebbing, and W. Kuhbauch. 2009. Long-term changes of the $\delta^{15}N$ natural abundance of plants and soil in a temperate grassland. Plant and Soil **325**:157-169.

Laubach, J., A. Taghizadeh-Toosi, S. J. Gibbs, R. R. Sherlock, F. M. Kelliher, and S. P. P. Grover. 2013. Ammonia emissions from cattle urine and dung excreted on pasture. Biogeosciences **10**:327-338.

Mariotti, A., J. C. Germon, P. Hubert, P. Kaiser, R. Letolle, A. Tardieux, and P. Tardieux. 1981. Experimental-determination of nitrogen kinetic isotope fractionation - some principles - illustration for the denitrification and nitrification processes. Plant and Soil **62**:413-430.

McDowell, R. W., T. Snelder, R. Littlejohn, M. Hickey, N. Cox, and D. J. Booker. 2011. State and potential management to improve water quality in an agricultural catchment relative to a natural baseline. Agriculture Ecosystems & Environment **144**:188-200.

McFarland, J. W., R. W. Ruess, K. Kielland, K. Pregitzer, R. Hendrick, and M. Allen. 2010. Cross-ecosystem comparisons of in situ plant uptake of amino acid-N and NH_4^+. Ecosystems **13**:177-193.

McIlvin, M. R. and M. A. Altabet. 2005. Chemical conversion of nitrate and nitrite to nitrous oxide for nitrogen and oxygen isotopic analysis in freshwater and seawater. Analytical Chemistry **77**:5589-5595.

Mengis, M., U. Walther, S. M. Bernasconi, and B. Wehrli. 2001. Limitations of using delta O-18 for the source identification of nitrate in agricultural soils. Environmental Science & Technology **35**:1840-1844.

Minet, E., C. E. Coxon, R. Goodhue, K. G. Richards, R. M. Kalin, and W. Meier-Augenstein. 2012. Evaluating the utility of N-15 and O-18 isotope abundance analyses to identify nitrate sources: A soil zone study. Water Research **46**:3723-3736.

Mobius, J. 2013. Isotope fractionation during nitrogen remineralization (ammonification): Implications for nitrogen isotope biogeochemistry. Geochimica Et Cosmochimica Acta **105**:422-432.

Moir, J. L., K. C. Cameron, H. J. Di, and U. Fertsak. 2011. The spatial coverage of dairy cattle urine patches in an intensively grazed pasture system. Journal of Agricultural Science **149**:473-485.

Nestler, A., M. Berglund, F. Accoe, S. Duta, D. M. Xue, P. Boeckx, and P. Taylor. 2011. Isotopes for improved management of nitrate pollution in aqueous resources: review of surface water field studies. Environmental Science and Pollution Research **18**:519-533.

Oenema, O., G. L. Velthof, S. Yamulki, and S. C. Jarvis. 1997. Nitrous oxide emissions from grazed grassland. Soil Use and Management **13**:288-295.

Orwin, K. H., J. E. Bertram, T. J. Clough, L. M. Condron, R. R. Sherlock, M. O'Callaghan, J. Ray, and D. B. Baird. 2010. Impact of bovine urine deposition on soil microbial activity, biomass, and community structure. Applied Soil Ecology **44**:89-100.

Powell, J. M., C. J. P. Gourley, C. A. Rotz, and D. M. Weaver. 2010. Nitrogen use efficiency: A potential performance indicator and policy tool for dairy farms. Environmental Science & Policy **13**:217-228.

Romera, A. J., G. Levy, P. C. Beukes, D. A. Clark, and C. B. Glassey. 2012. A urine patch framework to simulate nitrogen leaching on New Zealand dairy farms. Nutrient Cycling in Agroecosystems **92**:329-346.

Schimel, J. P. and J. Bennett. 2004. Nitrogen mineralization: Challenges of a changing paradigm. Ecology **85**:591-602.

Schrama, M., G. F. Veen, E. S. Bakker, J. L. Ruifrok, J. P. Bakker, and H. Olff. 2013. An integrated perspective to explain nitrogen mineralization in grazed ecosystems. Perspectives in Plant Ecology Evolution and Systematics **15**:32-44.

Sherlock, R. R. and K. M. Goh. 1985. Dynamics of ammonia volatilization from simulated urine patches and aqueous urea applied to pasture. 2. the theoretical derivation of a simplified model Fertilizer Research **6**:3-22.

Smith, P., D. Martino, Z. Cai, D. Gwary, H. Janzen, P. Kumar, B. McCarl, S. Ogle, F. O'Mara, C. Rice, B. Scholes, O. Sirotenko, M. Howden, T. McAllister, G. Pan, V. Romanenkov, U. Schneider, S. Towprayoon, M. Wattenbach, and J. Smith. 2008. Greenhouse gas mitigation in agriculture. Philosophical Transactions of the Royal Society B-Biological Sciences **363**:789-813.

Stark, J. M. and S. C. Hart. 1996. Diffusion technique for preparing salt solutions, Kjeldahl digests, and persulfate digests for nitrogen-15 analysis. Soil Science Society of America Journal **60**:1846-1855.

Stevenson, B. A., R. L. Parfitt, L. A. Schipper, W. T. Baisden, and P. Mudge. 2010. Relationship between soil delta N-15, C/N and N losses across land uses in New Zealand. Agriculture Ecosystems & Environment **139**:736-741.

Uemura, S., S. Suzuki, K. Abe, A. Ohashi, H. Harada, M. Ito, H. Imachi, and T. Tokutomi. 2011. Partial nitrification in an airlift activated sludge reactor with experimental and theoretical assessments of the pH gradient inside the sponge support medium. International Journal of Environmental Research **5**:33-40.

Venterea, R. T., A. D. Halvorson, N. Kitchen, M. A. Liebig, M. A. Cavigelli, S. J. Del Grosso, P. P. Motavalli, K. A. Nelson, K. A. Spokas, B. P. Singh, C. E. Stewart, A. Ranaivoson, J. Strock, and H. Collins. 2012. Challenges and opportunities for mitigating nitrous oxide emissions from fertilized cropping systems. Frontiers in Ecology and the Environment **10**:562-570.

Xue, D. M., J. Botte, B. De Baets, F. Accoe, A. Nestler, P. Taylor, O. Van Cleemput, M. Berglund, and P. Boeckx. 2009. Present limitations and future prospects of stable isotope methods for nitrate source identification in surface- and groundwater. Water Research **43**:1159-1170.

Plate 3 **Clockwise from top: rice crop in long-term fallowing experiment photographed in September 2010 (following the studied dry season fallow); fallow treatment 'R' (natural wetting and drying with rainfall), with and without straw removal; fallow treatment 'D' (constant drying, covered with tarp overnight and during rainfall; fallow treatment 'F' (kept continuously flooded, note cyanobacteria mat formed in bottom right of photograph).**

Chapter 5

Nitrate dual isotopes reveal the impact of the intercrop period on accumulation versus attenuation of soil nitrogen in a tropical lowland rice system

A version of this chapter was submitted for publication in January 2014. Wells, N.S., T.J. Clough, S.E. Johnson-Beebout, R.J. Buresh. In review. Land preparation controls the soil inorganic nitrogen balance (accumulation v. attenuation) in a tropical lowland rice system. Nutrient Cycling in Agroecosystems

5.1 Abstract

Sustainable production of lowland rice (*Oryza sativa* L.) hinges on minimising undesirable soil nitrogen (N) losses via nitrate (NO_3^-) leaching and denitrification. Thus effective paddy management is limited by the lack of information on the N transformations during the intercrop period (fallow and land preparation) that control indigenous N availability for the subsequent crop. In order to redress this knowledge gap, changes in NO_3^- isotopic composition ($\delta^{15}N$ and $\delta^{18}O$) in soil and water were measured from harvest through fallow, land preparation, and crop establishment in a long-term field trial. During the intercrop period, plots were maintained either completely flooded, completely dried, or alternated between wet-dry with rainfall, with a split-plot treatment of ± crop residue incorporation and no N additions. Nitrogen accumulation during the fallow (20 kg NH_4^+-N ha^{-1} in flooded treatments v. 10 kg NO_3^--N ha^{-1} in aerobic treatments) did not influence N availability for the subsequent crop. Nitrate isotope fractionation patterns indicated that denitrification drove this homogenisation: during land preparation ~50% of available N in the soil (top 10 cm) was denitrified, and by two weeks after seedling transplanting this increased to >80% of available N, regardless of fallow management. The 17 days between fallow and crop growth controlled not only N attenuation (3 to 7 kg NO_3^--N ha^{-1} denitrified), but also N inputs (3 to 14 kg NO_3^--N ha^{-1} from nitrification), meaning denitrification was dependent on soil nitrification rates. While incorporation of crop residues delayed the timing of N attenuation, they ultimately did not impact indigenous N supply. By measuring NO_3^- isotopic composition over depth and time, this study provides unique *in situ* measurements of the pivotal role of land preparation in determining paddy soil indigenous N supply.

Keywords: paddy soils, indigenous nitrogen, nitrate isotopes, denitrification, fallow management

Terminology *Floodwater* refers to the ~6 cm of irrigation+rainwater overlaying submerged paddy soil, the *oxic layer* is at the top 2 cm of soil, defined by the depth to which atmospheric O_2 will diffuse; the *plough layer* represents bulk soil between the oxic and the plough pan (10 – 20 cm depth), defined as the depth at which NO_3^- is consumed; the *hardpan* is the impermeable layer underlying the paddy (~50 cm depth). The *intercrop* period occurs between the two annual rice crops (*crop growth*) and consists of a *fallow* (no crops or management activities) and *land preparation* (including re-flooding, harrowing, hydrotilling prior to seedling transplanting).

5.2 Introduction

Over 95% of rice (*Oryza sativa* L.), the staple food for the majority of the global population, is cultivated under submerged conditions in paddy soils (Buresh et al. 2008). The poor natural production, and rapid losses, of plant-available nitrogen (N) under submerged conditions have resulted in a reliance on costly N fertiliser inputs in order to obtain good crop yields (Buresh and Witt 2008). However, chronic inefficiencies in fertiliser use (Cassman and Buresh, Witt) incur further environmental costs as excess N additions contaminate adjacent waters (Bouman et al. 2002, Xiong et al. 2010) or are lost to the atmosphere in gaseous forms, including the greenhouse gas nitrous oxide (N_2O) (Cai et al. 1997, Zhang et al. 2011). In order to minimise these undesirable N losses while maximising crop yields, research has focused on fertiliser management (timing, quantity, and location of N application) (Cassman et al. 1998, Cassman et al. 2003, Dobermann and Cassman 2005). However, advances in conserving paddy soil N stocks are limited by a poor understanding of fluctuations its 'baseline' sources and sinks within the paddy environment, particularly during the intercrop period (fallow and land-preparation) (e.g., Akiyama et al. 2005).

The oscillating aerobic and anaerobic conditions inherent to lowland rice cultivation are considered the primary biogeochemical drivers for N cycling, and major determinants of paddy soil indigenous N supply (Buresh et al. 1993, George et al. 1993, Cai et al. 1997). Indigenous soil N supply is the soil N available to crops pre-fertilisation ($N_{indigenous}$), defined here as the net difference between N inputs (N_{input}) and losses (N_{out}) (Eq. 5.1):

$$N_{indigenous} = N_{input} - N_{out}$$

$$N_{input} = N_{miner} + N_{BNF} \quad (5.1)$$

$$N_{out} = N_{denit} + N_{leach}$$

where N inputs (N_{input}) come from mineralised soil organic material (N_{miner}) and/or biological fixation of atmospheric N_2 (BNF) and N losses (N_{out}) are denitrification (permanent removal, or attenuation, of nitrate (NO_3^-) via its step-wise heterotrophic conversion to N_2O and dinitrogen (N_2) (using carbon (C) as an electron donor)) (N_{denit}) and leaching (N_{leach}).

The highly anaerobic conditions that form beneath paddy floodwater inhibit the mineralisation of organic N into biologically available forms (predominantly ammonium (NH_4^+ and nitrate (NO_3^-)) (Bird et al. 2001, Bird et al. 2002). Nitrogen mineralisation rates also depend on the frequency and duration of wetting-drying cycles (Schimel and Bennett 2004, Borken and Matzner 2009, Austin and Strauss 2011), and can change synergistically with management of crop residues (Witt et al. 2000, Bird et al. 2002, Bierke et al. 2008). Due to the oxygen (O_2) limitation in paddy soils, nitrification (autotrophic oxidation of ammonia (NH_3) to nitrate (NO_3^-)) is generally the limiting step to NO_3^- accumulation, and thus N losses, from these systems, as NO_3^- is the most mobile form of N (Henckel and Conrad 1998). Anaerobic, submerged paddy soils maximise N_{out} due to the rapid denitrification of any NO_3^- that forms (generally in the thin oxidised surface soil or in root rhizophere) (DeDatta 1995, Buresh et al. 2008). If NO_3^- is not denitrified or taken up by the plants, it can be leached into the groundwater (Bouman et al. 2007).

Thus management of submerged v. dry soil periods drives both N_{input} and N_{out} in paddy systems: in lowland tropical rice cultivation fields are typically flooded two weeks prior to transplanting rice seedlings, submerged with ~6 cm of water throughout the growing period, left to 'dry down' two weeks prior to harvest, and then left fallow for one to two months before the next crop. During low rainfall fallow periods the top 10-20 cm of the paddy soil dries out (Ringrose-Voase et al. 2000), increasing O_2 penetration and altering redox potential. Accordingly, mineralisation and nitrification rates are maximised during the fallow (Buresh et al. 1989). Oxygen concentrations ≥4 mg l^{-1} inhibit denitrification (Rivett et al. 2008), meaning that NO_3^- can accumulate between the harvest of one crop and the planting of the next. Additionally, reincorporation of crop residues can either conserve N losses by returning organic N to the soil, or cause net immobilisation of dissolved inorganic N (DIN), depending primarily on the residue's C/N ratio (Rasche and Cadisch 2013).

Despite recognition of the importance of these wetting-drying cycles on paddy soil N cycling during the growing season (Buresh et al. 1993; Dong et al. 2012; Berger et al. 2013), the impact of the dramatic dry-down, re-flooding and turbation during the intercrop period is rarely assessed. Exceptions include George et al. (1993) and Becker et al. (2007), both of whom found that, regardless of the quantity of DIN initially present, NO_3^- concentrations were 'virtually negligible' within weeks of re-flooding. However, information is still needed on the relative importance of denitrification versus leaching to net N losses and how management can control the timing and rate of these pathways. Additionally, relying on DIN concentration data to assess paddy soil nutrient dynamics can lead to an underestimation of N_{input} due to the tight spatial and temporal coupling between nitrification and denitrification in paddy soils (Buresh et al. 2008).

To address these research gaps, this study identified and quantified nitrification and denitrification in paddy soils during the intercrop period by measuring changes in the natural abundance of NO_3^- stable isotopes ($^{15/14}N$ and $^{18/16}O$). As 'light' isotopes of NO_3^- are used preferentially during biological reactions, the change in isotope abundance over distance and/or time (R/R_0) can be

quantitatively related to the change in substrate concentration (C/C_0) based on the degree of isotopic preference for the given reaction (α, the fractionation factor) using the Rayleigh equation (Kendall 1998) (Eq. 5.2).

(5.2) $$\frac{R}{R_0} = \left(\frac{C}{C_0}\right)^{1/(\alpha-1)}$$

During denitrification both $\delta^{18}O\text{-}NO_3^-$ and $\delta^{15}N\text{-}NO_3^-$ are enriched in parallel, meaning that ratios of $\delta^{18}O{:}\delta^{15}N$ of 1:1 (Granger et al. 2008) or 1:2 (Kendall 1998) can be used to fingerprint attenuation. Nitrate stable isotopes have been effectively used to quantify N sources (e.g., N from mineralised organic matter and BNF from manure derived or fertiliser derived N) and sinks in marine (Sigman et al. 2003) and freshwater (Barnes and Raymond 2010) environments, as well as in aerobic soils (Koba et al. 1997). As $\delta^{15}N$ and $\delta^{18}O$ are minimally influenced by non-biological changes in DIN concentration (e.g., immobilisation, mineralisation (Möbius 2013)) and integrate microscale changes in concentration over time and space (e.g., Koba et al. 1997), the objective of this study was to use changes in their composition to quantify how water and residue management specifically affected the biological (nitrification and denitrification) controls on N_{inputs} and N_{out} during the intercrop period in a rice paddy system.

5.3 Material & methods

5.3.1 Field site

The study was carried out in a long-term field trial (established in November 2003) at the International Rice Research Institute's experimental farm in Los Baños, Laguna, Philippines (14º1'N, 121º15'E). The climate is tropical (mean annual temperature of 25ºC), with most of the 1900 mm precipitation per year received July–February. The soil was an Aquandic Epiaquoll soil (62% clay and 9% sand) (Bierke et al. 2008). During the fallow, water and crop residues were managed such that main plots were either: continuously flooded (F), continuously dried (D), or allowed to naturally alternate between wet and dry with rainfall (R). Treatments, replicated four times, were laid out in a randomised split-plot block design (Bierke et al. 2008). Split-plots (4.5 m x 4.7 m) had rice straw residues from the previous crop either removed after harvest (*ns*) or left standing during the fallow and then incorporated into the soil during land preparation (*s*). Rain was excluded from D plots using tarpaulin tents (open at the ends to allow free airflow). Neither soil nor air temperatures changed significantly under rain-exclusion tents (R.J. Buresh, unpubl.). Due to the lack of precipitation during the fallow (April-June 2010), plots in treatment R were irrigated for ~4 h on day 20 to simulate a rainfall event.

The fallow period lasted 33 days, and were followed by 17 days of land preparation, beginning with the re-flooding of all plots on day 33 and including the reincorporation of crop residues

into *s* treatments (Fig. 5.1). On day 53 seedlings (variety NSIC Rc158) were transplanted into all treatments. During the growing season all plots were managed identically, including basal application of phosphorus, potassium, and zinc (40, 20, and 10 kg ha^{-1} of P, K, and Zn, respectively) and three splits of 60 kg urea-N ha^{-1}.

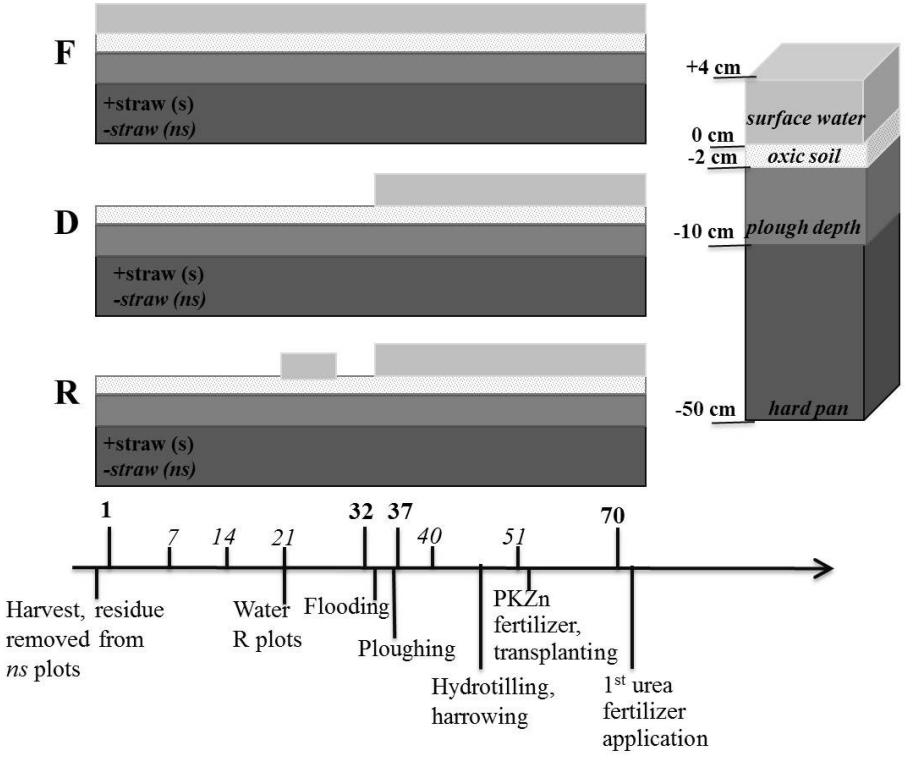

Figure 5.1 **Schematic diagram showing treatment management, where treatments were kept either continuously flooded (F), continuously dried (D), or allowed to alternate wet-dry (R) during the fallow with split-plots of ± crop residue incorporation; the inset depicts the stratification of where samples were collected from surface water, oxic soil (0-2 cm), plough layer soil (2-10 cm) and immediately above the hardpan (50 cm) (inset)**

5.3.2 Sample collection

Samples were collected from plots' floodwater, oxic soil (0-2 cm), plough layer soil (2-10 cm), and the hardpan (porewater at 40 cm depth) nine times over 70 days. Sampling was timed to land management: *ns* split-plots of treatments F, D, and R were sampled five times over the fallow (day 1 – 32; fallow), thrice during land-preparation (day 34 – 51; land preparation), and once during the first 18 days of crop growth (day 52 – 70; crop) (Fig. 5.1). In the *s* split-plots, samples were collected on twice during the fallow (days 1 and 32), once during land preparation (day 37), and once during crop growth (day 70). Final samples (day 70) were collected immediately prior to the first urea fertiliser application.

5.3.3 Redox, pH, temperature

Soil, redox potential, pH, and temperature were measured in-situ during sample collection. To measure redox, six platinum electrodes were permanently installed in each *ns* plot on day 1 (see Johnson-Beebout et al. (2009) for electrode details). Electrodes were removed for land preparation on day 33 and reinstalled following transplanting (day 52) (Fig. 5.1). Electrode placement corresponded to sampled soil depths at 2 and 10 cm depths, and a total of 12 electrodes were installed per treatment per depth. Measurements were taken between 11:00 and 14:00 h using an Ag/AgCl reference electrode corrected based on hydrogen probe readings. Soil pH was measured simultaneously on the same probe. A mercury thermometer was used to measure soil temperature at 10 cm depth in each plot.

5.3.4 Soil sampling and measurements

During soil sampling, cores (10 cm length x 5 cm diameter) were collected from four randomly selected locations within each split-plot. Soil cores were separated into 0-2 cm (oxic) and 2-10 cm (plough) sections, and bulked to create homogenised samples for each soil depth per split-plot. Bulked soils were sealed into polypropylene bags and kept on ice until they were returned to the laboratory for extractions.

For soil NH_4^+ measurements, 7 g (fresh weight) of soil was extracted with 35 ml of 1M KCl (shaken for 30 min on a rotary shaker, centrifuged for 15 min at 3500 rpm, and then passed through Whatman 42 filter paper). Nitrate was measured in water extractions: 7 g (fresh weight) soil was mixed with 35 ml deionised water for 1 h on a rotary shaker, centrifuged at 3500 rpm for 15 min, and then passed through Whatman 1 filter paper. All filtrates were stored in acid-washed plastic vials at -4ºC for ≤48 h prior to chemical analyses, with aliquots frozen at -20ºC until isotope analysis. Soil gravimetric moisture (θ_g) was determined on 10 g sub-samples after drying at 105°C for 48 h (Blakemore et al. 1987). Following drying, sub-samples of soils from days 32 and 70 were finely ground in a mechanical mixer for total N and C analysis.

5.3.5 Water sampling and measurement

Soil porewater above the hardpan (Fig. 5.1) was collected using Rhizon soil solution samplers (RSSS) (Eijkelkamp Agrisearch Equipment, Giesbeek, Netherlands) installed at 40 cm depth in each of the 24 split-plots on day 1. Samplers were removed on day 32 for land preparation and then reinstalled after transplanting. Porewater was collected via suction using 50 ml single-use syringes, after which extraction volume was recorded and then injected into a 15 ml pre-evacuated glass vial fitted with a rubber stopper. Soil dryness prevented consistent collection of porewater in both aerobic treatments (D and R) during the fallow period. Additional porewater samples were collected from R plots (both *s* and *ns*) starting 4 h prior to the simulated rainfall event on day 20, and continuing for 36 h at 2 – 6 h intervals.

Floodwater samples were collected, and floodwater depth measured, from treatment F throughout the trial period, and from treatments D and R following re-submergence for land preparation on day 37. Irrigation water used to flood the plots for land preparation was sampled on day 37. All water samples were collected in 100 ml acid-washed Nalgene bottles, and immediately passed through Whatman GF/F filter paper upon return to the laboratory. Filtrates were stored (≤48 h) at 4ºC until chemical analysis and then frozen at -20ºC until isotope analysis.

5.3.6 Chemical analysis

Nitrate concentrations were measured in soil porewater, floodwater, and water extracts of oxic and plough layer soils using an ELIT 8021 ion selective electrode (www.nico2000.net). Approximately 10% of samples were re-analysed on a Dionex suppressed ion exchange chromatograph (Lincoln University, NZ) to ensure that there was no matrix interference. Ammonium concentrations were determined in acidified porewater and floodwater samples (as per Dobermann et al. (1994)) and on 1M KCl soil extracts. These samples were analysed using the salicylate method (Kempers and Zweers 1986), with absorbance read at 650 nm on a DU-730 UV-*vis* spectrophotometer (International Rice Research Institute). Total N and C of soils collected on days 32 and 70 were measured via combustion on an EA-TCD (Analytical Services Laboratory, International Rice Research Institute) (precision of ±0.04).

Nitrate isotopes ($^{15}N/^{14}N$ and $^{18}O/^{16}O$) were measured using the cadmium reduction- azide reaction method (McIlvin and Altabet 2005). Each batch contained duplicates of three international standards (IAEA-N3, USGS-34, and USGS-32), two internal standards, and water blanks. The $\delta^{18}O$ and $\delta^{15}N$ of resultant N_2O were measured on a Europa PDZ (SerCon) 20-20 IR-MS at Lincoln University (NZ), and the values of $\delta^{18}O$- $\delta^{15}N$- NO_3^- were calculated based on calibration of the international standards. Method accuracy was calculated as 0.8‰ for $\delta^{18}O$- NO_3^- and 0.6‰ for $\delta^{15}N$- NO_3^-. Isotope results are reported in δ‰ (Eq. 5.3):

$$\delta‰ = \frac{(R_{sample} - R_{standard})}{R_{standard}} \times 1000 \quad (5.3)$$

where the isotope mass ratio of the sample (R_{sample}) is reported with respect to internationally recognised standards ($R_{standard}$) (AIR for N and VSMOW for O).

5.3.7 Data analysis

Differences between treatments over time were assessed using a mixed model with sampling date or phase (fallow, land preperation, crop) as repeated measures. Water management, residue management, and time variables were treated as fixed factors (Type III), with residue nested within water (as per the split-plot experimental design), using Least Significant Difference to analyse means (SPSS ver.20, New York, IBM Inc.). Changes in soil chemistry over vertical profiles (e.g., oxic versus

plough soils) were established via paired t-tests, and differences between treatments within a single phase or sampling date were established using a nested two-way ANOVA (Sidak post-hoc). Relationships between parameters were determined with Spearman rank-order correlation. Linear regression between variables was evaluated for goodness of fit (r^2) and significance (SigmaPlot ver.12; SPSS ver.20). All isotope calculations and mathematical manipulations were performed in Mathematica (ver. 7.0.1.; Wolfram Research). Significant results for all tests were defined as $p<0.05$, and values are reported as treatment mean ±SE unless otherwise noted.

5.4 Results

5.4.1 Soil chemistry

Soil total N and C content did not change over soil depth or with fallow management. From the fallow end (day 32) to immediately prior to the first N fertiliser application (day 70) total soil N decreased ($p<0.05$) from 0.177 ±0.004% (by mass) to 0.143 ±0.01%. Total C decreased ($p<0.05$) from 1.90 ±0.04% to 1.57 ±0.1% over the same period, meaning soil C/N ratios remained constant at 11.5 ±0.1.

Within the oxic and plough soil layers, moisture varied over time with water management ($p<0.001$; $p<0.001$). Soil in treatment F had consistently higher θ_g values than treatments R or D, even following re-flooding and transplanting (Fig. 5.2d). Residue incorporation increased θ_g by an average of 8% over all sampling dates and water treatments ($p<0.001$). Plough layer soil had lower ($p<0.001$) redox potential than oxic layers over all treatments and sampling dates (37.0 ±9 v. 75.0 ±11 Eh, respectively).[1] During the fallow, submerged soil in F treatments had lower redox potentials than the drying soils in the R and D treatments ($p<0.01$) (Fig. 5.2c). Re-flooding for land preparation caused the pH of the oxic soil layer to increase in both aerobic treatments: in D from 6.2 ±0.2 (fallow mean) to 7.4 ±0.1 and in R from 7.3 ±0.1 to 7.5 ±0.1. The pH in F treatments remained constant throughout the sampling period (7.1 ±0.1). By day 70, following land preparation and transplanting, soil pH in all treatments was ~7.0 and redox potential in the plough layer was 33.7 ±20 Eh (Fig. 5.2c). Soil temperatures were 35 ±4°C and did not exhibit any significant trends (data not shown).

1Redox potential could not be measured in treatment D on days 1 and 32 due to extreme soil dryness causing the electrode to lose contact with the soil

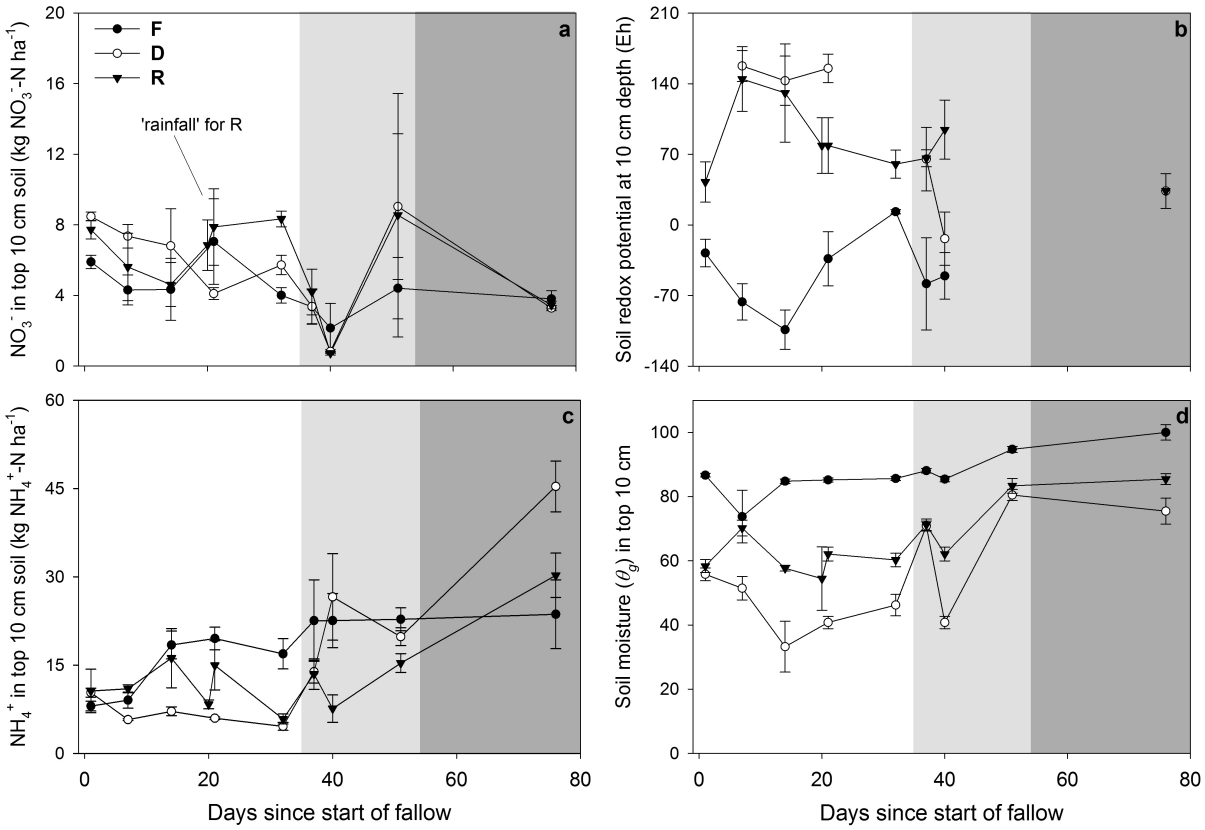

Figure 5.2 **Nitrate (a), redox potential (b), NH_4^+ (c), and soil gravimetric water content (d) in the top 10 cm of paddy soil over time in fields maintained either continuously submerged (F), continuously dry (D) or with natural wetting-drying with rainfall (R) during the fallow period. Grayscale gradations indicate the phase of crop management, from fallow (white), to land prep (light) to crop growth (dark). Data points represent treatment mean ± SE (n = 4)**

5.4.2 Inorganic N (soil and water)

Concentrations of NO_3^- and NH_4^+ varied over time in depth partitions (floodwater, oxic, plough, and hardpan) (Table 5.1). Immediately following the harvest of the previous crop (day 1), NO_3^- concentrations in the top 10 cm of soil (0-2 cm + 2-10 cm) in both aerobic treatments (D and R) increased relative to treatment F (Fig. 5.2a). By the end of the fallow period (day 32) DIN availability was lowest in treatment D (12.0 ±3 kg N ha^{-1}) and highest in F (25.2 ±9 kg N ha^{-1}). Residue treatments did not influence DIN concentration (Table 5.1).

The highest concentrations of NO_3^- in floodwater were measured in treatment F on the first day of the fallow (equivalent to ~0.127 ±0.004 kg NO_3^--N ha^{-1}). For all treatments, the lowest (p<0.001) NO_3^- concentration occurred during land preparation (0.049 ±0.004 kg NO_3^--N ha^{-1}), which increased to 0.086 ±0.004 kg NO_3^--N ha^{-1} after transplanting (Table 5.1).

Nitrate and NH_4^+ concentrations in the oxic soil layers were influenced by fallow management of water and residues. Over time, NO_3^- concentrations were highest during the fallow in treatments D and R with residues returned (s), while NH_4^+ concentrations were highest in D+s treatments during

crop growth (Table 5.1). During land preparation intra-treatment concentrations of NO_3^- and NH_4^+ in the oxic layer became highly variable (Fig. 5.2). In the plough layer NH_4^+ accumulation was influenced by water management, and was highest in treatment D on day 70 (Table 5.1, Fig. 5.2c). Flooding aerobically fallowed plots (D and R) for land preparation increased the concentration of DIN in the plough layer from 7.3 ±0.5 µg N g^{-1} soil (day 32) to 20 ±2 µg N g^{-1} soil (day 37), with NH_4^+ increasing from 4.0 ±0.4 to 13 ±1 µg NH_4^+-N g^{-1} and NO_3^- decreasing from 3.8 ±0.3 to 1.9 ±0.2 µg NO_3^--N g^{-1} soil (Fig. 5.2). In the total top 10 cm of soil of all treatment, only 3 kg NO_3^--N ha^{-1} was left after land preparation, representing <20% of the NO_3^- present on day 32.

Table 5.1 **Mixed model analysis of the importance of fallow management in controlling soil DIN variability over time (with the strength of the factor's impact on the model as F (df) and significance as $p<0.05$). For water (W) treatments fields were kept fields were kept either continuously flooded, continuously dried, or allowed to wet-dry with rainfall over the fallow period (W) and then subdivided into two straw treatments (S) (crop residues either removed or returned to the soil) (n = 4 per split-plot per sampling date). Water treatments were assessed based on a total of 10 sampling dates (5 during fallow, 3 during land prep, and 1 during crop growth) and straw treatments were assessed based on 5 sampling dates (2 during fallow, 1 during land prep, and 1 during crop growth)**

Oxic	NH_4^+	21.0 (9)***	0.234 (2)	2.05 (1)	2.29 (2)	6.68 (16)***	5.09 (3)**	4.40 (2)**
(0-2 cm)	NO_3^-	20.4 (9)***	13.7 (2)***	4.94 (1)*	11.2 (2)***	7.39 (16)**	4.98 (3)*	5.15 (6)**
	$\delta^{15}N\text{-}NO_3^-$	34.2 (8)***	0.790 (2)	2.50 (1)	0.293 (2)	1.61 (14)	0.938 (2)	0.107 (4)
	$\delta^{18}O\text{-}NO_3^-$	6.66 (8)*	2.31 (2)	1.99 (1)	1.76 (2)	1.47 (14)	1.56 (2)	0.935 (4)
Plough	NH_4^+	13.9 (9)***	2.84 (2)	1.19 (1)	0.614 (2)	5.44 (16)***	1.05 (3)	0.807 (6)
(2-10 cm)	NO_3^-	12.3 (9)***	0.244 (2)	1.52 (1)	0.148 (2)	2.32 (16)	0.513 (3)	0.840 (6)
	$\delta^{15}N\text{-}NO_3^-$	25.1 (8)***	0.957 (2)	5.37 (1)*	0.953 (2)	1.10 (14)	0.777 (2)	0.496 (4)
	$\delta^{18}O\text{-}NO_3^-$	22.8 (8)**	1.32 (2)	3.29 (1)	1.78 (2)	1.03 (14)	1.67 (2)	1.49 (4)
Hardpan	NO_3^-	56.2 (6)***	2.37 (2)	0.56 (1)	0.64 (2)	1.53 (5)	6.34 (2)	0.907 (1)
(50 cm)	$\delta^{15}N\text{-}NO_3^-$	1.44 (5)*	0.433 (2)	1.15 (1)	0.132 (2)	0.125 (4)	1.25 (1)	
	$\delta^{18}O\text{-}NO_3^-$	3.54 (5)	1.93 (2)	1.35 (1)	1.73 (2)	0.321 (4)	3.86 (1)	

***$p<0.001$
**$p<0.01$
*$p<0.05$

Porewater NO_3^- concentrations at the hardpan of treatments F and R had a mean value of 0.45 ±0.05 mg NO_3^--N l^{-1} (~1.76 g N kg^{-1} soil) during the fallow. (Drying during the fallow made it impossible to collect porewater from treatment D on days 1 through 32 or from treatment R on day 14.) Once land preparation commenced, NO_3^- concentrations at the hardpan below treatments F, D and R decreased to a mean of 0.55 ±0.1 µg NO_3^--N g^{-1} soil, and did not change significantly following transplanting (Table 5.1). Ammonium was not present in detectable concentrations at the hardpan on any date in any treatment.

5.4.3 Nitrate isotopes

Values of $\delta^{15}N\text{-}NO_3^-$ and $\delta^{18}O\text{-}NO_3^-$ were dynamic over time in the floodwater, oxic soil, plough soil, and porewater at the hardpan (Table 5.1). Variations in $\delta^{15}N\text{-}NO_3^-$ and $\delta^{18}O\text{-}NO_3^-$ were positively correlated with each other across all samples (r =0.385, p<0.01). Although $\delta^{15}N\text{-}NO_3^-$ was higher in treatments without residue incorporation (14.5 ±1‰) than those with (13.0 ±2‰) (p<0.05)), vertical (surface water v. oxic v. plough v. hardpan) and temporal variations in $\delta^{15}N$- $\delta^{18}O$- NO_3^- were not influenced by residue or water management. Both NO_3^- isotopes became more enriched in all treatments over all sampling dates (p<0.001), but the dynamics within each layer was distinct over time, as was the degree of change over depth.

The isotopic composition of NO_3^- in floodwater in treatment F was 9.75 ±4‰ for $\delta^{15}N$ and 4.80 ±5‰ for $\delta^{18}O$ during the fallow, statistically similar to their composition in the adjacent oxic soil layer (Fig. 5.3). Following flooding during land preparation, floodwater enrichment in both NO_3^- heavy isotopes increased (p<0.05) to 19.9 ±4‰ ($\delta^{15}N$) and 19.5 ±6‰ ($\delta^{18}O$), and did not change significantly following transplanting (or vary between treatments) (Table 5.1). The slope of the linear regression of $\delta^{18}O\text{-}NO_3^-$ v. $\delta^{15}N\text{-}NO_3^-$ in floodwater over time was 0.46 (r^2 = 0.30, p<0.05,) (data not shown).

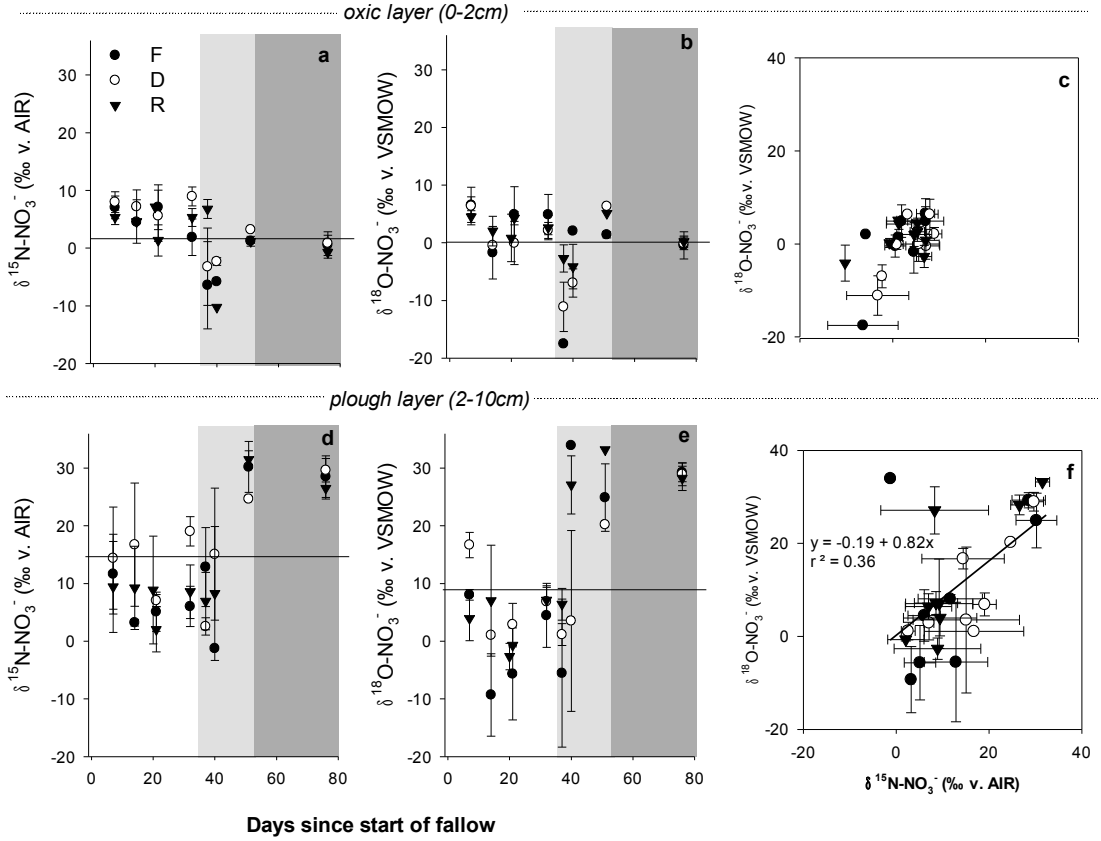

Figure 5.3 **Composition of $\delta^{15}N\text{-}NO_3^-$ and $\delta^{18}O\text{-}NO_3^-$ in the oxic (a, b) and plough (d, e) layers of soil over time, and plotted verse each other (c, f). Measurements were taken during the fallow (white; days 1-32), land preparation (light grey; days 37-50) and crop growth (dark grey; day 70). During the fallow plots were maintained as either continuously flooded (F), continuously dried (D), or with natural wetting-drying (R). The solid lines in a, b, d, and e indicate the mean isotope composition for all treatments and sampling dates, which were: 2.82 ±6‰ (a), 0.231 ±7 (b), 14.0 ±10 (d), and 9.88 ±10 (e). Data is plotted as treatment means (±SE) (*n* = 3).**

In the oxic soil layer $\delta^{15}N\text{-}NO_3^-$ and $\delta^{18}O\text{-}NO_3^-$ became slightly less enriched over time, declining from +5.64 ±1‰ ($\delta^{15}N$) and +3.24 ±1‰ ($\delta^{18}O$) during the fallow to +0.423 ±0.6‰ ($\delta^{15}N$) and -0.114 ±1‰ ($\delta^{18}O$) by day 70 (Fig. 5.3). Changes in $\delta^{15}N\text{-}NO_3^-$ did not co-vary with those in $\delta^{18}O\text{-}NO_3^-$ within this soil layer (Fig. 5.3c). Instead, $\delta^{15}N\text{-}NO_3^-$ values in the oxic soil depended on the relative concentration of NO_3^- to NH_4^+: the lower the NO_3^--N to NH_4^+-N ratios the less enriched the $\delta^{15}N\text{-}NO_3^-$ (Fig. 5.4).

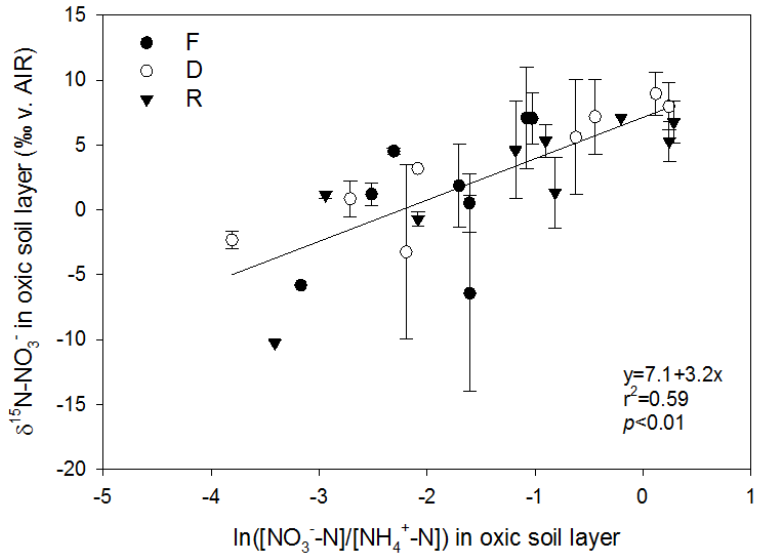

Figure 5.4 **A Rayleigh-type plot of $\delta^{15}N\text{-}NO_3^-$ versus the natural log of the concentration ratio of NO_3^--N to NH_4^+-N in the oxic soil layer over time and treatments (either continuously flooded (F), continuously dried (D), or allowed to naturally wet-dry (R) during the fallow). Error bars represent ±SE for treatment means per sampling date (n = 3).**

Within the plough layer $\delta^{18}O\text{-}NO_3^-$ co-varied with $\delta^{15}N\text{-}NO_3^-$, yielding a slope of 0.82 for changes $\delta^{18}O$:$\delta^{15}N$ over time and between replicates (Fig. 5.3f). Both O and N in the plough layer were isotopically lightest during land preparation, when intra-plot variability was greatest (Fig. 5.3). The difference in enrichment of $\delta^{15}N\text{-}NO_3^-$ and $\delta^{18}O\text{-}NO_3^-$ between plough and oxic soil layers increased over time, with NO_3^- in the plough layer heaviest relative to NO_3^- in the oxic layer during crop growth ($\delta^{15}N\text{-}NO_3^-$: p<0.001; $\delta^{18}O\text{-}NO_3^-$: p<0.001). These changes in isotopic composition over soil depth occurred with a linear slope of 1.15 for $\delta^{18}O$ v. $\delta^{15}N$ (p<0.001, r^2 = 0.95) (Fig. 5.5a).

The isotopic composition of NO_3^- at the hardpan was 12.6 ±3‰ for $\delta^{15}N$ and 12.7 ±4‰ for $\delta^{18}O$ during the fallow (Fig. 5.5b). Enrichment of $\delta^{18}O\text{-}NO_3^-$, but not $\delta^{15}N\text{-}NO_3^-$, occurred during land preparation (Table 5.1, Fig. 5.5b), resulting in a weak relationship between the two isotopes over time and space, with an $r^2 = 0.17$ ($p<0.05$) for the slope of $\delta^{18}O$ v. $\delta^{15}N$ (Fig. 5.5b). The exception to this trend was the samples collected from treatment R following the simulated rainfall event on day 20, as discussed below.

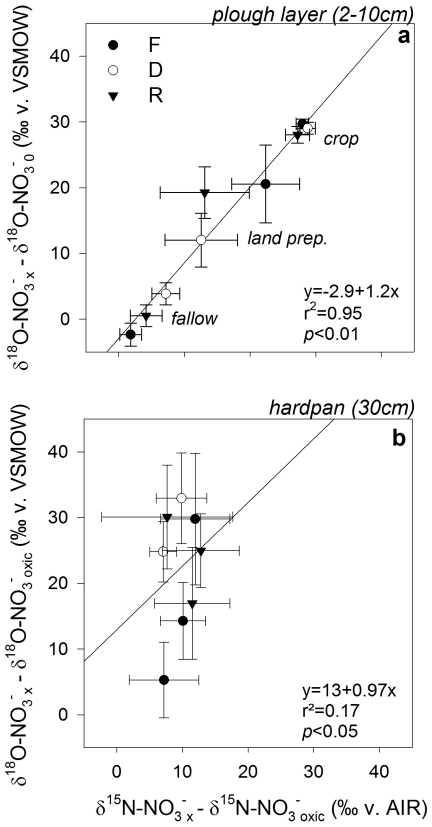

Figure 5.5 **The difference between $\delta^{15}N\text{-}NO_3^-$ and $\delta^{18}O\text{-}NO_3^-$ in the plough soil layer (2-10 cm) and at the hardpan and that in the oxic soil layer (0-2 cm) (a and b, respectively). Samples were collected on nine sampling dates during the dry season fallow (sampled x5 over 30 days), land-preparation (sampled x3 over 19 days), and cropping (sampled once 19 days post-transplanting, pre-fertilisation) from paddies that were kept either continuously flooded (F), continuous dried (D), or allowed natural drying-rewetting with rainfall (R) during the fallow.**

5.4.4 Site-specific ε_{denit}

Nitrate concentrations at the hardpan reached a maximum between 10 and 18 h post-wetting (Fig. 5.6a). From 20 h onwards NO_3^- concentrations decreased while becoming progressively enriched in both ^{18}O and ^{15}N ($\delta^{18}O$:$\delta^{15}N$ linear relationship of ~1 ($p<0.01$, $r^2 = 0.6$)) (Fig. 5.6). The inverse relationship between NO_3^- concentrations and $\delta^{15}N$- $\delta^{18}O$- NO_3^- enrichment after the 20 h 'tipping point' was used to calculate a site-specific enrichment factor for denitrification (ε_{denit}; $\varepsilon = (\alpha\text{-}1)\times1000$) using the modified Rayleigh equation (Eq. 5.3) of Mariotti et al. (1981) (Eq. 5.4):

$$\delta^{15}N_x = \delta^{15}N_0 + \varepsilon \times ln\left(\frac{f}{1-f}\right)$$

(5.4)

$$f = \frac{C_x}{C_0}$$

where the proportion of the maximum NO_3^- concentration measured during peak leaching (20 h) (C_0) remaining at the sampling point (C_x) was defined as *f*, and related to the co-occurring changes in $\delta^{15}N$ enrichment ($\delta^{15}N_x$ v. $\delta^{15}N_0$) via ε_{denit}. The same equation was also used to calculate ε_{denit} based on $\delta^{18}O$-NO_3^-. From Eq. 5.4, ε_{denit} for both $\delta^{15}N$-NO_3^- and $\delta^{18}O$-NO_3^- was calculated as -16‰ (r^2 = 0.67 and 0.61, respectively (p<0.01)) (Fig. 5.6c).

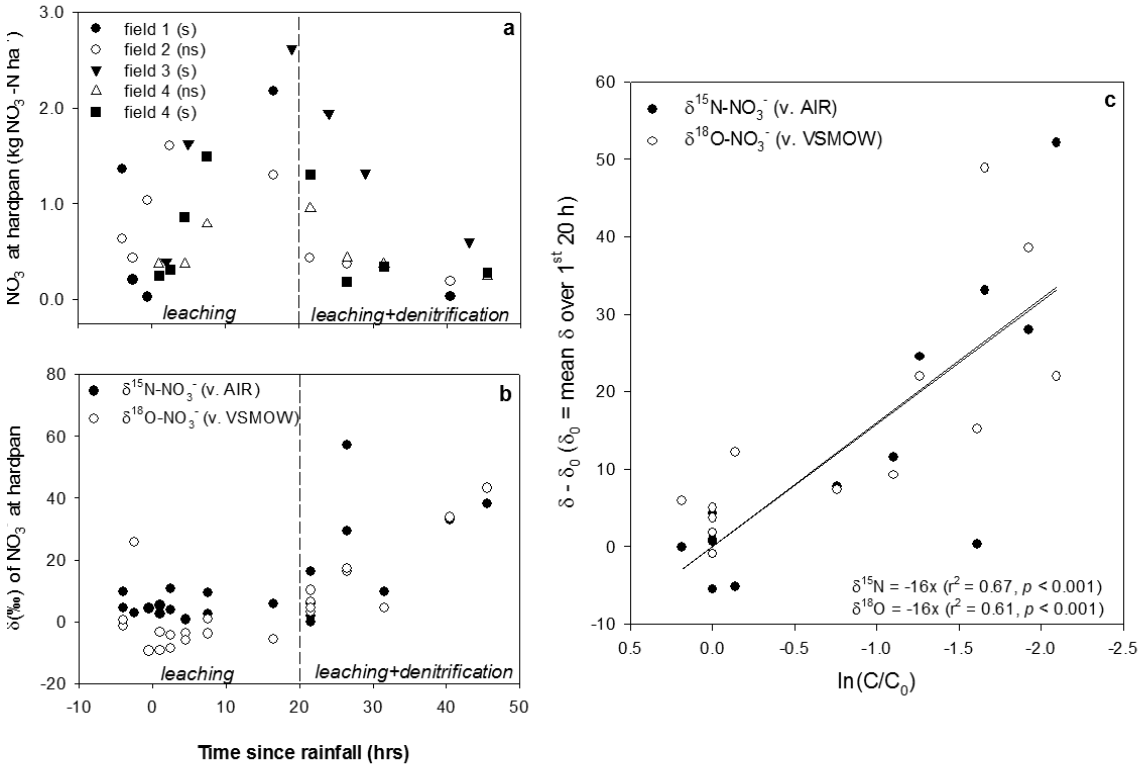

Figure 5.6 **The concentration of NO_3^- (a) and its isotopes ($\delta^{15}N$ and $\delta^{18}O$) (b) in soil porewater measured above the hardpan (40 cm depth) in treatment R (wetting-drying, both with and without residue amendments) during a mid-fallow (day 20-21) simulated rainfall event. The relationship between NO_3^- concentrations and isotopic composition over this period were then used to calculate ε_{denit} (c).**

5.5 Discussion

5.5.1 Overview

Similar spatial and temporal trends in isotopic composition across all plots indicated that NO_3^- production and reduction was controlled by the same processes, regardless of treatment. Thus the measured differences in DIN concentrations between treatments reflected differences in process rates. The changes in paddy soil chemistry over time and between treatments followed anticipated trends (e.g., Buresh et al. (1989) and Becker et al. (2007) also found that N oxides accumulated over aerobic fallows were lost from the soil within ~2 weeks of flooding), making the N balance calculated from the NO_3^- isotope data broadly applicable. The strong redox gradient over depth (similar to that observed by others, e.g., Johnson-Beebout et al. 2009) indicates that denitrification should dominate below the 2 cm oxic layer. The lack of a significant relationship between $\delta^{15}N\text{-}NO_3^-$ and $\delta^{18}O\text{-}NO_3^-$ in the oxic soil layer likewise indicated that denitrification not the dominant impact on the surface NO_3^- pool, while the ~1:1 enrichment ratio for $\delta^{15}N{:}\delta^{18}O$ in the plough layer soil confirms that the NO_3^- pool below 2 cm depth was governed by denitrification. As only trace concentrations of DIN were measured in floodwater or at the hardpan, only the top 10 cm of the paddy soil were used to quantify N transformations. This simplification is supported by previous findings that, due to steep redox gradients, the top ~10 cm of paddy soil is the dominant N cycling zone (Buresh et al. 2008; Endo et al. 2012), and that fallow drying affects only the top 10-15 cm of soil (Ringrose-Voase et al. 2000). Building on the vertical trends observed across all treatments, a simple two-box model was constructed to quantify N_{input} v. N_{out} (and thus indigenous N, as per Eq. 1) over time (Fig. 5.7), with the oxic soil layer (Box 1 in Fig. 5.7) as N_{input} and the anaerobic plough soil (Box 2 in Fig. 5.7) as N_{out}.

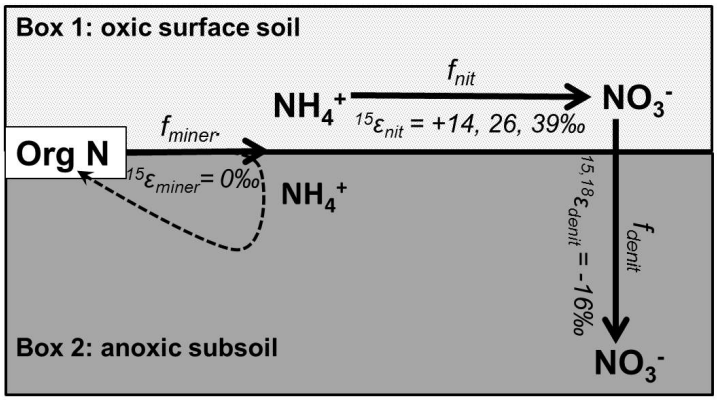

Figure 5.7 **A two-box model describing N, and N isotope, cycling in paddy soils. The concentration of NH_4^+ is determined by the mineralisation rate for disolved organic N (DON) and biologically fixed N (BNF) (or molar fraction of organic N mineralised, f_{miner}), and the isotopic signature of this pool should directly reflect that of soil organic N (org N), given the associated N enrichment factor for mineralisation (ε_{miner}) of 0‰ (Hogberg 1997). Under anaerobic conditions (Box 2) NH_4^+ can be immobilised back to organic N (no known fractionation factor). Ammonium in the oxic layer (Box 1) will be nitrified to NO_3^-, meaning that the size of the NO_3^- pool is a product of the nitrification rate (or, the molar fraction of NH_4^+ oxidised to NO_3^-, f_{nit}) and that $\delta^{15}N$ of NO_3^- in the oxic layer reflects f_{nit} and the enrichment factor of nitrification (+18‰, +26‰, +38‰ (Casciotti et al. 2003)). Once NO_3^- moves into the anaerobic soil zone (Box 2) it is consumed by denitrifiers (f_{denit} = proportion of NO_3^- from Box 1 remaining) and the isotopic composition of both $\delta^{15}N$ and $\delta^{18}O$ of NO_3^- in Box 2 reflect the enrichment factor for denitrification (ε_{denit}, determined as -16‰ from experimental data).**

5.5.2 Nitrogen inputs

As $\delta^{15}N\text{-}NO_3^-$ composition in the oxic soil layer was primarily determined by ammonia oxidation (Fig. 5.4, 5.7), N_{input} can be estimated by quantitatively relating the variations in $\delta^{15}N\text{-}NO_3^-$ over time to the fraction of substrate nitrified (f_{nit}) as per Rayleigh fractionation (Eq. 5.5):

(5.5) $$f_{nit} = \left(\frac{R_{NO3}}{R_{SON}}\right)^{1/\alpha nit}$$

in which the composition of $\delta^{15}N\text{-}NO_3^-$ at sampling time (R_{NO3}) as compared to the original $\delta^{15}N$ composition of soil organic N (R_{SON}) is used to calculate the net conversion of NH_4^+ to NO_3^- (f_{nit}) based on the fractionation factor for nitrification (α_{nit}). Here a range of ε_{nit} ($\varepsilon_{nit} = (\alpha_{nit}\text{-}1)\times 1000$) values from +14‰ to +38‰ (as reported by Casciotti et al. (2003)) were used as the variable DIN pool size caused by on-going mineralisation and BNF made an empirical ε_{nit} measurement implausible (Hogberg 1997). The $\delta^{15}N$ composition of soil organic N was estimated to be 7.14 ±1‰ based on the mean $\delta^{15}N\text{-}NO_3^-$ composition across all depths and treatments on day 1, which falls within the +5‰ to +9‰ $\delta^{15}N$ soil N range expected for clay soils (Hobbie and Ouimette 2009). Given these assumptions, the proportion of the available N pool represented by the measured NO_3^- concentration, and thus total N_{input} within each plot over time, were calculated. The key outcomes of these calculations were that, 1) higher nitrification rates in D plots did not result in higher net accumulation of DIN during the fallow, 2)

nitrification in submerged soils, particularly when fallow, was significant, and, 3) land preparation 'spiked' N_{input} (Fig. 5.8a).

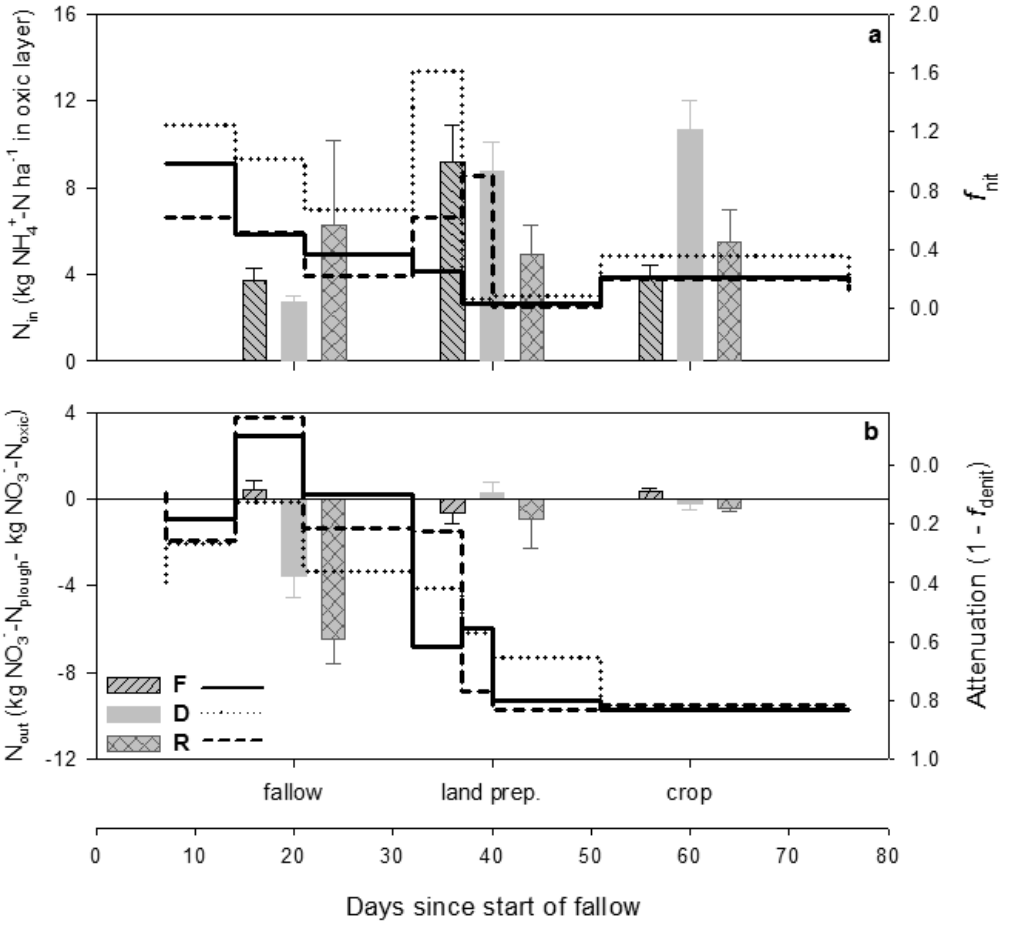

Figure 5.8 **The N balance in paddy soils kept either continuously flooded (F), continuously dried (D), or with wetting-drying (R) during the intercrop period. Nitrogen inputs (a) are represented as the mean (±SE) NH_4^+ concentration in the oxic soil layer during fallow, land preparation, and cropping (bars) as compared to the calculated turnover rate of reduced N to NO_3^- via nitrification (f_{nit}) (lines). Nitrogen losses are shown as the mean (±SE) change in NO_3^- concentration between the oxic and plough soil layers during fallow, land preparation, and cropping (bars) as compared to attenuation rate (1-f_{denit}), which was calculated based on Rayleigh fractionation of NO_3^- dual isotopes over depth.**

The measured fallow was particularly intense in terms of temperature and lack of moisture, making it more probable that low NO_3^- accumulation rates over the fallow in treatment D were caused by low mineralisation rates rather than nitrification inhibition (as discussed by Stark and Firestone (1995)). The breakdown and mineralisation of soil organic matter decreases with increasing intensity of drying periods in wetting-drying cycles (Yao et al. 2011), meaning very little inorganic N was available for nitrifiers, which can in turn be inhibited due to moisture stress (Austin and Strauss 2011). On the opposite end of the water stress spectrum, submerging paddy soils during the fallow is seen as

a way to maximise N storage by inhibiting nitrification (Bird et al. 2002; Linquist et al. 2006; Bierke et al. 2008). However, here the isotope data clearly shows that nitrification occurred in treatment F during the fallow, with f_{nit} ranging from 0.12 (near the end of fallow) to 0.5 (at the beginning of the fallow) (Fig. 5.8a). Therefore the high DIN accumulation during the fallow in this treatment cannot be fully explained by differences in turnover rates, which were not consistently different between treatments, and is instead hypothesised to come from BNF by cyanobacteria. This hypothesis is supported by observed cyanobacterial mats in the floodwaters during this dry season fallow, and is in keeping with findings of George et al. (1993) that BNF can be a significant N source in plant-free submerged paddies. However, NO_3^- dual isotope data could not be used to distinguish between mineralisation and BNF derived N due to the variability in ε_{nit} during NO_3^- production (Buchwald et al. 2012). Despite this limitation, the similar nitrification rates recorded across treatments with different measured DIN pools highlights the importance of 'new' N inputs (as opposed to internal DIN cycling) in determining N_{input}.

Increased nitrification rates immediately following re-flooding, which could explain the measured shifts in soil pH (Kogel-Knabner et al. 2010), also supports reports of increasing ammonia oxidising bacterial abundance following both re-flooding and ploughing (Fujii et al. 2010; Kogel-Knabner et al. 2010). The isotopically depleted $\delta^{18}O\text{-}NO_3^-$ measured following re-flooding (~ -15‰) contributes to mounting evidence that $\delta^{18}O$ of NO_3^- formed via nitrification will vary inversely with the rate of formation (Fang et al. 2012) as the shifting balance between O exchange with the adjacent H_2O and kinetic fractionation during O incorporation means that the faster nitrification occurs, the less O exchange occurs, and the more isotopically depleted the resultant $\delta^{18}O\text{-}NO_3^-$ is (Casciotti et al. 2010). This evidence for a 'hot moment' of NO_3^- production during land preparation adds complexity to the conventional understanding of paddy field N dynamics (i.e., temporally isolated production (aerobic fallow) and reduction (anaerobic land preparation)).

5.5.3 Nitrogen losses

Attenuation of N_{inputs} within the treatments could then be calculated from the difference in $\delta^{18}O\text{-}NO_3^-$ and $\delta^{15}N\text{-}NO_3^-$ enrichment between Box 1 (oxic soil) and Box 2 (plough layer soil) (Fig. 5.7) using a modified Rayleigh equation where the initial NO_3^- pool size ($f_{denit} = N_{plough}/N_{input}$) is defined as N_{input} from Box 1 (Eq. 5.6):

$$\frac{R_{oxic}}{R_{plough}} = \left(f_{denit}\right)^{\alpha denit - 1} \qquad (5.6)$$

$$Attenuation = 1 - f_{denit}$$

where NO_3^- isotopic composition in the plough layer (R_{plough}) relative to the oxic layer (R_{oxic}) is related to the proportion of produced NO_3^- (kg N ha^{-1}) denitrified (f_{denit}) via the site-specific α_{denit} value

calculated following the simulated leaching event in treatment R during the fallow (Fig. 5.6). The ε_{denit} of -16‰ calculated for this paddy soil falls within the range of -5‰ to -25‰ measured in pure cultures of denitrifiers (Granger et al. 2008) and the reported range of ε_{denit} in soil (from -5‰ to -33‰ (Mariotti et al. 1981; Koba et al. 1997)). Interestingly, even under the high mean soil temperatures of 35ºC (far higher than that in any other published field studies of NO_3^- isotope dynamics) denitrifier – driven isotope fractionation does not deviate from the expected range, despite the fact that temperature is a key regulator of denitrifier activity (Braker et al. 2010), and was previously found to alter denitrifier associated isotopic fractionation (Mariotti et al. 1982).

The major assumption of this calculation is that denitrification is the primary driver of NO_3^- fractionation and N attenuation. While the consistent ~1:1 ratio between $\delta^{18}O\text{-}NO_3^-$ and $\delta^{15}N\text{-}NO_3^-$ measured both within plough layer soil over time validates the dominance of denitrification in the plough layer, all calculations were performed using the mean of $\delta^{18}O\text{-}NO_3^-$ and $\delta^{15}N\text{-}NO_3^-$ enrichment in order to compensate for any other fractionating processes that could occur. It is notably that, in contrast to the consistent 1:1 $\delta^{18}O$:$\delta^{15}N$ ratio across the redox gradient from oxic to plough layer soils, $\delta^{18}O$- $\delta^{15}N$- NO_3^- in the floodwater (presumably a mixture of NO_3^- diffused from oxic and plough depths) was enriched at a 1:2 ratio over time. This contrast provides further evidence that the 1:2 enrichment ratios often attributed to denitrification in soils and freshwater environments (Kendall 1998) is actually an artefact of spatially and/or temporally coupled nitrification-denitrification, as is becoming increasingly clear from marine research (Casciotti et al. 2013).

Model confidence is also increased by the lack of reported evidence for non-denitrification N removal processes in paddy soils. Briefly, abiotic NO_3^- assimilation during iron (Fe(II)) reduction (Davidson et al. 2003) (which can create 1:2 enrichment of ^{18}O v. $\delta^{15}N$) is not empirically proven to occur in soil (Canfield et al. 2010), dissimilatory reduction of NO_3^- to NH_4^+ (DNRA) (Rutting et al. 2011) most likely only influences N isotopes, and is thought to 'dampen' their enrichment relative to that of $\delta^{18}O\text{-}NO_3^-$ (Dhondt et al. 2003). Based on this relationship, DNRA might explain the high ratio of $\delta^{18}O$:$\delta^{15}N$ at the hardpan (Fig. 5.5), but there is minimal evidence for the process in paddy soils (Buresh and Patrick 1978; Buresh et al. 2008). Finally, attenuation via nitrifier-denitrification, in which nitrifying microbes reduce nitrite (NO_2^-) directly to N_2O+N_2 without producing NO_3^- (Kool et al. 2010), could not be accounted for using these measurements of NO_3^- stable isotopes. However, this process is unlikely to go forward in such O_2 depleted settings (Kool et al. 2010), and there is no evidence for it in paddy soils (Ishii et al. 2011).

With no evidence for non-denitrification pathways influencing NO_3^- isotopic composition Eq. 5.6 could be confidently used to reveal attenuation dynamics in each treatment over time (Fig. 5.8b). Nitrate removal varied over time by management phase (fallow v. land prep v. crop) (p<0.001). The lowest attenuation rates for all treatments occurred during the fallow and the highest following transplanting, by which point 83.1 ±2% of NO_3^- was attenuated across all treatments (Fig. 5.8b). Calculated attenuation rates were also used to estimate net N_{denit} (Eq. 5.1) in each treatment over time

(Table 5.2). In contrast to previous assumptions (Santiago-Ventura et al. 1986), fallow management impacted the rate (e.g., occurred most rapidly in *ns* plots and slowest in *s* split-plots of D treatments), but not the quantity, of denitrification (Table 5.2). Differences in NO_3^- concentrations over depth followed the opposite temporal trend to attenuation rates, with the greatest concentration differences between oxic and plough depths found in treatment R during the fallow (Fig. 5.8b). As the experimental fields were kept weed-free during the fallow (plant N uptake ~0), we conclude that NO_3^- leaching (which causes no isotope fractionation) rather than denitrification accounted for the majority of DIN lost from aerobic treatments over the fallow.

Table 5.2 **Net attenuation of NO_3^- from paddy soils kept either continuously flooded (F), continuously dried (D), or with wetting-drying (R), with or without reincorporation of rice residues (*s* v. *ns*, respectively). Results are reported in kg NO_3^--N ha^{-1} in the top 10 cm of soil (±SE) based on stable isotope modelling of N inputs and outputs and measured NO_3^- and NH_4^+ soil concentrations during the 30 day fallow period, 19 days of active land preparation (including re-flooding, hydrotilling, and harrowing), and 11 days after transplanting of the next season's crop (but prior to the first N fertiliser application). Letters indicate significant difference between treatments (p<0.05)**

Treatment		*Modelled N losses (kg N-NO_3^- ha^{-1})*[1]		
		Fallow	Land prep.	Crop
F	*ns*	2.17 (0.5)^{b}	7.12 (1)^{c}	2.23 (0.3)^{b}
	s	1.64 (0.4)^{b}	1.93 (0.2)^{b}	2.93 (0.7)^{b,c}
D	*ns*	1.57 (0.5)^{b}	6.34 (2)^{c,d}	5.74 (0.5)^{d}
	s	1.28 (0.3)^{b}	3.16 (1)^{b,c}	8.59 (2)^{d}
R	*ns*	3.83 (0.6)^{c}	4.03 (1)^{c}	2.19 (1)^{b}
	s	1.45 (0.7)^{a}	0.53 (0.3)^{a}	5.16 (2)^{c,d}

[1]*Soil bulk density = 1.4*

Although NO_3^- leaching from paddy soils is assumed to be minimal (Bouman et al. 2002), evidence here for management-driven, acute NO_3^- leaching is corroborated by recent reports of fallow period spikes in NO_3^- concentrations in aquifers under lowland rice production (Jin et al. 2012). However, the lack of measurable denitrification in treatment F during the fallow was surprising given the highly reducing conditions measured in the plough layer soil and evidence for high N inputs (as discussed in the previous section). This lack of measurable NO_3^- fractionation with depth may have been caused by the fact that, in the absence of active plant roots, the movement of NO_3^- within the soil profiles was dominated by diffusion (Chen et al. 2007), which could 'mask' the isotope signature of denitrification (e.g., Sebilo et al. 2003, Chapter 2, Chapter 3). Additionally, the anomalous NO_3^- isotope patterns measured at 40 cm depth in this study may indicate that the NO_3^- leached from the plough zone is attenuated by a non-denitrifying process below the denitrifying zone, meaning that the rates calculated here represent the 'minimum' net attenuation.

5.5.4 Implications

While water management did not impact indigenous N supply or N biogeochemistry, isotope modelling revealed that high fluxes of nitrification-produced NO_3^- (enabled in treatment D by rapid increases in mineralisation) combined with increasing denitrification rates created a 'hot moment' of NO_3^- loss during land preparation that resulted in the fairly homogeneous indigenous N availability observed across all treatments. The concurrent decreases in total C and N following land preparation corroborate the conclusion that net mineralisation of the organic matter (accumulated over the fallow) during active land turbation (Olk et al. 2006) creating a temporal asynchronicity between N availability and demand. This evidence that N losses during land preparation hinge on co-occurring nitrification and denitrification indicates that application of nitrification inhibitors prior to the growing season could minimise the need for N fertilisers use, a finding that contrasts previous assessments that these amendments would not impact paddy N losses.

Although residue incorporation did not change the net N balance over the measured period, it did delay N losses from land preparation (when the majority of N was lost from all *ns* plots) to the period following transplanting (Table 5.2). This short duration of the stabilising effect of organic amendments in submerged soils has been reported previously (George et al. 1993), and supports the finding of Bierke et al. (2008) that residue management during fallow has no long-term effect on soil N stores. Unlike Linquist et al. (2006), who linked residue incorporation in continuously flooded soils to increased N mineralisation and availability, in this experiment the highest grain yields occurred in fields kept continuously flooded *without* residue additions (R.J. Buresh, unpubl.). Indeed residue incorporation within the different water treatments consistently inhibited rice production: grain yields were on average decreased by 0.75 ±0.4 Mg ha^{-1} in *s* v *ns* split-plots ($p<0.001$). Any beneficial stabilisation of available N caused by residue incorporation did not occur over a timeframe that was useful to the rice plants, highlighting the importance of the timing of residue incorporation on its impact (Witt et al. 1998).

5.6 Conclusions

By overlaying NO_3^- stable isotope data onto DIN concentration data over time and depth, the, "highly complex and heterogeneous" biogeochemical and physiochemical reactions triggered by re-wetting and dynamic land turbation were disentangled, contributing to the growing body of knowledge on the biogeochemical effects of soil re-wetting. We found that, for soils not receiving organic amendments, the majority of production and reduction of DIN occurred in the first few days of land preparation, particularly in soils dried over the intercrop period due to rapid mineralisation, nitrification, and denitrification as the soil was wetted and disturbed. Based on this quantification of the importance of activities during land preparation in limiting indigenous N, the clear next step in

creating more fertile, and thus sustainable, lowland rice production is to test the impact of modifying the land preparation regimen, rather than the fallow, on paddy soil N stocks.

5.7 Acknowledgements

Thanks to Angel Bautista, Sonny Pantoja, and Jerone Onoya for assistance with field work at the IRRI experimental farm and to Mia Bunquin (International Rice Research Institute) for assistance in preparing samples for isotope analysis. Thanks especially to Jun Correa for management oversight of the field trial. Thanks to Roger Cresswell and Joy Jiao at Lincoln University for analytical assistance. This project was funded in part by a U.S. Student Fulbright scholarship to N.S. Wells, with additional assistance from Lincoln University and W. Troy Baisden at GNS Science.

Sarah Beebout and Tim Clough both provided editorial assistance, and Roland Buresh shared his wealth of knowledge of paddy soil N cycling, access to his long-term experimental sites, and the previous 10 years of data collected from the 'B9b' experiment.

5.8 References

Akiyama, H., K. Yagi, and X. Y. Yan. 2005. Direct N_2O emissions from rice paddy fields: Summary of available data. Global Biogeochemical Cycles **19**:10.

Austin, B. J. and E. A. Strauss. 2011. Nitrification and denitrification response to varying periods of desiccation and inundation in a western Kansas stream. Hydrobiologia **658**:183-195.

Barnes, R. T. and P. A. Raymond. 2010. Land-use controls on sources and processing of nitrate in small watersheds: insights from dual isotopic analysis. Ecological Applications **20**:1961-1978.

Becker, M., F. Asch, S. L. Maskey, K. R. Pande, S. C. Shah, and S. Shrestha. 2007. Effects of transition season management on soil N dynamics and system N balances in rice-wheat rotations of Nepal. Field Crops Research **103**:98-108.

Berger, S., I. Jang, J. Seo, H. Kang, G. Gebauer. 2013. A record of N_2O and CH_4 emissions and underlying soil processes of Korean rice paddies as affected by different water management practices. Biogeochemistry **115**:317-332.

Bierke, A., K. Kaiser, and G. Guggenberger. 2008. Crop residue management effects on organic matter in paddy soils - The lignin component. Geoderma **146**:48-57.

Bird, J. A., W. R. Horwath, A. J. Eagle, and C. van Kessel. 2001. Immobilization of fertilizer nitrogen in rice: Effects of straw management practice. Soil Science Society of America Journal **65**:1143-1152.

Bird, J. A., C. van Kessel, and W. R. Horwath. 2002. Nitrogen dynamics in humic fractions under alternative straw management in temperate rice. Soil Science Society of America Journal **66**:478-488.

Blakemore, L. C., P. L. Searle, and B. K. Daly. 1987. Methods for chemical analysis of soils. NZ Soil Bureau Scientific report 80:7.

Borken, W. and E. Matzner. 2009. Reappraisal of drying and wetting effects on C and N mineralization and fluxes in soils. Global Change Biology **15**:808-824.

Bouman, B. A. M., A. R. Castaneda, and S. I. Bhuiyan. 2002. Nitrate and pesticide contamination of groundwater under rice-based cropping systems: past and current evidence from the Philippines. Agriculture Ecosystems & Environment **92**:185-199.

Bouman, B. A. M., E. Humphreys, T. P. Tuong, and R. Barker. 2007. Rice and water. Pages 187-237 *in* D. L. Sparks, editor. Advances in Agronomy, Vol 92. Elsevier Academic Press Inc, San Diego.

Braker, G., J. Schwarz, and R. Conrad. 2010. Influence of temperature on the composition and activity of denitrifying soil communities. FEMS microbiology ecology **73**:134-148.

Buchwald, C., A. E. Santoro, M. R. McIlvin, and K. L. Casciotti. 2012. Oxygen isotopic composition of nitrate and nitrite produced by nitrifying cocultures and natural marine assemblages. Limnology and Oceanography **57**:1361-1375.

Buresh, R. J., E. G. Castillo, and S. K. Dedatta. 1993. Nitrogen losses in puddled soils as affected by timing of water-deficit and nitrogen-fertilization. Plant and Soil **157**:197-206.

Buresh, R. J. and W. H. Patrick, Jr. 1978. Nitrate reduction to ammonium in anaerobic soil. Soil Science Society of America Journal **42**:913–918.

Buresh, R. J., K. R. Reddy, and C. van Kessel. 2008. Nitrogen Transformations in Submerged Soils. Pages 401-436 Nitrogen in Agricultural Systems.

Buresh, R. J. and C. Witt. 2008. Balancing fertilizer use and profit in Asia's irrigated rice systems. Better Crops with Plant Food **92**:18-21.

Buresh, R. J., T. Woodhead, K. D. Shepherd, E. Flordelis, and R. C. Cabangon. 1989. Nitrate accumulation and loss in a mungbean lowland rice cropping system. Soil Science Society of America Journal **53**:477-482.

Cai, Z. C., G. X. Xing, X. Y. Yan, H. Xu, H. Tsuruta, K. Yagi, and K. Minami. 1997. Methane and nitrous oxide emissions from rice paddy fields as affected by nitrogen fertilisers and water management. Plant and Soil **196**:7-14.

Canfield, D. E., A. N. Glazer, and P. G. Falkowski. 2010. The evolution and future of earth's nitrogen cycle. Science **330**:192-196.

Casciotti, K.L., C. Buchwald, and M. McIlvin. 2013. Implications of nitrate and nitrite isotopic measurements for the mechanisms of nitrogen cycling in the Peru oxygen deficient zone. Deep-Sea Research Part I-Oceanography Research Papers **80**:78-93.

Casciotti, K. L., M. McIlvin, and C. Buchwald. 2010. Oxygen isotopic exchange and fractionation during bacterial ammonia oxidation. Limnology and Oceanography **55**:753-762.

Casciotti, K. L., D. M. Sigman, and B. B. Ward. 2003. Linking diversity and stable isotope fractionation in ammonia-oxidizing bacteria. Geomicrobiology Journal **20**:335-353.

Cassman, K.G., A. Dobermann, D.T. Walters. 2002. Agroecosystems, nitrogen-use efficiency, and nitrogen management. Ambio **31**:132-140.

Cassman, K. G., A. Dobermann, D. T. Walters, and H. Yang. 2003. Meeting cereal demand while protecting natural resources and improving environmental quality. Annual Review of Environment and Resources **28**:315-358.

Cassman, K. G., S. Peng, D. C. Olk, J. K. Ladha, W. Reichardt, A. Dobermann, and U. Singh. 1998. Opportunities for increased nitrogen-use efficiency from improved resource management in irrigated rice systems. Field Crops Research **56**:7-39.

Chen, M., H. Wu, and F. Wo. 2007. Nitrate vertical transport in the main paddy soils of Tai Lake region, China. Geoderma **142**:136-141.

Davidson, E. A., J. Chorover, and D. B. Dail. 2003. A mechanism of abiotic immobilization of nitrate in forest ecosystems: the ferrous wheel hypothesis. Global Change Biology **9**:228-236.

DeDatta, S. K. 1995. Nitrogen transformations in wetland rice ecosystems. Fertilizer Research **42**:193-203.

Dhondt, K., P. Boeckx, O. Van Cleemput, and G. Hofman. 2003. Quantifying nitrate retention processes in a riparian buffer zone using the natural abundance of N-15 in NO3. Pages 2597-2604 *in* Meeting of the Stable-Isotope-Mass-Spectrometry-Users-Group. John Wiley & Sons Ltd, Bristol, England.

Dobermann, A. and K. G. Cassman. 2005. Cereal area and nitrogen use efficiency are drivers of future nitrogen fertilizer consumption. Science in China Series C-Life Sciences **48**:745-758.

Dobermann, A., J. L. Gaunt, H. U. Neue, I. F. Grant, M. A. Adviento, and M. F. Pampolino. 1994. Spatial and temporal variability of ammonium in flooded rice fields. Soil Science Society of America Journal **58**:1708-1717.

Dong, N. M., K. K. Brandt, J. Sorensen, N. N. Hung, C. V. Hach, P. S. Tan, and T. Dalsgaard. 2012. Effects of alternating wetting and drying versus continuous flooding on fertilizer nitrogen fate in rice fields in the Mekong Delta, Vietnam. Soil Biology & Biochemistry **47**:166-174.

Endo, A., S.-I. Mishima, and K. Kohyama. 2012. Nitrate percolation and discharge in cropped Andosols and Gray lowland soils of Japan. Nutrient Cycling in Agroecosystems:1-21.

Fang, Y. T., K. Koba, A. Makabe, F. F. Zhu, S. Y. Fan, X. Y. Liu, and M. Yoh. 2012. Low delta O-18 values of nitrate produced from nitrification in temperate forest soils. Environmental Science & Technology **46**:8723-8730.

Fujii, C., T. Nakagawa, Y. Onodera, N. Matsutani, K. Sasada, R. Takahashi, and T. Tokuyama. 2010. Succession and community composition of ammonia-oxidizing archaea and bacteria in bulk soil of a Japanese paddy field. Soil Science and Plant Nutrition **56**:212-219.

George, T., J. K. Ladha, R. J. Buresh, and D. P. Garrity. 1993. Nitrate dynamics during the aerobic soil phase in lowland rice-based cropping systems. Soil Science Society of America Journal **57**:1526-1532.

Granger, J., D. M. Sigman, M. F. Lehmann, and P. D. Tortell. 2008. Nitrogen and oxygen isotope fractionation during dissimilatory nitrate reduction by denitrifying bacteria. Limnology and Oceanography **53**:2533-2545.

Henckel, T. and R. Conrad. 1998. Characterization of microbial NO production, N_2O production and CH_4 oxidation initiated by aeration of anoxic rice field soil. Biogeochemistry **40**:17-36.

Hobbie, E. A. and A. P. Ouimette. 2009. Controls of nitrogen isotope patterns in soil profiles. Biogeochemistry **95**:355-371.

Hogberg, P. 1997. Tansley review No 95 - N-15 natural abundance in soil-plant systems. New Phytologist **137**:179-203.

Ishii, S., S. Ikeda, K. Minamisawa, and K. Senoo. 2011. Nitrogen cycling in rice paddy environments: Past achievements and future challenges. Microbes and Environments **26**:282-292.

Jin, Z. F., Z. Y. Pan, M. T. Jin, F. L. Li, Y. Wan, and B. Gu. 2012. Determination of nitrate contamination sources using isotopic and chemical indicators in an agricultural region in China. Agriculture Ecosystems & Environment **155**:78-86.

Johnson-Beebout, S. E., O. R. Angeles, M. C. R. Alberto, and R. J. Buresh. 2009. Simultaneous minimization of nitrous oxide and methane emission from rice paddy soils is improbable due to redox potential changes with depth in a greenhouse experiment without plants. Geoderma **149**:45-53.

Kempers, A. J. and A. Zweers. 1986. Ammonium determination in soil extracts by the salicylate method. Communications in Soil Science and Plant Analysis **17**:715-723.

Kendall, C. 1998. Tracing Nitrogen Sources and Cycling in Catchments *in* C. Kendall and J. J. Mcdonell, editors. Isotope Tracers in Catchment Hydrology. Elsevier Science B.V., Amsterdam.

Koba, K., N. Tokuchi, E. Wada, T. Nakajima, and G. Iwatsubo. 1997. Intermittent denitrification: The application of a N-15 natural abundance method to a forested ecosystem. Geochimica Et Cosmochimica Acta **61**:5043-5050.

Kogel-Knabner, I., W. Amelung, Z. H. Cao, S. Fiedler, P. Frenzel, R. Jahn, K. Kalbitz, A. Kolbl, and M. Schloter. 2010. Biogeochemistry of paddy soils. Geoderma **157**:1-14.

Kool, D. M., N. Wrage, S. Zechmeister-Boltenstern, M. Pfeffer, D. Brus, O. Oenema, and J. W. Van Groenigen. 2010. Nitrifier denitrification can be a source of N_2O from soil: a revised approach to the dual-isotope labelling method. European Journal of Soil Science **61**:759-772.

Linquist, B. A., S. M. Brouder, and J. E. Hill. 2006. Winter straw and water management effects on soil nitrogen dynamics in California rice systems. Agronomy Journal **98**:1050-1059.

Mariotti, A., J. C. Germon, P. Hubert, P. Kaiser, R. Letolle, A. Tardieux, and P. Tardieux. 1981. Experimental-determination of nitrogen kinetic isotope fractionation - some principles - illustration for the denitrification and nitrification processes. Plant and Soil **62**:413-430.

Mariotti, A., J. C. Germon, and A. Leclerc. 1982. Nitrogen isotope fractionation associated with the NO_2--N_2O step of denitrification in soils. Canadian Journal of Soil Science **62**:227-241.

McIlvin, M. R. and M. A. Altabet. 2005. Chemical conversion of nitrate and nitrite to nitrous oxide for nitrogen and oxygen isotopic analysis in freshwater and seawater. Analytical Chemistry **77**:5589-5595.

Möbius, J. 2013. Isotope fractionation during nitrogen remineralization (ammonification): Implications for nitrogen isotope biogeochemistry. Geochimica et Cosmochimica Acta **105**:422-432.

Olk, D. C., K. G. Cassman, K. Schmidt-Rohr, M. M. Anders, J. D. Mao, and J. L. Deenik. 2006. Chemical stabilization of soil organic nitrogen by phenolic lignin residues in anaerobic agroecosystems. Soil Biology & Biochemistry **38**:3303-3312.

Rasche, F., G. Cadisch. 2013. The molecular microbial perspective of organic matter turnover and nutrient cycling in tropical agroecosystems - What do we know? Biological Fertility of Soils **49**:251-262.

Ringrose-Voase, A. J., J. M. Kirby, G. Djoyowasito, W. B. Sanidad, C. Serrano, and T. M. Lando. 2000. Changes to the physical properties of soils puddled for rice during drying. Soil & Tillage Research **56**:83-104.

Rivett, M. O., S. R. Buss, P. Morgan, J. W. N. Smith, and C. D. Bemment. 2008. Nitrate attenuation in groundwater: A review of biogeochemical controlling processes. Water Research **42**:4215-4232.

Ros, G.H., E. Hoffland, C. van Kessel, E.J.M. Temminghoff. 2009. Extractable and dissolved soil organic nitrogen - A quantitative assessment. Soil Biology & Biochemistry **41**:1029-1039.

Rutting, T., P. Boeckx, C. Muller, and L. Klemedtsson. 2011. Assessment of the importance of dissimilatory nitrate reduction to ammonium for the terrestrial nitrogen cycle. Biogeosciences **8**:1779-1791.

Santiago-Ventura, T., M. Bravo, C. Daez, V. Ventura, I. Watanabe, and A. A. App. 1986. Effects of N-fertilizers, straw, and dry fallow on the nitrogen balance of a flooded soil planted with rice. Plant and Soil **93**:405-411.

Schimel, J. P. and J. Bennett. 2004. Nitrogen mineralization: Challenges of a changing paradigm. Ecology **85**:591-602.

Sebilo, M., G. Billen, M. Grably, and A. Mariotti. 2003. Isotopic composition of nitrate-nitrogen as a marker of riparian and benthic denitrification at the scale of the whole Seine River system. Biogeochemistry **63**:35-51.

Sigman, D. M., R. Robinson, A. N. Knapp, A. van Geen, D. C. McCorkle, J. A. Brandes, and R. C. Thunell. 2003. Distinguishing between water column and sedimentary denitrification in the Santa Barbara Basin using the stable isotopes of nitrate. Geochemistry Geophysics Geosystems **4**:20.

Stark, J. M. and M. K. Firestone. 1995. Mechanisms for soil-moisture effects on activity of nitrifying bacteria. Applied and Environmental Microbiology **61**:218-221.

Witt, C., K. G. Cassman, D. C. Olk, U. Biker, S. P. Liboon, M. I. Samson, and J. C. G. Ottow. 2000. Crop rotation and residue management effects on carbon sequestration, nitrogen cycling and productivity of irrigated rice systems. Plant and Soil **225**:263-278.

Witt, C., K. G. Cassman, J. C. G. Ottow, and U. Biker. 1998. Soil microbial biomass and nitrogen supply in an irrigated lowland rice soil as affected by crop rotation and residue management. Biology and Fertility of Soils **28**:71-80.

Xiong, Z. Q., T. Q. Huang, Y. C. Ma, G. X. Xing, and Z. L. Zhu. 2010. Nitrate and ammonium leaching in variable- and permanent-charge paddy soils. Pedosphere **20**:209-216.

Yao, S. H., B. Zhang, and F. Hu. 2011. Soil biophysical controls over rice straw decomposition and sequestration in soil: The effects of drying intensity and frequency of drying and wetting cycles. Soil Biology & Biochemistry **43**:590-599.

Zhang, J. S., F. P. Zhang, J. H. Yang, J. P. Wang, M. L. Cai, C. F. Li, and C. G. Cao. 2011. Emissions of N_2O and NH_3, and nitrogen leaching from direct seeded rice under different tillage practices in central China. Agriculture Ecosystems & Environment **140**:164-173.

Plate 4 **Clockwise from top right: Heathcote River and adjacent structural damage at reach 10 in March 2011, days after the main earthquake; wastewater entering the river above reach 6 in the days following the February earthquake; Heathcote River at reach 7 hours after a significant aftershock in June 2011 (note whitening of water and high water mark left on the bank by liquefaction of fine sediments).**

Chapter 6
Biogeochemistry and community ecology in a spring-fed urban stream following a major earthquake

A version of this chapter was published. Wells, N.S., T.J. Clough, L.M. Condron, W.T. Baisden, J.S. Harding, Y. Dong, G.D. Lewis, G. Lear. 2013. Biogeochemistry and community ecology in a spring-fed urban stream following a major earthquake. Environmental Pollution **182:**190-200

6.1 Abstract

In February 2011 a major 6.3M_W earthquake in Christchurch, New Zealand inundated urban waterways with sediment from liquefaction and triggered sewage spills. The impacts of, and recovery from, this natural disaster on the stream biogeochemistry and biology were assessed over six months along a longitudinal impact gradient in an urban river. The impact of liquefaction was masked, particularly in the lower reaches, by earthquake triggered sewage spills (~20,000 m^3 sewage day^{-1} entering the river for one month). Within 10 days of the earthquake dissolved oxygen in the lowest reaches was <1 mg l^{-1}, in-stream denitrification accelerated (attenuating 40-80% of sewage nitrogen), microbial biofilm communities changed, and several benthic invertebrate taxa disappeared. Following sewage system repairs, the river recovered in a reverse cascade, and within six months there were no significant differences in water chemistry, nutrient cycling, or benthic biological communities between severely and minimally impacted reaches.

Keywords: stream biofilm; stable isotopes; sewage contamination; liquefaction; natural disaster recovery

6.2 Introduction

On the 22nd of February 2011 a 6.3 magnitude (M_W) earthquake hit the Canterbury region of New Zealand's South Island (epicentre at 43°58'S, 172°68"E), leaving 185 people dead in the city of Christchurch (population ~370,000). Strong shaking (peak ground acceleration of >2.2*g*) brought ~580,000 tonnes of silt and sand to the surface (liquefaction), damaging infrastructure and rupturing land surfaces (Christchurch City Council, pers. comm.; Segou and Kalkan, 2011 and references therein). The environmental degradation, particularly to surface waters, caused by such an earthquake impacts urban recovery and rebuild (e.g., Menoni, 2001; Halvorson and Hamilton 2010), yet the functional response of rivers to earthquakes has rarely been assessed.

Earthquakes are known to influence hydrology, changing spring locations and river heights (Mohr et al., 2012), which could in turn influence aquatic biogeochemical cycles (Lohse et al., 2009). Liquefaction caused by abrupt hydrologic shifts (described in Muir-Wood and King (1993) and Wang and Manga (2010)), could result in further biogeochemical disruptions similar to those associated with chronic sediment loading of waterways (Wood and Armitage, 1997), while also smothering streambed communities in the short-term. Additionally, in urban ecosystems prolonged contamination can occur due to leaks from pipes, septic tanks, pumping systems, and wastewater treatment facilities damaged by the earthquake. The excess nutrients discharged in these sewage spills affect in-stream biogeochemical cycling (Kaushal et al., 2011), resulting in the decay of benthic (Wright et al., 1995) and microbial (Wakelin et al., 2008) communities as rapid biological growth causes overconsumption of oxygen and eutrophication.

From the ecological perspective, this type of abrupt, discrete ecosystem disturbance is recognised as an important driver of stream composition and function (Sousa, 1984). Resilience of fish, invertebrates, and algae to natural disturbances such as flooding (Boulton et al., 1992), debris flows (Lamberti et al., 1991), and hurricanes (Shiller et al., 2012) is frequently observed, yet has rarely been linked with disturbance effects at fundamental trophic levels (i.e., microbial cycling of key nutrients). Furthermore, due presumably to their relatively infrequent occurrence, the impact of earthquake related disturbances on freshwater systems has never been rigorously quantified.

In order to assess the magnitude and duration of the impact of the 22nd February 2011 earthquake on local rivers, I integrated traditional indicators of stream health (water chemistry, *Escherichia coli* (*E. coli*) counts and benthic invertebrate metrics) with emerging isotopic and microbial techniques. I deployed these measures along a longitudinal impact gradient in the Heathcote River/ Ōpawaho (one of two major river systems with its catchment entirely within the city of Christchurch) for six months following the initial quake. I believe this to be the first comprehensive study of the interactions between earthquakes and urban surface water health.

6.3 Materials and methods

6.3.1 Study site

The Heathcote River/ Ōpawaho is a spring-fed 5th order urban river (mean discharge of 990 l s^{-1}) running from the western suburbs of Christchurch, New Zealand to the Heathcote-Avon Estuary/ Ihutai east of the city (Wilson, 1976); it has a total length of 62 km. Ten reaches were selected to cover the range of earthquake impact (Fig. 6.1): minimally impacted upstream (S1 – S3, A); moderately impacted by liquefaction and sub-surface sewage leaks (S4 – S6); severely impacted by liquefaction and both sub-surface and direct discharge of untreated sewage (S7 – S10). Sites S1 through S10 were located along the main stem of the river while site A was an upstream tributary (draining residential and pasture land with minimal earthquake damage). Additional measurements were taken at sites 'B' and 'C' on 09-Mar-2011 (Fig. 6.1). Biological samples (biofilms and benthic invertebrates) were not collected from S10 as it was affected by salinity from the estuary, and thus communities could not be usefully compared to those upstream. Direct sewage influx occurred at S6, S9 and S10, with the duration of 'spill' decreasing from west to east as repairs were completed more rapidly in less damaged areas (New Zealand Civil Defence, 2011).

Sewage input was characterised from samples collected from an open discharge pipe upstream of S6 on 09-Mar-2011. Liquefaction sediment was collected from Tai Tapu (15 km southwest of Christchurch) following the 04-Sep-2010 Greendale Fault earthquake (Fig. 6.1). This sediment was derived from the same ancient alluvial deposits as those under Christchurch, and thus chemically analogous to liquefaction deposits following the 22-Feb earthquake. To account for any seasonally driven variation, daily climate data (rainfall, air temperature, wind direction) was obtained from a continuous monitoring site at the Christchurch International Airport (CliFlo: NIWA's Climate Database Online (http://cliflo.niwa.co.nz). Retrieved 10-Oct-2011).

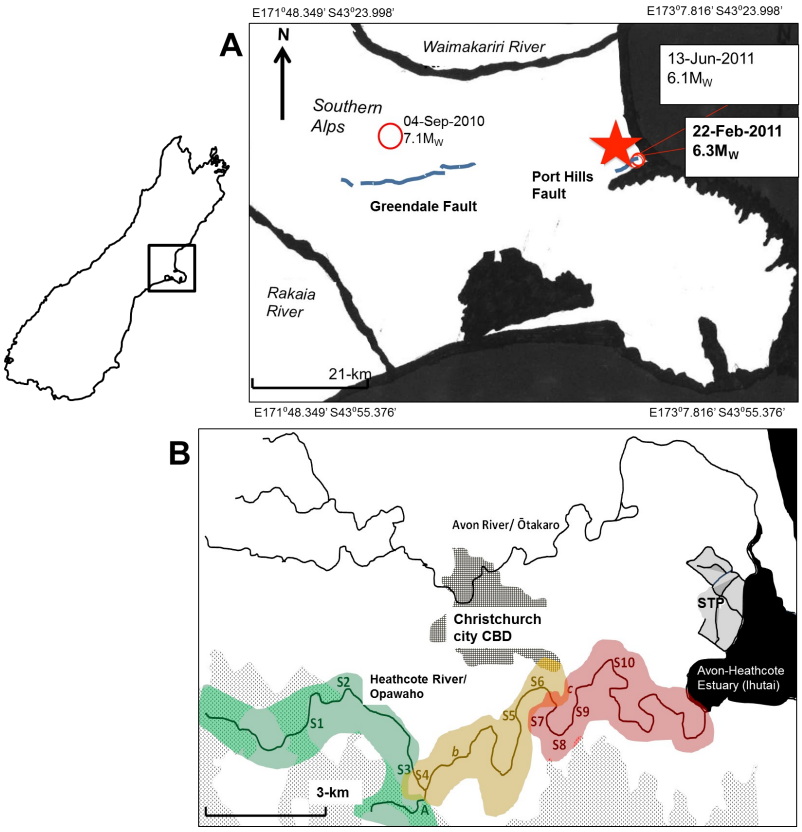

Figure 6.1 **The Canterbury region of New Zealand's South Island (pictured on left) affected by the 22-Feb-2011 6.3M_W and 13-Jun-2011 6.1M_W earthquakes along the Port Hills Fault (A). Within Christchurch city (starred on map A), the Heathcote River/ Ōpawaho study area (B) spanned an impact gradient from minimally affected headwaters in the west through severely affected reaches in the east (minimally, moderately, and severely affected zones indicated with shading). The River drains into the Avon-Heathcote Estuary/ Ituhai to the east, where the Bromley Sewage Treatment Plant (STP) is also located. Sampling reaches are labelled S1-S10, plus A, B, C, with S1 through S3 and A minimally impacted by the earthquakes, S4 through S6 moderately impacted (liquefaction and some sewage), and S7 through S10 severely impacted (from both sewage and liquefaction).**

6.3.2 Surface water sampling

Sampling was synchronised with periods of likely acute change (i.e., following the 22-Feb-2011 6.3M_W earthquake and a significant 6.1M_W aftershock on 13-Jun-2011). Samples were collected weekly for the first month, biweekly through Jun-2011 and monthly for Jul-2011 and Aug-2011. Additional samples were collected on 13-Jun-2011 (1st samples collected ~3-hrs after the 6.1M_W quake), 14-Jun-2011, and 16-Jun-2011.

At each site dissolved oxygen (DO) and water temperature were measured at 20 cm depth using a portable hand-held meter (550A YSI, Yellow Springs, OH). One litre of water was collected from the thalweg of the stream in an acetiline bottle (using a reaching pole to minimize sediment disturbance), headspace air removed, and stored on ice for <2 hr. Upon return to the laboratory, 5-ml of each sample were set aside for *E.coli* counts and the remainder was passed through GF/F (Whatman) filter paper and filtrate stored at -20ºC until chemical and isotopic analyses.

Concentrations of nitrate (NO_3^-), chloride (Cl^-), and bromide (Br^-) were measured in filtered water samples on a Dionex suppressed ion exchange chromatograph. Chloride and Br- concentrations were included as their relative proportion to NO_3^- can distinguish biological NO_3^- uptake from dilution (e.g., Trisk et al., 1993). Dissolved organic carbon (DOC) content was measured on a Shimadzu TOC-5000A total organic carbon analyser fitted with an ASI-5000A auto sampler. Ammonium (NH_4^+) concentrations were measured on acidified samples (as per Dobermann et al., (1994)) using the salicylate method (Kempers and Zweers 1986) on an UVmini-1240 spectrophotometer (Shimadzu). *E. coli* abundance was measured using Petrifilm *E.coli* count plates, as per manufacturer's instructions (3M, USA).

Water samples from 09-Mar-2011, 13-Jun-2011, and 23-Aug-2011 were screened for a suite of elements (Al, As, B, Ba, Ca, Cu Fe, K, Li, Mg, Mn, Na, P, S, Si, Sr, Zn) on an inductively coupled plasma optical emission spectrophotometer (Varian 720). Filtered water samples were introduced using an SP3 autosampler (concentrated with a Cetac U5000AT Ultrasonic Nebulizer) in aerosol form and light intensity measured in one simultaneous reading covering wavelengths 167–785 nm at 7 pm resolution.

6.3.3 Nitrate isotopes

Nitrate (N and O) and H_2O (D and O) dual isotopes were measured in all surface water samples. All isotope results are reported in respect to internationally recognised standards (Eq. 6.1).

$$\delta ‰ = \frac{(R_{sample} - R_{standard})}{R_{standard}} \times 1000 \quad (6.1)$$

For N-NO_3^- the isotope mass ratio of the sample (R_{sample}) is reported with respect to AIR; the isotope mass ratios of O-NO_3^-, D-H_2O, and O-H_2O are reported with respect to VSMOW.

Nitrate isotopes can be used to quantify nitrogen (N) sources (sewage-N is typically enriched in $\delta^{15}N$ relative to soil-N sources) and sinks ($\delta^{15}N$ and $\delta^{18}O$ of NO_3^- become progressively enriched during denitrification) (reviewed by Xue et al., 2009)). Denitrification (the anaerobic microbial reduction of reactive NO_3^- to N_2O and N_2 gases using C as an electron donor) (as reviewed by Seitzinger et al., 2006; Groffman et al., 2009) was of particular interest as it would be favoured under the conditions created by effluent discharge. Water isotopes were measured to assess hydrologic changes and differentiate water sources (Reddy et al., 2011; Wassenaar et al., 2011)

Nitrogen and O isotopes of NO_3^- were measured using the Cd reduction- azide reaction (McIlvin and Altabet, 2005). Each batch contained duplicates of three international standards (IAEA-N3, USGS-34, and USGS-32), two internal standards, and water blanks. The $\delta^{18}O$ and $\delta^{15}N$ of resultant N_2O were measured at Lincoln University on a Europa PDZ (SerCon) 20-20 IR-MS. Method precision was calculated as 0.8‰ for $\delta^{18}O$- NO_3^- and 0.6‰ for $\delta^{15}N$- NO_3^-.

Water isotopes were measured at the National Isotope Centre (GNS Science, Lower Hutt) or the University of California Davis Stable Isotope Lab. At the National Isotope Centre, samples were run in duplicate on a dual inlet IsoPrime mass spectrometer using the equilibration method at 25ºC for $\delta^{18}O\text{-}H_2O$ and continuous flow using injections to a Chrome HD for $\delta D\text{-}H_2O$. Results were normalized to two internal standards and analytical precision was 0.1‰ for $\delta^{18}O$ and 1.0‰ for δD. At the University of California Davis samples were determined via laser spectroscopy (Los Gatos Research Instruments). Analytical precision was reported as 0.1‰ for $\delta^{18}O$ and 0.5‰ for δD.

6.3.4 Biofilms

Recognising that biofilms microbial communities are both facilitators and indicators of stream function (Lear et al., 2011), epilithic biofilms were collected from S2, S3, A, S4, S5, S6 and S9 (Fig. 6.1) on 09-Mar-2011, 31-Mar-2011, 05-May-2011, 04-Jun-2011 and 05-Jul-2011 and used to complement process-level NO_3^- stable isotope information. Sites S7 and S8 were not routinely monitored as they lacked the hard substrates required for the development of epilithic biofilms, or were entirely inundated with silt. Rocks (3 – 5) were collected from each reach and biofilm biomass recovered from the surface abrasion using a Speci-Sponge™. Individual samples were sealed and stored at -20ºC until analysis, at which point the sponges were masticated and DNA extracted (as per Miller et al. 1999) and community structures characterised using ARISA (as per Lear et al., 2009).

6.3.5 Benthic invertebrates

Benthic invertebrates were collected using a standard kick net (500 µm mesh) from S2, S3, A, S4, S5, S6, S7, S8 and S9 in Mar-2011, May-2011, and Sep-2011. The bed was disturbed at five locations (selected to represent a range of habitats) per reach. Samples were preserved in the field in 70% ethanol, pooled to create a single composite sample at each reach (as per Stark et al., 2001), and transported to the laboratory, where community composition was determined by identifying to the lowest practicable taxonomic level (generally genus) using the keys of Winterbourn (1973) and Winterbourn et al. (2000). (Density data was not collected due to human health risks.)

6.3.6 Statistics/ Quantitative methods

Differences between sites, impact groups, and over time were determined using a one-way ANOVA with a Sidak post-hoc test (SPSS ver.20). Relationships between parameters were determined as Pearson's correlations (SPSS ver.20). Linear regression between variables was evaluated for goodness of fit (r^2) and significance (SigmaPlot ver.12, SPSS ver.20). Reaches were compared over time using two-way ANOVA (data was tested for normality and heterogeneity and transformed where appropriate) (SigmaPlot ver.11; Systat Software, 2008). Significant results for all tests were defined as $p < 0.05$. Values are reported as means ±SD, unless otherwise indicated.

Nitrate attenuation was calculated for dates with linear relationships between change in $\delta^{18}O\text{-}NO_3^-$, $\delta^{15}N\text{-}NO_3^-$ and distance using a modified Rayleigh kinetic fractionation model (Eq. 6.2) (Ostrom et al., 2002):

(6.2) $$Attenuation = 1 - e^{(\delta - \delta_0)/\varepsilon_{denit}}$$

Upstream (S1, S2, A) values were taken as the unfractionated isotopic source signature (δ_0) and compared to the enrichment downstream (δ). This equation was solved using enrichment factors (ε_{denit}) of -2‰ and -10‰ (reflecting the reported range for ε_{denit} in surface water (-14.8‰ (Chen et al., 2009) to -1.5‰ (Sebilo et al., 2003)), and are comparable to the modelling range recommended by Barnes and Raymond (2010)). All attenuation calculations were based on the composition of $\delta^{18}O\text{-}NO_3^-$, which is thought to be less impacted by source mixing than $\delta^{15}N\text{-}NO_3^-$ (Barnes and Raymond, 2010), particularly in New Zealand where input of $\delta^{18}O$ enriched atmospheric NO_3^- is negligible (Parfitt et al., 2006). The resultant attenuation rates were combined with stream flow (Environment Canterbury) and direct sewage discharge (Dewson and Stevenson, 2011) data to quantify sewage-N removal during downstream transport.

For biofilm samples, Genemapper software (version 3.7; ABI Ltd., Melbourne, Australia) was used to assign a fragment length (in nucleotide base pairs) to ARISA peaks via comparison with a standard ladder (LIZ1200; ABI Ltd.). Data were then standardised as per Lear et al. (2009). To assess the extent of difference between bacterial community in the post-earthquake Heathcote River and those in other regional waterways, Heathcote River biofilms were run against biofilm samples collected from 51 different streams in the Canterbury Region in Feb/Mar-2010, including from S3 on the Heathcote River. (See Lewis et al. (2010) for more details).

To test for differences in bacterial community structure among samples, ARISA data were analysed using permutational multivariate analysis of variance (PERMANOVA, Anderson 2002, McArdle and Anderson 2001) on the basis of the Bray Curtis similarity measure (a value of 0 indicates no similarity and one of 100 indicates community equality). All tests were performed using type III sums of squares (as missing data points cause the data to unbalance) and 9999 permutations under the reduced model (Anderson and Gorley 2008). Multivariate patterns in biofilm community structure (based on the ARISA data), were tested using multidimensional scaling (MDS) and Bray Curtis similarity. All multivariate analyses were performed using the PRIMER v.6 computer program (Clarke and Gorley 2006) with the additional add-on package PERMANOVA+ (Anderson and Gorley 2008).

A range of metrics were calculated for benthic invertebrate communities in order to classify stream health over distance and time. Metrics included: total taxonomic richness, the number of pollution sensitive EPT taxa (Ephemeroptera, Plecoptera and Trichoptera or mayflies, stoneflies and caddis flies) and the Macroinvertebrate Community Index (MCI). The MCI is widely used as a water quality monitoring index in New Zealand, and is calculated by allocating pollution tolerance scores to

each individual taxa and then summing these scores for each site (see Stark (1993) and Stark (1998) for detailed explanation).

6.4 Results

6.4.1 Hydrology

Although abrupt increases in river discharge were observed following the 22-Feb and 13-Jun quakes, these fluctuations were not statistically significant on the time scale relevant to this study. Variations in δD- H_2O v. $\delta^{18}O$-H_2O in Heathcote River had a slope of 7.62 (r^2 =0.92, p<0.001), roughly equivalent to the global meteoric water line (GMWL) (slope =8), with a mean δD-H_2O of -55.8 ±3 ‰ and $\delta^{18}O$-H_2O of -8.28 ±0.5 ‰ (Fig. 6.2). Both δD and $\delta^{18}O$ decreased significantly over river distance, with respective slopes of -0.193 m^{-1} (r^2 =0.037, p<0.05) and -0.222 m^{-1} (r^2 =0.049, p<0.05). Outlier values were collected following extreme weather events: a storm from the south-west on 23-Mar-2011 and one from the north-west on 06-Apr-2011. However, $\delta^{18}O$ or δD of water collected during the high-flow event immediately following the 13-Jun 6.1M_W quake were not significantly different in mean or slope. Water temperature did not vary significantly with either spatial or temporal proximity to the earthquakes (data not shown). Nor did proximity to the earthquakes change the elemental composition of river water: there were no significant changes in concentrations of Al, As, B, Ba, Ca, Cu Fe, K, Li, Mg, Mn, Na, P, S, Si, Sr, or Zn between reaches or dates (13-Jun-2011, Mar-2011, Aug-2011). Phosphorous (P) was elevated in severely impacted reaches in Mar-2011 (impact zone x time: F =15.5, p<0.001). Liquefaction sediments had very low concentrations of major nutrients (1.0 mg g^{-1} Olsen P, <10.0 mg g^{-1} total C, <4.0 mg g^{-1} total N), high base saturation (82%) and neutral pH (7.01).

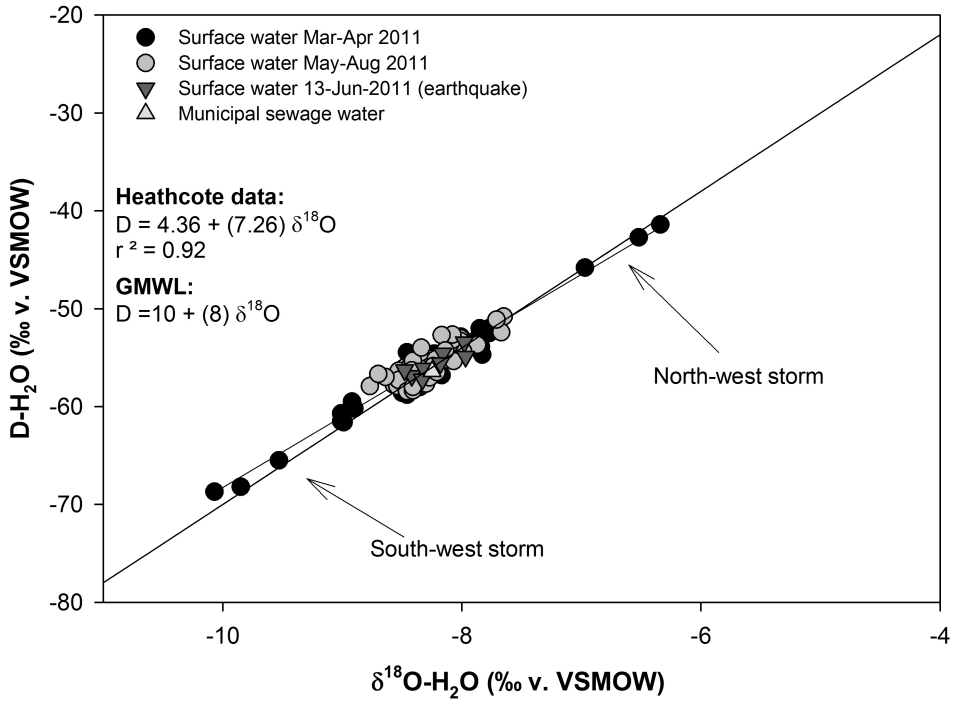

Figure 6.2 **Water isotopes (D-H_2O v. $\delta^{18}O$-H_2O, measured v. VSMOW) of surface water samples collected from 10 sites along the Heathcote River on 14 dates from 09-Mar-2011 through 28-Aug-2011. Values for municipal wastewater/ sewage collected on 09-Mar-2011 are also shown. Data is grouped by dates: 09-Mar-2011 through 21-Apr-2011 versus 05-May-2011 through 23-Aug-2011, with 13-Jun-2011 isolated (water collected ~3 h after 6.1M_W earthquake).**

6.4.2 Water chemistry

Sewage entering the Heathcote River on 09-Mar-2011 had significantly elevated concentrations of dissolved organic carbon (78.1 ±4 mg DOC l^{-1}), ammonium (20.5 ±2 mg N-NH_4^+ l^{-1}), total P (4.15 ±0.03 mg P l^{-1}; impact group x time) and copper (0.004 ±0.0005 mg Cu l^{-1}) relative to river water in minimally, moderately and severely impacted reaches. Nitrate isotopes of sewage (+2.2‰ of δ^{15}N-NO_3^-, +9‰ of δ^{18}O-NO_3^-) were not significantly different from upstream NO_3^- or the reported soil-N range (Xue et al., 2009).

Primary indicators of sewage contamination (*E. coli,* NH_4^+, DOC) were elevated in severely impacted reaches relative to both upstream reaches from Mar-2011 through Jul-2011(impact zone x time: *E.coli* ($F = 12.5$, $p < 0.001$), NH_4^+ ($F = 30.9$, $p < 0.001$), DOC ($F = 2.02$, $p < 0.05$)) (Fig. 6.3).

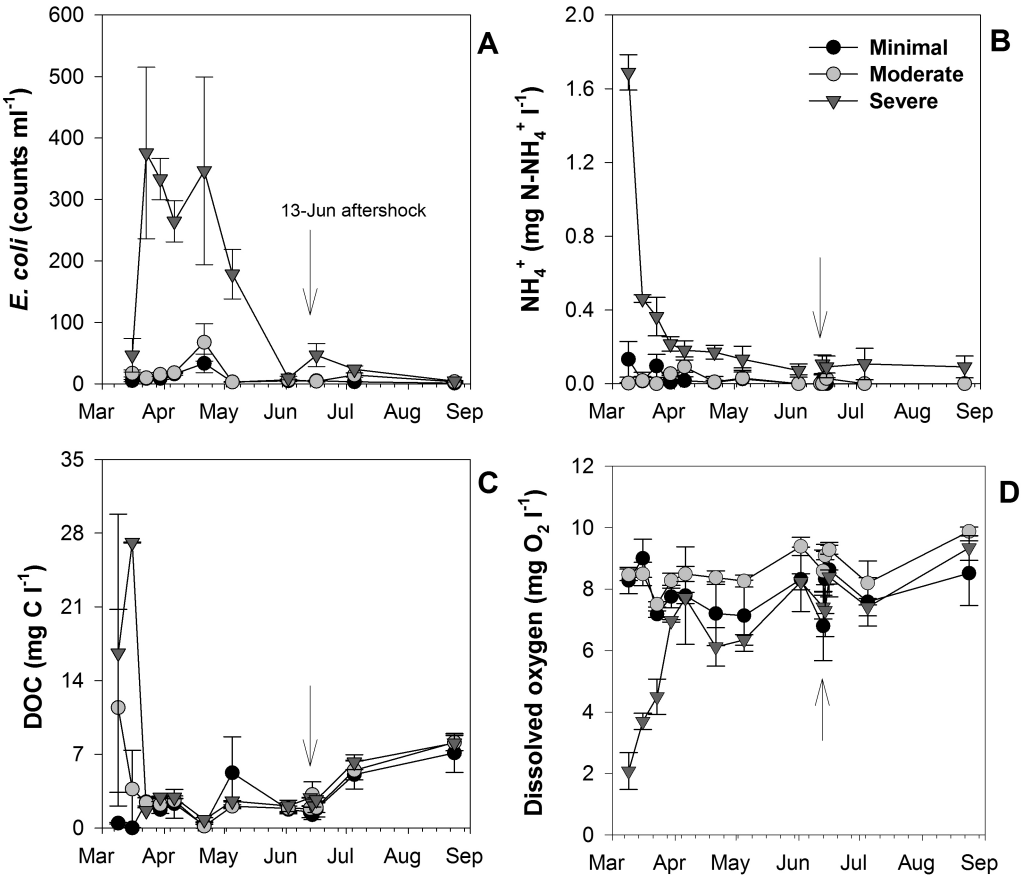

Figure 6.3 **Concentrations of *E. coli* (A), NH_4^+ (B), DOC (C), and DO (D) in the Heathcote River across each of the three identified impact zones (minimal (black circles), moderate (grey circles) and severe (grey triangles)) over a 6-month period following the 22-Feb-2011 Christchurch earthquake. Arrows point to the 6.1M_W earthquake on 13-Jun-2011. Data are mean ± SE (*n* =4 for minimal, *n* =3 for moderate and severe).**

Dissolved oxygen was significantly lower in severely impacted reaches relative to moderately impacted ones through Apr-2011 ($p<0.01$), with the lowest mean value of 2 mg O_2 l^{-1} measured in severely impacted reaches on 09-Mar-2011. Concentrations of Cl^- and Br^- were significantly elevated in severely impacted reaches ($p<0.01$), while NO_3^- was significantly depleted ($p<0.05$). In the six months following the 22-Feb earthquake anion concentrations in minimally impacted reaches did not change significantly, whereas in severely impacted reaches NO_3^- increased significantly ($p<0.05$) over time and Cl^- and Br^- decreased ($p<0.05$). Both the DIN concentration (DIN = NH_4^+-N + NO_3^--N) and the ratio of NO_3^- to Cl^- were negatively correlated with stream distance ($p<0.001$, n =105). Flux of DIN out of the Heathcote River was 1.5 ±0.3 g N s^{-1}, and did not change significantly over the six-month monitoring period (Table 6.1).

Table 6.1 **Nitrogen (N) export gives the flux of DIN (NH_4^+-N + NO_3^--N) measured at S10 as a proportion of gauged stream flow (l s^{-1}). On the far left, days since the 22-Feb-2011 earthquake are demarcated, with a dashed line highlighting 13-Jun-2011 earthquake. Estimates of the direct sewage inflow into the Heathcote River (Dewson and Stevenson (2011), numbers prior to 08-Mar-2011 are approximate), reported in m^3 day^{-1}, and the calculated proportion of total daily stream discharge that sewage accounted for. Attenuation was calculated using a Rayleigh kinetic – based model for $\delta^{18}O\text{-}NO_3^-$ fractionation on sampling dates where in-situ continuous denitrification dominated the isotopic signature using enrichment factors (ε_{denit}) of -2‰ and -10‰ for $\delta^{18}O\text{-}NO_3^-$ to provide possible range. These rates were then used to calculate net N removal in terms of total sewage loading in kg DIN day^{-1}. From 05-May-2011 onward attenuation could not be calculated, as isotope data did not fit model assumptions.**

		Sewage loading	N export	Attenuation	
		m^3 day^{-1} (% streamflow)	*g DIN s^{-1} to estuary*	*% N removed*	*kg DIN day^{-1} removed*
Day 0	*22-Feb*	~20,000 (?)		-	-
	09-Mar	12,500 (16%)	1.61	87 → 56	230,000 → 150,000
	16-Mar	12,500 (17%)	1.59	51 → 25	140,000 → 66,000
	23-Mar	15,000 (18%)	1.92	56 → 28	120,000 → 55,000
	30-Mar	10,000 (14%)	0.747	28 → 12	58,000 → 26,000
	06-Apr	4,500 (4%)	1.66	36 → 16	34,000 → 15,000
	21-Apr	4,300 (6%)	1.41	71 → 40	65,000 → 36,000
	05-May	4,300 (6%)	1.08	-	-
	02-Jun	4,000 (5%)	1.43	-	-
	13-Jun	18,000 (20%)	1.54	-	-
	14-Jun	18,000 (20%)	0.91	-	-
	16-Jun	17,000 (21%)	1.66	-	-
	05-Jul	5,000 (6%)	1.57	-	-
Day 185	*23-Aug*	100 (<0.01%)	2.57	-	-

6.4.3 Nitrogen cycling

For 40-days following the 22-Feb earthquake, $\delta^{15}N\text{-}NO_3^-$ was enriched relative to a 'natural' soil-N range across all Heathcote River sites (Fig. 6.4). The ratio of $\delta^{18}O\text{-}NO_3^-$ to $\delta^{15}N\text{-}NO_3^-$ was positively correlated with DOC concentration in severely impacted reaches (p<0.05, n=12). By 21-Apr-2011 the mean $\delta^{15}N\text{-}NO_3^-$ within all three impact groups had decreased to fall within the typical 'soil-N'/ recycled-N range (as defined by Xue et al., 2009) (Fig 6.4). Surface water $\delta^{15}N$- $\delta^{18}O$- NO_3^- during winter months (Jun., Jul., and Aug.) was again enriched at a 1:1 ratio relative to soil-N (Fig. 6.4).

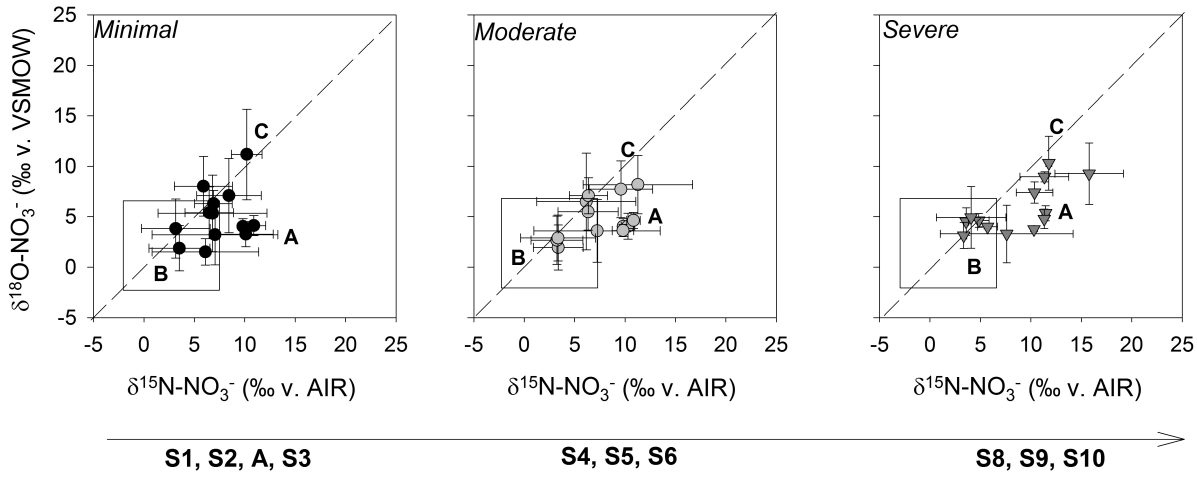

Figure 6.4 **Shifts in mean $\delta^{15}N\text{-}NO_3^-$ versus $\delta^{18}O\text{-}NO_3^-$ over time for each impact group (minimally impacted comprised of sites S1, S2, S3, A on far left, moderately impacted comprised of sites S4, S5, S6 in centre, and severely impacted comprised of sites S7, S9, S10 on far right). 'A' demarcates the value at initial sampling on 09-Mar-2011, 'B' sampling on 05-May-2011, and 'C' the final sampling on 28-Aug-2011, 6-months after the initial earthquake. The box in the lower-left of each graph delineates the range of isotopic composition associated with soil-N derived NO_3^- (Xue et al. 2009) and the dashed line draws the 1:1 $\delta^{15}N$- $\delta^{18}O$- NO_3^- enrichment associated with denitrification (Granger et al. 2008). Isotope values are reported as mean ±SD for each impact zone (*n* =4 for minimal, *n* =3 for moderate and severe)**

Enrichment in $\delta^{15}N\text{-}NO_3^-$ and $\delta^{18}O\text{-}NO_3^-$ increased downstream (Fig. 6.5). This parallel enrichment increased linearly with river distance from Mar-2011 through the end of Apr-2011 (r^2 =0.4, p<0.01) (Fig. 6.5A). Significant linear relationships between $\delta^{18}O$ and $\delta^{15}N$ of surface water NO_3^- were found for all dates except 13-Jun-2011 (Fig. 6.5), but the slope of this relationship decreased from 1.07 ± 0.1 (r^2 =0.62 to 0.98, p<0.001) (1st three samplings) to 0.66 ± 0.2 (r^2 =0.33 to 0.53, p<0.001) (all subsequent dates). Although the change in $\delta^{15}N\text{-}NO_3^-$ v. change in $\delta^{18}O\text{-}NO_3^-$ over distance was consistent from Mar-2011 through Apr-2011, the actual $\delta^{15}N$ and $\delta^{18}O$ enrichment became significantly depleted in heavy isotopes by 21-Apr-2011 (p<0.05) (Fig. 6.5A, Fig. 6.4). From May-2011 onward changes in NO_3^- isotopes were no longer significantly correlated with river distance (Fig. 6.5B), despite a brief resurgence of sewage contamination following the 13-Jun aftershock (Table 6.1). Nitrate isotopes in surface water samples collected hours after this aftershock exhibited no significant relationship between $\delta^{18}O$- and $\delta^{15}N$- of NO_3^- or enrichment of either isotope over distance (Fig. 6.5C).

Calculated DIN removal declined over time from 190 ±40 T DIN day^{-1} in Mar-2011 to 55 ±10 T DIN day^{-1} in the end of Apr-2011 as sewage inputs decreased (Table 6.1). However, there were no clear temporal trends in N attenuation rates, in part due to uncertainty associated with ε_{denit} (Table 6.1). From May-2011 onward, attenuation was not calculated as there was no significant relationship between $\delta^{18}O\text{-}NO_3^-$, $\delta^{15}N\text{-}NO_3^-$, and river distance (Fig. 6.5B), violating the assumption of continuous reaction in Eq. 6.2.

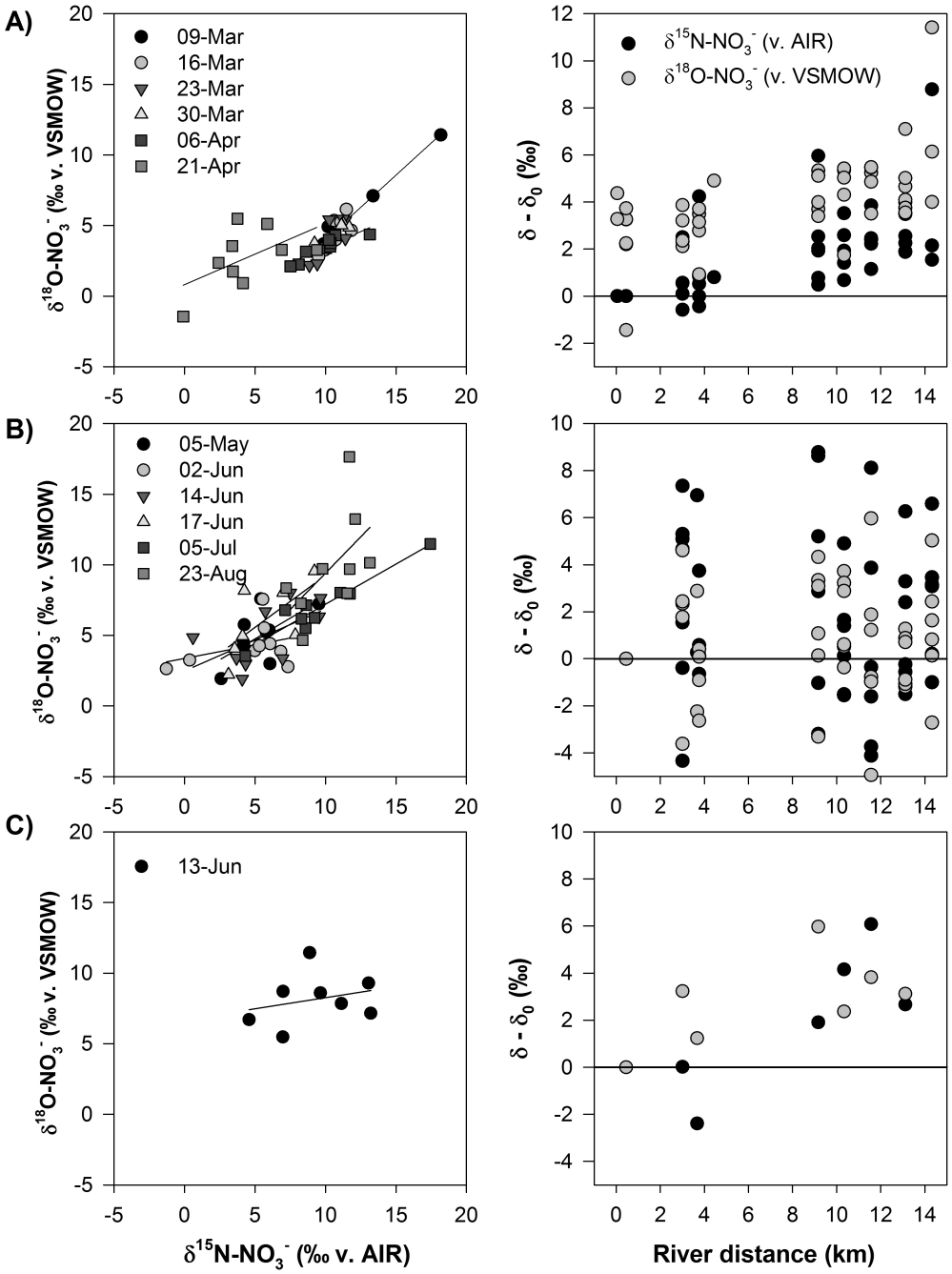

Figure 6.5 **Change in $\delta^{15}N\text{-}NO_3^-$ versus change in $\delta^{18}O\text{-}NO_3^-$ (left) and change in $\delta^{15}N\text{-}NO_3^-$ and $\delta^{18}O\text{-}NO_3^-$ over distance (right) measured in surface water of the Heathcote River over the 6-months following the 22-Feb-2011 Christchurch earthquake. Lines in left-hand figures indicate linear regression of $\delta^{15}N\text{-}NO_3^-$ v. $\delta^{18}O\text{-}NO_3^-$. The data is separated by date into (A) period of whole-stream continuous processing directly following the main earthquake, (B) re-equilibration with multiple source mixing and ex-situ and in-situ processes contributing to the $\delta^{15}N$:$\delta^{18}O$ relationship, and, (C) hours after the 13-Jun-2011 6.1M_W aftershock, when there is no significant relationship between $\delta^{15}N\text{-}NO_3^-$ and $\delta^{18}O\text{-}NO_3^-$, nor any clear spatial trends.**

6.4.4 Stream biota

Post-earthquake microbial communities detected in biofilms in the Heathcote River were significantly different from both those detected in the same section of river in 2010 (PERMANOVA, P<0.0001) and those measured in any other stream sampled within the region (Pairwise PERMANOVA, P<0.0001) (Fig. 6.6). Additionally, this community composition within each reach changed over the sampling period (Fig. 6.7). The magnitude of shifts was greater in downstream reaches: the average Bray-Curtis similarity between samples collected on either 09-Mar-2011 or 05-Jul-2011 in S2, S3 and S4 was 40, 35 and 35, respectively, whereas in reaches S5, S6 and S9 the similarity was 27, 17 and 29, respectively. Pre-earthquake community composition was more similar to that in minimally impacted reaches than to that in severely impacted reaches (Fig. 6.7). However, the distances in ordination space between minimally impacted/ pre-earthquake reaches and severely impacted reaches decreased over time. Winter samples (Jul-2011) displayed a re-divergence from pre-earthquake composition.

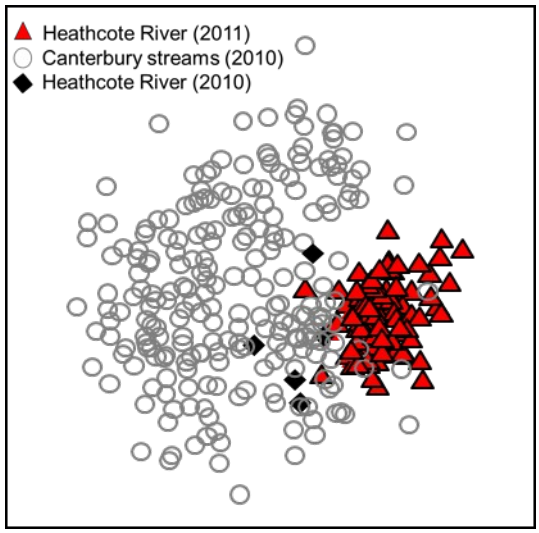

Figure 6.6 **Comparison of bacterial community profiles from biofilm sampled within the Heathcote River post 22-Feb-2011 earthquake, the Heathcote River in Feb-2010, and within a range of other streams sampled in the Canterbury region in February/March 2010 (Lewis et al. 2010). Plot is derived from non-metric multi-dimensional scaling of ARISA traces using a Bray Curtis similarity measure, 2D stress, 0.27; 3D stress, 0.21. Between three and five rocks (pseudo-replicates) were sampled within each stream site.**

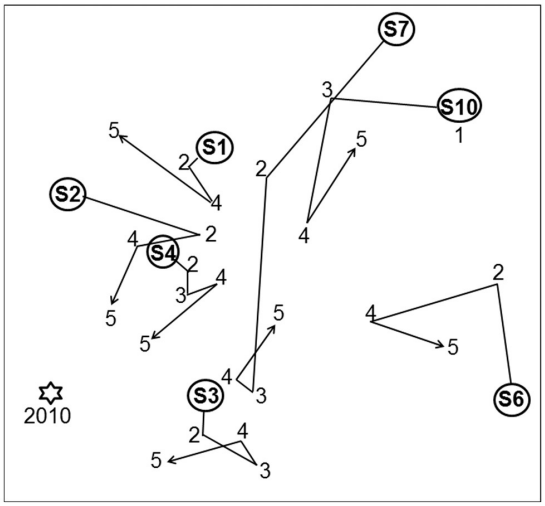

Figure 6.7 **Temporal difference in bacterial community profiles from biofilms sampled within sections S2, S3, A, S4, S5, S6 and S9 of the Heathcote River. Plot is derived from non-metric multidimensional scaling of ARISA traces using a Bray Curtis similarity measure. Trajectories show variation in the bacterial communities in each section of the Heathcote River over time: (1) 09-Mar-2011; (2) 31-Mar-2011; (3) 05-May-2011; (4) 04-Jun-2011; (5) 05-Jul-2011, and data collected from the Heathcote River (S3) in Feb-2010 (indicated with star). All data points are average data obtained from the analysis of three stream rocks for each stream section and date. 2D stress is 0.21.**

Despite degradation of Heathcote River benthic invertebrate communities (mean taxonomic richness of 12 taxa, EPT number of 2 taxa, and MCI value of ~70), there was a marked post-earthquake deterioration of downstream EPT communities (Fig. 6.8). The number of EPT taxa in moderately impacted reaches recovered to upstream levels by May-2011, and by Sep-2011 the severely impacted reaches had likewise recovered. Although taxonomic richness did not differ between reaches, there was a significant increase in the number of taxa from Mar-2011 to Sep-2011. Over this time the mean number of taxa in severely impacted reaches increased from 8 to 17. There were no changes in MCI, either over distance or over time.

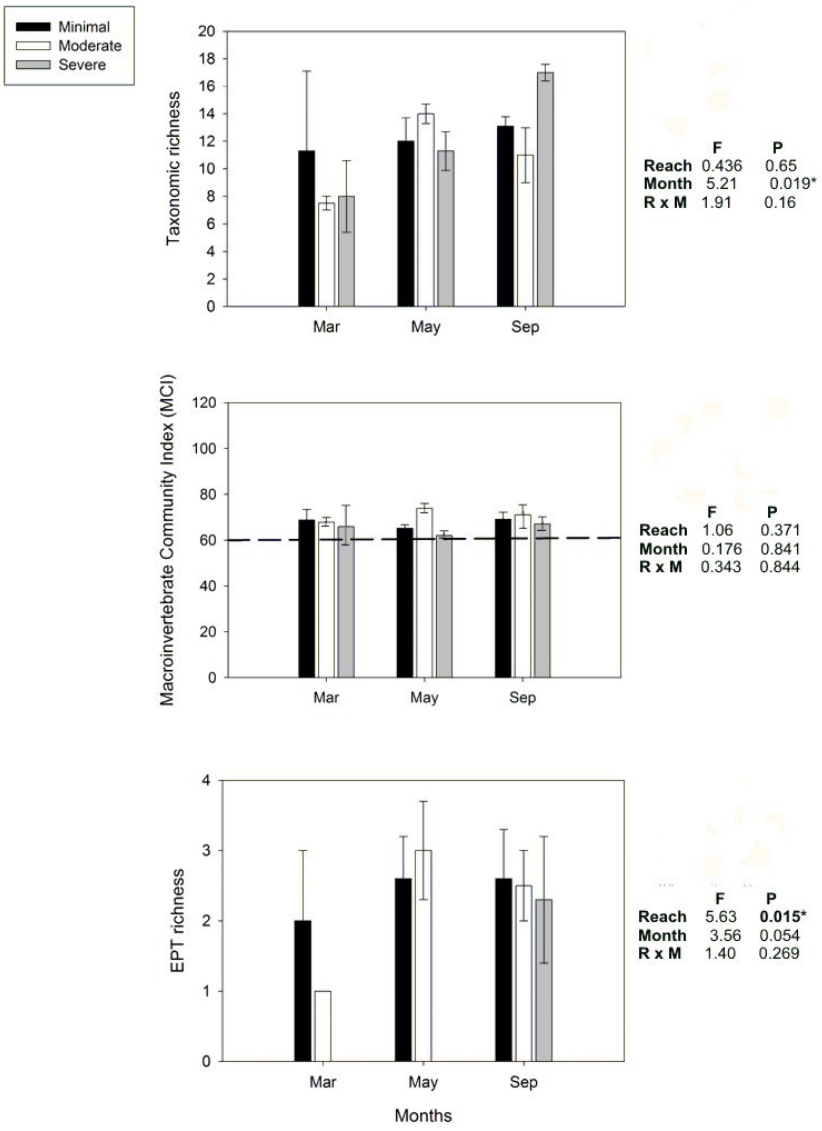

Figure 6.8 **Mean benthic invertebrate taxonomic richness, EPT richness and Macroinvertebrate Community Index values (mean ±SE) for minimally, moderately and severely impacted reaches along the Heathcote River. Results from the two-way ANOVA comparisons of metrics over distance (reaches), time (months), and reaches x months (RxM). The dashed line (MCI = 60) is the indicator point for categorising water quality as 'severely impacted' (Stark 1998) ('*' indicates p <0.05).**

6.5 Discussion

The 22-Feb-2011 Christchurch earthquake and associated destruction caused immediate damage to the Heathcote River ecosystem, particularly in the lower reaches of the river (corresponding geographically to the most damaged parts of the city). By studying changes in key biological communities and their relationship to biogeochemical function I found sewage was the primary vector of earthquake-induced damage, and that recovery from this damage occurred in an inverse cascade, with surface water chemistry returning to baseline immediately after sewage discharge was curtailed, then in-stream biogeochemistry (N cycling and benthic microbial composition) resuming more typical function within another one to three weeks, and finally the re-establishment of benthic invertebrate communities in the most severely impacted reaches four months later.

The broad spatial patterns of sewage discharge were geographically congruent to the most extreme hydrologic earthquake effects, making it difficult to separate the impact of the two forces. So although anecdotal hydrologic disruptions were observed (e.g., river 'whitening' following both the 22-Feb and 13-Jun earthquakes), any effect that they had on river function was masked by the overwhelming impact of the sewage being discharged. However, the consistent downstream pattern of H and O isotope ratios and water temperatures in the stream over the course of the study (showing no relationship to distance from either the 22-Feb or 13-Jun earthquakes) indicate that liquefaction did not meaningfully alter hydrology relevant to community structure and biogeochemical function. Furthermore, both the water and sediments associated with earthquake-triggered liquefaction were chemically unremarkable and essentially biologically inert. Given that the region's surface waters and shallow groundwater, the source of hydrologic disturbances following the earthquake (Cox et al., 2012), share the same source (Stewart, 2012) the lack of chemical and isotopic indicators of earthquake hydrology in the Heathcote River was unsurprising. Thus the lack of clear indicators of lasting hydrologic change make it reasonable to interpret my results on the biogeochemical and biological community response to the 22-Feb earthquake entirely in the context of the sewage spills it triggered.

The drastic changes to the macronutrient composition (DOC, NO_3^-, NH_4^+ and DO) of surface water in the Heathcote River clearly indicate the magnitude of sewage contamination. Changes were tightly coupled, both spatially and temporally, with earthquake damage, and surface water chemical composition across the entire river returned to typical urban stream levels once sewage inputs decreased. The lack of $\delta^{15}N$ enrichment in sewage-NO_3^- reflects the fact that the 'heavy' signature commonly associated with sewage-N is a product of the treatment process, when ammonia volatilisation preferentially removes 'light' N. Although a precise isotopic source signature for sewage-N could not be constrained, the dominance of this nutrient source in the river system was clearly identified as it drove in-situ denitrification, resulting in increasingly enriched $\delta^{15}N$ and $\delta^{18}O$ of NO_3^- in the river.

Nitrate fractionation by denitrifiers could be used to quantify in-stream N-attenuation, and thus sewage-N loading, over the first 40-days following the 22-Feb earthquake. Over this period $\delta^{18}O$-NO_3^- and $\delta^{15}N$-NO_3^- were enriched in parallel as they moved downstream, fingerprinting denitrification as the primary N fractionating process in the system. The overwhelming volume of sewage entering the river (~20% of upstream discharge and >10x baseline DIN discharge) provided a roughly homogenous N source. This assumption is further validated by the lack of variation in $\delta^{18}O$-H_2O between NO_3^- sources (sewage and river water), meaning NO_3^- in either source would have formed from isotopically identical O-H_2O and O-O_2, creating homogenous $\delta^{18}O$-NO_3^- (Kool et al. 2009).

The calculated N attenuation (removing up to 80% of N entering the waterway) explains the consistency of the N flux out of the Heathcote River despite the extreme changes in sewage N loading. Based on this high attenuation efficiency, the elevated DIN concentrations reported in the Avon-

Heathcote Estuary at the mouth of the Heathcote River post-earthquake (Bolton-Ritchie 2012) must have resulted from either, 1) an additional sewage source downstream of the sampled reaches, or, 2) an elevated N discharge from the Heathcote prior to commencement of sampling in Mar-2011. The latter indicates a delayed response of denitrifier communities to the sewage influx consistent with the lack of significant changes to NO_3^- isotope dynamics during the three days of re-elevated sewage discharge following the 13-Jun earthquake. A similarly delayed response followed the cessation of sewage discharge in Apr-2011, when $\delta^{15}N$- NO_3^- returned to the soil-N range one week prior to the loss functional dominance of in-stream denitrification. These measurements constrain the response time of Heathcote River denitrifying communities to changes in N supply to ~7 days (3-15 days).

The continuous enrichment of $\delta^{15}N$ and $\delta^{18}O$ of NO_3^- as it was transported downstream ceased after 70 days, indicating that in-situ denitrification was no longer controlling the DIN pool. This assumption is supported by the loss of in-stream conditions favouring denitrification (high DOC and low DO) as sewage inputs decreased. The linear relationship between $\delta^{15}N$-NO_3^- and $\delta^{18}O$-NO_3^- persisted in winter months. However, this enrichment did not occur continuously down the river, and thus probably reflects a mixing of heterogeneously denitrified soil-N sources caused by the seasonal increase in rainfall accelerating leaching and denitrification of soil-N (Di and Cameron 2002). The hypothesis of winter leaching, rather than renewed sewage contamination, driving a seasonal isotopic enrichment of NO_3^- in river water is supported by the parallel elevation in DOC concentrations in July and August (which occurred independently of an increase in *E.coli* numbers or depletion of DO).

Interestingly, as river conditions became increasingly aerobic and the availability of electron donors (DOC) reverted back to more typical freshwater levels, the $\delta^{18}O$- $\delta^{15}N$- NO_3^- enrichment ratio shifted from 1:1 (the ratio at which denitrifiers isolated from a range of environments will fractionate NO_3^- under optimal laboratory conditions (Granger et al. 2008, Wunderlich et al. 2012)) to 1:2 (the value traditionally assigned to fractionation by denitrifiers in freshwater systems (Xue et al. 2009)). This shift indicates either a change in cellular-level fractionation as C become more limiting (Wunderlich et al. 2012) or that increasing oxygen availability in the surface water caused diffusive fractionation as denitrified NO_3^- moved from the anaerobic sediments into the aerobic surface water (Lehmann et al. 2003). This unique empirical data set highlights the need to better quantify the controls on NO_3^- fractionation across scales.

The response of biofilm microbes to earthquake damage confirms their sensitivity to dramatic shifts in ecosystem function (Allison and Martiny 2008) and nutrient uptake (Hoellein et al. 2009). For instance, reach S6, which consistently had the highest *E.coli* counts, also underwent the most extreme changes in microbial community composition. The temporal correlation between the changes in NO_3^- isotope cycling and benthic biofilm microbial communities provides an intriguing possible link between composition and function, emphasising the potential insight that could come from novel combinations of these two indicators (e.g., Merbt et al. 2011) in order to resolve community function v. structure (e.g., Frossard et al. 2012). The 'regression' in Jun-2011 could indicate some of the

'increased system variability' sometimes found following a disturbance (Lamberti et al. 1991). However, in light of the continuous recovery of benthic invertebrates over the study period, it seems likely that the potential re-divergence of biofilm communities sampled in Jul-2011 is a result of seasonal change. During winter months the concentration of DOC in the surface water increased and the temperature decreased, both of which could cause a community shift (Battin 2000, de la Rua et al. 2011).

The recovery of benthic invertebrate populations lagged behind that of organisms at lower trophic levels: all seven genera of caddisflies found in minimally impacted reaches were still absent from severely impacted reaches in Sep-2011. However, all other metrics showed complete recovery within six months, placing the recovery of the Heathcote River at the rapid end of the spectrum of what has been observed in streams impacted by natural disasters, which span from months (Anderson 1992, Snyder and Johnson 2006) to >10 years (Cover et al 2010, Mundahl and Hunt 2011). The relatively slow recovery of higher trophic levels is in keeping with previously observed stream recovery patterns (e.g., Lamberti et al. 1991, Mundahl and Hunt 2011). In this case, slower recovery of benthic invertebrates reflects their reliance on the recovery of water chemistry and basal food resources as well as the time needed for re-colonisation of severely impacted reaches (Sousa 1984).

6.6 Conclusions

In addition to enabling more accurate quantification of sewage-N attenuation, NO_3^- isotope measures, when used in combination with other biological and chemical metrics, proved a clear 'added value' as indicators of stream impact and recovery from an acute event. Although the hydrologic changes triggered by large earthquakes do not appear to cause significant disturbance to the biological communities in the receiving surface water, sewage spills triggered by earthquakes in urban zones do pose a significant risk to stream health. However, my finding that stream organisms, from microbes to macroinvertebrates, recovered within six months of the earthquake confirm that the city's decision to discharge effluent directly into the rivers will have no long-term environmental cost, supporting the use of such short-term dumping as an effective natural disaster mitigation strategy. More studies are needed to determine how stream health (urbanisation) prior to such a natural disaster dictates its resilience to acute change. It should be highlighted that *E. coli* values returned to background levels relatively quickly after sewage discharge ceased, meaning that relying on *E. coli* as the sole measure of 'water health', as most monitoring agencies do, would result in a misrepresentation of ecosystem recovery.

In light of my findings, I reiterate Lindenmayer and colleagues' (2010) call to focus resources (both monetary and intellectual) on ensuring rapid scientific response to catastrophic events. As cities grow in area and density worldwide, the probability of major earthquakes occurring within an urban centre is likewise growing, as has been reflected in the recent spate of catastrophic urban earthquakes (e.g., 2003 Bam (Iran), 2009 L'Aquila (Italy) and 2010 Port-au-Prince (Haiti)). Thus the motivation to characterise the effect of these events on freshwater systems comes not only from scientific curiosity,

but also from acknowledgement of the human need for clean water. By identifying the impacts that earthquakes can have on surface water resources, recovery efforts can be more precisely focused to minimise long-term ecosystem degradation. These findings on the impact and recovery of multiple trophic levels in an urban stream following a catastrophic earthquake highlight the need for rapid and effective scientific study of these events.

6.7 Acknowledgements

Like the earthquake that precipitated it, this research was unanticipated. As such, funding was pulled from many sources and assistance offered by many generous individuals, making this a truly collaborative product. Funding for chemical and isotopic analyses was made available from a FRST grant (C05X0803) to W.T. Baisden / GNS Science, with additional support from Lincoln University. Microbial analysis was funded by RSNZ Marsden Fund (LU10901) to Gavin Lear.

I would like to thank Environment Canterbury for providing background data for the Heathcote River, particularly Martin Neale (Auckland Council) and Michele Stevenson (Environment Canterbury) and Vidya Washington (University of Auckland) for provision of bacterial community data from the wider Canterbury region and Tony Gray (Environment Canterbury) for hydrologic data.

Thanks to Andy Phillips and Cedric Douence at the National Isotope Centre of New Zealand and Lynne Clucas and Joy Jiao at Lincoln University for analytical assistance, and Milen Marinov and Hayley Stoddart at the University of Canterbury for processing benthic invertebrate samples.

Finally, thanks to my endlessly supportive co-authors: Gavin Lear, Jon Harding, Leo Condron, Tim Clough, Troy Baisden, Y. Ding and Gillian Lewis, without whom this manuscript would be much poorer. Leo, Tim, and Gavin helped propose the mad idea of doing 'some sampling', Troy ran the initial batches of NO_3^- and H_2O batches, Lewis and Ding helped process the microbial data (Fig. 6.6 and Fig 6.7 reproduced with permission), and Jon collected invertebrate data (Fig. 6.8 reproduced with permission). Special thanks to Gavin, Tim, and Jon for pointing out which bits of the manuscript were, 'unreadable'.

6.8 References

Allison, S. D. and J. B. H. Martiny. 2008. Resistance, resilience, and redundancy in microbial communities. Proceedings of the National Academy of Sciences of the United States of America **105**:11512-11519.

Anderson, M.J. 2002. A new method for non-parametric multivariate analysis of variance. Austral Ecology **26**: 32-46.

Anderson, N. H. 1992. Influence of disturbance on insect communities in pacific-northwest streams. Hydrobiologia **248**:79-92.

Barnes, R. T., P. A. Raymond, and K. L. Casciotti. 2008. Dual isotope analyses indicate efficient processing of atmospheric nitrate by forested watersheds in the northeastern US. Biogeochemistry **90**:15-27.

Battin, T. J. 2000. Hydrodynamics is a major determinant of streambed biofilm activity: From the sediment to the reach scale. Limnology and Oceanography **45**:1308-1319.

Bolton-Ritchie, L. 2012. Earthquake impacts on estuary water quality. Environment Canterbury. Accessed online at: http://ecan.govt.nz on 08-Jun-2012.

Boulton, A. J., C. G. Peterson, N. B. Grimm, and S. G. Fisher. 1992. Stability of an aquatic macroinvertebrate community in a multiyear hydrologic disturbance regime. Ecology **73**:2192-2207.

Chen, F. J., G. D. Jia, and J. Y. Chen. 2009. Nitrate sources and watershed denitrification inferred from nitrate dual isotopes in the Beijiang River, south China. Biogeochemistry **94**:163-174.

Clarke, K.R., Gorley, R.N., 2006. PRIMER v6: User Manual/Tutorial. PRIMER-E, Plymouth, UK.

Cover, M. R., J. A. de la Fuente, and V. H. Resh. 2010. Catastrophic disturbances in headwater streams: the long-term ecological effects of debris flows and debris floods in the Klamath Mountains, northern California. Canadian Journal of Fisheries and Aquatic Sciences **67**:1596-1610.

Cox, S. C., H. K. Rutter, A. Sims, M. Manga, J. J. Weir, T. Ezzy, P. A. White, T. W. Horton, and D. Scott. 2012. Hydrological effects of the M-W 7.1 Darfield (Canterbury) earthquake, 4 September 2010, New Zealand. New Zealand Journal of Geology and Geophysics **55**:231-247.

de la Rua, A., B. Rodelas, J. Gonzalez-Lopez, and M. A. Gomez. 2011. Submerged filter biofilm formation by nitrate-contaminated groundwater microbiota. Journal of Environmental Science and Health Part a-Toxic/Hazardous Substances & Environmental Engineering **46**:1113-1121.

Di, H. J. and K. C. Cameron. 2002. Nitrate leaching in temperate agroecosystems: sources, factors and mitigating strategies. Nutrient Cycling in Agroecosystems **64**:237-256.

Dobermann, A., J. L. Gaunt, H. U. Neue, I. F. Grant, M. A. Adviento, and M. F. Pampolino. 1994. Spatial and temporal variability of ammonium in flooded rice fields. Soil Science Society of America Journal **58**:1708-1717.

Frossard, A., L. Gerull, M. Mutz, and M. O. Gessner. 2012. Disconnect of microbial structure and function: enzyme activities and bacterial communities in nascent stream corridors. Isme Journal **6**:680-691.

Granger, S. J., T. H. E. Heaton, R. Bol, G. S. Bilotta, P. Butler, P. M. Haygarth, and P. N. Owens. 2008. Using $\delta^{15}N$ and $\delta^{18}O$ to evaluate the sources and pathways of NO_3^- in rainfall event discharge from drained agricultural grassland lysimeters at high temporal resolutions. Rapid Communications in Mass Spectrometry **22**:1681-1689.

Groffman, P. M., K. Butterbach-Bahl, R. W. Fulweiler, A. J. Gold, J. L. Morse, E. K. Stander, C. Tague, C. Tonitto, and P. Vidon. 2009. Challenges to incorporating spatially and temporally explicit phenomena (hotspots and hot moments) in denitrification models. Biogeochemistry **93**:49-77.

Halvorson, S. J. and J. P. Hamilton. 2010. In the aftermath of the Qa'yamat: the Kashmir earthquake disaster in northern Pakistan. Disasters **34**:184-204.

Hoellein, T. J., J. L. Tank, E. J. Rosi-Marshall, and S. A. Entrekin. 2009. Temporal variation in substratum-specific rates of N uptake and metabolism and their contribution at the stream-reach scale. Journal of the North American Benthological Society **28**:305-318.

James, A., and S. McMurtie. 2012. Post-quake ecology of the lower Avon River: current state of the fish and invertebrate community. EOS Ecology Report No: 11012

Kaushal, S. S., P. M. Groffman, L. E. Band, E. M. Elliott, C. A. Shields, and C. Kendall. 2011. Tracking nonpoint source nitrogen pollution in human-impacted watersheds. Environmental Science & Technology **45**:8225-8232.

Kempers, A. J. and A. Zweers. 1986. Ammonium determination in soil extracts by the salicylate method. Communications in Soil Science and Plant Analysis **17**:715-723.

Kool, D. M., C. Muller, N. Wrage, O. Oenema, and J. W. Van Groenigen. 2009. Oxygen exchange between nitrogen oxides and H2O can occur during nitrifier pathways. Soil Biology & Biochemistry **41**:1632-1641.

Lamberti, G. A., S. V. Gregory, L. R. Ashkenas, R. C. Wildman, and K. M. S. Moore. 1991. Stream ecosystem recovery following a catastrophic debris flow. Canadian Journal of Fisheries and Aquatic Sciences **48**:196-208.

Lear, G., I. K. G. Boothroyd, S. J. Turner, K. Roberts, and G. D. Lewis. 2009. A comparison of bacteria and benthic invertebrates as indicators of ecological health in streams. Freshwater Biology **54**:1532-1543.

Lear, G., A. Dopheide, P. Ancion, and G. D. Lewis. 2011. A comparison of bacterial, ciliate and macroinvertebrate indicators of stream ecological health. Aquatic Ecology **45**:517-527.

Lehmann, M. F., P. Reichert, S. M. Bernasconi, A. Barbieri, and J. A. McKenzie. 2003. Modelling nitrogen and oxygen isotope fractionation during denitrification in a lacustrine redox-transition zone. Geochimica Et Cosmochimica Acta **67**:2529-2542.

Lewis, G.D., V. Washington, G. Lear, K. Roberts, J. Curran, V. Fan, M.W. Neale. 2010. A bacterial

community index (BCI) for New Zealand streams- Year 1. Auckland Regional Council Technical Report 2010/068.81

Lindenmayer, D. B., G. E. Likens, and J. F. Franklin. 2010. Rapid responses to facilitate ecological discoveries from major disturbances. Frontiers in Ecology and the Environment **8**:527-532.

Lohse, K. A., P. D. Brooks, J. C. McIntosh, T. Meixner, and T. E. Huxman. 2009. Interactions Between Biogeochemistry and Hydrologic Systems. Annual Review of Environment and Resources **34**:65-96.

McArdle, B. H. and M. J. Anderson. 2001. Fitting multivariate models to community data: A comment on distance-based redundancy analysis. Ecology **82**:290-297.

McIlvin, M. R. and M. A. Altabet. 2005. Chemical conversion of nitrate and nitrite to nitrous oxide for nitrogen and oxygen isotopic analysis in freshwater and seawater. Analytical Chemistry **77**:5589-5595.

Menoni, S. 2001. Chains of damages and failures in a metropolitan environment: some observations on the Kobe earthquake in 1995. Journal of Hazardous Materials **86**:101-119.

Merbt, S. N., J. C. Auguet, E. O. Casamayor, and E. Marti. 2011. Biofilm recovery in a wastewater treatment plant-influenced stream and spatial segregation of ammonia-oxidizing microbial populations. Limnology and Oceanography **56**:1054-1064.

Miller, D. N., J. E. Bryant, E. L. Madsen, and W. C. Ghiorse. 1999. Evaluation and optimization of DNA extraction and purification procedures for soil and sediment samples. Applied and Environmental Microbiology **65**:4715-4724.

Mohr, C. H., D. R. Montgomery, A. Huber, A. Bronstert, and A. Iroume. 2012. Streamflow response in small upland catchments in the Chilean coastal range to the M-W 8.8 Maule earthquake on 27 February 2010. Journal of Geophysical Research-Earth Surface **117**.

Muirwood, R. and G. C. P. King. 1993. Hydrological signatures of earthquake strain. Journal of Geophysical Research-Solid Earth **98**:22035-22068.

Mundahl, N. D. and A. M. Hunt. 2011. Recovery of stream invertebrates after catastrophic flooding in southeastern Minnesota, USA. Journal of Freshwater Ecology **26**:445-457.

New Zealand Civil Defence. 2011. Media release, received 04-Apr-2011.

Ostrom, N. E., L. O. Hedin, J. C. von Fischer, and G. P. Robertson. 2002. Nitrogen transformations and NO_3^- removal at a soil-stream interface: A stable isotope approach. Ecological Applications **12**:1027-1043.

Parfitt, R. L., L. A. Schipper, W. T. Baisden, and A. H. Elliott. 2006. Nitrogen inputs and outputs for New Zealand in 2001 at national and regional scales. Biogeochemistry **80**:71-88.

Reddy, D. V., P. Nagabhushanam, and B. S. Sukhija. 2011. Earthquake (M 5.1) induced hydrogeochemical and delta O-18 changes: validation of aquifer breaching-mixing model in Koyna, India. Geophysical Journal International **184**:359-370.

Sebilo, M., G. Billen, M. Grably, A. Mariotti. 2003. Isotopic composition of nitrate-nitrogen as a marker of riparian and benthic denitrification at the scale of the whole Seine River system. Biogeochemistry **63:** 35-51.

Segou, M. and E. Kalkan. 2011. Ground motion attenuation during M 7.1 Darfield and M 6.2 Christchurch, New Zealand, earthquakes and performance of global predictive models. Seismological Research Letters **82**:866-874.

Seitzinger, S., J. A. Harrison, J. K. Bohlke, A. F. Bouwman, R. Lowrance, B. Peterson, C. Tobias, and G. Van Drecht. 2006. Denitrification across landscapes and waterscapes: A synthesis. Ecological Applications **16**:2064-2090.

Shiller, A. M., M. J. Shim, L. D. Guo, T. S. Bianchi, R. W. Smith, and S. W. Duan. 2012. Hurricane Katrina impact on water quality in the East Pearl River, Mississippi. Journal of Hydrology **414**:388-392.

Snyder, C. D. and Z. B. Johnson. 2006. Macroinvertebrate assemblage recovery following a catastrophic flood and debris flows in an Appalachian mountain stream. Journal of the North American Benthological Society **25**:825-840.

Sousa, W. P. 1984. The role of disturbance in natural communities. Annual Review of Ecology and Systematics **15**:353-391.

Stark, J. D. 1993. Performance of the macroinvertebrate community index - effects of sampling method, sample replication, water depth, current velocity, and substratum on index values. New Zealand Journal of Marine and Freshwater Research **27**:463-478.

Stark, J. D. 1998. SQMCI: a biotic index for freshwater macroinvertebrate coded abundance data. New Zealand Journal of Marine and Freshwater Research **32**:55-66.

Stark, J.D., I.K. Boothroyd, J.S. Harding, J.R. Maxted, M.R. Scarsbrook. 2001. Protocols for sampling macroinvertebrates in wadeable streams. New Zealand Macroinvertebrate Working Group Report No. 1., Ministry for the Environment, Wellington. 57 p.

Stewart, M. K. 2012. A 40-year record of carbon-14 and tritium in the Christchurch groundwater system, New Zealand: Dating of young samples with carbon-14. Journal of Hydrology **430**:50-68.

Triska, F. J., J. H. Duff, and R. J. Avanzino. 1993. The role of water exchange between a stream channel and its hyporheic zone in nitrogen cycling at the terrestrial aquatic interface. Hydrobiologia **251**:167-184.

Wakelin, S. A., M. J. Colloff, and R. S. Kookana. 2008. Effect of wastewater treatment plant effluent on microbial function and community structure in the sediment of a freshwater stream with variable seasonal flow. Applied and Environmental Microbiology **74**:2659-2668.

Wang, C. Y. and M. Manga. 2010. Hydrologic responses to earthquakes and a general metric. Geofluids **10**:206-216.

Wassenaar, L. I., P. Athanasopoulos, and M. J. Hendry. 2011. Isotope hydrology of precipitation, surface and ground waters in the Okanagan Valley, British Columbia, Canada. Journal of Hydrology **411**:37-48.

Wilson, D. D. 1976. Hydrogeology of metropolitan Christchurch. Journal of Hydrology (N.Z.) **15**:101-120.

Winterbourn, M.J. 1973. A guide to the freshwater Mollusca of New Zealand. Tuatara **20**: 141-159.

Winterbourn, M.J., K.L.D. Gregson, C.H. Dolpin. 2000. Guide to aquatic insects of New Zealand. Bulletin of the Entomological Society of New Zealand **14**: 1-108.

Wood, P. J. and P. D. Armitage. 1997. Biological effects of fine sediment in the lotic environment. Environmental Management **21**:203-217.

Wright, I. A., B. C. Chessman, P. G. Fairweather, and L. J. Benson. 1995. Measuring the impact of sewage effluent on the macroinvertebrate community of an upland stream - the effect of different levels of taxonomic resolution and quantification. Australian Journal of Ecology **20**:142-149.

Wunderlich, A., R. Meckenstock, and F. Einsiedl. 2012. Effect of different carbon substrates on nitrate stable isotope fractionation during microbial denitrification. Environmental Science & Technology **46**:4861-4868.

Xue, D. M., J. Botte, B. De Baets, F. Accoe, A. Nestler, P. Taylor, O. Van Cleemput, M. Berglund, and P. Boeckx. 2009. Present limitations and future prospects of stable isotope methods for nitrate source identification in surface- and groundwater. Water Research **43**:1159-1170.

Plate 5 **Top to bottom: dairy herd grazing near irrigation line adjacent to reach 'C' in Harts Creek (Canterbury, New Zealand); Harts Creek as it nears its confluence with Lake Ellesmere (reach 'D'). Both photographs taken in February (summer) 2012.**

Chapter 7

Nitrate stable isotopes reveal climate controls on nitrogen attenuation and discharge in a stream draining intensive pastoral agriculture (Canterbury, New Zealand)

A version of this chapter will be submitted for publication. Wells, N.S., W.T. Baisden, T. Horton, T.J. Clough. In prep. Tracing the fate of nitrogen inputs into pastoral agroecosystems using nitrate isotopes. Biogeochemistry.

7.1 Abstract

Precise indicators of when and where reactive nitrogen (N) is 'leaking' from grazed pasture ecosystems are needed in order to mitigate the threat that intensifying production poses to water quality. The natural abundance isotopic composition ($\delta^{15}N$ and $\delta^{18}O$) is tipped as a potential means of improving N loss measurements based on the knowledge that changes in isotopic composition caused by denitrification can be quantitatively related to attenuation once the original isotopic composition of the source is known. We demonstrate that NO_3^- stable isotopes ($\delta^{15}N$ and $\delta^{18}O$) can play an important role in elucidating spatial-temporal variations in the sources and sinks of NO_3^- in a catchment dominated by pastoral livestock production. An agricultural stream (mean NO_3^--N of 6 mg l^{-1}) was sampled monthly over a two-year period for NO_3^- isotopes along four reaches. In all but three months, NO_3^- in the lowest reaches reflected nitrification of pasture nitrogen sources (urine and fertilisers, $\delta^{15}N$-NO_3^- of ~0‰), indicating that catchment nitrogen inputs are in excess of its attenuation capacity. It was concluded that the nitrate (mean NO_3^--N of 6 mg l^{-1} and $\delta^{15}N$-NO_3^- of 0‰) at the stream mouth reflected nitrification of these pasture nitrogen sources, which became progressively enriched at a $\delta^{18}O$:$\delta^{15}N$ ratio of ~0.6 in shallower upstream reaches. Using a Rayleigh model, monthly attenuation rates for the catchment could thus be calculated for 16 sampling dates. Nitrate discharged from the stream reflected from 10 to 90% of N lost from the catchment. Attenuation was negatively correlated with streamwater nitrate concentration, and highly responsive to rainfall: 93% of calculated attenuation (20 kg NO_3^--N ha^{-1} y^{-1}) occurred within 48 h of rainfall. These findings demonstrate the power of dense measurements of NO_3^- stable isotope for distinguishing temporal and spatial trends in NO_3^- loss pathways, allowing for improved catchment-scale management of agricultural intensification.

Keywords: Nitrate, $\delta^{15}N$- $\delta^{18}O$- NO_3^-, nitrogen attenuation, New Zealand, stable isotopes, denitrification

7.2 Introduction

Increasing reactive nitrogen (N) inputs to agricultural systems have not been accompanied by a commensurate increase in crop N use efficiency (Dobermann and Cassman 2005), creating a cascade of undesirable environmental outcomes as excess N is transferred from land to water. Excess reactive N applied to soils as fertilisers and livestock excreta can cause eutrophication of water bodies, declining quality of potable water, and emission of the greenhouse gas nitrous oxide (N_2O) (Galloway et al. 2003). The need to manage agricultural N inputs in order to minimise losses is especially pertinent in New Zealand, where increasing nitrate (NO_3^-) concentrations in waterways have been linked to enhanced N leaching from intensifying pastoral ecosystems (Hamill and McBride 2003, Parfitt et al. 2008, Matthaei et al. 2010).

In order to successfully manage N loading from intensive agriculture, a more mechanistic understanding of how changing land-use and climate influence the proportional export of N from watersheds is needed (e.g., Kroeze et al. 2012). The major 'missing' sink for NO_3^- during land-to-water transfers is denitrification, the microbial step-wise reduction of reactive/ mobile NO_3^- to N gasses (N_2O, and ultimately inert dinitrogen (N_2)). Denitrification is the dominant pathway through which N is attenuated (i.e., permanently removed from the ecosystem) (Galloway et al. 2003). Once NO_3^- is available, denitrification only proceeds under anaerobic conditions and in the presence of a suitable electron donor such as carbon (C) (Seitzinger et al. 2006; Wallenstein et al. 2006). The factors controlling C, O_2, and NO_3^- availability (e.g., water saturation (Hefting et al. 2004), particle size (Findlay et al. 2011), land use (Barnes and Raymond 2010, Sudduth et al. 2013), climate (Mulholland et al. 2008), nutrient stoichiometry (Taylor and Townsend 2010), and C quality (Barnes et al. 2012) vary at micro to landscape scales, causing denitrification to occur in 'hot spots' and 'hot moments' of activity, rather than linearly over time and space. Furthermore, additions of ^{15}N- enriched tracers to whole-streams found that in-stream denitrification efficiency decreases as N loading increases (Mulholland et al. 2008). This resultant complexity in the rates and occurrence of denitrification has made accurate measurements of NO_3^- attenuation a challenge, bringing significant uncertainty to catchment- landscape scale assessments of N cycling (Galloway et al. 2003, Groffman et al. 2009).

Kinetic fractionation of NO_3^- isotopes ($\delta^{18}O$ and $\delta^{15}N$) during denitrification provides a potential tool to integrate spatio-temporal variability in attenuation, and have been used successfully to identify (e.g., Chen et al. 2009) and quantify (e.g., Ostrom et al. 2002, Cohen et al. 2012) the importance of denitrification in a range of ecosystems. The method quantifies denitrification fluxes (attenuation) using a closed-system Rayleigh kinetic type model (Nestler et al. 2011) (Eq. 7.1):

$$\frac{C}{C_0} = \left(\frac{R}{R_0}\right)^{1/(\alpha\, denit - 1)} \tag{7.1}$$

which relates the enrichment of isotope pool and substrate (NO_3^-) concentration measured at any point (R and C, respectively) to the original isotopic composition (R_0) and concentration (C_0) of the NO_3^- pool using the fractionation factor for denitrification (α_{denit}). Thus, the $\delta^{15}N$ $\delta^{18}O$ of exported NO_3^- could provide the needed precise and accurate measure of N attenuation, and N loading, needed to successfully manage the excess N from intensifying pastoral agriculture in New Zealand (where the lack of atmospheric N deposition means there are fewer potential sources to convolute this signal (Parfitt et al. 2006)).

Since the 1980's New Zealand agriculture has undergone rapid land-use conversion from low-intensity sheep grazing to high-intensity dairy production (Parfitt et al. 2006). This shift is reflected in the increased use of N fertilisers (from 50 Gg nationally in 1980 to 350 Gg in 2005) with the average dairy farm applying 150 kg N ha^{-1} y^{-1} (typically as urea) (Parfitt et al. 2008). Land conversion entails higher stocking rates, increased N mineralisation and turnover from animal excreta (urine and manure), urea fertiliser application, and area cover of pasture legumes that biologically fix atmospheric N (BNF) (e.g., Lucerne (*Medicago sativa* L.), white clover (*Trifolium repens* L.)), combined with increased irrigation and subsequent physical nutrient leaching (McDowell et al. 2011a, McDowell et al. 2011b). Surface water quality monitoring schemes carried out since 1989 have documented an increase in N exports (in the form of NO_3^-) from agricultural regions of New Zealand (e.g., Stevenson et al. 2010) and an overall decline in water quality (Alexander et al. 2002, Larned et al. 2004). Concern is growing over the cost of declining water quality, both in terms of ecosystem services and the maintenance of a 'clean' national environmental image, motivating new mitigation efforts. For example, the 2003 Dairying and Clean Streams Accord between monitoring agencies and dairy farmer cooperative groups focused on stock exclusion fencing around flowing waters and riparian re-planting in order to lower surface water N concentrations (Bewsell et al. 2007).

Using the SCOPE-N model (Boyer et al. 2002), Parfitt et al. (2006) calculated that 40.5 kg N ha^{-1} are lost from New Zealand soils annually. Lacking functional data, the authors assumed a constant rate of NO_3^- attenuation during land-to-water transfers, designating losses as directly proportional to inputs. However, in North American watersheds 'proportional N export' (percent of N inputs discharged downstream v. denitrified during transport) was found to range from 7 – 80% over climate gradients (Schaefer and Alber 2007, Schaefer et al. 2009).

In order to more accurately assess the impact of agriculture on water quality, I test the hypothesis that NO_3^- dual isotopes can provide a means of both quantifying N attenuation, and thus its proportional export, from at-risk New Zealand pastoral catchments and identifying the spatial and temporal (weather and season) controls on these losses.

7.3 Materials and methods

7.3.1 Site description

Stream water was sampled monthly from four reaches along the length of Birdlings Brook/ Harts Creek (Waitatari) (subsequently referred to as Harts Creek) (mean discharge at mouth 1,500 m^3 s^{-1}) on the South Island of New Zealand (Fig. 7.1). Harts Creek drains into Lake Ellesmere (Te Waihora), a large brackish lake with a ~256,000 ha catchment bounded by the Rakaia and Waimakariri Rivers to the south and north, respectively, and the Canterbury foothills to the west (Gough and Ward 1996). Regional land-use is dominated by agriculture (>80% of area), which has undergone rapid intensification in production: between 1992 and 2004 urea fertiliser use in Canterbury increased from 10,000 tonnes to >90,000 tonnes and dairy cattle numbers increased six-fold to ~600,000 (Ford and Taylor 2006). Based on satellite images (accessed on GoogleEarth, 01/06/2012) the catchment area of Harts Creek was estimated to be 11,482 ha, with an elevation change from 100 to 0 m above sea level from west to east. Nitrate flux from Harts Creek into Lake Ellesmere increased from 1993 (beginning of monitoring) to 2012 (present) (Environment Canterbury, unpublished data), reflecting the national trend of increasing land-to-water nutrient loss (Parfitt et al. 2012) and contributing to the eutrophic state of the lake (in which >95% of excess nutrients enter via such spring-fed streams) (Department of Conservation 2005). In the 1980's extensive bank restoration was undertaken between reaches C and D and a vegetated buffer strip (5 to 8 m in width) has been maintained since with the objective of decreasing nutrient inputs to the creek by maximising plant uptake and/or denitrification (Collins 2011).

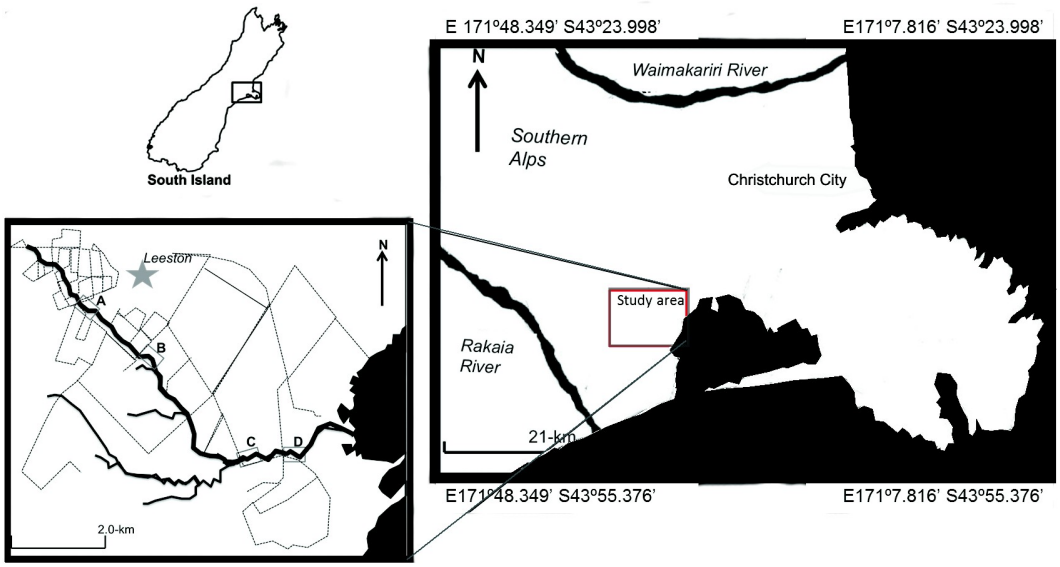

Figure 7.1 **The study area is located in the Canterbury Central Plains (between the Rakaia and Waimakariri Rivers, and the Southern Alps), on New Zealand's South Island. Samples were collected from Birdlings Brook/ Harts Creek (running from the town of Leeston (43°46'1.99"S, 172°16'57.79"E) to Lake Ellesmere/ Te Waihora) (inset) from Feb-2010 through Jan-2012. The three main spring-fed tributaries enter Birdlings Brook/ Harts Creek between reaches B and C, and numerous ephemeral drainage ditches intersect with the river along its length (dashed lines) (locations of ditches and tributaries based on satellite images accessed via GoogleEarth on 20-Jul-2012).**

7.3.2 Sample collection

Four reaches along Harts Creek were sampled monthly from Feb-2010 through Jan-2012. Sampling location were spread across the ~10 km of stream length, from the spring-fed source (A) to ~1 km above the confluence with Lake Ellesmere (D) (Fig. 7.1, inset). Surface water samples were collected from the thalweg of the stream using a reaching pole (to minimise sediment disturbance) holding a 500 ml sampling bottle. Four pseudo-replicates were collected from each reach at equal distances along a 100 m longitudinal transect, creating a nested sampling design of 16 total samples per month. Headspace air was removed by overfilling bottles and samples were stored on ice until return to the lab, where they were passed through Whatman GF/F filter paper and stored at -20°C until analysis.

Dissolved oxygen and water temperature were measured in-situ at each reach using a portable hand-held meter (550A YSI, Yellow Springs, OH). Stream depth was measured at upstream sites (A and B) using a metre stick and at downstream sites (C and D) using stream depth gauges previously installed by the regional council (Environment Canterbury). Daily climate data (soil moisture, rainfall, air temperature, wind direction, and wind run) were obtained from the Leeston/ Harts Creek climate station (43°46'1.99"S, 172°16'57.79"E) (<1 km from site A) (CliFlo: NIWA's Climate Database Online (http://cliflo.niwa.co.nz), data retrieved 06-Jun-2011, 11-Nov-2011, and 01-Feb-2012) (Fig.

7.2). Stream flow data was obtained from the Environment Canterbury gauging station at site D (water depth measured every 15 min, depth and width gauged monthly) (Fig. 7.2).

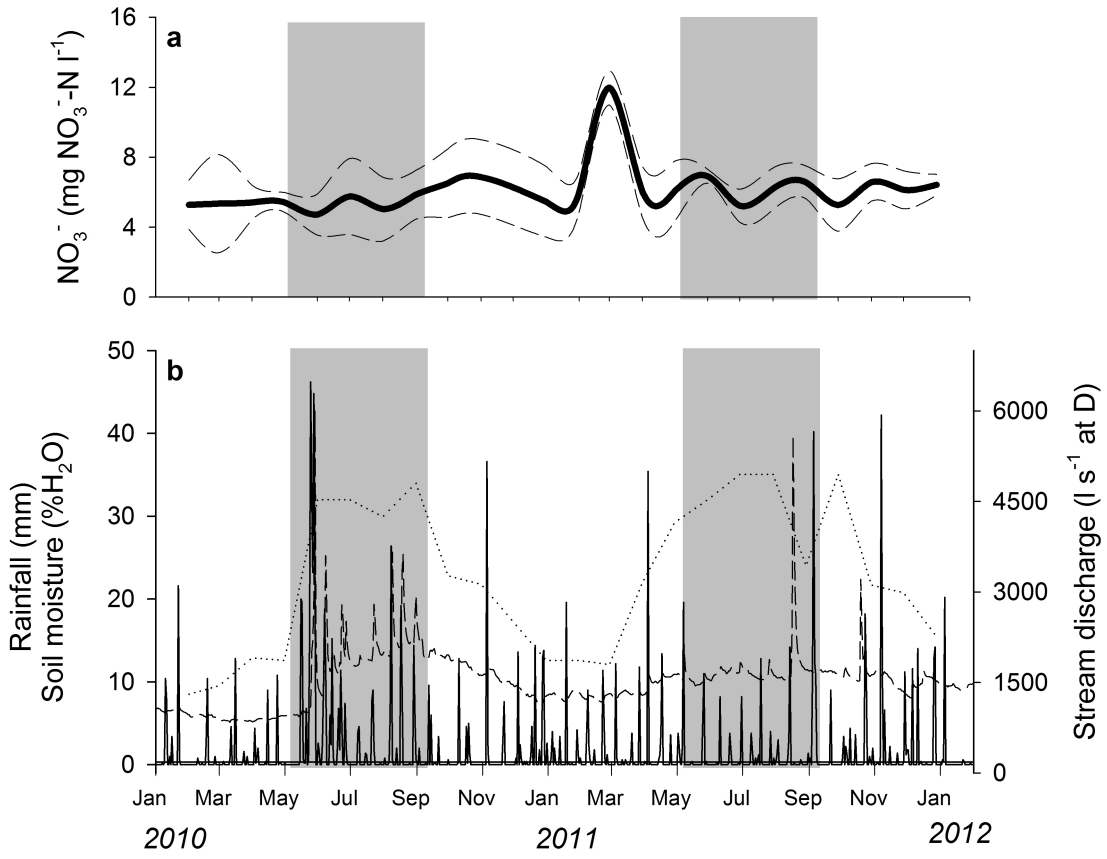

Figure 7.2 **Mean NO_3^- concentration in the surface water of all Harts Creek sites (solid line) ±1 SD (dashed lines) (a) (lines represent spline curves fitted to monthly data); and climate-driven hydrological conditions (soil moisture (dotted line), stream discharge (dashed line), and daily rainfall (solid line)) in the Harts Creek catchment (b) over the measurement period (Feb-2010 through Jan-2012). Shaded areas indicate winter months. (Climate data from the Leeston Harts Creek climate station, located <1 km from site A (CliFlo: NIWA's Climate Database Online (http://cliflo.niwa.co.nz)).**

7.3.3 Chemical analysis

Anion concentrations (NO_3^-, Cl^-, and Br^-) were measured in filtered water samples on a Dionex DX-120 Ion Chromatograph with an AS-50 Autosampler (IonPac AG9-SC column). Dissolved organic carbon (DOC) content was analysed on a total organic carbon analyser (Shimadzu TOC-5000A) fitted with an ASI-5000A auto sampler. Ammonium (NH_4^+) concentrations were measured using the salicylate method (Kempers and Zweers 1986) on acidified samples as per Dobermann et al. (1994), and the absorbance read at 650 nm on a UV-*vis* spectrophotometer (UVmini-1240, Shimadzu).

All isotope results are reported in δ notation expressed in per mil (‰). For N-NO_3^- the isotope mass ratio of the sample is reported with respect to AIR; for O-NO_3^- and D- O- H_2O the isotope mass ratios are reported with respect to VSMOW. Nitrate (N and O) isotopes were measured using the Cd reduction- azide reaction method described by McIlvin and Altabet (2005). Each batch of samples

contained duplicates of three international standards (IAEA-N3, USGS-34, and USGS-32), two internal standards (1 KNO_3, 1 KNO_2), and water blanks. The $\delta^{18}O$ and $\delta^{15}N$ values of the produced N_2O were measured on a Europa PDZ (SerCon) 20-20 IR-MS at Lincoln University and the values of $\delta^{18}O$- and $\delta^{15}N$- NO_3^- calculated based on linear calibration of the international standards. Method precision was 0.8‰ for $\delta^{18}O$- NO_3^- and 0.6‰ for $\delta^{15}N$- NO_3^-.

Water isotopes ($^{2/1}H$ and $^{18/16}O$) were measured in 50 randomly selected samples at the University of Canterbury (NZ) Department of Geology. All results were reported in δ‰ with respect to VSMOW. Samples were analysed on a Picarro L1102-i liquid water isotope analyser with dry N_2 gas (3 psi) as the sample analysis atmosphere. Analytical precision was <0.15‰ ($\delta^{18}O$) and <0.5‰ (δD) for all samples (based on 5x replicate analysis of samples, with the first two discarded). All samples were normalised to the VSMOW scale based on replicate (20x) analysis of international standards (SMOW2 and SLAP certified reference materials). GISP was used as an internal standard demonstrating accuracy of better than 0.2‰ for $\delta^{18}O$ and better than 1.0‰ for δD.

7.3.4 Quantitative analysis

Differences between variables, grouped by sampling date, site, model fit, and/or season, were determined based on a one-way ANOVA test (with Tukey's post-hoc test for multiple groups) and interactions between these grouped variables with a two-way ANOVA (SPSS ver.20) (with repeated measures when over time, and date and location treated as fixed effects). In order to analyse precipitation patterns, samples were categorised as either being collected within 24 h of rainfall (1), 48 h of rainfall (2), or >48 h after the most recent rainfall (3). Due to the limited number of sampling dates, these categories could not be further subdivided into seasons. Pearson correlation was used to determine relationships between individual variables over distance and time. Linear regression was determined using a least-squared approach and forward variable selection (p<0.05), with goodness of fit measured as r^2 (SigmaPlot ver.12, SPSS ver.20). Significance for all tests was defined as p<0.05 and all values in the text are reported as mean ± standard deviation, unless otherwise noted.

7.3.4.1 Nitrate attenuation and fluxes

The total NO_3^- load of Harts Creek (N_{total}) was defined as the quantity of NO_3^--N inputs into the catchment (N_{input}) times the stream's flow rate (Q) (Eq. 7.2):

$$N_{total} = N_{input} \times Q \tag{7.2}$$

where N_{input} is defined as the measured NO_3^- flux at site D (N_D) with respect to the proportion of NO_3^- attenuated during transport ($atten_{net}$) (Eq. 7.3):

$$N_{input} = N_D + \left(atten_{net} \times N_D\right) \tag{7.3}$$

Attenuation was calculated based on Rayleigh fractionation NO_3^- isotopes (Eq. 7.4) (Ostrom et al. 2002):

$$Attenuation = 1 - f = 1 - e^{\left(\frac{\delta - \delta_0}{\varepsilon_{denit}}\right)}$$

$$atten_{net} = \int_0^x \frac{d[Attenuation]}{dx} \quad (7.4)$$

where the proportion of attenuation at a given site (*Attenuation*) was calculated using a modified version of Eq. 7.1 ($f = C/C_0$) based on the difference in the composition of $\delta^{18}O$ and $\delta^{15}N\text{-}NO_3^-$ measured at a given site at a given time (δ) versus their original (pre-denitrification) composition (δ_0), with respect to the enrichment factor for denitrification (ε_{denit}, $\varepsilon_{denit}=1000\times(\alpha_{denit}-1)$). The δ_0 for Harts Creek was defined as the NO_3^- isotopic composition at site D (as explained further in the discussion). Enrichment factors of -2‰ and -10‰ were used for all attenuation calculations, which were selected to span the reported range for denitrification measured in surface waters from -14.8‰ (Chen et al. 2009) to -1.5‰ (Sebilo et al. 2003)). Net attenuation for the catchment ($atten_{net}$) resulted from calculting *Attenuation* occurring at each location (x) downstream and integrating the area under the curve (Eq. 7.4). Using Eq. 7.4 to calculate attenuation assumes that, 1) there is constant mixing between 'denitrified' NO_3^- from anoxic microsites and 'non-denitrified' NO_3^- in oxic waters (as discussed by, e.g., Mariotti et al. (1988) and Green et al. (2010)), all of which originated from a single homogeneous and diffuse N source, meaning that, 2) all variation in $\delta^{18}O\text{-}NO_3^-$ and $\delta^{15}N\text{-}NO_3^-$ is assumed to be caused by denitrification. Assumption (2) was validated by testing the isotopic fingerprint of denitrification (i.e., for significant deviation in the ratio of $\delta^{18}O\text{-}NO_3^-$ to $\delta^{15}N\text{-}NO_3^-$ from the predicted 2:1 (Nestler et al. 2011) to 1:1 (Granger et al. 2008a) denitrification fractionation pattern). Since divergence from this relationship indicates mixing by heterogeneous sources or significant nitrification (Wankel et al. 2007), the standard deviation of attenuation calculated for the mean changes in both $\delta^{15}N\text{-}NO_3^-$ and $\delta^{18}O\text{-}NO_3^-$ reflects uncertainty in the given assumptions of a single source of fractionation and N in the system.

7.4 Results

7.4.1 Stream water chemistry

Isotope ratios of water ranged from -8.8‰ to -7.5‰ (mean of -8.66 ±0.2‰) for $\delta^{18}O\text{-}H_2O$ and from -78‰ to -51‰ (mean of -64.4 ±5‰) for $\delta D\text{-}H_2O$. Water isotopic composition was relatively consistent over time (i.e., minimal response to climate factors) in downstream reaches (C and D), whereas $\delta^{18}O$- δD- H_2O in reaches A and B became more negative in winter months (δD: $F = 3.0$, $p<0.05$; $\delta^{18}O$: $F = 4.0$, $p<0.05$) and varied from the mean (in either direction) in the 24 h following rainfall. Upstream reaches (A and B) had lower dissolved oxygen (DO), higher DOC, and higher NO_3^-

concentrations relative to the downstream reaches (C and D) across all seasons (Table 7.1). Channel depth increased over distance from 0.29 ±0.02 m in A to 0.95 ±0.1 m in D. In the summer, water temperature decreased (p<0.01) over distance from 12ºC in reaches A and B to 10ºC in reaches C and D, whereas water temperature remained a constant 10ºC across all reaches during winter months (May-Sep) (Table 7.1). Mean summer and winter air temperatures over the sampling period were 13 ±4ºC and 7.5 ±4ºC, respectively (data not shown). Winter months were characterised by higher (p<0.001) stream flow into Lake Ellesmere (1380 ±50 l s^{-1} in summer versus 1730 ±50 l s^{-1} in winter) and soil moisture (p<0.001) (Fig. 7.2). Concentrations of DOC were higher (p<0.001) in winter (3.22 ±0.2 mg C l^{-1}) than in summer (2.29 ±0.2 mg C l^{-1}) in all reaches (Table 7.1). Concentrations of NH_4^+ were typically <0.1 mg NH_4^+-N l^{-1} and did not vary significantly with season or stream distance (Table 7.1). The ratio of Cl^- to Br^- in surface water (481 ±10) likewise did not change significantly over distance or time (data not shown). However, the NO_3^--N:Cl^- ratio increased with stream distance throughout the two-year sampling period (Fig. 7.3).

Table 7.1 **Chemical composition (NH_4^+, NO_3^-, DO, DOC, and temperature) of surface water measured at 4 sites along Harts Creek (Canterbury, New Zealand), moving from source (A, 1.7 km) to mouth (D, 9.9 km). Means (±SE) for each site are presented for monthly samplings in winter (May-Sep) versus summer (Oct-Apr) collected Feb-2010- Jan-2012 (n = 4 per site per month). Superscript letters (a, b, c, d) denote significant differences (p<0.05) between sites within a given season.**

	Winter					*Summer*				
	DO* *mg O_2 l^{-1}*	**DOC^** *mg C l^{-1}*	**T_{H2O}¥** *℃*	**NO_3^-§** *mg NO_3^- N l^{-1}*	**NH_4^+** *mg NH_4^+N l^{-1}*	**DO** *mg O_2 l^{-1}*	**DOC** *mg C l^{-1}*	**T_{H2O}** *℃*	**NO_3^-** *mg NO_3^- N l^{-1}*	**NH_4^+** *mg NH_4^+N l^{-1}*
A	7.81(0.3)^a	8.42(0.7)^a	10.8(0.2)^a	6.26(0.3)^a	0.11(0.8)^a	7.42(0.2)^a	5.32(0.3)^a	14.2(0.3)^a	6.97(0.4)^a	0.045(0.01)^a
B	8.58(0.2)^b	5.00(0.3)^b	10.8(0.2)^a	6.09(0.2)^{a,b}	0.032(0.04)^a	8.56(0.01)^b	3.19(0.2)^b	13.4(0.2)^b	7.27(0.3)^a	0.052(0.02)^a
C	9.02(0.2)^b	2.24(0.2)^c	11.0(0.1)^a	5.56(0.2)^{a,b}	0.024(.01)^a	9.11(0.1)^c	1.29(0.2)^c	12.4(0.1)^c	5.86(0.3)^{a,b}	0.031(0.01)^a
D	9.07(0.2)^b	2.11(0.2)^c	11.0(0.1)^a	5.41(0.2)^b	0.019(0.01)^a	9.13(0.1)^c	1.23(0.2)^c	12.5(0.1)^c	5.71(0.3)^b	0.013(0.01)^a

*season×site: p<0.001, F =17.2
^season×site: p<0.001, F =53.2
¥season×site: p<0.001, F = 16.4
§season×site: p<0.001, F = 5.00

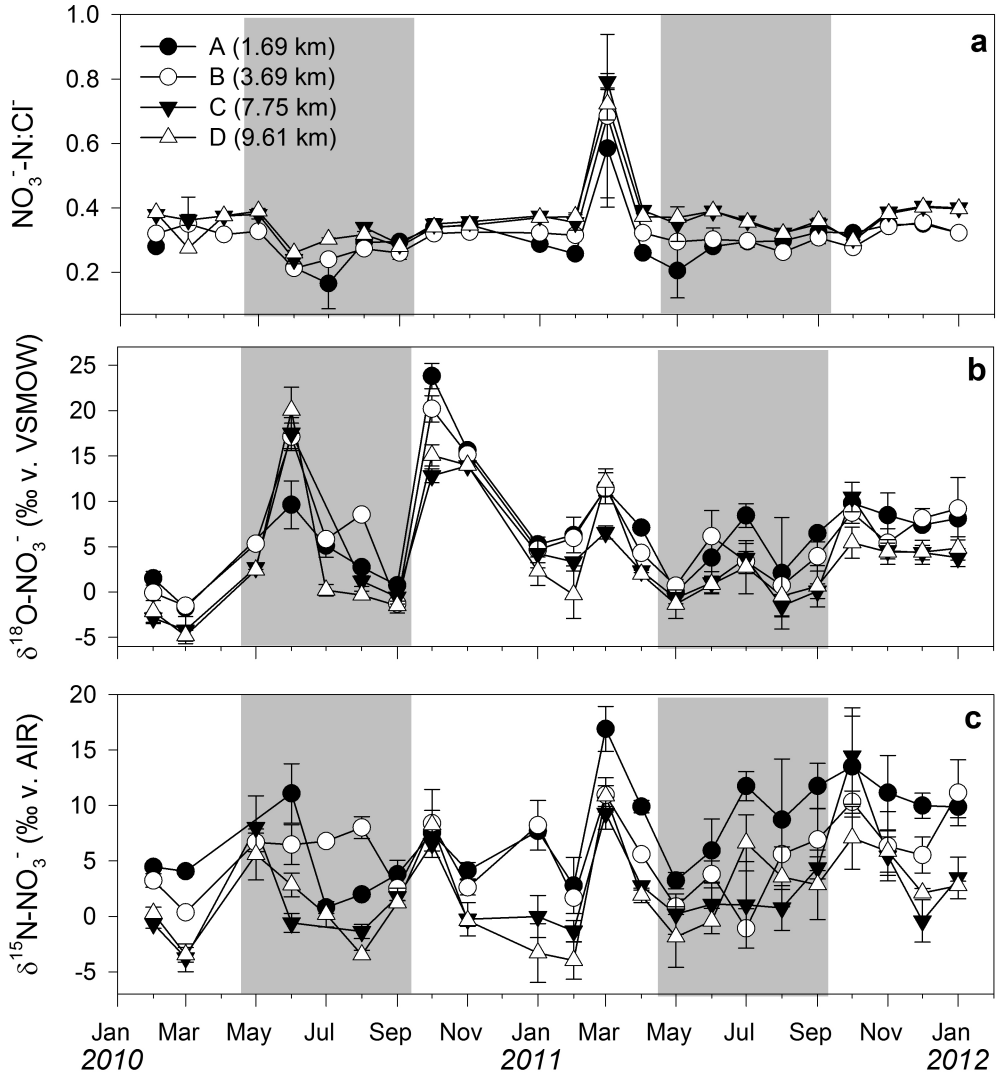

Figure 7.3 **Mean NO_3^- isotopic composition in Harts Creek over two winter-summer cycles (winter months shaded), as expressed through: a) NO_3^-:Cl^- ratio, b) $\delta^{18}O$-NO_3^-, and, c) $\delta^{15}N$-NO_3^-. Points represent the mean ±SE (n = 4) composition at four reaches (located at 1.7 km, 3.9 km, 7.7 km, and 9.9 km from the source spring) sampled monthly from Feb-2010 through Jan-2012. Over this period there were two significant effluent spills in the catchment: farm effluent in Oct-2010 (spill 1) and municipal sewage diversion following the 22-Feb-2011 Christchurch earthquake in Mar-2011 samples (spill 2).**

The concentration of NO_3^- in the surface water was lower than the maximum acceptable value of 11.3 mg NO_3^--N l^{-1} for New Zealand drinking water on all dates except for Mar-2011 (mean concentration of 12.0 ±0.3 mg NO_3^--N l^{-1} over all reaches). The Mar-2011 peak correlates with sustained dumping of municipal sewage into the catchment following the 22-Feb-2011 Christchurch earthquake. Although NO_3^- concentrations were lower (p<0.01) in winter than in summer months (5.81 ±1 mg NO_3^--N l^{-1} versus 6.45 ±0.2 mg NO_3^--N l^{-1} in summer), NO_3^- discharge into Lake Ellesmere was greater (p<0.05) during the wetter and colder winter months than during the summer months, increasing from 7.66 ±0.5 g NO_3^--N s^{-1} in the summer to 9.34 ±0.4 g NO_3^--N s^{-1} in the winter (Fig. 7.2, Table 7.1). This discharge of NO_3^- out of Harts Creek (NO_3^- flux at D) was positively correlated with soil moisture (p<0.01, r = 0.46). Controlling for seasonal variation, NO_3^- discharge increased (p<0.01) over time in the lowest reach (Fig. 7.3). In contrast, concentrations of DOC and Cl^-

remained stable and monthly rainfall showed no significant trends (mean annual precipitation of 256 mm) over the two year sampling period.

7.4.2 Nitrate isotopes

Values of $\delta^{18}O\text{-}NO_3^-$ and $\delta^{15}N\text{-}NO_3^-$ in streamwater became less enriched in heavy isotopes over stream distance (A,B v. C,D) ($p<0.01$) (Fig. 7.3, Fig. 7.4). In Mar-2011, both $\delta^{18}O\text{-}NO_3^-$ and $\delta^{15}N\text{-}NO_3^-$ in the lowest reach were highly enriched compared to all other sampling dates and were not significantly different from $\delta^{15}N$- $\delta^{18}O$- NO_3^- in the upper reaches. Both $\delta^{15}N\text{-}NO_3^-$ and $\delta^{18}O\text{-}NO_3^-$ correlated positively with NO_3^- concentrations over all sampling dates ($p<0.001$ and $r = 0.28$ and 0.24, respectively), but not with the ratio of NO_3^--N to Cl^-. While the concentration ratio of NO_3^--N to Cl^- in streamwater remained constant at 0.34 ±0.1 over the sampling period (excluding Mar-2011), NO_3^- isotopic composition ($\delta^{18}O$ and $\delta^{15}N$) varied between months (Fig. 7.3). The spike in the NO_3^--N:Cl^- ratio in Mar-2011 (~0.80) corresponded with isotopic enrichment of both $\delta^{18}O\text{-}NO_3^-$ and $\delta^{15}N\text{-}NO_3^-$ (Fig. 7.3). Conversely, streamwater in Oct-2010 and Nov-2010, collected following an illegal discharge of dairy effluent into the catchment in mid Oct-2010 (Environment Canterbury, pers. comms.), had anomalously enriched $\delta^{18}O\text{-}NO_3^-$ and produced anomalously low NO_3^--N:Cl^- ratios (Fig. 7.3).

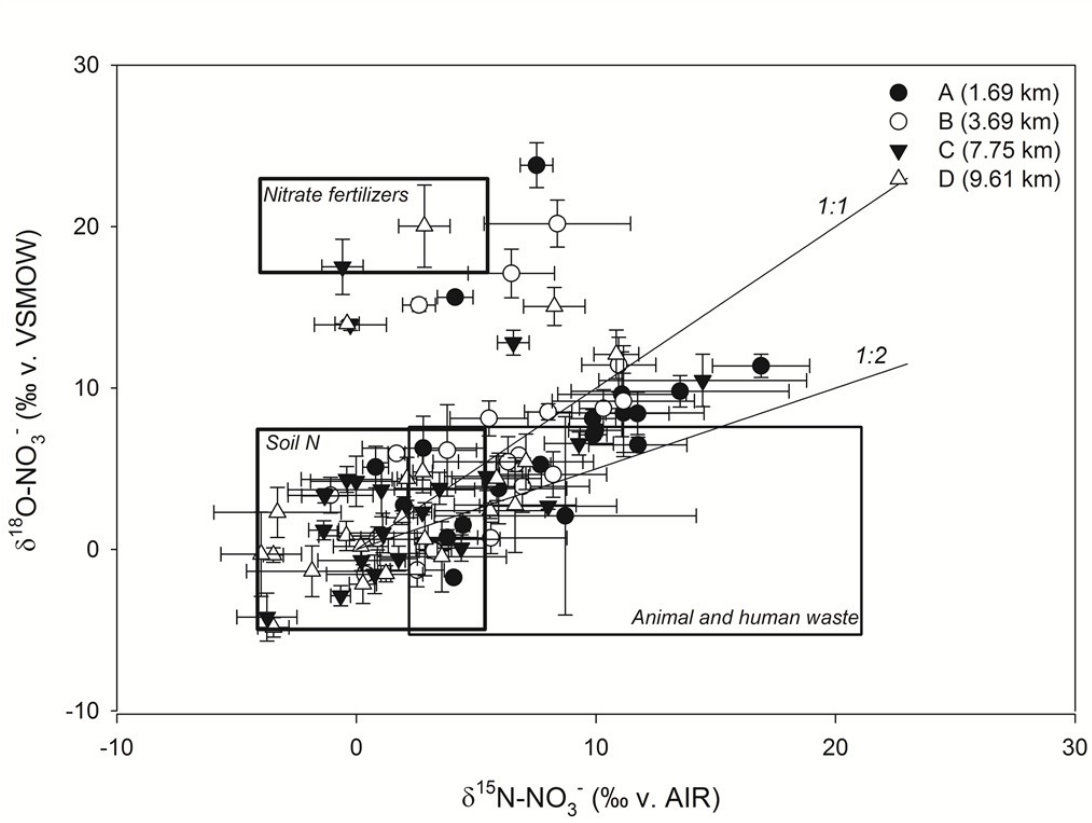

Figure 7.4 **The monthly mean composition of surface water $\delta^{18}O$ versus $\delta^{15}N$ of NO_3^- at each of the four sampled reaches in Harts Creek (Canterbury, New Zealand). Samples were collected from Feb-2010 through Jan-2012. Boxes represent ranges reported in literature for potential NO_3^- sources: NO_3^- fertilisers (from Haber-Bosch), soil N, and effluent (livestock manure and urine, human sewage) (Nestler et al. 2011). Denitrification would result in a movement along a 1:1 (Granger et al. 2008a) or 1:2 (Nestler et al. 2011) enrichment line (solid lines). Error bars represent ±SE for each reach x month ($n = 4$).**

Despite these fluctuations, the isotopic composition of NO_3^- ($\delta^{18}O\text{-}NO_3^-$ v. $\delta^{15}N\text{-}NO_3^-$) fell predominantly within the range reported for 'soil-N' derived NO_3^-, with deviation from this zone moving along a linear denitrification line (Fig. 7.4). Samples from Jun-2010 (following 230 mm rainfall over the previous 30 days (Fig. 7.2)), Oct-2010, Nov-2010, and Oct-2011 were the exception to this trend: the relatively enriched $\delta^{18}O\text{-}NO_3^-$ (~15‰ measured across the entire stream length on these dates) placed their composition closer to that of atmospherically derived fertiliser NO_3^- (Fig. 7.4). Variation in $\delta^{15}N\text{-}NO_3^-$ over stream distance linearly paralleled that of $\delta^{18}O\text{-}NO_3^-$ ($r^2 \geq 0.5$, $p<0.05$) in 16 out of the 22 months sampled. Slope of the $\delta^{18}O$:$\delta^{15}N$ relationship did not vary significantly, with a mean value of 0.67 ±0.1 for sampling dates with $r^2 \geq 0.50$. Months when variation in $\delta^{15}N$ explained <50% of the variation in $\delta^{18}O$ of streamwater NO_3^-, and thus Eq. 7.4 could not be applied ($n = 6$), had significantly higher concentrations of NO_3^- (but not Cl^-), lower concentrations DOC, lower stream flows, warmer water temperatures, lower cumulative rainfall over the previous 30 days, and higher net rainfall over the previous 48 h (Table 7.2). Mean $\delta^{18}O\text{-}NO_3^-$ was more enriched in months that did not fit the Rayleigh model (Eq. 7.4), whereas there were no significant differences in mean $\delta^{15}N\text{-}NO_3^-$ between the two groups (Table 7.2).

Table 7.2 **Conditions in Harts Creek (Canterbury, New Zealand) on days that fulfilled the requirements ($n = 16$) for application of a NO_3^- stable isotope based attenuation model (linear relationship between enrichment in $\delta^{15}N$- and $\delta^{18}O$- of NO_3^- over stream length) versus those that did not ($n = 7$). Values for rainfall are expressed as net precipitation over the 48 h prior to sampling, and % soil moisture is based on gravimetric water content (from the Leeston Harts Creek climate station, located <1 km from site A (CliFlo: NIWA's Climate Database Online (http://cliflo.niwa.co.nz)). Samples were collected monthly from Feb-2010 through Jan-2012. Values are given as mean of 4 sites (x4 reps at each site, $n = 16$ per monthly sampling) ±standard error of the mean (SE) and significance was tested using 1-way ANOVA.**

Model fit?	NO_3^- *mg NO_3^-N l^{-1}*	DO *mg O_2 l^{-1}*	DOC *mg C l^{-1}*	Flow *l s^{-1}*	$\delta^{15}N\text{-}NO_3^-$ *‰ v. AIR*	$\delta^{18}O\text{-}NO_3^-$ *‰ v. VSMOW*	T_{H2O} *°C*	Soil %moisture	$Rain_{48h}$ *mm*
Yes *(n=16)*	6.52(0.2)***	8.50(0.1)	2.32(0.2)	1480(50)	3.69(0.4)	4.08(0.4)	12.7(.1)***	20.7(0.6)	5.30(.4)***
No *(n=7)*	5.80(0.2)	8.83(0.1)*	3.35(0.2)***	1670(50)*	5.68(0.5)**	6.71(0.7)***	11.3(0.1)	27.9(0.6)***	0.98(0.2)

*Significantly greater, $p< 0.05$
**Significantly greater, $p<0.01$
***Significantly greater, $p<0.001$

Variation in $\delta^{18}O\text{-}NO_3^-$ within each reach was correlated primarily with climate: stream flow ($r = 0.29$, $p<0.01$), wind run ($r = 0.31$, $p<0.001$), air temperature ($r = 0.15$, $p<0.01$), and rainfall over the previous 30-days ($r = 0.31$, $p<0.001$) (Fig. 7.2, Fig. 7.3). In contrast, variations in $\delta^{15}N\text{-}NO_3^-$ within reaches were correlated with variations in stream water chemistry: concentration of NH_4^+ ($r = -0.13$, $p<0.05$), and DO ($r = 0.12$, $p<0.05$). The $\delta^{15}N$ enrichment of NO_3^- in Harts Creek increased over the sampling period (site×time: $F = 1.4$, $p<0.05$), coinciding with the increase in the flux of NO_3^- out of the stream. Variations in NO_3^- in the surface water (including concentration, $\delta^{15}N\text{-}NO_3^-$, $\delta^{18}O\text{-}NO_3^-$, NO_3^--N:Cl^-, and NO_3^- flux (g N s^{-1})) over stream distance were controlled by rainfall in the catchment over the 48 h prior to sample collection (rain×distance: $F = 6.1$, $p<0.05$ ($\delta^{18}O\text{-}NO_3^-$); $F = 2.1$, $p<0.05$ ($\delta^{15}N\text{-}NO_3^-$); $F = 2.8$, $p<0.01$ (mg NO_3^--N l^{-1})). Additionally, rainy versus clear days also differed with

regards to NH_4^+ concentration (F = 7.8, $p<0.01$), DO (F = 5.9, $p<0.05$), stream flow (F = 39, $p<0.001$) and the Cl^-:Br^- ratio (F = 5.1, $p<0.05$). However, there was no quantifiable relationship between NO_3^- isotopic composition and the *quantity* of rainfall (cumulative or daily). Seasonal variation (winter versus summer months) also appeared to influence NO_3^- composition, with higher $\delta^{15}N\text{-}NO_3^-$ (F = 6.5, $p<0.01$) and $\delta^{18}O\text{-}NO_3^-$ (F = 6.9, $p<0.001$) and lower NO_3^- fluxes ($p<0.05$) in the summer.

7.4.3 Nitrate attenuation

Monthly $atten_{net}$ rates were calculated for the 16 sampling dates that fitted the assumptions in Eq. 7.4 (i.e., had continuous, parallel enrichment of both NO_3^- isotopes over stream length) (Fig. 7.5). Based on these calculations, NO_3^- inputs into Harts Creek (Eq. 7.3) ranged from 6.3 ±1 g NO_3^--N s^{-1} in Mar-2010 to 47 ±3 g NO_3^--N s^{-1} in Oct-2011 (when ε_{denit} = -2‰), equating to 1.8 and 4.0 -fold, respectively, the measured NO_3^- discharge (Fig. 7.5). On a monthly basis, attenuation rates were negatively correlated with NO_3^- concentrations ($p<0.05$, r = -0.49 (ε_{denit} = -2‰) and r = -0.52 (ε_{denit} = -10‰)) and positively correlated with rainfall over the 24 h preceding sampling ($p<0.01$, r = 0.56 (ε_{denit} = -2‰) and r = 0.57 (ε_{denit} = -10‰)). Step-wise linear regression of N_{total} v. climate variables found soil moisture (r^2 = 0.28, $p<0.01$) to be the primary driving factor of variation, as compared to N_{input}, where the quantity of rainfall over the previous 24 h (r^2 = 0.58, $p<0.01$) was the controlling factor.

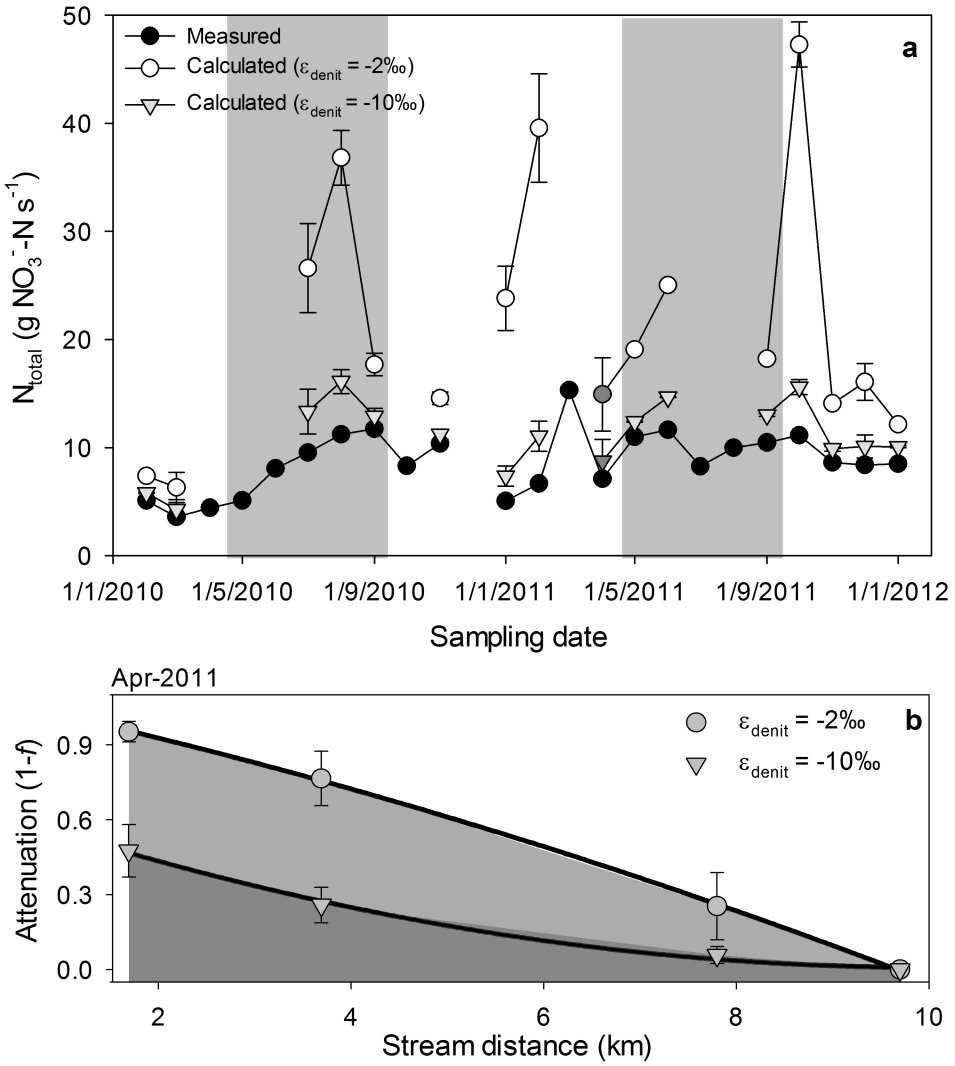

Figure 7.5 **The actual (measured) export of NO_3^- from Harts Creek into Lake Ellesmere compared to the calculated range of NO_3^- export rates that would occur if in-stream attenuation had not occurred (a). The range of monthly total N export rates (discharge + attenuation) for Harts Creek between Feb-2010 and Jan-2012 was calculated for sampling dates with wherein $\delta^{15}N$- $\delta^{18}O$- NO_3^- measured at 16 sites along the stream length exhibited the fingerprint for denitrification. Calculations were based on the measured NO_3^--N flux at site D and $atten_{net}$ (Eq. 7.4), which integrates site-by-site attenuation rates based on ε_{denit} values of -2‰ and -10‰ over stream distance, as depicted in (b) for Apr-2011. (Error bars represent ±SD for attenuation calculated for $\delta^{15}N$-NO_3^- and $\delta^{18}O$-NO_3^-).**

Grouping isotopic data by significant climate variables (precipitation grouping (as discussed in methods) and season (winter v. summer)) enabled calculation of $atten_{net}$ for each grouping, which was then extrapolated into an estimate of annual NO_3^- export for the Harts Creek catchment (Fig. 7.6). Over the sampling period ~60% of the days had rainfall within the previous 48 h, yet, according to these calculations, these days accounted for 93% of N_{total} (discharge plus attenuation). Based on

precipitation groupings, total N export (discharge plus attenuation) from the catchment was from 25 kg N ha^{-1} y^{-1} (ε_{denit} = -2‰) to 2.2 kg N ha^{-1} y^{-1} (ε_{denit} = -10‰). Seasonal groupings resulted in similar annual flux estimates (21 kg N ha^{-1} y^{-1} (ε_{denit} = -2‰) to 4.6 kg N ha^{-1} y^{-1} (ε_{denit} = -10‰), with 60% occurring during summer months (defined as 7 out of 12 months, or 58% of days per year).

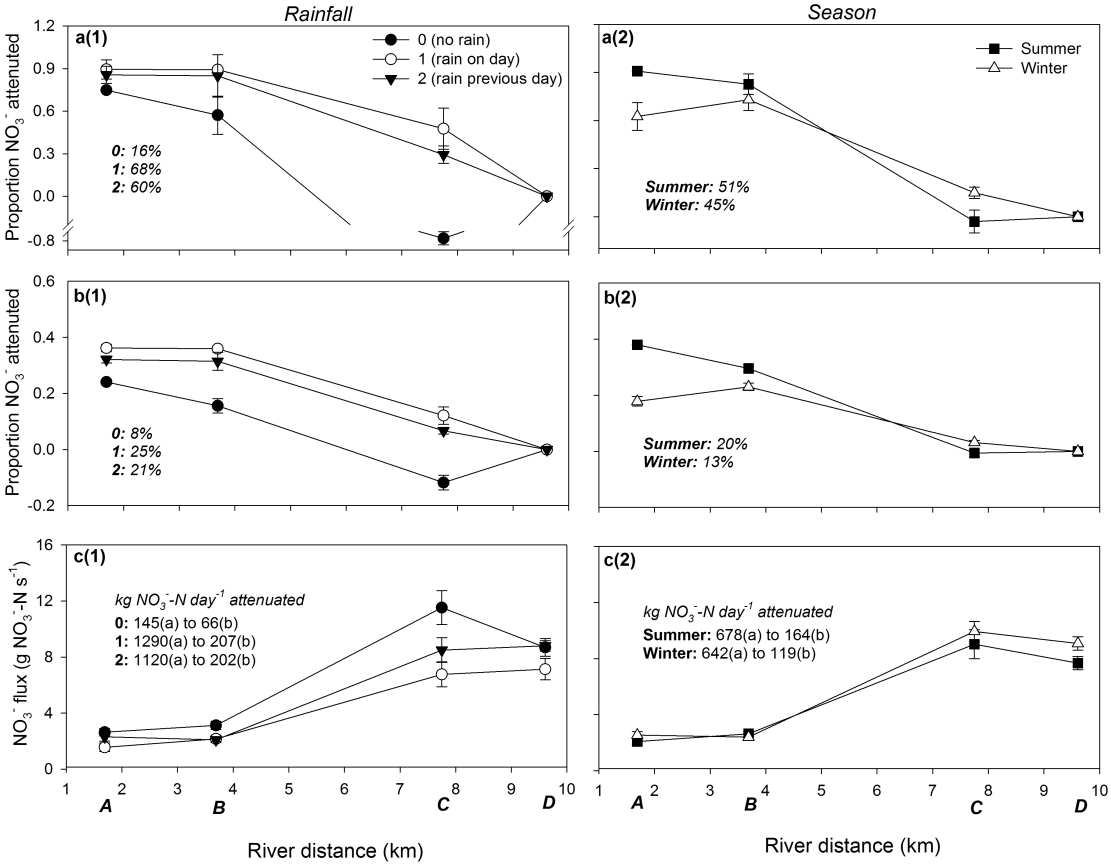

Figure 7.6 **Nitrate attenuation rates in Harts Creek, based on enrichment factors of either -2‰ (a) or -10‰ (b), and mean NO_3^- fluxes (c) over stream distance (from reaches A, B, C, D). Attenuation rates and NO_3^- fluxes were calculated using mean (±SE) $\delta^{18}O$- NO_3^-, [NO_3^-], and flow values for rainfall (1) and seasonal (2) categories. For rainfall, sampling dates were categorised as either, 0 (no rain within 48 h of sampling, *n* = 9), 1 (rainfall within 24 h of sampling, *n* = 6), or, 2) (rainfall within 48 h (±24 h) of sampling, *n* = 8). Seasons were defined as summer (Oct-May, *n* =13) or winter (Jun-Sep, *n* = 10). Percentage values in figures (a) and (b) indicate cumulative attenuation over the stream length; attenuation rates in terms of flux (kg NO_3^--N day^{-1}), shown in (c), were calculated from (a) and (b) cumulative rates.**

7.5 Discussion

7.5.1 Nitrogen inputs

The δD and $\delta^{18}O$ values for Harts Creek surface water indicate a consistent hydrologic source throughout the catchment, in keeping with recent findings that shallow groundwater in the region is dominated by a single source (Stewart 2012). Based on the strong variations measured in local precipitation, as compared to groundwater, H_2O isotopes by Blackstock (2011), the slight climate-

driven variations in δD- $\delta^{18}O$- H_2O observed in the upstream reaches corroborate evidence from the water temperature data indicating that increased discharge downstream was due to increasing groundwater infiltration (i.e., precipitation had a greater relative impact on the shallow upstream reaches). The surface water Cl^-:Br^- ratios, which fell within the expected range for water carrying NO_3^- derived from livestock, provide additional evidence that the NO_3^- in Harts Creek was derived from a relatively uniform agricultural source (Koh et al. 2010, Katz et al. 2011).

Upstream values of $\delta^{15}N$-NO_3^- and $\delta^{18}O$-NO_3^- tended to follow a linear enrichment line from the 'δ_0' isotopic composition in site D, confirming that variations in $\delta^{15}N$-NO_3^- and $\delta^{18}O$-NO_3^- over the stream length reflected differing degrees of denitrification of an isotopically homogeneous source. Although it seems counter-intuitive to use the most downstream site to calculate δ_0, uniform catchment hydrology and NO_3^- sources indicate that residual 'upstream' δ_x is diluted by incoming, less denitrified, NO_3^- during downstream transport such that $NO_3^-{}_0$>>>$NO_3^-{}_{A,B}$ by site D. The isotope ratios of NO_3^- in the lowest reach fell within the expected range for nitrified N from BNF ($\delta^{15}N$=0‰) and/or urea fertilisers ($\delta^{15}N$ of -0.4 (Minet et al. 2012) to +1.2‰ (Frank et al. 2004)). Previous measurements of NO_3^- leached from pasture soils with BNF present reported $\delta^{15}N$-NO_3^- between +0.3‰ to +5.1‰ (Oelmann et al. 2007, Rock et al. 2011), and from +0.4‰ to +6.6‰ from urea fertilised pastures (Minet et al. 2012). Since pasture soil zone studies have found that bovine urine, rather than fertilisers or BNF, is the dominant source of NO_3^- leached from pastoral systems (e.g., Decau et al. 2004; Monaghan et al. 2005), the NO_3^- isotope signature at site D cannot be taken as evidence for the dominance of a single input, but rather is assumed to reflect a mixed 'pasture-N' signal (as discussed by, e.g., Romera et al. 2012). Most importantly, the more negative isotope ratios of NO_3^- downstream indicate that N inputs are overwhelming the system's attenuation capacity (i.e., denitrification is limited by C or O_2, not NO_3^-, and nitrification and denitrification are decoupled).

However, anomalous $\delta^{18}O$-NO_3^- values measured across the stream's length in Oct-2010, Nov-2010, and Mar-2011 show that there were deviations from this constant 'pasture' NO_3^- source. In Oct-2010 and Nov-2010 $\delta^{18}O$-NO_3^- values fell within the range of atmospherically-derived fertiliser N (Nestler et al. 2011). While NO_3^- fertilisers are not commonly used in Canterbury (<10% (by mass) of applied fertiliser (A. Roberts, pers. comms.), the association between enriched $\delta^{18}O$-NO_3^- and storm events does make it more likely that these values do indeed reflect an influx of atmospherically-derived fertilisers. However, it should also be noted that all three of the dates that did not show a consistent 'pasture N' source were associated with known effluent spills: in Mar-2011 municipal effluent was being diverted directly into the Lake Ellesmere catchment following earthquake damage to city infrastructure (Chapter 6), and in Oct-2010 there was a spill of dairy effluent into the catchment (Environment Canterbury, pers. comms.). In Mar-2011, the equally enriched $\delta^{15}N$-NO_3^- and $\delta^{18}O$-NO_3^- across stream distance following sewage discharge (Fig. 7.3) points to denitrification of the sewage-N during transport (as also found by, e.g., Anisfeld et al. 2007, Chapter 6). Given that agricultural soils (with temperatures >4ºC) have typically been found to 'reset' the $\delta^{18}O$ signal from atmospheric fertilisers due to N cycling in the soil column (Mengis et al. 2001, Deutsch et al. 2005, Granger et al.

2008b), and that the low concentration of NO_3^- (compared to Cl^-) and high DOC in Oct-2010 and Nov-2010 support the dominance of a nitrified effluent-N source, it is not possible to isolate which anthropogenic disturbance (effluent or fertilisation) caused the loss of the typical spatial NO_3^- isotope patterns. While the direct mechanism cannot be conclusively proven, for the purposes of this study it is sufficient to identify that there is a rationale for why these months deviated from the expected isotopic patterns, and thus should be excluded from monthly attenuation calculations.

7.5.2 Spatial patterns to N losses

As NO_3^- was transported from low dissolved oxygen, high DOC, shallow conditions near the spring-fed source through a 10-km reach of pastoral land towards the mouth (high water volume and oxygen saturation, ~0 DOC), $\delta^{15}N$- and $\delta^{18}O$- NO_3^- became lighter. Previous longitudinal stream studies have likewise found denitrification activity to be concentrated in shallow headwaters, and to decrease as the depth-to-width ratio increased further downstream (Findlay et al. (2011) and references therein). The higher density and connectivity of farm drains and ditches within the upper reaches of the stream, as compared to the lower reaches (Fig. 7.1), further corroborates this spatial denitrification pattern as the shallow waters, high DOC loads, and fine bottom sediments commonly found in agricultural drainage ditches can create hot-spots of NO_3^- attenuation (Alexander et al. 2000, Herzon and Helenius 2008, Powell and Bouchard 2010). The spatial variation in attenuation rates indicates that the restored riparian zone/ bank replanting between reaches C and D is not significantly denitrifying the N inputs as they are received, and that further steps are need to optimise conditions for attenuation (e.g., C additions). Overall, the spatial trends in $\delta^{15}N$- and $\delta^{18}O$- NO_3^- effectively captured attenuation during transport to the stream water sampling locations through the soil, riparian, and/or hyporheic zones (dominant areas of denitrification (Seitzinger et al. 2006)), enabling the values to be used to estimate whole-catchment N losses.

The exceptions to the spatial trend of decreasing attenuation downstream came from the sampling dates when anthropogenic activities (Oct-2010, Nov-2010, Mar-2011) and/or storms (Jun-2010, Oct-2011) also resulted in relatively enriched $\delta^{18}O$-NO_3^-. Without a consistent trend in NO_3^- isotopic composition over distance, monthly attenuation rates could not be calculated. Theoretically there was either no significant NO_3^- attenuation on these dates, or else the mixing of different signals (effluent & baseline soil N) masked the denitrification fractionation pattern. Cooler temperatures and faster flows (both associated with these 'anomalous' sampling dates) have previously been found to minimise attenuation at the catchment scale (Schaefer and Alber 2007, Schaefer et al. 2009)). Yet given the lack of seasonal trends in N dynamics for the watershed and the fact that temperatures in the region rarely dipped below the 12ºC 'breakpoint' for denitrification activity (Schaefer and Alber 2007), it seems more likely that the spatial relationship observed on the other sampling dates was merely masked by source mixing (i.e., high inputs from fertilisers and/or effluent). Mixing could also have come from variable fluxes of minimally-denitrified NO_3^- entering the main stem from the two major tributaries between reaches B and C following rainfall (Fig. 7.6). Vitally, while mixing of

isotopically distinct NO_3^- sources is often seen to obscure the fractionation pattern of denitrification (making isotope-based quantification of attenuation unreliable), the data collected on 'anomalous' sampling dates from Harts Creek did contribute to attenuation calculations measured over greater time intervals, making it possible to assess temporal variations in NO_3^- attenuation beyond the month-to-month sampling framework.

7.5.3 Role of season and climate in regulating N losses

Under baseline conditions (no storms or effluent spills) variation from the 'soil N' isotopic zone moved along a linear denitrification enrichment line with a slope of ~0.6 (comparable to the expected ratio for fresh surface water systems (e.g., 0.5 reported by Burns et al. (2009) for streams in an agriculture region of the United States). Attenuation rates calculated for monthly data sets were highly variable (7 – 48% removal), in keeping with previous date-to-date rates calculated based on NO_3^- isotopes in river surface water, e.g., tributaries of the Mississippi River, USA (10 – 40% (Panno et al. 2006)) and the Beijing River, China (10 – 48% (Chen et al. 2009)). In contrast to these previous works, the duration and frequency of sampling in the current study enabled climatic controls on monthly variations in N attenuation in Harts Creek to be quantified.

Direct evidence for the impact of rainfall on N dynamics found in this catchment supports previous evidence for the influence of precipitation on streamwater nutrient dynamics (Buda and DeWalle 2009, Goswami et al. 2009, Burt et al. 2010). In Harts Creek, NO_3^- attenuation and inputs increased in response to rainfall that occurred within 24 to 48 h of sampling: the ratio of NO_3^- attenuated v. discharged downstream decreased rapidly in response to local rainfall. This relationship further highlights that the NO_3^- isotopes reflected denitrification during transport to the stream (as high flow rates generally inhibit denitrification by decreasing the residence time of NO_3^- in the water column (Alexander et al. 2009)). High attenuation and proportional N export following rainfall could have been caused by precipitation flushing partially denitrified NO_3^- from the hyporheic zone into the surface water (Cirmo and McDonnell 1997), or overland flow rapidly exporting NO_3^- (Monaghan et al. 2007). High DOC loads were measured during these rainfall-induced N transport periods, which could further promote denitrification by providing a terminal electron donor to NO_3^- reducers (Seitzinger et al. 2006). However, although the majority of rainfall in the study region fell during winter months, no seasonal effect of N response to precipitation could be detected as the sample size was not robust enough to have significant 'season × precipitation' groupings. My findings highlight the regulatory role of daily weather variations on proportional N export, emphasising the importance of high frequency sampling in order to accurately quantify N losses, and thus inputs.

Previous mass-balance approaches used to identify N loss pathways are limited in scale by the availability of N input data (typically only reported on the annual scale at the catchment or regional scale) (e.g., Boyer et al. 2002, Schaefer and Alber 2007, Parfitt et al. 2006). The annual N losses (discharge + attenuation) calculated for the Harts Creek catchment using NO_3^- stable isotopes align with the 22 kg N ha^{-1} y^{-1} calculated to be lost from the Canterbury region (Parfitt et al. 2006).

Furthermore, by monitoring both temporal and spatial variations in NO_3^- isotopes this study provides a more nuanced understanding of not just how much, but also how and when, NO_3^- is entering and exiting pastoral catchments. Quantifying this type of sensitivity of catchment N losses to rainfall is a fundamental piece of information for enabling accurate predictions of local responses to future climate change – driven changes in rainfall patterns.

7.6 Conclusions

The template for calculating NO_3^- attenuation developed here placed established isotope methods (e.g., Groffman et al. 2006; Nestler et al. 2011) into the framework of a catchment-scale effective NO_3^- export model (Boyer et al. 2002, Schaefer et al. 2009).The contrast between my finding of highly variable NO_3^- attenuation rates (over distance and time) and the relatively consistent NO_3^- concentrations measured in Harts Creek reveals the impossibility in identifying when and where anthropogenic activities are changing effective N export based solely on changes in streamwater concentration (the typical monitoring measurement). Indeed, despite the low precision of attenuation measurements generated using the dual isotope method (due primarily to uncertainty in ε_{denit}), the consistent spatial trends across the stream length should be used to inform future agricultural intensification in the catchment. Vitally, my data reveals that N inputs should be minimised in the downstream region of the catchment, where negligible attenuation rates mean that any increase in N_{inputs} will be directly reflected in greater NO_3^- discharge into Lake Ellesmere.

This multi-year longitudinal study of NO_3^- isotope dynamics within a small agricultural catchment highlights the key components required to compile a functional and quantitative understanding of the sources and sinks of N in a pastoral ecosystem. I further emphasise that seasonal controls on denitrification need to be incorporated into modelling of watershed NO_3^- exports, even when mean annual temperatures are relatively constant. These findings highlight the importance of sampling frequency in NO_3^- isotope studies, and it is likely that increasing to weekly, daily, or hourly time scales would further clarify NO_3^- stable isotope based attenuation calculations. The successful use of NO_3^- isotopes to tease apart the controls on attenuation v. discharge of NO_3^- at the catchment scale, demonstrated here over a sustained period of time despite occasional variations in NO_3^- sources, provides a viable tool to better understand the effects of anthropogenic changes (to land use and climate) on the fate of N in catchments.

7.7 Acknowledgements

Thanks to Tony Gray and Julie Edwards from Environment Canterbury for assistance with site selection and sharing of hydrologic data, Joy Jaio and Roger Cresswell at Lincoln University for analytical assistance, and Aimee Robinson for field assistance. Research was funded by FRST (Foundation for Research, Science and Technology, New Zealand) grant C05X0803 to W.T. Baisden / GNS Science.

My co-authors on this manuscript were Troy Baisden, who pushed my ideas to greater nuance, Tim Clough, who shared his wealth of knowledge about pasture ecosystems, as well as editorial zeal, and Travis Horton, who helped analyse the water isotopes.

7.8 References

Alexander, R. B., J. K. Bohlke, E. W. Boyer, M. B. David, J. W. Harvey, P. J. Mulholland, S. P. Seitzinger, C. R. Tobias, C. Tonitto, and W. M. Wollheim. 2009. Dynamic modeling of nitrogen losses in river networks unravels the coupled effects of hydrological and biogeochemical processes. Biogeochemistry **93:**91-116.

Alexander, R. B., A. H. Elliott, U. Shankar, and G. B. McBride. 2002. Estimating the sources and transport of nutrients in the Waikato River Basin, New Zealand. Water Resources Research **38.**

Alexander, R. B., R. A. Smith, and G. E. Schwarz. 2000. Effect of stream channel size on the delivery of nitrogen to the Gulf of Mexico. Nature **403:**758-761.

Anisfeld, S. C., R. T. Barnes, M. A. Altabet, and T. X. Wu. 2007. Isotopic apportionment of atmospheric and sewage nitrogen sources in two Connecticut rivers. Environmental Science & Technology **41**:6363-6369.

Barnes, R. T. and P. A. Raymond. 2010. Land-use controls on sources and processing of nitrate in small watersheds: insights from dual isotopic analysis. Ecological Applications **20:**1961-1978.

Barnes, R. T., R. L. Smith, and G. R. Aiken. 2012. Linkages between denitrification and dissolved organic matter quality, Boulder Creek watershed, Colorado. Journal of Geophysical Research-Biogeosciences **117**.

Bewsell, D., R. M. Monaghan, and G. Kaine. 2007. Adoption of stream fencing among dairy farmers in four New Zealand catchments. Environmental Management **40:**201-209.

Blackstock, J. M. 2011. Isotope study of moisture sources, recharge areas, and groundwater flow paths within the Christchurch Groundwater System. MSc Thesis: University of Canterbury, Christchurch.

Boyer, E. W., C. L. Goodale, N. A. Jaworsk, and R. W. Howarth. 2002. Anthropogenic nitrogen sources and relationships to riverine nitrogen export in the northeastern USA. Biogeochemistry **57:**137-169.

Buda, A. R. and D. R. DeWalle. 2009. Dynamics of stream nitrate sources and flow pathways during stormflows on urban, forest and agricultural watersheds in central Pennsylvania, USA. Hydrological Processes **23:**3292-3305.

Burns, D. A., E. W. Boyer, E. M. Elliott, and C. Kendall. 2009. Sources and Transformations of Nitrate from Streams Draining Varying Land Uses: Evidence from Dual Isotope Analysis. Journal of Environmental Quality **38:**1149-1159.

Burt, T. P., N. J. K. Howden, F. Worrall, and M. J. Whelan. 2010. Long-term monitoring of river water nitrate: how much data do we need? Journal of Environmental Monitoring **12:**71-79.

Chen, F. J., G. D. Jia, and J. Y. Chen. 2009. Nitrate sources and watershed denitrification inferred from nitrate dual isotopes in the Beijiang River, south China. Biogeochemistry **94:**163-174.

Cirmo, C. P. and J. J. McDonnell. 1997. Linking the hydrologic and biogeochemical controls of nitrogen transport in near-stream zones of temperate-forested catchments: a review. Journal of Hydrology **199:**88-120.

Cohen, M. J., J. B. Heffernan, A. Albertin, and J. B. Martin. 2012. Inference of riverine nitrogen processing from longitudinal and diel variation in dual nitrate isotopes. Journal of Geophysical Research-Biogeosciences **117.**

Collins, K. E. 2011. Benefits of riparian planting: A case study of lowland streams in the Lake Ellesmere catchment. MSc. Thesis: Lincoln University, Canterbury.

Decau, M. L., J. C. Simon, and A. Jacquet. 2004. Nitrate leaching under grassland as affected by mineral nitrogen fertilization and cattle urine. Journal of Environmental Quality **33:**637-644.

Department of Conservation Te Papa Atawhai (2005) Te Waihora Joint Management Plan Department of Conservation, Christchurch, NZ ISBN: 0-478-14059-2

Deutsch, B., I. Liskow, P. Kahle, and M. Voss. 2005. Variations in the delta N-15 and delta O-18 values of nitrate in drainage water of two fertilized fields in Mecklenburg-Vorpommern (Germany). Aquatic Sciences **67:**156-165.

Dobermann, A. and K. G. Cassman. 2005. Cereal area and nitrogen use efficiency are drivers of future nitrogen fertilizer consumption. Science in China Series C-Life Sciences **48:**745-758.

Dobermann, A., J. L. Gaunt, H. U. Neue, I. F. Grant, M. A. Adviento, and M. F. Pampolino. 1994. Spatial and temporal variability of ammonium in flooded rice fields. Soil Science Society of America Journal **58:**1708-1717.

Findlay, S. E. G., P. J. Mulholland, S. K. Hamilton, J. L. Tank, M. J. Bernot, A. J. Burgin, C. L. Crenshaw, W. K. Dodds, N. B. Grimm, W. H. McDowell, J. D. Potter, and D. J. Sobota. 2011. Cross-stream comparison of substrate-specific denitrification potential. Biogeochemistry **104:**381-392.

Ford R. K. and Taylor K. 2006. Managing Nitrate Leaching to Groundwater: An Emerging Issue for Canterbury. In Proceedings of the Fertiliser and Lime Research Centre Workshop 8-9 February 2006, “Implementing Sustainable Nutrient Management Strategies in Agriculture”,

Currie L.D. and J.A. Hanly (eds.), Occasional Report No. 19: 48-67. Fertiliser and Lime Research Centre, Massey University, Palmerston North.

Frank, D. A., R. D. Evans, and B. F. Tracy. 2004. The role of ammonia volatilization in controlling the natural N-15 abundance of a grazed grassland. Biogeochemistry **68:**169-178.

Galloway, J. N., J. D. Aber, J. W. Erisman, S. P. Seitzinger, R. W. Howarth, E. B. Cowling, and B. J. Cosby. 2003. The nitrogen cascade. Bioscience **53:**341-356.

Goswami, D., P. K. Kalita, R. A. C. Cooke, and G. F. McLsaac. 2009. Nitrate-N loadings through subsurface environment to agricultural drainage ditches in two flat Midwestern (USA) watersheds. Agricultural Water Management **96:**1021-1030.

Gough, J. D. and J. C. Ward. 1996. Environmental decision-making and lake management. Journal of Environmental Management **48:**1-15.

Granger, J., D. M. Sigman, M. F. Lehmann, and P. D. Tortell. 2008a. Nitrogen and oxygen isotope fractionation during dissimilatory nitrate reduction by denitrifying bacteria. Limnology and Oceanography **53:**2533-2545.

Granger, S. J., T. H. E. Heaton, R. Bol, G. S. Bilotta, P. Butler, P. M. Haygarth, and P. N. Owens. 2008b. Using delta N-15 and delta O-18 to evaluate the sources and pathways of NO3- in rainfall event discharge from drained agricultural grassland lysimeters at high temporal resolutions. Rapid Communications in Mass Spectrometry **22:**1681-1689.

Green, C. T., J. K. Bohlke, B. A. Bekins, and S. P. Phillips. 2010. Mixing effects on apparent reaction rates and isotope fractionation during denitrification in a heterogeneous aquifer. Water Resources Research **46:**19.

Groffman, P. M., M. A. Altabet, J. K. Bohlke, K. Butterbach-Bahl, M. B. David, M. K. Firestone, A. E. Giblin, T. M. Kana, L. P. Nielsen, and M. A. Voytek. 2006. Methods for measuring denitrification: Diverse approaches to a difficult problem. Ecological Applications **16:**2091-2122.

Groffman, P. M., K. Butterbach-Bahl, R. W. Fulweiler, A. J. Gold, J. L. Morse, E. K. Stander, C. Tague, C. Tonitto, and P. Vidon. 2009. Challenges to incorporating spatially and temporally explicit phenomena (hotspots and hot moments) in denitrification models. Biogeochemistry **93:**49-77.

Hamill, K. D. and G. B. McBride. 2003. River water quality trends and increased dairying in Southland, New Zealand. New Zealand Journal of Marine and Freshwater Research **37:**323-332.

Hefting, M., J. C. Clement, D. Dowrick, A. C. Cosandey, S. Bernal, C. Cimpian, A. Tatur, T. P. Burt, and G. Pinay. 2004. Water table elevation controls on soil nitrogen cycling in riparian wetlands along a European climatic gradient. Biogeochemistry **67:**113-134.

Herzon, I. and J. Helenius. 2008. Agricultural drainage ditches, their biological importance and functioning. Biological Conservation **141:**1171-1183.

Katz, B. G., S. M. Eberts, and L. J. Kauffman. 2011. Using Cl/Br ratios and other indicators to assess potential impacts on groundwater quality from septic systems: A review and examples from principal aquifers in the United States. Journal of Hydrology **397:**151-166.

Kempers, A. J. and A. Zweers. 1986. Ammonium determination in soil extracts by the salicylate method. Communications in Soil Science and Plant Analysis **17:**715-723.

Koh, D. C., B. Mayer, K. S. Lee, and K. S. Ko. 2010. Land-use controls on sources and fate of nitrate in shallow groundwater of an agricultural area revealed by multiple environmental tracers. Journal of Contaminant Hydrology **118:**62-78.

Kroeze, C., L. Bouwman, and S. Seitzinger. 2012. Modeling global nutrient export from watersheds. Current Opinion in Environmental Sustainability **4:**195-202.

Larned, S. T., M. R. Scarsbrook, T. H. Snelder, N. J. Norton, and B. J. F. Biggs. 2004. Water quality in low-elevation streams and rivers of New Zealand: recent state and trends in contrasting land-cover classes. New Zealand Journal of Marine and Freshwater Research **38:**347-366.

Mariotti, A., A. Landreau, and B. Simon. 1988. N-15 isotope biogeochemistry and natural denitrification process in groundwater - application to the chalk aquifer of northern france. Geochimica Et Cosmochimica Acta **52:**1869-1878.

Matthaei, C. D., J. J. Piggott, and C. R. Townsend. 2010. Multiple stressors in agricultural streams: interactions among sediment addition, nutrient enrichment and water abstraction. Journal of Applied Ecology **47:**639-649.

McDowell, R. W., T. Snelder, R. Littlejohn, M. Hickey, N. Cox, and D. J. Booker. 2011a. State and potential management to improve water quality in an agricultural catchment relative to a natural baseline. Agriculture Ecosystems & Environment **144:**188-200.

McDowell, R. W., T. J. van der Weerden, and J. Campbell. 2011b. Nutrient losses associated with irrigation, intensification and management of land use: A study of large scale irrigation in North Otago, New Zealand. Agricultural Water Management **98:**877-885.

McIlvin, M. R. and M. A. Altabet. 2005. Chemical conversion of nitrate and nitrite to nitrous oxide for nitrogen and oxygen isotopic analysis in freshwater and seawater. Analytical Chemistry **77**:5589-5595.

Mengis, M., U. Walther, S. M. Bernasconi, and B. Wehrli. 2001. Limitations of using delta O-18 for the source identification of nitrate in agricultural soils. Environmental Science & Technology **35:**1840-1844.

Minet, E., C. E. Coxon, R. Goodhue, K. G. Richards, R. M. Kalin, and W. Meier-Augenstein. 2012. Evaluating the utility of N-15 and O-18 isotope abundance analyses to identify nitrate sources: A soil zone study. Water Research **46:**3723-3736.

Monaghan, R. M., R. J. Paton, L. C. Smith, J. J. Drewry, and R. P. Littlejohn. 2005. The impacts of nitrogen fertilisation and increased stocking rate on pasture yield, soil physical condition and nutrient losses in drainage from a cattle-grazed pasture. New Zealand Journal of Agricultural Research **48:**227-240.

Monaghan, R. M., R. J. Wilcock, L. C. Smith, B. Tikkisetty, B. S. Thorrold, and D. Costall. 2007. Linkages between land management activities and water quality in an intensively farmed catchment in southern New Zealand. Agriculture Ecosystems & Environment **118:**211-222.

Mulholland, P. J., A. M. Helton, G. C. Poole, R. O. Hall, S. K. Hamilton, B. J. Peterson, J. L. Tank, L. R. Ashkenas, L. W. Cooper, C. N. Dahm, W. K. Dodds, S. E. G. Findlay, S. V. Gregory, N. B. Grimm, S. L. Johnson, W. H. McDowell, J. L. Meyer, H. M. Valett, J. R. Webster, C. P. Arango, J. J. Beaulieu, M. J. Bernot, A. J. Burgin, C. L. Crenshaw, L. T. Johnson, B. R. Niederlehner, J. M. O'Brien, J. D. Potter, R. W. Sheibley, D. J. Sobota, and S. M. Thomas. 2008. Stream denitrification across biomes and its response to anthropogenic nitrate loading. Nature **452:**202-U246.

Nestler, A., M. Berglund, F. Accoe, S. Duta, D. M. Xue, P. Boeckx, and P. Taylor. 2011. Isotopes for improved management of nitrate pollution in aqueous resources: review of surface water field studies. Environmental Science and Pollution Research **18:**519-533.

Oelmann, Y., Y. Kreutziger, R. Bol, and W. Wilcke. 2007. Nitrate leaching in soil: Tracing the NO3- sources with the help of stable N and O isotopes. Soil Biology & Biochemistry 39:3024-3033.

Ostrom, N. E., L. O. Hedin, J. C. von Fischer, and G. P. Robertson. 2002. Nitrogen transformations and NO3- removal at a soil-stream interface: A stable isotope approach. Ecological Applications **12:**1027-1043.

Panno, S. V., K. C. Hackley, W. R. Kelly, and H. H. Hwang. 2006. Isotopic evidence of nitrate sources and denitrification in the Mississippi River, Illinois. Journal of Environmental Quality **35:**495-504.

Parfitt, R. L., W. T. Baisden, L. A. Schipper, and A. D. Mackay. 2008. Nitrogen inputs and outputs for New Zealand at national and regional scales: past, present and future scenarios. Journal of the Royal Society of New Zealand **38:**71-87.

Parfitt, R. L., L. A. Schipper, W. T. Baisden, and A. H. Elliott. 2006. Nitrogen inputs and outputs for New Zealand in 2001 at national and regional scales. Biogeochemistry **80:**71-88.

Parfitt, R. L., B. A. Stevenson, J. R. Dymond, L. A. Schipper, W. T. Baisden, and D. J. Ballantine. 2012. Nitrogen inputs and outputs for New Zealand from 1990 to 2010 at national and regional scales. New Zealand Journal of Agricultural Research **55:**241-262.

Powell, K. L. and V. Bouchard. 2010. Is denitrification enhanced by the development of natural fluvial morphology in agricultural headwater ditches? Journal of the North American Benthological Society **29:**761-772.

Rock, L., B. H. Ellert, and B. Mayer. 2011. Tracing sources of soil nitrate using the dual isotopic composition of nitrate in 2 M KCl-extracts. Soil Biology & Biochemistry **43:**2397-2405.

Romera, A. J., G. Levy, P. C. Beukes, D. A. Clark, and C. B. Glassey. 2012. A urine patch framework to simulate nitrogen leaching on New Zealand dairy farms. Nutrient Cycling in Agroecosystems **92:**329-346.

Schaefer, S. C. and M. Alber. 2007. Temporal and spatial trends in nitrogen and phosphorus inputs to the watershed of the Altamaha River, Georgia, USA. Biogeochemistry 86:231-249.

Schaefer, S. C., J. T. Hollibaugh, and M. Alber. 2009. Watershed nitrogen input and riverine export on the west coast of the US. Biogeochemistry **93:**219-233.

Sebilo, M., G. Billen, M. Grably, and A. Mariotti. 2003. Isotopic composition of nitrate-nitrogen as a marker of riparian and benthic denitrification at the scale of the whole Seine River system. Biogeochemistry **63:**35-51.

Seitzinger, S., J. A. Harrison, J. K. Bohlke, A. F. Bouwman, R. Lowrance, B. Peterson, C. Tobias, and G. Van Drecht. 2006. Denitrification across landscapes and waterscapes: A synthesis. Ecological Applications **16:**2064-2090.

Stevenson, B. A., R. L. Parfitt, L. A. Schipper, W. T. Baisden, and P. Mudge. 2010. Relationship between soil delta N-15, C/N and N losses across land uses in New Zealand. Agriculture Ecosystems & Environment **139**:736-741.

Stewart, M. K. 2012. A 40-year record of carbon-14 and tritium in the Christchurch groundwater system, New Zealand: Dating of young samples with carbon-14. Journal of Hydrology **430:**50-68.

Sudduth, E. B., S. S. Perakis, and E. S. Bernhardt. 2013. Nitrate in watersheds: Straight from soils to streams? Journal of Geophysical Research: Biogeosciences:n/a-n/a.

Taylor, P. G. and A. R. Townsend. 2010. Stoichiometric control of organic carbon-nitrate relationships from soils to the sea. Nature **464:**1178-1181.

Wallenstein, M. D., D. D. Myrold, M. Firestone, and M. Voytek. 2006. Environmental controls on denitrifying communities and denitrification rates: Insights from molecular methods. Ecological Applications **16**:2143-2152.

Wankel, S. D., C. Kendall, J. T. Pennington, F. P. Chavez, and A. Paytan. 2007. Nitrification in the euphotic zone as evidenced by nitrate dual isotopic composition: Observations from Monterey Bay, California. Global Biogeochemical Cycles **21:**13.

Chapter 8

Synthesis and conclusions

8.1 Key findings

The work described in this thesis contributes to the understanding of NO_3^- isotope dynamics in soils and surface water, by, 1) untangling the biological and hydrological controls on ε_{denit}, and, 2) showing that, by using prior site information to separate $\delta^{15}N$- $\delta^{18}O$- NO_3^- data, Rayleigh-based fractionation models can be effectively used to constrain N attenuation across landscapes. The key trends that emerged over the course of this research for defining the fundamental isotope effects relevant to denitrification during land-to-water N transfers and then effectively applying these values to develop field → catchment scale NO_3^- isotope based attenuation measurements are discussed below.

8.1.1 Defining ε_{denit} (Objective #1)

A) Variability in fractionation is unavoidable in unconstrained systems. The mathematical modelling, incubation experiments, and preliminary stream sampling in Chapter 3 combine to confirm that assigning a precise value of ε_{denit} to dynamics and heterogeneous environments such as streams could result in a misrepresentation of N cycling due to the mixing of NO_3^- pools affected by different ε_{denit} and oscillations in hydrologic controls on the expression of ε_{denit}. Incubations of sediments and submerged soils revealed that biologically-driven variation in ε_{denit} occurs at the metre-kilometre, not the biome or catchment, scale. So what does control ε_{denit}? The literature synthesis in Chapter 2 highlighted inconsistencies in previously reported links between ε_{denit}, k_{denit}, and C, while incubations in Chapter 3 found a strong relationship between C and ε_{denit}, but not k_{denit}, potentially reflecting a structural, rather than functional, difference in denitrifier communities over space. Simultaneously, the diffusion of NO_3^- through the denitrification zone to the aerobic surface water, where measurements are generally taken, causes a convergence of ε_{denit} around relatively low values. Field sampling along stream reaches over time emphasised that nutrient spiralling effects (i.e., nitrification and denitrification occurring simultaneously), coupled with typical diffuse NO_3^- inputs, mean that basing Rayleigh-type attenuation measurements on empirically calculated ε_{denit} could cause a dramatic underestimating of attenuation. In identifying an 'effective' ε_{denit} range of -2 to -10‰ for measurements in aerobic systems, these findings pave the way for expanding the use of NO_3^- isotopes as quantifiers of denitrification, and eliminate the perceived need to limit such quantifications to environments where decreasing NO_3^- concentrations are coupled with isotopic enrichment.

However, environments where denitrification occurs in discrete periods over time (scenario B from Chapter 2) may be the exception to this rule. The contained hydrology of submerged rice paddies (i.e., closer to the idealised 'closed systems' of a true Rayleigh fractionation relationship) is hypothesised to explain the equivalent ε_{denit} values measured both empirically in the field and in soil mesocosms idealised for denitrification with added C, NO_3^-, and no O_2. Site-specific ε_{denit} values can, and should, be calculated for more 'closed' denitrifying environments. But how universal are these trends?

B) The ratio of $^{18}\varepsilon_{denit}$ to $^{15}\varepsilon_{denit}$ varies from 0.5 to 1.0, shifting towards 1.0 as the strength of the reducing zone increases. Based on the literature synthesis in Chapter 2, it was hypothesised that the trend of decreasing enrichment ratios in aerobic environments was caused by mixing of nitrification and denitrification. While this still seems a viable explanation, my experimental results also suggest that variations in this relationship may result from a suite of biological drivers. Even in sediments and soils incubated under identical O_2-depleted, C-enriched conditions, the $\delta^{18}O$:$\delta^{15}N$ enrichment ratio varied from ~0.5 to ~1.0, with samples collected from more aerobic and C-rich environments tending towards the former. This rejects the hypothesis that pure denitrification created ubiquitous 1:1 enrichment of the two isotope species (e.g., Kritee et al. 2012). Furthermore, the trends between C, O_2, and $\delta^{18}O$:$\delta^{15}N$ are particularly interesting as the former two variables were also found to control biological ε_{denit}.

Scaling these results up to the field, the 0.25 relationship between $\delta^{18}O$-NO_3^- and $\delta^{15}N$-NO_3^- measured during denitrification in a pasture soil, hypothesised to be a bi-product of co-occurring nitrification, occurred in the most consistently O_2- rich environment measured. In this light, the 0.25 enrichment ratio in aerobic soils contributes to the overall trend, whether through external environmental effects or a fundamental difference in biological fractionation, of $\delta^{18}O$ and $\delta^{15}N$ fractionation becoming more similar the stronger the denitrifying zone (and vice-versa): highly reducing paddy soils had a consistent ~1:1 enrichment ratio, both in the field and in the lab, an abrupt shift between 1:1 and 1:2 was observed in the Heathcote River following the cessation of direct sewage dumping into the waterway (and thus increase in O_2), while $\delta^{18}O$ v. $\delta^{15}N$ variations in surface water NO_3^- in Harts Creek followed a ~0.6 line, in contrast to the enrichment ratios of between 0.5 and 1.0 calculated for anaerobic sediments collected from four sites along the stream.

Do these trends reflect a functional effect on NO_3^- processing, or result from a more distal forcing on communities? Additionally, the trends between C, O_2, and $\delta^{18}O$:$\delta^{15}N$ are particularly interesting as the former two variables were also found to control biological ε_{denit}. Targeted research is needed into the impact of C on denitrifier communities, and of denitrifier communities on $\delta^{18}O$:$\delta^{15}N$ ratios.

8.1.2 Rayleigh fractionation of NO_3^- isotopes can be used to constrain denitrification across diverse environments (Objective #2)

C) The isotopic fingerprint of denitrification is evident in all NO_3^- pools once a high enough density of measurements is obtained. Application of a stable-isotope based attenuation assessment is primarily limited by sampling density. On 4 out of 24 sampling dates source mixing, rather than denitrification, dominated the NO_3^- isotopic signature in the surface water along the length of an agricultural, spring-fed, stream (Chapter 7). However, by collating these seemingly 'anomalous' points with the entire two years worth of data collected from four locations within four reaches, they contributed both to the overall denitrification line of 0.6 $\delta^{18}O$ v. $\delta^{15}N$ and the calculations of climate-driven clustering of attenuation rates. Similarly, even with ~40% of the N pool removed via NH_3 volatilisation and the high

nitrification rates that followed urine application to an aerobic soil (Chapter 4), the composition of whole-field $\delta^{15}N\text{-}NO_3^-$ and $\delta^{18}O\text{-}NO_3^-$ within these systems reflected the imprint of denitrification. Up-scaling these observations, I found that there was a clear, denitrification-driven, relationship between $\delta^{18}O$ and $\delta^{15}N$ (Pearson's correlation: $r = 0.58$, $p<0.001$) over all of the individual NO_3^- isotope measurements collected from all field sites ($n = 566$): surface water and porewater of two ditches, aerobic soils following urine deposition, submerged paddy soils from fallow through crop transplanting, surface water of an agricultural stream, and surface water of an urban stream following an acute sewage influx event (Fig. 8.1a). It should be acknowledged that the consistency of the 'denitrification' fingerprint across large spatial and temporal scales could be enabled by the fact that both main sampling locations (Canterbury, New Zealand and Luzon, Philippines) have very low rates of atmospheric N deposition and minimal use of NO_3^- fertilisers. As the 'atmospheric' level $\delta^{18}O\text{-}NO_3^-$ values in Harts Creek were associated with difficulty in measuring denitrification rates for the specific sampling date, the relatively heavy $\delta^{18}O$ from atmospheric sources noted in other locations (e.g., Anisfeld et al. 2007) may make it more difficult to tease out the denitrification signal, and should be critically evaluated. However, based on the Harts Creek data set in particular, I hypothesise that, with sufficient density of data, attenuation trends could be teased out of even the most impacted catchments.

Previous work by Houlton and Bai (Houlton and Bai 2009, Bai et al. 2012) indicated that, at a global scale, soil $\delta^{15}N$ is controlled exclusively by denitrification, but the current study is the first clear indication that this rule holds true for compound-specific N isotopes. With increasing density of data over time and/or space, NO_3^- isotopes tended to plot along the linear space between $\delta^{18}O$ and $\delta^{15}N$, and by clumping data points (by, e.g., site, location, site×location) the significance and slope of this line invariably increased (Fig. 8.1b). But what does a global denitrification fingerprint on NO_3^- isotopes mean for assessing attenuation at the catchment and field scales of most relevance for improving environmental management? With this foundation, the challenge then becomes translating these denitrification 'fingerprints' into quantitative measurements of N losses. The strength of the denitrification signature increases confidence in interpreting NO_3^- isotopic results in terms of % attenuation, creating a scenario where, “The *irregularity* of environmental data does not detract from its utility but often provides the only really useful information.” (Ginevan and Splitstone 2004).

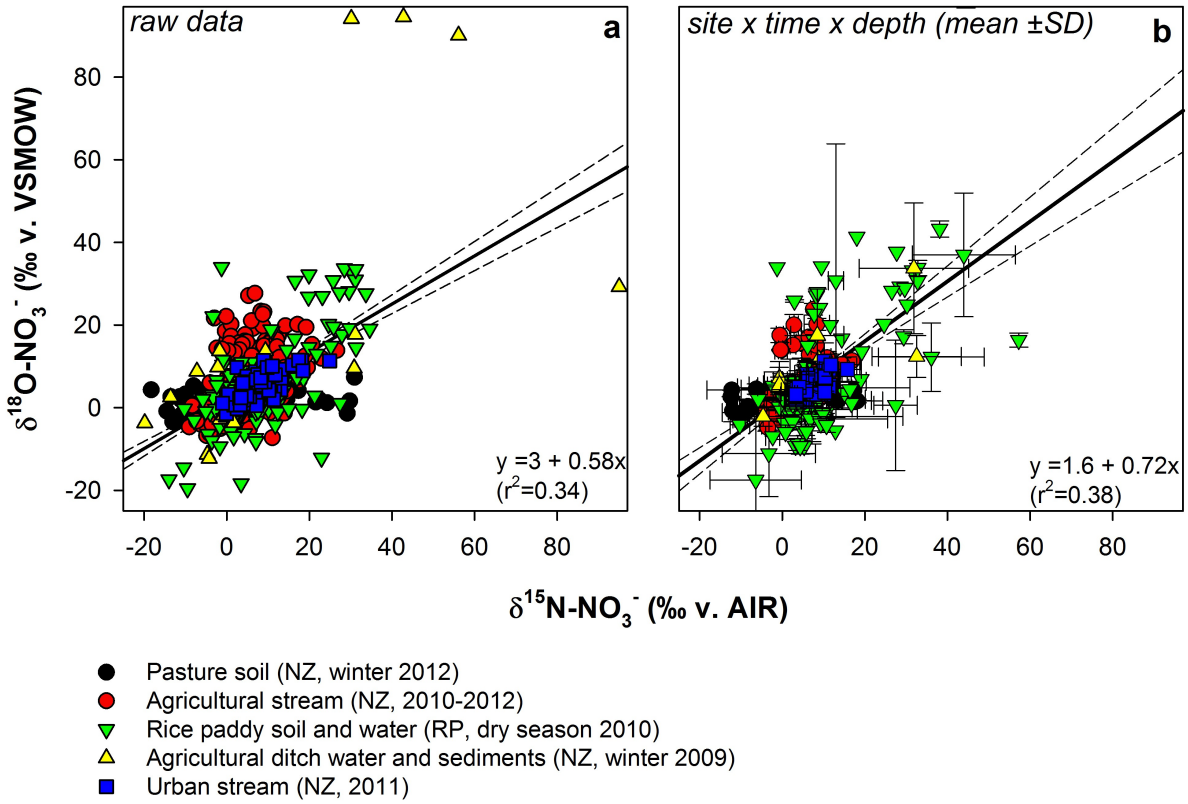

Figure 8.1 **Plotting $\delta^{15}N\text{-}NO_3^-$ v. $\delta^{18}O\text{-}NO_3^-$ for all empirical measurements made from: an aerobic pasture soil over 17 days following urine deposition, the surface water and porewater of two agriculture drainage ditches (ditches), surface water measured in 10 reaches along the length of an urban stream over a six month period following a catastrophic earthquake and effluent dumping, surface water measured monthly in four reaches along a spring-fed stream draining an intensive pastoral agricultural catchment, and from tropical rice paddy soil, floodwater, and poor water subjected to variable water and organic amendment management, which were sampled on 10 occasions over a 70 day period. The slope of the linear line through all data is ~0.5, with dotted lines indicating 95% CI (r^2 =0.34, p<0.001); sampling dates and locations (RP: Philippines; NZ: New Zealand) are indicated in parenthesis. Condensing the data into mean ±SD for each site (defined as treatments in the two soil studies and reaches in the stream studies) moved the slope of the best fit linear regression closer to 0.72 (r^2 = 0.38, p<0.001) (b).**

D) Separating isotope data based on complementary site information reveals 'hot spots' and 'hot moments' of denitrification. Whereas the identification of the isotopic fingerprint depends on data density, translating this data into estimates of attenuation depends on the ability to distinguish sources and processes (i.e., remove the 'noise' around the parallel ~1:1 $\delta^{18}O$:$\delta^{15}N$ enrichment line). Rates of N attenuation could be calculated for differently managed paddy soils over time, effluent discharged into an urban stream, and a whole-catchment draining pastoral agriculture by separating collected $\delta^{18}O$-$\delta^{15}N$- NO_3^- data, subsequently referred to as 'prior-information'. Within the rice paddies, soil redox potential was used to partition isotope data into a two-box model of N inputs (aerobic) and N attenuation (anaerobic), while $\delta^{18}O$- $\delta^{15}N$- NO_3^- within the effluent contaminated river was contextualised based on information on effluent influxes, stream chemistry (particularly O_2 and C) and microbial biofilm populations. The importance of detailed prior-information is emphasised by the relative ease in quantifying attenuation of N from an acute sewage spill (Chapter 6) versus from

chronic, diffuse agricultural sources (Chapter 7). However, adapting the partitioning techniques developed to quantify fluxes within paddy soils (Chapter 5) and following acute pollution in the urban stream (Chapter 7) to separate streamwater NO_3^- isotope data into 'source versus sink' (based on stream depth, chemistry, and climate conditions) in conjunction with the ε_{denit} information developed in the previously, enabled the identification and quantification of hot spots and hot moments of attenuation within this chronically loaded system. The ability to use dense measurements of NO_3^- isotopes to calculate net attenuation rates comparable to those provided through labour- intensive nutrient balances confirmed the viability of using NO_3^- isotopes as integrative measures of denitrification across scales and locations. Moreover, in all of the case studies here, overlaying NO_3^- isotopes onto chemical data enabled identification of when and where attenuation happens, presenting a vital step-forward for improving catchment-scale N management.

E) Practical considerations for method application. To answer the originally posed questions of when, where, and how a stable isotope – based attenuation assessment should be deployed: by using independent site information to constrain sources and collecting a dense enough data set to reveal the trends beneath the 'noise', this methodology could be used anywhere. However, the analytical and sampling demands of constructing such a data set lead me to conclude that NO3- dual isotopes are optimanally used to provide additional information on N fluxes following specific events (e.g., sewage spills) or to tackle targeted chronic problems (e.g., agricultural intensification), rather than as part of a broad monitoring scheme.

8.2 Suggestions for future work

Looking between the conclusions described above, key areas for future research that have emerged from this thesis are:

- Intersection of C availability (including quality), microbial population structure, denitrification rates, and ε_{denit}, particularly $^{18}\varepsilon_{denit}$ v. $^{15}\varepsilon_{denit}$
- Reconcile variations in ε_{denit} at the field-scale with measured strain-to-strain variations – do intrinsic or extrinsic factors create the observed 'site specificity' of NO_3^- fractionation dynamics?
- There is a need to resolve discrepancies in $\delta^{18}O\text{-}NO_3^-$ dynamics, particularly in regards to $\delta^{18}O{:}\delta^{15}N$ fractionation ratios. In light of new information on the various fractionation processes impacting $\delta^{18}O$ during nitrification, attention should especially be paid to how the presence of NO_2^- removal processes such as anammox , co-denitrification, and nitrifier-denitrification impact the isotopic composition of the adjacent NO_3^-, and thus R_0 for traditional denitrification, and potentially ε_{denit}.

- How much mixing is too much? The data here implies that, with sufficient sampling density and prior site information, NO_3^- isotopes can be used to constrain attenuation fluxes in any environment. But what exactly defines 'sufficient density'? Is there a quantifiable relationship between sampling demands and hydrologic / biogeochemical complexity?
- The isotopic measurements in both the aerobic pasture soils and the submerged paddy soils revealed considerable inputs from soil-N following urine deposition and re-flooding/ tilling, respectively. As measurements of these compound-specific N compounds at the natural abundance level become increasingly viable for use in the soil-zone, the effect that the continuous turnover of the much larger organic pool will need to be considered.

8.3 Final comments

As the price of NO_3^- isotope analyses (both in terms of money and time) drops, the value of this methodology will become limited by interpretive power rather than finances. The previous six chapters reveal that, without sensible separation of data sets by known variables, NO_3^- isotopes cannot be accurately used as measures of ecosystem function and/or denitrification. With the power of the isotopes only as good as the prior information for the site, the most potential 'added value' from this sort of functional measurement most likely comes from adding NO_3^- isotope measurements to intensive study areas: this thesis lays out a solid starting point for any organisation interested in quantifying N losses from key catchments, or the impact of acute events on ecosystem function in freshwater or terrestrial sites.

8.4 References

Anisfeld, S. C., R. T. Barnes, M. A. Altabet, and T. X. Wu. 2007. Isotopic apportionment of atmospheric and sewage nitrogen sources in two Connecticut rivers. Environmental Science & Technology **41**:6363-6369.

Bai, E., B. Z. Houlton, and Y. P. Wang. 2012. Isotopic identification of nitrogen hotspots across natural terrestrial ecosystems. Biogeosciences **9**:3287-3304.

Ginevan, M.E., D.E. Splitstone. 2004. Statistical Tools for Environmental Quality Measures. Chapman & Hall/CRC, Boca Raton, Florida. p. 135

Houlton, B. Z. and E. Bai. 2009. Imprint of denitrifying bacteria on the global terrestrial biosphere. Proceedings of the National Academy of Sciences of the United States of America **106**:21713-21716.

Kritee, K., D. M. Sigman, J. Granger, B. B. Ward, A. Jayakumar, and C. Deutsch. 2012. Reduced isotope fractionation by denitrification under conditions relevant to the ocean. Geochimica Et Cosmochimica Acta **92**:243-259.

Appendix A
Meta-analysis of fractionation of nitrate isotopes during denitrification

A.1 Methods

Studies producing unique enrichment factors for NO_3^- isotopes (N ($^{15}\varepsilon_{denit}$) and/or O ($^{18}\varepsilon_{denit}$)) during denitrification were identified by searching titles and abstracts on ISI Web of Science using the search query, "enrichment OR fractionation" AND "denit* AND isotop*". References were also taken from citations in Lund et al. (2000), Lehmann et al. (2003), and Kritee et al. (2012). All significantly different ε_{denit} values within each publication (e.g., if ε_{denit} varied with laboratory conditions, environmental conditions, between sites, etc.) were used. Enrichment factors were calculated for O in dual isotope studies that reported the fractionation ratio between O:N and $^{15}\varepsilon_{denit}$, but not $^{18}\varepsilon_{denit}$. Enrichment factors for $^{15}\varepsilon_{denit}$ were estimated for three studies (Kellman and Hillaire-Marcel 1998, Kellman and Hillaire-Marcel 2003, Kellman 2004) that supplied Rayleigh plots, attributed isotopic and concentration variation directly to denitrification, but did not include the value for the slope of the relationship between the two in their manuscripts.

In addition to enrichment factors and O:N ratios (when applicable) each manuscript was also reviewed for: 1) mean ambient temperature (for laboratory studies this would be the T set for the experiment, for field experiments this was defined as either the mean annual air temperature at the site of data collection or the mean water temperature for marine studies); 2) method of NO_3^- isotope analysis (categorised as either steam distillation, diffusion, silver nitrate, denitrifier, Cd-azide, or other); 3) calculation used to generate the ε_{denit} value (e.g., Rayleigh, advection-diffusion, etc.); 4) wether measurements were based on NO_3^- within the denitrifying zone or post-transport into, e.g., oxic streamwater; 5) categorised as either 'field' or 'lab'. All manipulative studies (i.e., wherein conditions for denitrification were controlled, substrates were added, etc.) were classified as 'lab' and all studies that based their calculations off values collected empirically in the environment were classified as 'field'.

For lab studies additional information was collected for: 6) electron donor additions (identity and concentration); 7) oxygen concentration (if available); 8) substrate of experiment (culture (bacteria, fungi, archaea on a growth media), sediment (marine, aquifers, or rivers), or soil); and, for culture experiments, 9) origin of denitrifier strain (marine, freshwater, terrestrial).

For the field studies additional classifications were made based on: 10) the sampling environment (marine oxygen minimum zones, coastal zones, and continental shelf; terrestrial soils, lakes, rivers and streams, wetlands, groundwater, and the surface-water groundwater interface (SWGW)); 11) dominant transport mechanism between source and sink, as per Seitzinger et al. (2006) (diffusion (A), temporal lag (B), or advection (C)); and, 12) estimated distance (mm to cm (1), cm to m (2), m to km (3), or km to 100 km (4)) and time (seconds to minutes (1), minutes to hours (2), hours to months (3), or months to centuries (4)) between N source and sink (based on information on flow rates, residence times, catchment size, etc. provided within the publication).

A.2 Data tables

TableA1 **Enrichment factors (ε_{denit}) calculated based on denitrification under controlled conditions (i.e., 'intrinsic' fractionation).**

Reference	Medium	Analytical method	Calculation	$^{15}\varepsilon_{denit}$ ‰	$^{18}\varepsilon_{denit}$ ‰	δO:δN	Temperature (ºC)	C added (type, quantity)	Oxygen conditions	Denitrifier strain
Barford et al. (1999)	Culture	Diffusion	Rayleigh	-28.6	-	-	30	Acetate, 20 mM	Anaerobic	Paracoccus denitrificans
Bates et al. (1998)	Sediment (aquifer)	Steam distillation	Rayleigh	-6.1	-	-	13	Ethanol, 200 mg l^{-1}	Aerobic/ saturated	-
Bates and Spalding (1998)	Sediment (aquifer)	Steam distillation	Rayleigh	-3.9	-	-	11.5	Ethanol, 50 mg l^{-1}	Anaerobic/ saturated	-
				-15.9	-	-				
				-2.5	-	-		Ethanol, 100 mg l^{-1}		
				-13.5	-	-				
Blackmer and Bremner (1977)	Soil	Steam distillation	Rayleigh	-14	-	-	30	Glucose, 0.75 mg g^{-1} soil	Anaerobic (He)	-
				-23	-	-				
Carroll et al. (2009)	Sediment	NH_4^+ removal + sediment combustion	Rayleigh	-17.6	-	-	23	Methanol, 0.75 mg g^{-1} sediment	Anaerobic (He)	-
Chien et al. (1977)	Soil	Steam distillation	Rayleigh	-19	-	-	35	Glucose, 1% (w/w)	Anaerobic	-
	Soil			-6.5	-	-				
Delwiche and Styen (1970)	Culture	Steam distillation	Rayleigh	-17.6	-	-	23	Glucose, no rate specified	Anaerobic	*Pseudomonas Denitricans*
Dhondt et al. (2003)	Sediment	Cd-azide	Rayleigh	-21.4	-	-	10	Wheat straw, 10 g 450 g^{-1} sediment	Anaerobic (He)	-
				-24.9	-	-	15			
Granger et al. (2008)	Culture	Denitrifier	Rayleigh	-17	-16	0.96	23	Casein, 0.2 g l^{-1}	Anaerobic	Pseudomonas stutzeri
				-22	-21	0.96				Ochrobactrum sp
				-24	-22	0.96				Paracoccus denitrificans
				-20	-20	0.96				Pseudomonas chlororaphis f. sp. aureofaciens
				-15	-9	0.96			Aerobic	Rhodobacter sphaeroides
Holl et al. (2011)	Aquaculture	Diffusion	Rayleigh	-6.3	-	-	28	-	Aerobic (DO=6)	-
Kellman (2004)	Sediment	Silver nitrate	Rayleigh	-4.19	-	-	23	-	Aerobic (DO=7)	-
Knoller et al. (2011)	Culture	Denitrifier	Rayleigh	-14.7	-5.97	0.41	23	Toluene, 20 mM	Anaerobic	Azoarcus sp.
				-11	-6.2	0.56		Succinate, 20 mM		Azoarcus sp.
				-15	-6	0.40		Succinate, 20 mM		Pseudomonas pseudoalcaligenes
Korom et al. (2005)	Sediment	Diffusion	Rayleigh	-20.4	-	-	?	No, but sulphate as electron donor	? (submerged)	-
Korom et al. (2012)	Sediment	Silver nitrate	Rayleigh	-4.86	-	-	?	-	? (submerged)	-
				-9.34	-	-		-		-
Kritee et al. (2012)	Culture	Denitrifier	Rayleigh	-9.3	-8.65	0.93	23	Acetate, glucose or bactopeptone +casein (lower with more complex C and higher O), 2 g l^{-1}	0 or 4 µM O_2	Pseudomonas chlororaphis
				-22.3	-20.7	0.93				Pseudomonas chlororaphis
				-11	-10.2	0.93				Paracoccus denitrificans
				-31	-28.8	0.93				Paracoccus denitrificans
				-14.8	-13.7	0.93				Marinobacter sp.
				-22.8	-21.2	0.93				Marinobacter sp.
Mariotti et al. (1981)	Soil	Diffusion	Rayleigh	-29.4	-	-	20	-	Anaerobic (He)	-
				-24.6	-	-	30			

Mariotti et al. (1982)	Soil	Diffusion	Rayleigh	-25.4	-	-	10	-	Anaerobic (He)	-
				-31.2	-	-	10			
				-13	-	-	30			
				-24.5	-	-	30			
				-11	-	-	20	Glucose, 0.5 g 100 g^{-1} soil		
Miyake and Wada (1971)[¥]	Culture	?	?	-14	-	-	?	?	?	Marine denitrifier
				-21	-	-				
Olleros (1983)[¥]	Culture	?	?	-30	-15	0.5	?	?	Anaerobic	?
Pintar et al. (2008)	Soil	Evaporation + combustion of salt	Rayleigh	-7.6	-	-	18	Glucose, 78.4 mg l^{-1}	Anaerobic	-
				-34.9	-	-				
Robinson and Conroy (1999)	Soil	Diffusion	Rayleigh	-4	-	-	23	No, soil C/N of 20	Aerobic	-
Sebilo et al. (2003)	Sediment (river)	Diffusion	Rayleigh	-18	-	-	20	No (but with nitrification inhibitor)	Anaerobic	-
				-3.6	-	-			Aerobic	
Shearer and Kohl (1988)	Culture	?	Rayleigh	-10	-	-	20	Succinate, 25 mM	Anaerobic	Pseudomonas stutzeri
				-20	-	-				Pseudomonas stutzeri
Sovik and Morkved (2007)	Sediment	Denitrifier	Rayleigh	-2.2	-	-	17	Glucose, 16.7 mg l^{-1}	Anaerobic	-
				-11.3	-	-		-		
Torrento et al. (2010)	Culture	Denitrifier	Rayleigh	-19	-13.5	0.88	?	-	Anaerobic	-
				-22	-15	0.85				
Torrento et al. (2011)	Sediment	Denitrifier	Rayleigh	-26.3	-20.4	0.9	?			
Tsushima et al. (2006)	Sediment	?	Rayleigh	-32.9	-	-	20	-	Anaerobic	-
				-34.1	-	-				
Warneke et al. (2011a)[*]	Bioreactor	Cd-azide	Rayleigh	-19.4	-	-	19.6	Woodchips (176x5x1.5 m)	Anaerobic	-
Wellman et al. (1968)	Culture	?	?	-20	-	-	?	?	Anaerobic (N_2)	Pseudomonas stutzeri
Wunderlich et al. (2012)	Culture	Resin exchange	Rayleigh	-22.1	-19.9	1	30	Acetate, 2 mM	Anaerobic	Thauera aromatica
				-18.9	-15.9	1		Benzoate, 0.8 mM		Thauera aromatica
				-18.1	-16.5	1		Toluene, 3 µL 50 l^{-1}		Thauera aromatica
				-23.5	-23.7	1		Acetate, 2 mM		Aromatoleum aromaticum (strain EbN1)
				-17.3	-16.1	1		Toluene, 3 µL 50 l^{-1}		Aromatoleum aromaticum (strain EbN1)

[¥]Values as reported in Lehmann et al. (2003)

[*]Information on T, C, and DO from Warneke et al. (2011b)

TableA2 **Enrichment factors (ε_{denit}) for denitrification calculated based on empirical measurements of NO_3^- and its isotopes under un-manipulated field conditions (i.e., 'effective' fractionation).**

Reference	Location	T (ºC)	Environment	Land use	Analytical method	Calculation	$^{15}\varepsilon_{denit}$	$^{18}\varepsilon_{denit}$	$\delta^{18}O:\delta^{15}N$	Transport		
										Type	Time	Distance
Albertin et al. (2012)	USA	20	GW	Mixed	Denitrifier	Rayleigh	-18	-9	0.59	C	3	3
Alkhatib et al. (2012)	Gulf of Lawrence	-	Marine (coastal)	-	Denitrifier	Advection-diffusion	-2	-	-	A	3	1
							-6	-	-			
Altabet et al. (1999a)	Open ocean	-	Marine (OMZ)	-	Diffusion	Rayleigh	-30	-	-	C	4	4
Altabet et al. (1999b)	Open ocean	-	Marine (OMZ)	-	Diffusion	Rayleigh	-22.7	-	-	C	4	4
Aravena and Robertson (1998)	Canada	6	GW	Urban	Silver nitrate	Rayleigh	-22.9	-11.5	0.5	C	3	4
Bohlke and Denver (1995)	USA	12.8	GW	Ag	Diffusion	Rayleigh	-10	-	-	C	3	3
Bottcher et al. (1990)	Germany	9.8	GW	Ag	Diffusion	Rayleigh	-15.9	-8	0.49	C	3	3
Brandes and Devol (1997)	-	-	Marine (coastal)	-	Diffusion	Rayleigh	0	-	-	A	1	1
Brandes et al. (1998)	Open ocean	-	Marine (OMZ)	-	Diffusion	Rayleigh	-22	-	-	C	4	4
							-25	-	-			
							-28	-	-			
Brandes and Devol (2002)	Ocean	-	Marine (shelf)	-	Diffusion	Rayleigh	-1.5	-	-	A	1	1
							-20	-	-	C	3	3
Burns et al. (2009)	USA	10	River	Ag	Denitrifier	Rayleigh	-4	-2	0.5	C	3	2
							-4.66	-2.33	0.5			
Chen and MacQuarrie (2004)	Canada	7	SWGW	Ag	Silver nitrate	Rayleigh	-6.5	-	-	C	3	2
Chen et al. (2009)	China	22	River	Ag	Silver nitrate	Rayleigh	-14.8	-8.5	0.52	C	3	2
Chen et al. (2006)	China	13	GW	Ag	Diffusion	Rayleigh	-7.5	-	-	C	3	3
Clement et al. (2003)	France	11	SWGW	Ag	Diffusion	Rayleigh	-8.38	-	-	C	2	2
Cline and Kaplan (1975)	Open ocean	7	Marine (OMZ)	-	Steam distillation	Rayleigh	-30	-	-	C	4	4
							-40	-	-			
Cohen et al. (2012)	USA	21	River	Mixed	Denitrifier	Rayleigh	-3.09	-3.09	0.97	C	3	2
							-3.08	-3.08	1.04			
Curie et al. (2009)	France	10.8	GW	Ag	Diffusion	Rayleigh	-2.9	-	-	C	3	2
			River				-3	-	-	C	2	2
Deutsch et al. (2005)	Germany	-	Soil	Ag	Silver nitrate	Rayleigh	-5.9	-2	0.4	B	1	2
Devito et al. (2000)	Canada	7	SWGW	Ag	Silver nitrate	Rayleigh	-4.98	-2.5	0.56	C	2	2
Dhondt et al. (2003)	Belgium	8	SWGW	-	Cd-azide	Rayleigh	-6	-	-	C	2	2
							-16.2	-	-			
Eguchi et al. (2009)	Japan	15.6	SWGW	Ag	Diffusion	Rayleigh	-12	-	-	B	2	3
Erler and Eyre (2010)	Australia	19	Wetland	Ag	Diffusion	Rayleigh	-5.44	-	-	A	1	1
Fryar et al. (2000)	USA	18	GW	Ag	Cu, combustion	Rayleigh	-3.6	-	-	B	2	3
Fustec et al. (1991)	France	11	SWGW	Ag	Steam distillation	Rayleigh	-5.2	-	-	C	2	2
Fukada et al. (2003)	Germany	7.8	SWGW	Ag	Silver nitrate	Rayleigh	-13.6	-9.8	0.76	C	3	3
Fukada et al. (2004)	UK	9.8	GW	Urban	Silver nitrate	Rayleigh	-13.7	-6.9	0.5	C	3	3
Granger et al. (2011)	Ocean	-	Marine (shelf)	-	Denitrifier	Rayleigh	-6.2	-6.2	1	A	1	1
						2-box model	-7.9	-7.9	1			
Green et al.	USA	13	GW	Ag	Denitrifier	Rayleigh	-5	-3.65	0.73	C	2	3

(2008)							-20	-14.6	0.73			
Green et al. (2010)	USA	-	GW	Ag	Denitrifier	Advection-diffusion	-5	-	-	C	3	3
							-16	-	-			
Griggs et al. (2003)	USA	24	GW	Urban	Freeze-drying+ combustion	Rayleigh	-12.4	-	-	C	2	3
Grischek et al. (1998)	Germany	7.8	SWGW	Urban	Steam distillation	Rayleigh	-14.6	-	-	C	2	2
Hatzinger (2009)	USA	13	GW	Urban	Denitrifier	Rayleigh	-8	-6.6	0.83	C	2	2
Heffernan et al. (2012)	USA	20	GW	Mixed	Denitrifier	Rayleigh	-7.37	-7.37	0.99	C	2	3
Itoh et al. (2011)	Mongolia	-2.4	SWGW	Urban	Denitrifier	Rayleigh	-6.7	-3.8	0.54	C	2	2
Kellman and Hillaire-Marcel (1998)	Canada	6	River	Ag	Anion exchange	Rayleigh	-9.97	-	-	C	3	2
Kellman and Hillaire-Marcel (2003)	Canada	6	SWGW	Ag	Anion exchange	Rayleigh	-2.18	-	-	C	3	2
							-4	-	-			
							-2.14	-	-			
Koba et al. (1997)	Japan	16	Soil	Forest	Diffusion	Rayleigh	-6	-	-	A	1	1
							-5.6	-	-			
Koh et al. (2012)	Korea	16	GW	Ag	Denitrifier	Rayleigh	-8.06	-4.01	0.46	C	3	3
Lehmann et al. (2003)	Switzer-land	13	Lake	Mixed	Denitrifier	Rayleigh	-11.2	-6.6	0.57	B	3	2
						Advection-diffusion	-20.7	-11	0.57			
Lehmann et al. (2007)	Ocean	4	Marine (shelf)	-	Denitrifier	Rayleigh	-5	-	-	A	1	1
							-15	-	-			
Lund et al. (2000)	USA	-	Wetland	Urban	Molecular seive		-2.51	-	-	C	2	2
Mariotti et al. (1988)	France	8	GW	Mixed	Diffusion	Rayleigh	-4.7	-	-	C	3	3
							-5	-	-			
McCallum et al. (2008)	Canada	-	GW		Silver nitrate	Rayleigh	-9.2	-6.9	1	C	3	3
McMahon and Bohlke (1996)	USA	10	SWGW	Ag	Diffusion	Rayleigh	-10	-	-	C	3	3
							-20	-	-			
McMahon et al. (1999)	USA	10	GW	Ag	Cu sorption+ combustion	Rayleigh	-20	-	-	C	3	4
							-13	-	-			
							-27	-	-			
McMahon et al. (2004)	USA	19	GW	Ag	Cu sorption+ combustion	Rayleigh	-10	-8.5	0.85	C	3	4
							-30	-25.5	0.85			
Mengis et al. (1999)	Canada	5	GW	Forest	Silver nitrate	Rayleigh	-27.3	-18.3	0.67	C	3	2
Miyajima et al. (2009)	Thailand	27	River	Urban	Denitrifier	Rayleigh	-16.3	-16.3	1	C	3	2
							-6.3	-3.1	0.5			
Naqvi et al. (1998)	Ocean	19	Marine (OMZ)	-	Cu sorption+ combustion	Rayleigh	-22	-	-	C	4	4
						Advection-diffusion model	-25	-	-			
Naqvi et al. (2006)	Ocean	19	Marine (coastal)	-	Cu sorption+ combustion	Rayleigh	-7.21	-	-	A	3	3
							-7.7	-	-			
Nishikiori et al. (2012)	Japan	14	River	Ag	Denitrifier	Rayleigh	-2.3	-2.3	1	C	3	2
Osaka et al. (2010)	Japan	13	GW	Forest	Denitrifier	Rayleigh	-1.1	-1.1	1	C	2	2
Otero et al. (2009)	Spain	13	GW	Ag	Denitrifier	Rayleigh	-4	-1.9	0.55	C	3	3
							-15.5	-8.9	0.55			
Prokopenko et al. (2011)	Ocean	-	Marine (coastal)	-	Denitrifier	Rayleigh	-20	-20	1	C	2	3
Reinhardt et al. (2006)	Switzerla nd	10	Wetland	-	Silver nitrate	Rayleigh	0	0	-	A	1	1
Ruehl et al. (2007)	USA	14	River	Ag	Denitrifier	Rayleigh	-6	-1.6	0.5	C	3	2
							-9	-9.7	1			
							-18.6	-18.5	1			

Ryabenko et al. (2012)	Ocean	5	Marine (OMZ)	-	Cd-azide	Rayleigh	-11.4	-	-	C	4	4
Schwarz et al. (2011)	Ecuador	15	Soil	Forest	Silver nitrate	Rayleigh	-4.9	-	-	B	1	3
							-2.6	-	-			
			River				-3.8	-	-	C	2	2
							-3.9	-	-			
							-1.5	-	-			
Sebilo et al. (2003)	France	12	River	Mixed	Diffusion	Rayleigh	-1.5	-	-	C	3	2
Sigman et al. (2003)	Ocean	-	Marine (coastal)	-	Denitrifier	Steady-state model	-25	-25	1	C	3	3
							-1.5	-1.5	1	A	1	1
						Rayleigh	-5	-5	1	B	3	3
Sigman et al. (2005)	Ocean	-	Marine (coastal)	-	Denitrifier	Steady-state model	-25	-25	1	C	4	4
Singleton et al. (2007)	USA	16	GW	Ag	Denitrifier	Rayleigh	-7	-3.5	0.47	C	3	3
							-57	-28	0.6			
Smith et al. (1991)	USA	8.9	GW	Urban	Diffusion	Rayleigh	-13.9	-	-	C	2	3
Sovik and Morkved (2008)	Norway	8	Wetland	Ag	Denitrifier	Rayleigh	-2.5			C	1	2
							-5.9				2	2
Spalding et al. (1993)	USA	11	GW	Ag	Steam distillation	Rayleigh	-7.7	-	-	C	2	3
							-5.7	-	-			
Spalding and Parrott (1994)	USA	11	GW	Ag	Steam distillation	Rayleigh	-9.6	-	-	C	2	3
Spoelstra et al. (2010)	Canada	5	Wetland	Forest	Silver nitrate	Rayleigh	-9	-4.5	0.5	C	1	2
							-30	-15	0.5		2	2
Sutka et al. (2004)	Ocean	-	Marine (OMZ)	-	Steam distillation	Advection-diffusion	-30	-	-	C	4	4
							-35	-	-			
Tsushima et al. (2002)	Japan	-	GW	Urban	?	Rayleigh	-17.9	-	-	C	3	3
Umezawa et al. (2009)	Indonesia	27	GW	Urban	Denitrifier	Rayleigh	-3	-1.5	0.51	C	3	3
Vogel et al. (1981)	Namibia	-	GW	-	Combustion to N_2	Rayleigh	-30	-	-	C	3	4
Voss et al. (2001)	Ocean	-	Marine (OMZ)	-	Diffusion	Rayleigh	-26.3	-	-	C	4	4
							-27.3	-	-			
						Advection-diffusion	-22.5	-	-			
							-37.5	-	-			
Voss et al. (2010)	Germany	5	Wetland	Urban	Diffusion	Rayleigh	0	-	-	A	1	1
Well et al. (2012)	Germany	8.9	GW	Ag	Cd-azide	Rayleigh	-13.7	-7.3	0.66	C	3	3
Wexler et al. (2011)	UK	11	River	Ag	Denitrifier	Rayleigh	-11.1	-8.3	0.75	C	3	2
Wexler et al. (2012)	UK	11	River	Ag	Denitrifier	Rayleigh	-5.8	-2.4	0.41	C	1	2
							-6	-3	0.49			
							-6.2	-3.4	0.5			
Zhang et al. (2012)	Nether-lands	4	GW	Ag	Silver nitrate	Rayleigh	-10.9	-9.1	1	C	3	3
							-2	-2	1			

A.3 References

Albertin, A. R., J. O. Sickman, A. Pinowska, and R. J. Stevenson. 2012. Identification of nitrogen sources and transformations within karst springs using isotope tracers of nitrogen. Biogeochemistry **108**:219-232.

Alkhatib, M., M. F. Lehmann, and P. A. del Giorgio. 2012. The nitrogen isotope effect of benthic remineralization-nitrification-denitrification coupling in an estuarine environment. Biogeosciences **9**:1633-1646.

Altabet, M. A., D. W. Murray, and W. L. Prell. 1999a. Climatically linked oscillations in Arabian Sea denitrification over the past 1 m.y.: Implications for the marine N cycle. Paleoceanography **14**:732-743.

Altabet, M. A., C. Pilskaln, R. Thunell, C. Pride, D. Sigman, F. Chavez, and R. Francois. 1999b. The nitrogen isotope biogeochemistry of sinking particles from the margin of the Eastern North Pacific. Deep-Sea Research Part I-Oceanographic Research Papers **46**:655-679.

Aravena, R. and W. D. Robertson. 1998. Use of multiple isotope tracers to evaluate denitrification in ground water: Study of nitrate from a large-flux septic system plume. Ground Water **36**:975-982.

Barford, C. C., J. P. Montoya, M. A. Altabet, and R. Mitchell. 1999. Steady-state nitrogen isotope effects of N_2 and N_2O production in Paracoccus denitrificans. Applied and Environmental Microbiology **65**:989-994.

Bates, H. K., G. E. Martin, and R. F. Spalding. 1998. Kinetic isotope effects in production of nitrite-nitrogen and dinitrogen gas during in situ denitrification. Journal of Environmental Quality **27**:183-191.

Bates, H. K. and R. F. Spalding. 1998. Aquifer denitrification as interpreted from in situ microcosm experiments. Journal of Environmental Quality **27**:174-182.

Blackmer, A. M. and J. M. Bremner. 1977. Nitrogen isotope discrimination in denitrification of nitrate in soils. Soil Biology & Biochemistry **9**:73-77.

Bohlke, J. K. and J. M. Denver. 1995. Combined use of groundwater dating, chemical, and isotopic analyses to resolve the histroy and fate of nitrate contamination in 2 agricultural watersheds, Atlantic coastal-plain, Maryland. Water Resources Research **31**:2319-2339.

Bottcher, J., O. Strebel, S. Voerkelius, and H. L. Schmidt. 1990. Using isotope fractionation of nitrate nitrogen and nitrate oxygen for evaluation of microbial denitrification in a sandy aquifer. Journal of Hydrology **114**:413-424.

Brandes, J. A. and A. H. Devol. 1997. Isotopic fractionation of oxygen and nitrogen in coastal marine sediments. Geochimica Et Cosmochimica Acta **61**:1793-1801.

Brandes, J. A. and A. H. Devol. 2002. A global marine-fixed nitrogen isotopic budget: Implications for Holocene nitrogen cycling. Global Biogeochemical Cycles **16**:14.

Brandes, J. A., A. H. Devol, T. Yoshinari, D. A. Jayakumar, and S. W. A. Naqvi. 1998. Isotopic composition of nitrate in the central Arabian Sea and eastern tropical North Pacific: A tracer for mixing and nitrogen cycles. Limnology and Oceanography **43**:1680-1689.

Burns, D. A., E. W. Boyer, E. M. Elliott, and C. Kendall. 2009. Sources and transformations of nitrate from streams draining varying land uses: Evidence from dual isotope analysis. Journal of Environmental Quality **38**:1149-1159.

Carroll, K. C., F. L. Jordan, E. P. Glenn, W. J. Waugh, and M. L. Brusseau. 2009. Comparison of nitrate attenuation characterization methods at the Uranium mill tailing site in Monument Valley, Arizona. Journal of Hydrology **378**:72-81.

Chen, D. J. Z. and K. T. B. MacQuarrie. 2004. Numerical simulation of organic carbon, nitrate, and nitrogen isotope behavior during denitrification in a riparian zone. Journal of Hydrology **293**:235-254.

Chen, F. J., G. D. Jia, and J. Y. Chen. 2009. Nitrate sources and watershed denitrification inferred from nitrate dual isotopes in the Beijiang River, south China. Biogeochemistry **94**:163-174.

Chen, J. Y., C. Y. Tang, and J. J. Yu. 2006. Use of O-18, H-2 and N-15 to identify nitrate contamination of groundwater in a wastewater irrigated field near the city of Shijiazhuang, China. Journal of Hydrology **326**:367-378.

Chien, S. H., G. Shearer, and D. H. Kohl. 1977. The nitrogen isotope effect associated with nitrate and nitrite loss from waterlogged soils. Soil Science Society of America Journal **41**:63-69.

Clement, J. C., R. M. Holmes, B. J. Peterson, and G. Pinay. 2003. Isotopic investigation of denitrification in a riparian ecosystem in western France. Journal of Applied Ecology **40**:1035-1048.

Cline, J. D. and I. R. Kaplan. 1975. Isotopic fractionation of dissolved nitrate during denitrification in the eastern tropical north pacific ocean. Marine Chemistry **3**:271-299.

Cohen, M. J., J. B. Heffernan, A. Albertin, and J. B. Martin. 2012. Inference of riverine nitrogen processing from longitudinal and diel variation in dual nitrate isotopes. Journal of Geophysical Research-Biogeosciences **117**.

Curie, F., A. Ducharne, M. Sebilo, and H. Bendjoudi. 2009. Denitrification in a hyporheic riparian zone controlled by river regulation in the Seine river basin (France). Hydrological Processes **23**:655-664.

Delwiche, C. C. and P. L. Steyn. 1970. Nitrogen isotope fractionation in soils and microbial reactions. Environmental Science & Technology **4**:929-935.

Deutsch, B., I. Liskow, P. Kahle, and M. Voss. 2005. Variations in the delta N-15 and delta O-18 values of nitrate in drainage water of two fertilized fields in Mecklenburg-Vorpommern (Germany). Aquatic Sciences **67**:156-165.

Devito, K. J., D. Fitzgerald, A. R. Hill, and R. Aravena. 2000. Nitrate dynamics in relation to lithology and hydrologic flow path in a river riparian zone. Journal of Environmental Quality **29**:1075-1084.

Dhondt, K., P. Boeckx, O. Van Cleemput, and G. Hofman. 2003. Quantifying nitrate retention processes in a riparian buffer zone using the natural abundance of N-15 in NO3. Pages 2597-2604 *in* Meeting of the Stable-Isotope-Mass-Spectrometry-Users-Group. John Wiley & Sons Ltd, Bristol, England.

Eguchi, S., Y. Nakajima, S. Yabusaki, M. Kasuya, H. Shibayama, A. Tsunekawa, and K. Imai. 2009. Denitrification during vertical upwelling at an alluvium-diluvium interface below the upland perimeter of a riparian paddy. Journal of Environmental Quality **38**:2198-2209.

Erler, D. V. and B. D. Eyre. 2010. Quantifying nitrogen process rates in a constructed wetland using natural abundance stable isotope signatures and stable isotope amendment experiments. Journal of Environmental Quality **39**:2191-2199.

Fryar, A. E., S. A. Macko, W. F. Mullican, K. D. Romanak, and P. C. Bennett. 2000. Nitrate reduction during ground-water recharge, Southern High Plains, Texas. Journal of Contaminant Hydrology **40**:335-363.

Fukada, T., K. M. Hiscock, and P. F. Dennis. 2004. A dual-isotope approach to the nitrogen hydrochemistry of an urban aquifer. Applied Geochemistry **19**:709-719.

Fukada, T., K. M. Hiscock, P. F. Dennis, and T. Grischek. 2003. A dual isotope approach to identify denitrification in groundwater at a river-bank infiltration site. Water Research **37**:3070-3078.

Fustec, E., A. Mariotti, X. Grillo, and J. Sajus. 1991. Nitrate removal by denitrification in alluvial ground-water - role of a former channel. Journal of Hydrology **123**:337-354.

Granger, J., M. G. Prokopenko, D. M. Sigman, C. W. Mordy, Z. M. Morse, L. V. Morales, R. N. Sambrotto, and B. Plessen. 2011. Coupled nitrification-denitrification in sediment of the eastern Bering Sea shelf leads to N-15 enrichment of fixed N in shelf waters. Journal of Geophysical Research-Oceans **116**.

Granger, J., D. M. Sigman, M. F. Lehmann, and P. D. Tortell. 2008. Nitrogen and oxygen isotope fractionation during dissimilatory nitrate reduction by denitrifying bacteria. Limnology and Oceanography **53**:2533-2545.

Green, C. T., J. K. Bohlke, B. A. Bekins, and S. P. Phillips. 2010. Mixing effects on apparent reaction rates and isotope fractionation during denitrification in a heterogeneous aquifer. Water Resources Research **46**:19.

Green, C. T., L. J. Puckett, J. K. Bohlke, B. A. Bekins, S. P. Phillips, L. J. Kauffman, J. M. Denver, and H. M. Johnson. 2008. Limited occurrence of denitrification in four shallow aquifers in agricultural areas of the United States. Journal of Environmental Quality **37**:994-1009.

Griggs, E. M., L. R. Kump, and J. K. Bohlke. 2003. The fate of wastewater-derived nitrate in the subsurface of the Florida Keys: Key Colony Beach, Florida. Estuarine Coastal and Shelf Science **58**:517-539.

Grischek, T., K. M. Hiscock, T. Metschies, and P. F. Dennis. 1998. Factors affecting denitrification during infiltration of river water into a sand and gravel aquifer in Saxony, Germany. Water Research **32**:450-460.

Hatzinger, P. B., J. K. Bohlke, N. C. Sturchio, B. Gu, L. J. Heraty, and R. C. Borden. 2009. Fractionation of stable isotopes in perchlorate and nitrate during in situ biodegradation in a sandy aquifer. Environmental Chemistry **6**:44-52.

Heffernan, J. B., A. R. Albertin, M. L. Fork, B. G. Katz, and M. J. Cohen. 2012. Denitrification and inference of nitrogen sources in the karstic Floridan Aquifer. Biogeosciences **9**:1671-1690.

Holl, C. M., C. T. Glazer, and S. M. Moss. 2011. Nitrogen stable isotopes in recirculating aquaculture for super-intensive shrimp production: Tracing the effects of water filtration on microbial nitrogen cycling. Aquaculture **311**:146-154.

Itoh, M., Y. Takemon, A. Makabe, C. Yoshimizu, A. Kohzu, N. Ohte, D. Tumurskh, I. Tayasu, N. Yoshida, and T. Nagata. 2011. Evaluation of wastewater nitrogen transformation in a natural wetland (Ulaanbaatar, Mongolia) using dual-isotope analysis of nitrate. Science of the Total Environment **409**:1530-1538.

Kellman, L. 2004. Nitrate removal in a first-order stream: reconciling laboratory and field measurements. Biogeochemistry **71**:89-105.

Kellman, L. and C. Hillaire-Marcel. 1998. Nitrate cycling in streams: using natural abundances of NO3--delta N-15 to measure in-situ denitrification. Biogeochemistry **43**:273-292.

Kellman, L. M. and C. Hillaire-Marcel. 2003. Evaluation of nitrogen isotopes as indicators of nitrate contamination sources in an agricultural watershed. Agriculture Ecosystems & Environment **95**:87-102.

Knoller, K., C. Vogt, M. Haupt, S. Feisthauer, and H. H. Richnow. 2011. Experimental investigation of nitrogen and oxygen isotope fractionation in nitrate and nitrite during denitrification. Biogeochemistry **103**:371-384.

Koba, K., N. Tokuchi, E. Wada, T. Nakajima, and G. Iwatsubo. 1997. Intermittent denitrification: The application of a N-15 natural abundance method to a forested ecosystem. Geochimica Et Cosmochimica Acta **61**:5043-5050.

Koh, E. H., D. Kaown, B. Mayer, B. R. Kang, H. S. Moon, and K. K. Lee. 2012. Hydrogeochemistry and isotopic tracing of nitrate contamination of two aquifer systems on Jeju Island, Korea. Journal of Environmental Quality **41**:1835-1845.

Korom, S. F., A. J. Schlag, W. M. Schuh, and A. K. Schlag. 2005. In situ mesocosms: Denitrification in the Elk Valley aquifer. Ground Water Monitoring and Remediation **25**:79-89.

Korom, S. F., W. M. Schuh, T. Tesfay, and E. J. Spencer. 2012. Aquifer denitrification and in situ mesocosms: Modeling electron donor contributions and measuring rates. Journal of Hydrology **432**:112-126.

Kritee, K., D. M. Sigman, J. Granger, B. B. Ward, A. Jayakumar, and C. Deutsch. 2012. Reduced isotope fractionation by denitrification under conditions relevant to the ocean. Geochimica Et Cosmochimica Acta **92**:243-259.

Lehmann, M. F., P. Reichert, S. M. Bernasconi, A. Barbieri, and J. A. McKenzie. 2003. Modelling nitrogen and oxygen isotope fractionation during denitrification in a lacustrine redox-transition zone. Geochimica Et Cosmochimica Acta **67**:2529-2542.

Lehmann, M. F., D. M. Sigman, D. C. McCorkle, J. Granger, S. Hoffmann, G. Cane, and B. G. Brunelle. 2007. The distribution of nitrate N^{15}/N^{14} in marine sediments and the impact of benthic nitrogen loss on the isotopic composition of oceanic nitrate. Geochimica Et Cosmochimica Acta **71**:5384-5404.

Lund, L. J., A. J. Horne, and A. E. Williams. 2000. Estimating denitrification in a large constructed wetland using stable nitrogen isotope ratios. Ecological Engineering **14**:67-76.

Mariotti, A., J. C. Germon, P. Hubert, P. Kaiser, R. Letolle, A. Tardieux, and P. Tardieux. 1981. Experimental-determination of nitrogen kinetic isotope fractionation - some principles - illustration for the denitrification and nitrification processes. Plant and Soil **62**:413-430.

Mariotti, A., J. C. Germon, and A. Leclerc. 1982. Nitrogen isotope fractionation associated with the NO_2--N_2O step of denitrification in soils. Canadian Journal of Soil Science **62**:227-241.

Mariotti, A., A. Landreau, and B. Simon. 1988. N-15 isotope biogeochemistry and natural denitrification process in groundwater - application to the chalk aquifer of northern France. Geochimica Et Cosmochimica Acta **52**:1869-1878.

McCallum, J. E., M. C. Ryan, B. Mayer, and S. J. Rodvang. 2008. Mixing-induced groundwater denitrification beneath a manured field in southern Alberta, Canada. Applied Geochemistry **23**:2146-2155.

McMahon, P. B. and J. K. Bohlke. 1996. Denitrification and mixing in a stream-aquifer system: Effects on nitrate loading to surface water. Journal of Hydrology **186**:105-128.

McMahon, P. B., J. K. Bohlke, and B. W. Bruce. 1999. Denitrification in marine shales in northeastern Colorado. Water Resources Research **35**:1629-1642.

McMahon, P. B., J. K. Bohlke, and S. C. Christenson. 2004. Geochemistry, radiocarbon ages, and paleorecharge conditions along a transect in the central High Plains aquifer, southwestern Kansas, USA. Applied Geochemistry **19**:1655-1686.

Mengis, M., S. L. Schiff, M. Harris, M. C. English, R. Aravena, R. J. Elgood, and A. MacLean. 1999. Multiple geochemical and isotopic approaches for assessing ground water NO_3^- elimination in a riparian zone. Ground Water **37**:448-457.

Miyajima, T., C. Yoshimizu, Y. Tsuboi, Y. Tanaka, I. Tayasu, T. Nagata, and I. Koike. 2009. Longitudinal distribution of nitrate delta N-15 and delta O-18 in two contrasting tropical rivers: implications for instream nitrogen cycling. Biogeochemistry **95**:243-260.

Miyake, Y. and E. Wada. 1971. The isotope effect on the nitrogen in biochemical, oxidation-reduction reactions. Rec. Oceanogr. Works Jpn. **11**:1-6.

Naqvi, S. W. A., H. Naik, A. Pratihary, W. D'Souza, P. V. Narvekar, D. A. Jayakumar, A. H. Devol, T. Yoshinari, and T. Saino. 2006. Coastal versus open-ocean denitrification in the Arabian Sea. Biogeosciences **3**:621-633.

Naqvi, S. W. A., T. Yoshinari, J. A. Brandes, A. H. Devol, D. A. Jayakumar, P. V. Narvekar, M. A. Altabet, and L. A. Codispoti. 1998. Nitrogen isotopic studies in the suboxic Arabian Sea. Proceedings of the Indian Academy of Sciences-Earth and Planetary Sciences **107**:367-378.

Nishikiori, T., T. Takamatsu, A. Kohzu, Y. Nakajima, and M. Watanabe. 2012. Distribution of nitrate in groundwater affected by the presence of an aquitard at an agricultural area in Chiba, Japan. Environmental Earth Sciences **67**:1531-1545.

Olleros, T. 1983. Kinetische Isotopeneffekte der Arginase- und Nitratreduktase-Reaktion: Ein Beitrag zur Aufkla¨rung der entsprechenden Reaktionsmechanismen. Tech. Univ. Mu¨nchen-Weihenstephan, Munich.

Osaka, K., N. Ohte, K. Koba, C. Yoshimizu, M. Katsuyama, M. Tani, I. Tayasu, and T. Nagata. 2010. Hydrological influences on spatiotemporal variations of delta N-15 and delta O-18 of nitrate in a forested headwater catchment in central Japan: Denitrification plays a critical role in groundwater. Journal of Geophysical Research-Biogeosciences **115**:14.

Otero, N., C. Torrento, A. Soler, A. Mencio, and J. Mas-Pla. 2009. Monitoring groundwater nitrate attenuation in a regional system coupling hydrogeology with multi-isotopic methods: The case of Plana de Vic (Osona, Spain). Agriculture Ecosystems & Environment **133**:103-113.

Pintar, M., S. V. Bolta, and F. Lobnik. 2008. Nitrogen isotope enrichment factor as an indicator of denitrification potential in top and subsoil in the Apace Valley, Slovenia. Australian Journal of Soil Research **46**:719-726.

Prokopenko, M. G., D. M. Sigman, W. M. Berelson, D. E. Hammond, B. Barnett, L. Chong, and A. Townsend-Small. 2011. Denitrification in anoxic sediments supported by biological nitrate transport. Geochimica Et Cosmochimica Acta **75**:7180-7199.

Reinhardt, M., B. Muller, R. Gachter, and B. Wehrli. 2006. Nitrogen removal in a small constructed wetland: An isotope mass balance approach. Environmental Science & Technology **40**:3313-3319.

Robinson, D. and J. P. Conroy. 1999. A possible plant-mediated feedback between elevated CO2, denitrification and the enhanced greenhouse effect. Soil Biology & Biochemistry **31**:43-53.

Ruehl, C. R., A. T. Fisher, M. Los Huertos, S. D. Wankel, C. G. Wheat, C. Kendall, C. E. Hatch, and C. Shennan. 2007. Nitrate dynamics within the Pajaro River, a nutrient-rich, losing stream. Journal of the North American Benthological Society **26**:191-206.

Ryabenko, E., A. Kock, H. W. Bange, M. A. Altabet, and D. W. R. Wallace. 2012. Contrasting biogeochemistry of nitrogen in the Atlantic and Pacific Oxygen Minimum Zones. Biogeosciences **9**:203-215.

Schwarz, M. T., Y. Oelmann, and W. Wilcke. 2011. Stable N isotope composition of nitrate reflects N transformations during the passage of water through a montane rain forest in Ecuador. Biogeochemistry **102**:195-208.

Sebilo, M., G. Billen, M. Grably, and A. Mariotti. 2003. Isotopic composition of nitrate-nitrogen as a marker of riparian and benthic denitrification at the scale of the whole Seine River system. Biogeochemistry **63**:35-51.

Shearer, G. and D. H. Kohl. 1988. Nitrogen isotopic fractionation and o-18 exchange in relation to the mechanism of denitrification of nitrite by pseudomonas-stutzeri. Journal of Biological Chemistry **263**:13231-13245.

Sigman, D. M., J. Granger, P. J. DiFiore, M. M. Lehmann, R. Ho, G. Cane, and A. van Geen. 2005. Coupled nitrogen and oxygen isotope measurements of nitrate along the eastern North Pacific margin. Global Biogeochemical Cycles **19**.

Sigman, D. M., R. Robinson, A. N. Knapp, A. van Geen, D. C. McCorkle, J. A. Brandes, and R. C. Thunell. 2003. Distinguishing between water column and sedimentary denitrification in the Santa Barbara Basin using the stable isotopes of nitrate. Geochemistry Geophysics Geosystems **4**:20.

Singleton, M. J., B. K. Esser, J. E. Moran, G. B. Hudson, W. W. McNab, and T. Harter. 2007. Saturated zone denitrification: Potential for natural attenuation of nitrate contamination in shallow groundwater under dairy operations. Environmental Science & Technology **41**:759-765.

Smith, R. L., B. L. Howes, and J. H. Duff. 1991. Denitrification in nitrate-contaminated groundwater - occurrence in steep vertical geochemical gradients. Geochimica Et Cosmochimica Acta **55**:1815-1825.

Sovik, A. K. and P. T. Morkved. 2007. Nitrogen isotope fractionation as a tool for determining denitrification in constructed wetlands. Water Science and Technology **56**:167-173.

Sovik, A. K. and P. T. Morkved. 2008. Use of stable nitrogen isotope fractionation to estimate denitrification in small constructed wetlands treating agricultural runoff. Science of the Total Environment **392**:157-165.

Spalding, R. F., M. E. Exner, G. E. Martin, and D. D. Snow. 1993. Effects of sludge disposal on groundwater nitrate concentrations. Journal of Hydrology **142**:213-228.

Spalding, R. F. and J. D. Parrott. 1994. Shallow groundwater denitrification. Science of the Total Environment **141**:17-25.

Spoelstra, J., S. L. Schiff, R. G. Semkin, D. S. Jeffries, and R. J. Elgood. 2010. Nitrate attenuation in a small temperate wetland following forest harvest. Forest Ecology and Management **259**:2333-2341.

Sutka, R. L., N. E. Ostrom, P. H. Ostrom, and M. S. Phanikumar. 2004. Stable nitrogen isotope dynamics of dissolved nitrate in a transect from the North Pacific Subtropical Gyre to the Eastern Tropical North Pacific. Geochimica Et Cosmochimica Acta **68**:517-527.

Torrento, C., J. Cama, J. Urmeneta, N. Otero, and A. Soler. 2010. Denitrification of groundwater with pyrite and Thiobacillus denitrificans. Chemical Geology **278**:80-91.

Torrento, C., J. Urmeneta, N. Otero, A. Soler, M. Vinas, and J. Cama. 2011. Enhanced denitrification in groundwater and sediments from a nitrate-contaminated aquifer after addition of pyrite. Chemical Geology **287**:90-101.

Tsushima, K., S. Ueda, and N. Ogura. 2002. Nitrate loss for denitrification during high frequency research in floodplain groundwater of the Tama River. Water Air and Soil Pollution **137**:167-178.

Tsushima, K., S. Ueda, H. Ohno, N. Ogura, T. Katase, and K. Watanabe. 2006. Nitrate decrease with isotopic fractionation in riverside sediment column during infiltration experiment. Water Air and Soil Pollution **174**:47-61.

Umezawa, Y., T. Hosono, S. Onodera, F. Siringan, S. Buapeng, R. Delinom, C. Yoshimizu, I. Tayasu, T. Nagata, and M. Taniguchi. 2009. Sources of nitrate and ammonium contamination in groundwater under developing Asian megacities. Science of the Total Environment **407**:3218-3231.

Vogel, J. C., A. S. Talma, and T. H. E. Heaton. 1981. Gaseous nitrogen as evidence for denitrification in groundwater. Journal of Hydrology **50**:191-200.

Voss, M., B. Deutsch, I. Liskow, M. Pastuszak, U. Schulte, and S. Sitek. 2010. Nitrogen retention in the Szczecin Lagoon, Baltic Sea. Isotopes in Environmental and Health Studies **46**:355-369.

Voss, M., J. W. Dippner, and J. P. Montoya. 2001. Nitrogen isotope patterns in the oxygen-deficient waters of the Eastern Tropical North Pacific Ocean. Deep-Sea Research Part I-Oceanographic Research Papers **48**:1905-1921.

Warneke, S., L. A. Schipper, D. A. Bruesewitz, and W. T. Baisden. 2011a. A comparison of different approaches for measuring denitrification rates in a nitrate removing bioreactor. Water Research **45**:4141-4151.

Warneke, S., L. A. Schipper, D. A. Bruesewitz, I. McDonald, and S. Cameron. 2011b. Rates, controls and potential adverse effects of nitrate removal in a denitrification bed. Ecological Engineering **37**:511-522.

Well, R., W. Eschenbach, H. Flessa, C. von der Heide, and D. Weymann. 2012. Are dual isotope and isotopomer ratios of N_2O useful indicators for N_2O turnover during denitrification in nitrate-contaminated aquifers? Geochimica Et Cosmochimica Acta **90**:265-282.

Wellman, R. P., F. D. Cook, and H. R. Krouse. 1968. Nitrogen-15: microbiological alteration of abundance. Science (New York, N.Y.) **161**:269-270.

Wexler, S. K., K. M. Hiscock, and P. F. Dennis. 2011. Catchment-scale quantification of hyporheic denitrification using an isotopic and solute flux approach. Environmental Science & Technology **45**:3967-3973.

Wexler, S. K., K. M. Hiscock, and P. F. Dennis. 2012. Microbial and hydrological influences on nitrate isotopic composition in an agricultural lowland catchment. Journal of Hydrology **468**:85-93.

Wunderlich, A., R. Meckenstock, and F. Einsiedl. 2012. Effect of different carbon substrates on nitrate stable isotope fractionation during microbial denitrification. Environmental Science & Technology **46**:4861-4868.

Zhang, Y. C., C. P. Slomp, H. P. Broers, B. Bostick, H. F. Passier, M. E. Bottcher, E. O. Omoregie, J. R. Lloyd, D. A. Polya, and P. Van Cappellen. 2012. Isotopic and microbiological signatures of pyrite-driven denitrification in a sandy aquifer. Chemical Geology **300**:123-132.

Appendix B

Modelling the impact of diffusion and mixing on the expression of the isotopic enrichment caused by denitrification

B.1 Derivation of equation to define diffusion-impacted R

By using Fick's Law, this model builds an isotopic dimension into the diffusion-based understanding of denitrification rates in sediments presented by Christensen et al. (1990), which defines k_{denit} and NO_3^- fluxes into and out of the denitrifying zone based on the depth of O_2 penetration (z) (Eq. B.1).

(B.1) $$0 = D_s \frac{\partial^2 C}{\partial z^2} - w \frac{\partial C}{\partial z} - F$$

where NO_3^- (as concentration, C) is transported vertically (over z) to and from the denitrifying zone (defined as an infinitely thin reactive layer, F, where denitrification occurs as per S1) via diffusion (Christensen et al., 1990; House, 2003; O'Connor and Hondzo, 2008). Availability of C for diffusion or consumption is controlled by physical advection (w) (cm s^{-1}). The diffusion term (D_s) is dependent on molecular diffusivity (D_m) of NO_3^- (1.33 x10^{-5} cm^2 s^{-1}), temperature, and sediment porosity (Φ), as defined by Eq. B.2 (Boudreau, 1997).

(B.2) $$D_s = \frac{D_m}{(1.0 - \ln \phi)}$$

Denitrification (F) is assumed to occur in isolation from transport terms over z, allowing Eq. B.1 to be simplified to:

(B.3) $$D \frac{\partial^2 C}{\partial z^2} = 0$$

boundary conditions $$\frac{\partial C}{\partial x} = -k_{denit} C$$

where the initial boundary condition describes 1st order reaction kinetics (S1). At steady state, consumption at L (penetration depth z of O_2 across the sediment-water interface, Fig. 3.1) is in equilibrium with diffusive transport of NO_3^- (C) across the aerobic-anaerobic boundary layer (z=0) (Eq. B.4):

(B.4) $$D \frac{\partial^2 C}{\partial z^2} = -k_{denit} C_{z=L}$$

boundary conditions $$C_{z=0} = -w\frac{dC}{dx}$$

where the upper boundary layer at z=0 is open, meaning substrate fluxes into the surface water in accordance with steady state demands, which is in turn controlled by downstream flow (w over x). Therefore, the NO_3^- concentration in the surface water reflects both the degree of denitrifcation and the effect of transport (w, D_s), and the flux across z=0 can be solved as the first derivative of Fick's Law (Eq. B.5).

(B.5) $$\frac{D_s \cdot k_{denit} \cdot C_w}{D_s + k_{denit} \cdot L} = -w\frac{\partial C_w}{\partial x}$$

Accordingly, the isotopic composition at z=0 reflects fractionation during from denitrification (α_{denit}) and transport (α_D); α_D is defined by Eq. B.6.

(B.6) $$\alpha_D = \sqrt{\frac{m(m^b + M)}{m^b(m + M)}}$$

where the square root of the relative masses of the heavy (m^b) and light (m) forms of NO_3^- (i.e., $^{15}N^{16}O_3^-$, $^{14}N^{18}O_3^-$) diffused in water (M= mass of H_2O) define the diffusive fractionation factor (α_D) (LaBolle et al., 2008; Richter et al., 2006). Using α_D and α_{denit}, the isotopic composition of NO_3^- (R) at depth z is calculated based on rates of consumption (k_{denit}) and transport (D_s) (Eq. B.7).

(B.7) $$R = \frac{C_0^b \cdot (D_s + k_{denit} L) \cdot (\alpha_D D_s + \alpha_{denit} k_{denit} (L - z))}{C_{0 \cdot} (D_s + k_{denit} (L - z)) \cdot (\alpha_D D_s + \alpha_{denit} k_{denit} L)}$$

The time required to establish the steady-state conditions assumed in the previous equations (t) is described in Eq. B.8,

(B.8) $$t = \frac{L^2 (1 - \ln [\phi^2])}{4D_s}$$

where the time to stead state (t) following a disturbance is determined by L squared and the sediment porosity (Φ) relative to its diffusivity (D_s) (Boudreau 1997).

B.2 Codes for S2 numerical results

The following formulae were used to generate numerical solutions for 'R' for various values of L, k_{denit}, ε_{denit}, D_s, and w (e.g., Fig. 3.1), which were then used to solve for ε_{eff} per the Rayleigh solutions developed by Mariotti et al. (1981).

```
Manipulate[Module[{S3A, S3sed, PlotS3a, PlotS3sed},
  S3A = NDSolve[{
     0 == - ((k1 Ds1 NO3A[x]) / (Ds1 + k1 Lz)) - w * D[NO3A[x], {x, 1}],
     0 == - ((((1 / αn2) * k1) (Ds1 * (αDn)) n15A[x]) / (Lz * ((1 / αn2) * k1) + ((αDn) * Ds1))) -
       w * D[n15A[x], {x, 1}],
     0 == - ((((1 / αo2) * k1) (Ds1 * (αDo)) o18A[x]) / (Lz * ((1 / αo2) * k1) + ((αDo) * Ds1))) -
       w * D[o18A[x], {x, 1}],
     NO3A[0] == A,
     n15A[0] == rn0 A,
     o18A[0] == ro0 A},
    {NO3A, n15A, o18A}, {x, 0, 10 000}];
  S3sed = NDSolve[{
     Ds1 D[NO3B[z], {z, 2}] == 0,
     (αDn) Ds1 D[n15B[z], {z, 2}] == 0,
     (αDo) Ds1 D[o18B[z], {z, 2}] == 0,

     Ds1 D[NO3B[z], {z, 1}] == -k1 NO3B[z] /. z → Lz,
     (αDn) Ds1 D[n15B[z], {z, 1}] == -k1 (1 / αn2) n15B[z] /. z → Lz,
     (αDo) Ds1 D[o18B[z], {z, 1}] == -k1 (1 / αo2) o18B[z] /. z → Lz,

     A == NO3B[z] /. z → 0,
     A rn0 == n15B[z] /. z → 0,
     A ro0 == o18B[z] /. z → 0},
    {NO3B, n15B, o18B}, {z, 0, Lz}];

  {PlotS3a = Dynamic[Plot[{Evaluate[NO3A[x] /. S3A],
        {δ[Evaluate[n15A[x] /. S3A] / Evaluate[NO3A[x] /. S3A], .003667]},
        {δ[Evaluate[o18A[x] /. S3A] / Evaluate[NO3A[x] /. S3A], .002008]}},
       {x, 0, 10 000}, AxesLabel → {x, "NO3- δ15N δ18O"},
       PlotLabel → "Surface water in S3", AxesOrigin → {0, 0}]]}

   {PlotS3sed = Dynamic[Plot[{Evaluate[NO3B[z] /. S3sed],
         {δ[Evaluate[n15B[z] /. S3sed] / Evaluate[NO3B[z] /. S3sed], .003667]},
         {δ[Evaluate[o18B[z] /. S3sed] / Evaluate[NO3B[z] /. S3sed], .002008]}},
        {z, 0, L - .01}, AxesLabel → {z, "NO3- δ15N δ18O"},
        PlotLabel → "Porewater in S3", AxesOrigin → {0, 0}]];}],

{{Ds1, Dh, "Diffusivity"}, Dh / 2, Dsand},
{{Lz, L, "diffusive distance"}, .1, 2}, {{k1, ka, "k_denit"}, .00000268, .008},
{{αn2, αn, "15ε_denit"}, αnMin, αnMax}, {{αo2, αo, "18ε_denit"}, αoMin, αoMax}]
```

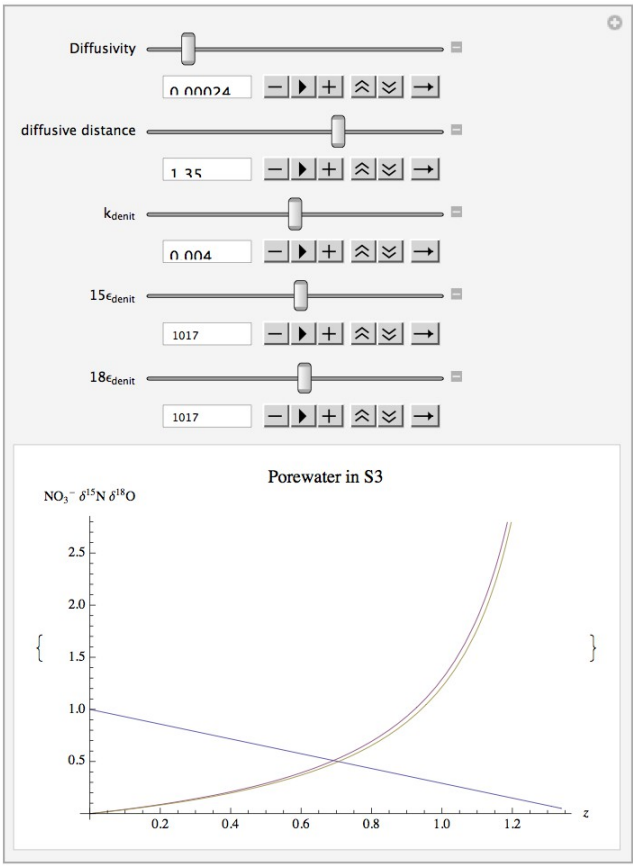

Figure B.1 **Output of dynamic model to describe how diffusive transport of NO_3^- over vertical distance (z) in the sediment porewater (a) and NO_3^- in the oxic surface water (b) over distance/ time (x) affects the net concentration of NO_3^- (blue line), $\delta^{15}N$-NO_3^- (‰ v AIR) (red line), and $\delta^{18}O$-NO_3^- (‰ v VSMOW) (yellow line), when sediment diffusivity (Diffusivity, in cm s^{-1}), diffusive distance (L, in cm), denitrification rate (k_{denit}, in µg N cm^{-2} s^{-1}), and fractionation factors for $\delta^{15}N$-NO_3^- ($^{15}\varepsilon_{denit}$, measured as α) and $\delta^{18}O$-NO_3^- ($^{18}\varepsilon_{denit}$, measured as α) are varied**

B.3 Codes for S3 numerical results

```
In[33]:= Manipulate[Module[{S2A, Plotsw, Plotall},
  S2A = NDSolve[{

    NO3sed'[x] == -ka NO3sed[x],
    n15sed'[x] == -ka (1 / αn) n15sed[x],
    o18sed'[x] == -ka (1 / αo) o18sed[x],

    NH4sw'[x] == -kn * NH4sw[x],
    n15sw'[x] == -(kn) (1 / αnit) n15sw[x],
    o18sw'[x] == -kn (1 / Oαnit1) o18sw[x],

    NO3sed[0] == A,
    n15sed[0] == rn0 A,
    o18sed[0] == ro0 A,


    NH4sw[0] == NH4,
    rn0 * NH4 == n15sw[x] /. x → 0,
    ro0 * NH4 == o18sw[x] /. x → 0},


   {NO3sed, n15sed, o18sed, NH4sw, n15sw, o18sw},
   {x, 0, 10000}];

 {Plotsw = Dynamic[Plot[{{A - Evaluate[NH4sw[x] /. S2A]}}, {x, 0, 10000}]],
  Dynamic[Plot[δ[{Evaluate[n15sw[x] /. S2A] / (Evaluate[NH4sw[x] /. S2A] / NHsw3)},
     .003667], {x, 0, 1000}]],
  Dynamic[Plot[{δ[(rn0 * NHsw3), .003667] + ((Nαnit1 - 1) * 1000) *
       (Evaluate[NH4sw[x] /. S2A] / NHsw3) * (Log[(Evaluate[NH4sw[x] /. S2A] / NHsw3)] /
         (1 - (Evaluate[NH4sw[x] /. S2A] / NHsw3)))}, {x, 0, 1000}]]};

 {Plotall =
   {Dynamic[Plot[{{NH4 - Evaluate[NH4sw[x] /. S2A]} + Evaluate[NO3sed[x] /. S2A]}, {x, 0,
        1000}, AxesOrigin → {0, 0}, ImageSize → {270, 188}, AxesLabel → {x, "NO3-"}]]}

    {Dynamic[
      Plot[{((δ[(rn0 / NH4), .003667] + ((αnit - 1) * 1000) * (Evaluate[NH4sw[x] /. S2A] /
                  NH4) * (Log[(Evaluate[NH4sw[x] /. S2A] / NH4)] / (1 - (Evaluate[
                    NH4sw[x] /. S2A] / NH4)))) * (NH4 - Evaluate[NH4sw[x] /. S2A])) +
           (δ[{Evaluate[n15sed[x] /. S2A] / Evaluate[NO3sed[x] /. S2A]},
              .003667] * Evaluate[NO3sed[x] /. S2A])) /
         (Evaluate[NO3sed[x] /. S2A] + (NH4 - Evaluate[NH4sw[x] /. S2A]))},
       {x, 0.1, 1000}, AxesLabel → {x, "δ"}, AxesOrigin → {0, 0},
       ImageSize → {270, 188}, PlotLabel → "δ15N- NO3- mixed"]]}


    {Dynamic[
      Plot[{((δ[(ro0 / NH4), .002008] + ((Oαnit1 - 1) * 1000) * (Evaluate[NH4sw[x] /. S2A] /
                  NH4) * (Log[(Evaluate[NH4sw[x] /. S2A] / NH4)] / (1 - (Evaluate[
                    NH4sw[x] /. S2A] / NH4)))) * (NH4 - Evaluate[NH4sw[x] /. S2A])) +
           (δ[{Evaluate[o18sed[x] /. S2A] / Evaluate[NO3sed[x] /. S2A]},
              .002008] * Evaluate[NO3sed[x] /. S2A])) /
         (Evaluate[NO3sed[x] /. S2A] + (NH4 - Evaluate[NH4sw[x] /. S2A]))},

       {x, 1, 1000}, AxesLabel → {x, "δ"}, AxesOrigin → {0, 0},
       ImageSize → {270, 188}, PlotLabel → "δ18O- NO3- mixed"]]}}],

{{NH4, A, "SW NO3-"}, 0, 4 * A}, {{kn, knit, "knit"}, 0, .007},
{{αnit, Nαnit1, "εnit"}, αnitHigh1, αnitLow1}]
```

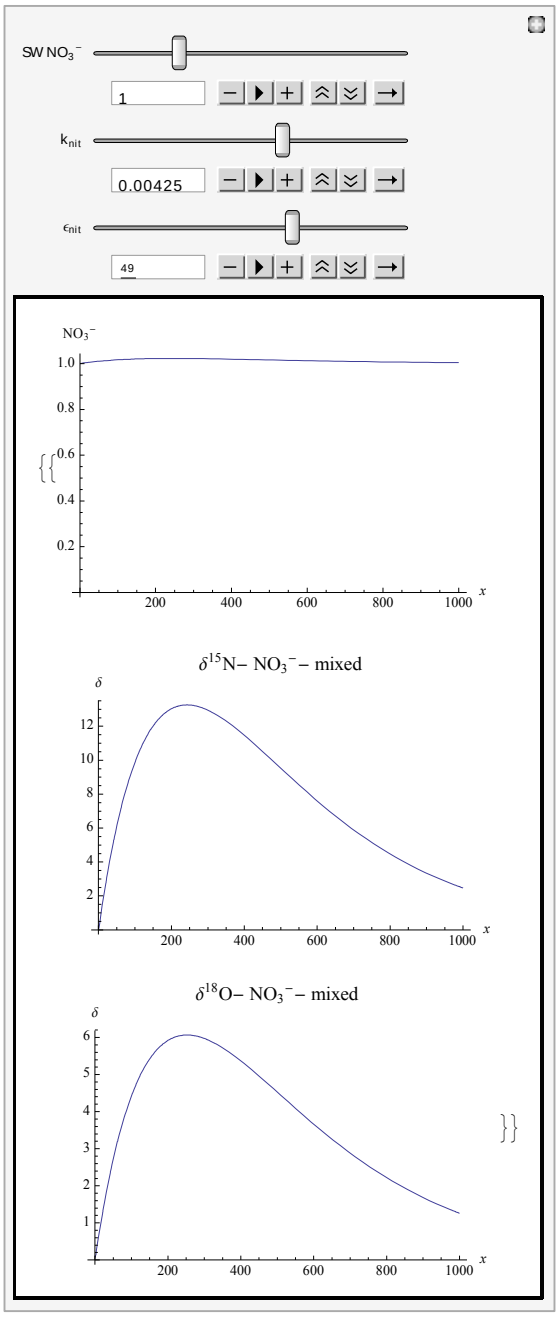

Figure B.2 **Output of dynamic model to describe how mixing of NO_3^- produced from nitrification and residual from denitrification mix to determine the net concentration of NO_3^- (top), $\delta^{15}N$-NO_3^- (‰ v AIR) (middle), and $\delta^{18}O$-NO_3^- (‰ v VSMOW) (bottom), when the total concentration of NO_3^- produced via nitrification (SW NO_3^-), the rate of nitrification (k_{nit}), and the fractionation factor for $\delta^{15}N$ during nitrification (ε_{nit}) are varied**